学位論文

Effective theory for the quark-hadron phase transition

(クォーク・ハドロン相転移の有効理論)

平成２６年１２月博士（理学）申請

東京大学大学院理学系研究科

物理学専攻

山崎　加奈子

Abstract

In this thesis, we propose an approach for describing the quark-hadron phase transition by using an effective model which is written in terms of quarks. Our starting point is the Nambu-Jona-Lasinio model with the Polyakov loop (PNJL model), that describes both the chiral phase transition and the de-confinement phase transition. Unlike many previous works based on the mean-field approximation, we take the mesonic and the baryonic fluctuations into account, because they play an important role in order to describe properly the hadronic phase at low temperatures and low densities.

Firstly, we include only the mesonic fluctuations into the two-flavour PNJL model at zero chemical potential. In this model, only the quarks and antiquarks are treated as dynamical variables, and the mesons are constructed from quarks and antiquarks as collective modes. They are introduced in the partition function as auxiliary fields. By considering their thermal fluctuations, their contribution to the equation of state can be calculated in the path integral method. We find that the pressure and the entropy are dominated by the mesonic fluctuations at low temperatures. On the other hand, the quarks and the gluons dominate at high temperatures after the mesons have melted into quarks and antiquarks. We also discuss at which temperature the mesons (the pions and the sigma mesons in the two-flavour case) change into quarks and antiquarks in order to obtain some informations of the transition region.

Next, we extend the two-flavour calculations to the three-flavour case. Due to the increased number of flavours, 18 species of mesons (9 scalar mesons and 9 pseudo-scalar mesons) appear. Since the heavy mesons are expected to give a very small contribution to the pressure at low temperatures, we take into account only the eight lightest species of mesons (three degenerated pions, four degenerated kaons and the sigma meson) and we neglect all the heavier mesons.

Finally, we extend the two-flavour PNJL model to the case of a finite chemical potential by including both the mesons and the baryons. By introducing an additional interaction term in the original Lagrangian, a diquark condensate can be described as well as the quark condensate. We assume that a diquark and a quark form a baryon, just like that a quark and an antiquark form a meson, so that we now insert auxiliary fields for mesons,

diquarks, anti-diquarks, baryons, and anti-baryons with an additional coupling between quarks and diquarks. We calculate analytically the pressure of the diquark fluctuations and of the baryonic fluctuations, and we discuss how they contribute to the pressure at low temperatures.

This thesis is based on the following papers:

[1] Quark-Hadron Phase transition in the PNJL model for interacting quarks,
Kanako Yamazaki, T. Matsui,
Nucl. Phys. **A913** (2013) 19.

[2] Quark-hadron phase transition in a three flavour PNJL model for interacting quarks,
Kanako Yamazaki, T. Matsui,
Nucl. Phys. **A922** (2014) 237.

[3] Entropy in the quark-hadron transition,
Kanako Yamazaki, T. Matsui, Gordon Baym,
Nucl. Phys. **A933** (2015) 245.

[4] Baryons in an extended PNJL model for quark-hadron phase transition,
Kanako Yamazaki, T. Matsui,
in preparation.

Contents

Chapter 1

Introduction

Investigating the phase structure of quantum chromodynamics (QCD) is probably one of the most fundamental problems in modern nuclear physics. It has been theoretically and also experimentally expected that there are several phases in QCD, for instance the hadronic phase at low temperatures and the quark-gluon plasma at high temperatures [5–8]. At low temperatures and low densities, free quarks and gluons have never been observed even though they are the most elementary particles in QCD. All the states which have been observed are colour singlet states, i.e. bound states made of colourless combinations of quarks. Therefore, this phase where coloured states are not allowed in the spectrum of excitations is called the confined phase or the hadronic phase. In addition, the chiral symmetry, which is an important approximate symmetry of the QCD Lagrangian, is broken in the low temperature and low density region. For the high temperature and low density region, the chiral symmetry is thought to be restored and colour degrees of freedom become de-confined simultaneously to the chiral symmetry restoration. This phase is called the de-confined phase or the quark-gluon plasma. This theoretical prediction has been confirmed by experiments in high energy heavy ion collisions [9–16]. Since there are two phases which have completely different features in different temperature regions, there could be phase transitions (or crossover transitions) between these two phases, whose study is important for understanding the dynamics of QCD.

On the other hand, colour superconductor phases are expected to exist, based on perturbative approaches in the high density region where a perturbative theory can be effective since the coupling becomes weak thanks to the asymptotic freedom of QCD [17, 18]. This can be understood by noticing that the one gluon exchange diagram (See Fig.1.1) generates an attraction in a colour anti-triplet channel, which leads to the formation of Cooper pairs [19–22].

These phases are represented on the $T - \mu$ plane where μ is the chemi-

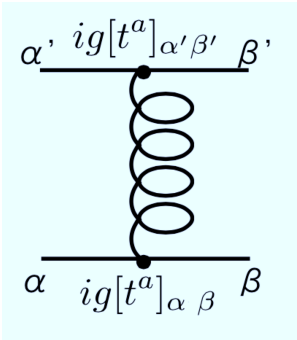

Figure 1.1: One gluon exchange. t^a is a generator of SU(3).

cal potential associated to baryon number conservation (originally $T - n_B$ plane where n_B is a baryon density) which is called the QCD phase diagram. In an early stage of development of the QCD phase diagram, only two phases were known: the confined phase and the de-confined phase [23] . These phases were predicted based on an interpretation of Hagedorn's temperature [24, 25], which is the highest temperature at which the partition function is stable. The phase transition at zero temperature and finite density was also discussed in this period [26, 27]. The phase diagram including both the chiral phase transition and the de-confinement transition was later suggested by [5,6]. The phases of nuclear matter have also been discussed in the Nambu-Jona-Lasinio (NJL) model [28–39] which includes a four point interaction of quark fields. The NJL model was originally designed to describe the chiral symmetry in hadron dynamics, in analogy with the BCS theory of superconductivity [40, 41]. This model therefore is useful to describe the chiral phase transition, but the colour confinement is dropped out. Therefore, if one calculates an equation of state in the hadronic phase by using the NJL model, the resulting pressure is a contribution from quark excitations in all regions, even though quarks should have been confined in hadrons in the hadronic phase.

Early applications of the NJL model to the chiral phase transition and/or the phase diagram have been done in the mean-field approximation. In this approximation, meson fields are treated as uniform background fields, namely their fluctuations are neglected. The merit of this approximation is to make the calculations simple, and in spite of its simplicity, this method can describe the chiral phase transition. However, this approximation has a serious shortcoming: mesonic excitations cannot be taken into account in this way even at low temperatures and low densities. It means that in the NJL model, a phase which has quark excitations and no hadronic excitations is realised at low temperatures instead of the hadronic phase that we have expected, where hadrons are excited and quarks are confined inside hadrons.

To improve the description of the hadronic phase, the mesonic fluctuations have been taken into account in the NJL model [42–45]. This improvement introduces mesonic fluctuations as corrections to the thermodynamic potential in the mean-field approximation by the method of steepest descent. These approaches made it possible to describe mesonic excitations at low temperatures and low densities. However, since there is no mechanism to confine quarks into hadrons, quark excitations and mesonic excitations coexist in the hadronic phase. This unsatisfactory situation has continued until the middle of the 2000s.

After the colour superconductor phase on the QCD phase diagram was first suggested at large chemical potential, many model calculations have tried to describe this phase [46–53]. In the NJL framework, quark-quark interactions can be introduced in order to generate diquark condensates in addition to the quark-antiquark interactions of the basic NJL model. Based on this, the simplest prediction of the phase diagram containing the colour superconductor phase leads to the hadronic phase at small temperatures and small chemical potential, the quark-gluon plasma at high temperatures, and the colour superconductor phase at small temperatures and large chemical potential (See Fig.1.2).

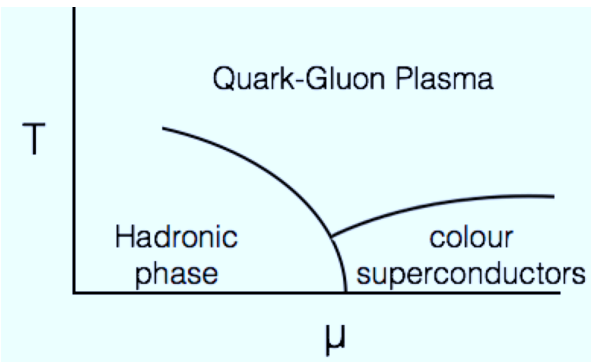

Figure 1.2: QCD phase diagram.

This situation that the hadronic phase is unphysical because of the lack of colour confinement was changed by the Nambu-Jona-Lasinio model with the Polyakov loop (PNJL model) that was proposed by Fukushima [54]. The PNJL model is a combination of the NJL model and the Polyakov loop [55, 56] which acts as an order parameter of the de-confinement phase transition [57–65]. The main effect of the Polyakov loop appears at low temperatures, where it suppresses quark excitations since quarks are not colour singlet states, and at high temperatures the quark suppression becomes weaker and weaker. Gluons are introduced by hand as an effective potential which gives a contribution to the thermodynamic potential only

at high temperatures, but the dynamics of gluons is not included in this model. For a convenience of calculations, the mean-field approximation has been performed in the PNJL model in the same way as in the NJL model. Since this approximation cannot describe the mesonic excitations and the quark excitations left are suppressed by the Polyakov loop, there are no excitations in the hadronic phase. To sum up, the dominant particles to the thermodynamical quantities calculated in the PNJL model under the mean-field approximation are quarks and gluons at high temperatures and nothing at low temperatures.

The next thing that we should do is to take the mesonic excitations into account in the hadronic phase in order to describe the change of degrees of freedom from hadrons to quarks. In this work, we have calculated the thermodynamic quantities by adding mesonic fluctuations to the mean-field approximation, and described the quark-hadron phase transition [1–3]. In a first step, we have focused on zero chemical potential and we have added mesonic excitations in the two and three-flavour PNJL model. Then, we have extended it to finite chemical potential. In this case, baryonic excitations are also taken into account in addition to the mesonic excitations.

This thesis is composed of a review part (Chapter 2, 3 and 4) and our original works (Chapter 5, 6, and 7). In Chapter 2, we will give a brief overview of the chiral phase transition and the de-confinement phase transition. In Chapter 3, some useful methods of quantum field theory at finite temperature are summarised. In Chapter 4, the two-flavour NJL model is reviewed. In the basic NJL model, the interaction term is a four-point interaction between quarks and antiquarks. Scalar and pseudo-scalar interactions with the same coupling are both required in order to keep the chiral symmetry when bare quark masses are zero. To describe the colour superconductor phase, a quark-quark four-point interaction is introduced. This interaction term has a different coupling from the quark-antiquark interaction term but the two couplings are connected by the Fierz transformation.

In Chapter 5, we discuss the quark-hadron phase transition in the two-flavour PNJL model at zero chemical potential. We begin with the basic PNJL model written in terms of quark and antiquark fields, and then introduce auxiliary meson fields in order to rewrite the four-point interactions as Yukawa interactions, so that the effective action becomes a function of the meson fields. The mesonic excitations are obtained by expanding the effective action up to the second order in the fluctuations around a stationary point which gives a local minimum value of the potential. Then, the thermodynamic potential is written as a sum of contributions from the mean-field and the mesonic excitations. We calculate the pressure and the entropy including mesonic excitations and we compare the results to those of the mean-field approximation. In the two-flavour case, three degenerate pion and sigma mesons are introduced as auxiliary fields so that we obtain their pressure and entropy separately. We also determine at which tempera-

ture the mesons as collective modes melt into quarks. This is a key to know what is happening through the transition region. In Chapter 6, we extend the contents of the previous chapter to the three-flavour case. The three-flavour PNJL model requires a six-point interaction [66, 67] which breaks axial $U(1)$ symmetry in addition to the four-point interaction. This is different from the two-flavour case that the effect of breaking $U(1)_A$ symmetry is already included in the four-point interaction. The six-point interaction can be treated approximately as a correction to the effective four-point interaction. Therefore, we can practically apply the same method to the three-flavour model and in the two-flavour case. The biggest difference between two-flavours and three-flavours is the number of mesons which appear in the thermodynamic quantities. In the three-flavour case, there are three pions, four kaons, an η meson, and an η' meson for pseudo scalar mesons and a sigma meson, four κ mesons, three a_0 mesons and an f_0 meson for scalar mesons. In Chapter 7, we discuss the PNJL model with both mesons and baryons at finite chemical potential. We assume that a baryon is constructed with a quark and a diquark so that we begin with the Lagrangian including the quark-antiquark interaction and the quark-quark interaction to make diquarks. Finally, we present our conclusions in Chapter 8.

Chapter 2

QCD phase transitions

QCD has a rich phase structure which is drawn in Fig.2.1. From the asymptotic freedom of QCD [17, 18], the coupling of the theory is weak in the high energy region where an analysis based on perturbation theory is possible. On the other hand, it becomes strong in the low energy region where perturbation theory fails and where non-perturbative phenomena like chiral symmetry breaking and colour confinement become essential. A phase transition from a phase where the chiral symmetry is broken and the colour is confined at low temperatures and low baryon densities to another phase called the quark-gluon plasma would happen as the temperature and/or the baryon density increase. This is strongly supported by the high energy heavy ion collision experiments at the RHIC and at the LHC. Although it is an interesting and important problem to determine the location of the transition from hadronic phase to the quark phase in the phase diagram, this is highly nontrivial since the phase transition happens in the non-perturbative region.

Lattice QCD simulations are often used for analysing this non-perturbative region [68–72]. In lattice calculations, the space-time is approximated as a finite grid of points, on which the matter fields (quarks) live, where the force carriers (gluons) are represented by links that connect the lattice sites. Physical quantities are calculated numerically using a Monte-Carlo sampling of the field configurations that exist on such a lattice. Lattice simulations have shown that the QCD phase transition at zero net baryon density is a cross-over transition, neither a first order nor a second order phase transition, and its pseudo-critical temperature is estimated between 150MeV and 170MeV. However, this method faces a serious difficulty at finite chemical potential because of the sign problem, namely the contribution from quarks to the path integral becomes complex once chemical potential is introduced. Therefore, it is exceedingly important to study the QCD phase transition by effective models to obtain informations at finite chemical potential. Indeed, there are many previous works using effective models such as the Nambu-

Jona-Lasinio (NJL) model [28–39], the random matrix model [73–75] and so on. However, most of them are based on the chiral symmetry breaking and its restoration, and they do not include any mechanism of the colour confinement. Although lattice QCD calculations have shown that the chiral cross-over transition and de-confinement cross-over transition happen at the same temperature at zero chemical potential, there is no reason why these two transitions should happen at the same critical temperature. In addition, it does not mean that these two transitions still happen at the same temperature at finite chemical potential. Therefore, a model which has only the chiral symmetry is not sufficient for describing the quark-hadron phase transition, and a model must also include the physics of colour confinement if we want to use it as an effective model of QCD.

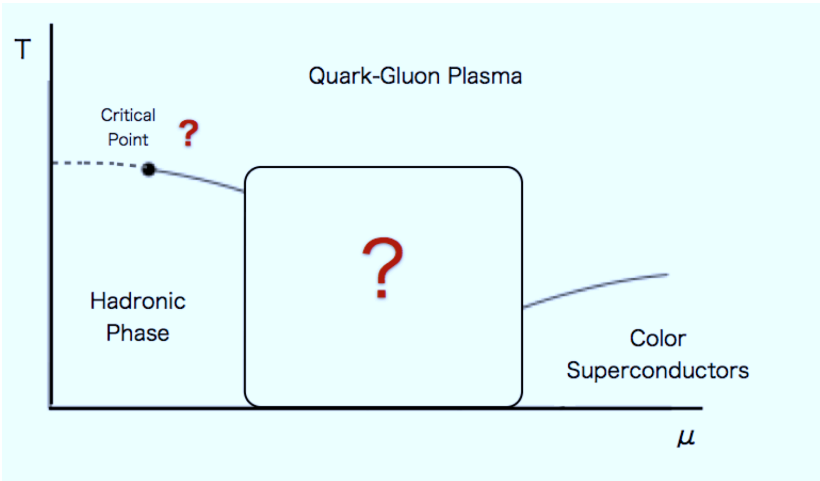

Figure 2.1: QCD phase diagram.

Before setting up an effective model including the chiral and the de-confinement phase transitions, we inspect their features in detail in this chapter.

We explain the chiral symmetry and how the chiral phase transition happens due to the change of temperature by using a toy model in the first section of this chapter. We begin with the free energy of the Ginzburg-Landau model which is a function of an order parameter of the chiral phase transition. The order parameter is determined by minimising the free energy at each temperature, and the behaviour of the order parameter as a function of temperature gives us informations on the phase transition. In Section 2.2, the de-confinement phase transition and its order parameter are explained. In Section 2.3, we summarise the behaviour of the order parameters of the chiral and the de-confinement phase transitions. To describe the quark-hadron phase transition, an effective model should be able to treat both the

chiral and de-confinement phase transitions at the same time. In addition, the effective Lagrangian should be written in terms of quarks, then hadrons should be constructed from quarks in order to describe the change of degrees of freedom from hadrons to quarks in an unified way. For this purpose, we start our discussion from the Nambu-Jona-Lasinio model with the Polyakov loop (the PNJL model), and construct hadrons as collective modes of quarks. The idea of making collective modes and the method are explained in Section 2.4.

2.1 Chiral phase transition

2.1.1 Chiral symmetry

The massless QCD Lagrangian with N_f flavours of quarks has an $U(N_f)_L \times U(N_f)_R$ chiral symmetry, namely the system is invariant under the individual transformation for the right-handed component and the left-handed component. To check this, divide the fermion fields into the right-handed component ψ_R and the left-handed component ψ_L by using the projection operators in

$$\psi_R = P_R\psi, \quad \psi_L = P_L\psi, \tag{2.1}$$

where the projection operators P_R and P_L are defined by

$$P_R \equiv \frac{1+\gamma_5}{2}, \quad P_L \equiv \frac{1-\gamma_5}{2}. \tag{2.2}$$

$\psi_{L/R}$ is an eigenstate of $\gamma_5 = i\gamma_0\gamma_1\gamma_2\gamma_3$

$$\gamma_5\psi_{L/R} = \mp\psi_{L/R}. \tag{2.3}$$

By applying separate transformations to the right-handed and the left-handed components,

$$\psi_L \to \exp\Big(i\sum_{a=0}^{N_f^2-1}\theta_L^a\tau^a\Big)\psi_L \tag{2.4}$$

$$\psi_R \to \exp\Big(i\sum_{a=0}^{N_f^2-1}\theta_R^a\tau^a\Big)\psi_R, \tag{2.5}$$

where

$$\exp\Big(i\sum_{a=0}^{N_f^2-1}\theta_L^a\tau^a\Big) \in U(N_f)_L \tag{2.6}$$

$$\exp\Big(i\sum_{a=0}^{N_f^2-1}\theta_R^a\tau^a\Big) \in U(N_f)_R, \tag{2.7}$$

one finds that the QCD Lagrangian

$$\begin{aligned}\mathcal{L}_{QCD} &= \bar{q}(i\not{D} - m)q - \frac{1}{4}F^a_{\mu\nu}F^{\mu\nu}_a \\ &= \bar{q}_L i\not{D} q_L + \bar{q}_R i\not{D} q_R - (\bar{q}_L m q_R + \bar{q}_R m q_L) - \frac{1}{4}F^a_{\mu\nu}F^{\mu\nu}_a \end{aligned} \tag{2.8}$$

with

$$F^a_{\mu\nu} = \partial_\mu A^a_\nu - \partial_\nu A^a_\mu + g f^{abc} A^b_\mu A^c_\nu \tag{2.9}$$

is invariant under these transformations when the quark mass is equal to zero, which means that the massless QCD has the chiral symmetry. If the quark mass is not zero, the chiral symmetry is not an exact symmetry but for a small quark mass the chiral symmetry is approximately realised.

To simplify, we consider the massless QCD which has the chiral symmetry $U(N_f)_L \times U(N_f)_R$. This symmetry group can also be written as

$$SU(N_f)_L \times SU(N_f)_R \times U(1)_B \times U(1)_A. \tag{2.10}$$

Note that this is the symmetry realised at the classical level. At the quantum level, the $U(1)_A$ subgroup is broken [76], which is called the $U(1)_A$ anomaly, so that the symmetry of the system is reduced to

$$SU(N_f)_L \times SU(N_f)_R \times U(1)_B. \tag{2.11}$$

It does not necessarily mean that the vacuum has this symmetry; there are in fact two possibilities. One is that the vacuum has the same symmetry as the action, which is called the Wigner mode. The other case is that the symmetry of the action is spontaneously broken in the vacuum, which is called the Nambu-Goldstone mode. Indeed the symmetry Eq.(2.11) is broken in the QCD vacuum to

$$SU(N_f)_V \times U(1)_B \tag{2.12}$$

and the broken $SU(N_f)$ generates $(N_f^2 - 1)$ Nambu-Goldstone bosons. In the two-flavour case, we therefore have three pions as NG bosons.

2.1.2 A simple example: Ginzburg-Landau model

The chiral phase transition is caused by the chiral symmetry breaking and its restoration. The massless QCD Lagrangian has the chiral symmetry, and the symmetry is spontaneously broken in the vacuum due to the strong interaction. It is thought to be restored as the temperature and/or the chemical potential increases. This transition is characterised by the chiral condensate $\langle \bar{q}q \rangle$ where $q(\bar{q})$ is a quark (anti-quark) field. Here we show how the chiral phase transition is caused by the change of the temperature

according to the change of $\langle \bar{q}q \rangle$ in the Ginzburg-Landau (GL) model [77,78]. The GL free energy is given as a function of the chiral condensate $\Phi^{ij} = \langle \bar{\psi}^i_R \psi^j_L \rangle$,

$$\Omega = \frac{a_0}{2}\mathrm{Tr}\Phi^\dagger\Phi + \frac{b_1}{4!}(\mathrm{Tr}\Phi^\dagger\Phi)^2 + \frac{b_2}{4!}\mathrm{Tr}(\Phi^\dagger\Phi)^2 - \frac{c_0}{2}(\det\Phi + \det\Phi^\dagger), \quad (2.13)$$

where the trace and the determinant are taken over the indices of flavour i, j. When $c_0 = 0$ in Eq.(2.13), this free energy has

$$SU_L(N_f) \times SU_R(N_f) \times U_B(1) \quad (2.14)$$

symmetry, while when $c_0 \neq 0$ it has a reduced symmetry

$$SU_L(N_f) \times SU_R(N_f), \quad (2.15)$$

because $U_B(1)$ is broken. Eq.(2.13) can be written in a much simpler form by assuming that Φ is a diagonal matrix whose diagonal elements are σ,

$$\Omega = \frac{a}{2}\sigma^2 - \frac{c}{3}\sigma^3 + \frac{b}{4}\sigma^4 - h\sigma. \quad (2.16)$$

When we consider the two-flavour case, c is equal to zero because a term which is proportional to σ^3 cannot appear since Φ is a 2×2 matrix in Eq.(2.13). On the other hand, the σ^3 term appears from the terms $\det\Phi$ and $\det\Phi^\dagger$ in Eq.(2.13) in the three-flavour case because Φ is a 3×3 matrix. First we consider the case that the coefficient c is equal to zero,

$$\Omega = \frac{a}{2}\sigma^2 + \frac{b}{4}\sigma^4 - h\sigma. \quad (2.17)$$

Assume that $b > 0$ and $h = 0$, and write the coefficient a as:

$$a = a' \frac{T - T_c}{T_c}. \quad (2.18)$$

In this case, the effective potential Eq.(2.17) shows a different behaviour as a function of σ, depending on whether the temperature T is smaller or larger than the critical temperature T_c, as shown in Fig.2.2.

Since the effective potential is an even function of σ, we concentrate on the region where $\sigma > 0$. At $T < T_c$, the minimum value of the potential is in the region where $\sigma > 0$, and as the temperature increases the σ which gives the minimum of the potential approaches zero, then it becomes zero as the temperature reaches the critical temperature T_c.

To see how the location of the minimum of the potential behaves as a function of temperature, we solve the following stationarity condition;

$$\frac{\partial\Omega}{\partial\sigma} = 0. \quad (2.19)$$

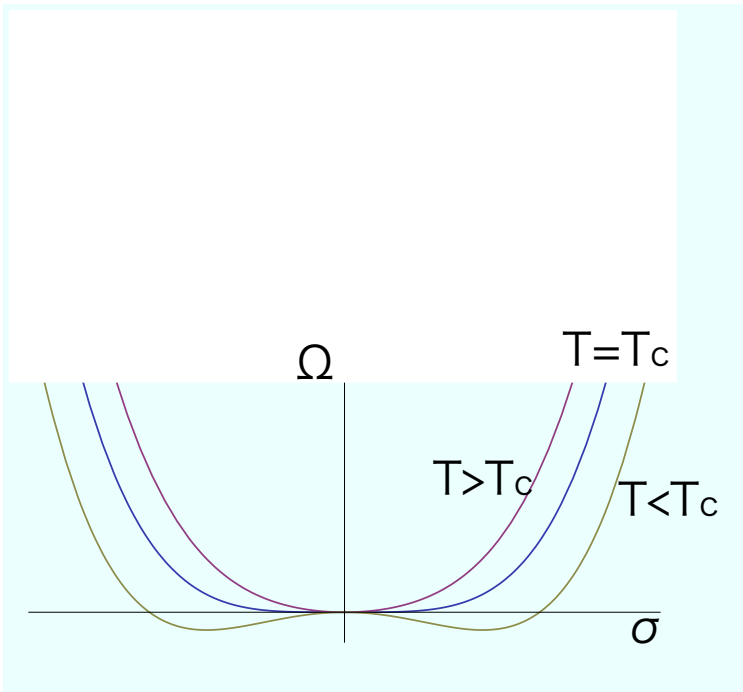

Figure 2.2: The Ginzburg-Landau potential as a function of σ for $T < T_c$, $T = T_c$ and $T > T_c$. In this calculation we set $c = 0$, $b > 0$, and $h = 0$.

From this condition, we get $\sigma = \pm(-a/b)^{1/2}$ at $T < T_c$ and $\sigma = 0$ at $T > T_c$, which is shown in Fig.2.3, so that we find that the phase transition in this case is second order.

Next, we assume that c is not equal to zero. In this case, the effective potential is given by

$$\Omega = \frac{a}{2}\sigma^2 - \frac{c}{3}\sigma^3 + \frac{b}{4}\sigma^4 - h\sigma. \tag{2.20}$$

To simplify we set $h = 0$, and show the behaviour of the effective potential Eq.(2.20) in Fig.2.4 as a function of σ ($b > 0$, $c > 0$). The value of σ for the minimum of the potential is located in the region where $\sigma > 0$ at $T > T_c$, then it discontinuously goes to zero when the temperature reaches the critical temperature. Again solving the stationarity condition

$$\frac{\partial \Omega}{\partial \sigma} = 0, \tag{2.21}$$

we get σ for the minimum of the potential as

$$\sigma = \frac{c \pm \sqrt{c^2 - 4ac}}{2b} \quad (T < T_c) \tag{2.22}$$

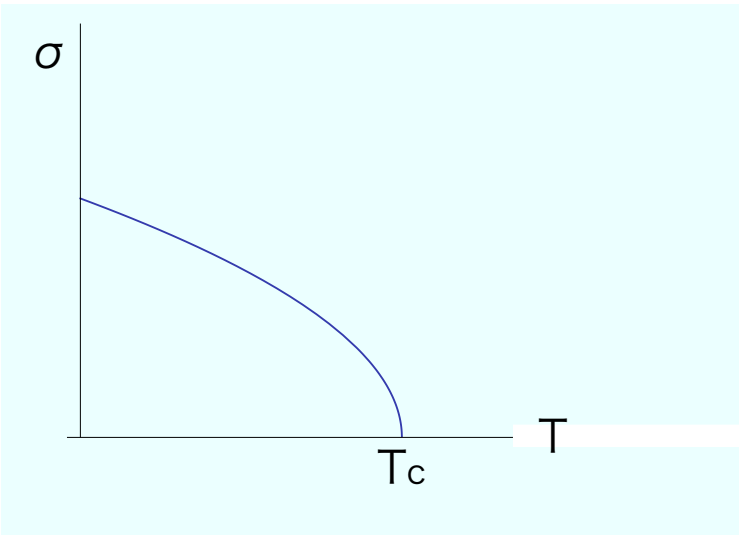

Figure 2.3: Value of σ at the minimum of the potential Eq.(2.17), as a function of temperature.

and

$$\sigma = 0 \quad (T > T_c) \tag{2.23}$$

which is shown in Fig.2.5 as a function of temperature. Clearly this is a first-order phase transition.

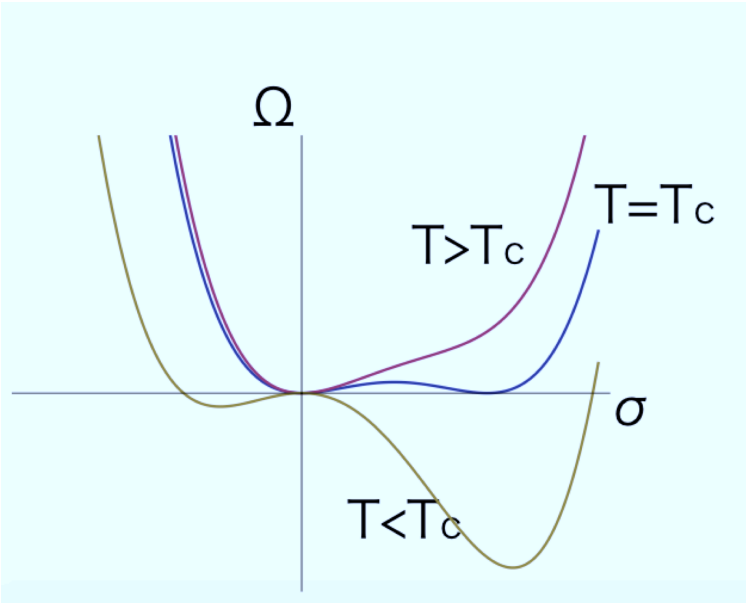

Figure 2.4: The Ginzburg-Landau potential as a function of σ for $T < T_c$, $T = T_c$ and $T > T_c$. In this calculation we set $c > 0$, $b > 0$, and $h = 0$.

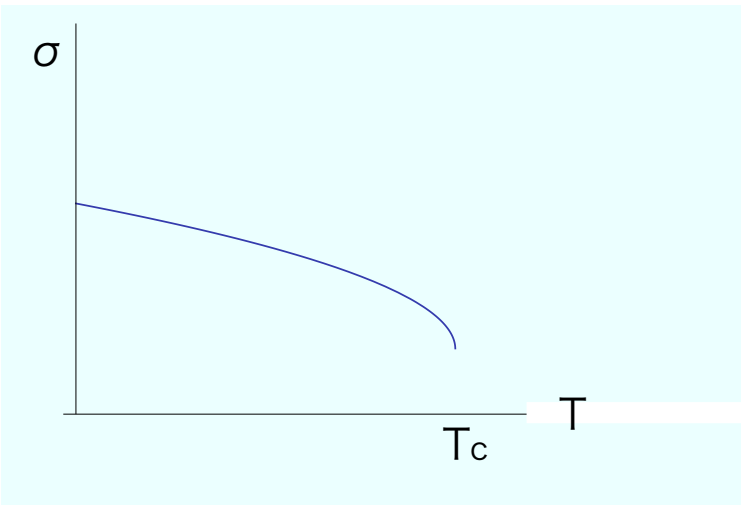

Figure 2.5: Value of σ at the minimum of the potential Eq.(2.20) as a function of temperature.

2.2 De-confinement phase transition

Another important phase transition is the de-confinement phase transition. At low temperatures, only hadrons which are colour singlet states are observed and quarks and gluons are confined in hadrons, so that this phase is called the confined phase or the hadronic phase. On the other hand, the colour confinement is supposed to be broken and a phase where the quarks and gluons degrees of freedom dominate appears at high temperatures. The transition between the confined phase and the de-confined phase is characterised by the expectation value of the Polyakov loop which is defined by

$$L(x) = \mathcal{P}\exp\left[-ig\int_0^\beta dx_4 A_4(\boldsymbol{x}, x_4)\right] \tag{2.24}$$

[55,56], where β is the inverse temperature $1/T$, $\mathcal{P}$ is the path ordering and x_4 is the Euclidean time. Its expectation value is written by

$$\Phi(\boldsymbol{x}) = \langle l(\boldsymbol{x})\rangle, \tag{2.25}$$

where

$$l = \frac{1}{N_c}\mathrm{tr}L. \tag{2.26}$$

To see that Φ characterises the de-confinement phase transition, it is helpful to consider the relation between the expectation value of the Polyakov loop and the quark free energy . This relation reads

$$\Phi = \langle l(\boldsymbol{x})\rangle = e^{-\beta f_q} \tag{2.27}$$

$$\bar{\Phi} = \langle l^\dagger(\boldsymbol{x})\rangle = e^{-\beta f_{\bar{q}}}. \tag{2.28}$$

Quarks which have colour are not allowed to exist in isolation in the confined phase, which implies that the free energy of a single quark is infinity. Then, Φ and $\bar{\Phi}$ become zero from Eqs. (2.27) and (2.28). On the other hand, the quark free energy can be finite in the de-confined phase since quark excitations are allowed, so that Φ and $\bar{\Phi}$ have a non-zero value.

As we see, the expectation value of the Polyakov loop has a relation to the free energy of a single quark, and its behaviour characterise the de-confinement phase transition. It seems that the expectation value of the Polyakov loop may be an order parameter of the phase transition. Indeed, it is an order parameter related to the centre symmetry breaking and its restoration.

The centre is a set of elements of a group G that commutes with all other elements of G. The group $SU(N_c)$ has the centre Z_{N_c} [79]. Assume

$U \in SU(N_c)$, $U = e^{i\theta \mathbf{1}}$ where $\mathbf{1}$ is the identity matrix $N_c \times N_c$. Because of $\det U = 1$,

$$\det U = e^{iN_c\theta} = e^{2\pi ik}, \tag{2.29}$$

where $\theta = 2\pi k/N_c$, so that the elements of Z_{N_c} can be written as $e^{2\pi ik/N_c}$ where $k = 0, \cdots, N_c - 1$. Considering the non-periodic gauge transformation,

$$V_k = (z_k \mathbf{1})^{x_4/\beta} \tag{2.30}$$

with

$$z_k = e^{2\pi ik/N_c}, \tag{2.31}$$

we find that the gauge action is invariant under this transformation. It means that the gauge action has the centre symmetry [80], not only the gauge symmetry. Next we check the transformation of the Polyakov loop. Since A_4 is transformed by

$$A_4 \to V_k[A_4 - (ig)^{-1}\partial_4]V_k^\dagger = A_4 - \frac{2\pi k}{gN_c\beta}, \tag{2.32}$$

the traced Polyakov loop l is transformed by

$$l \to z_k l, \tag{2.33}$$

which is invariant only the case $l = 0$. Therefore the centre symmetry is broken except when $\Phi = 0$.

2.3 Behaviour of the order parameters

We summarise the behaviour of the order parameters for the chiral and the de-confinement phase transitions in Fig.2.6. Note that Fig.2.6 is the case of massless quarks for the chiral condensate, and of a infinite quark mass for the expectation value of the Polyakov loop.

The chiral condensate $\langle \bar{q}q \rangle$ which is an order parameter of the chiral phase transition has non-zero value at $T < T_c$ and becomes zero above T_c. On the other hand, the expectation value of the Polyakov loop which is an order parameter of the de-confinement phase transition becomes zero below T_c and has non-zero value above T_c. As we have seen, these two order parameters show an opposite behaviour with respect to the temperature. Note that when the quarks have a finite mass, both the chiral condensate and the expectation value of the Polyakov loop do not become exactly zero at high and low temperatures respectively.

Usually "order parameters" are zero in a disordered phase and non-zero in an ordered phase. In this sense, the behaviour of the expectation value

	chiral condensate	Expectation value of Polyakov loop
low temperature	$\langle \bar{q}q \rangle \neq 0$	$\Phi = 0$
high temperature	$\langle \bar{q}q \rangle = 0$	$\Phi \neq 0$

Figure 2.6: order parameters.

of the Polyakov loop is not exactly that of an "order parameter". However, based on the relation to the centre symmetry breaking and its restoration, it can be viewed as an order parameter. Therefore, we use the term "order parameter" for both the chiral condensate and the expectation value of the Polyakov loop to avoid confusion.

2.4 Choice of the model

We need to select an effective model which can describe both the chiral and the de-confinement phase transitions in order to study the quark-hadron transition. The Lagrangian of the model should be written in terms of quarks because our purpose is to see how hadrons as collective modes of quarks melt into quarks in the transition region. Unlike the NJL type models, the PNJL model has an order parameter for the de-confinement phase transition. Therefore, by using the PNJL model, we could remove the unphysical quark excitations at low temperatures.

Since we use the PNJL model as an effective model of QCD, it is useful to explain the relation between this model and QCD. First, the PNJL model (the NJL model also) is adjusted to QCD in the vacuum, namely the model parameters are tuned to reproduce the experimental data on meson properties in the vacuum. Table 2.1 shows the meson properties calculated in the NJL model [38], compared to the experimental data [81]. Since the Polyakov loop does not play any role in the PNJL model in the vacuum, the PNJL model is equivalent to the NJL model at zero temperature. Therefore, the parameters in the quark sector of the PNJL model can be chosen as in the NJL model. The model contains 5 parameters, the bare mass of u-quark m_u, the bare mass of s-quark m_s, the coupling constant of the four point interaction G, the coupling constant of the six point interaction K and the cutoff

Λ. The value of m_u is chosen by hand [38]. The remaining 4 parameters are tuned in order to reproduce the masses m_π, m_K and $m_{\eta'}$ and the pion decay constant f_π. Then, when we calculate physical quantities at finite temper-

Table 2.1: Meson properties calculated in the NJL model [38] and the experimental data [81]. The model parameters are chosen as follows: $m_u = 5.5$ MeV, $m_s = 140.7$ MeV, $G\Lambda^2 = 1.835$, $K\Lambda^5 = 12.36$ and $\Lambda = 602.3$ MeV [38]. These parameters are adjusted to reproduce the experimental values of the pion mass $m_\pi = 135.0$ MeV, the kaon mass $m_K = 497.7$MeV, the η' meson mass $m_{\eta'} = 957.8$ MeV and the pion decay constant $f_\pi = 92.4$ MeV. The value of u-quark mass is fixed at $m_u = 5.5$ MeV [38]. The input values are indicated by *.

	NJL model	Experiment
f_π [MeV]	92.4	92.4* [82]
m_π [MeV]	135.0	135.0*
m_K [MeV]	497.7	497.6*
m_η [MeV]	514.8	547.8
$m_{\eta'}$ [MeV]	957.8	957.8*
m_{a_0} [MeV]	880.2	980 $\pm$ 20
m_κ [MeV]	1050.5	1425 $\pm$ 50
m_σ [MeV]	728.9	400 - 550
m_{f_0} [MeV]	1198.3	990 $\pm$ 20

atures, we keep the parameters obtained in the vacuum. Even though the model with this set of parameters can reproduce the experimental values of the meson masses in the vacuum, it is non-trivial that the model still agrees with QCD at finite temperatures. In order to check this, we show in Fig. 2.7 the behaviour of the order parameters as a function of the temperature calculated in the PNJL model (upper panel) and in lattice QCD [83] (lower panels) at zero chemical potential. In the upper panel, the red line is the chiral condensate and the blue line is the expectation value of the Polyakov loop. The left lower panel shows the expectation value of the Polyakov loop and the right one shows the chiral condensate. From Fig. 2.7, one sees that the behaviour of both the chiral condensate and the expectation value of the Polyakov loop in the PNJL model qualitatively agree with those of the lattice QCD simulation.

From the comparison of the PNJL model with the experimental data and the lattice QCD calculation, the use of the PNJL model as an effective model of QCD appears to be reasonable. On the other hand, there are still deficiencies in this model, especially in the treatment of the colour confinement. Although the PNJL model describes a picture in which the quark excitations are suppressed in the confined phase, the mechanism for

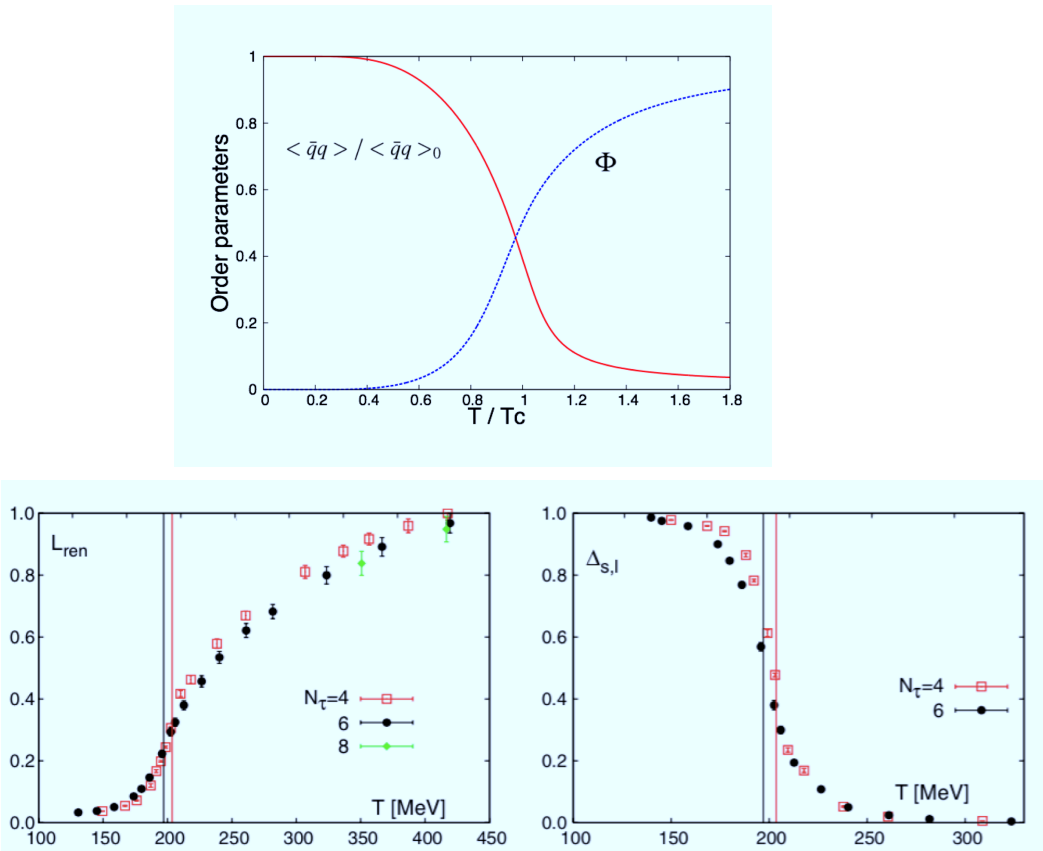

Figure 2.7: Temperature dependence of the the chiral condensate and the expectation value of the Polyakov loop: the top panel is calculated in the PNJL model and the bottom panels show the results of the lattice simulations [83].

the quark suppression in the confined phase is different from QCD. In the PNJL model, the quark distribution function, that depends on the Polyakov loop, controls the thermal excitations of quarks. In the confined phase, the Polyakov loop strongly suppresses the quark excitations, while in the de-confined phase, the effect of the Polyakov loop becomes weak so that the quarks can be easily excited. The Polyakov loop encapsulates in an effective way the effect of gluons, whose exchanges control the strength of the force between quarks and anti-quarks in QCD. In a sense, the PNJL model could be viewed as the effective theory one would obtain by integrating out the gluons. However, it is not exactly equivalent to QCD since it makes some drastic simplifications in doing so, and it is therefore not surprising to observe some differences between the predictions of the PNJL model and the results of lattice QCD computations.

Although the PNJL model does not describe the colour confinement in exactly the same way as QCD, it effectively works to suppress the coloured states in the confined phase and to release these states in the de-confined phase. In the sense of the suppression of coloured states, the confinement is phenomenologically included. Therefore, we use this model in order to describe the quark-hadron phase transition as an effective model.

When one calculates physical quantities within the PNJL model, the mean-field approximation has often been used. In the PNJL model (the NJL model also), meson fields are introduced as auxiliary fields and they are frozen by neglecting their fluctuations in the mean-field approximation. However, this is not enough to describe a physical hadronic phase. Although the quarks are suppressed by the Polyakov loop at low temperatures, it just means that the pressure in the hadronic phase becomes zero or very small and there are still no hadronic excitations. Since hadronic excitations dominate the system in the hadronic phase, we should take them into account when we describe the hadronic phase. This is possible if we go beyond the mean-field approximation.

In the (P)NJL model, the coupling between quarks and antiquarks is controlled by a parameter, that we determine in the vacuum. Once this parameter is fixed, we do not change it at non-zero temperature and chemical potential. However, this coupling could depend on the temperature and/or the chemical potential. Indeed, there are some models considering the temperature dependence of the coupling, for instance [84] by Bernard, Meissner and Zahed. In [84], they assume a certain form of the temperature dependence of the coupling of the original NJL model based on a discussion of the string tension between a quark and an antiquark [85]. It corresponds to taking the effect of the confinement partially into account.

For this coupling, other treatments have been used. In the non-local (P)NJL model [86–88], a running coupling is used. Since the running coupling suppresses the quark excitations at high momentum scale, the cutoff parameter which is necessary in the standard (P)NJL model is not necessary

anymore. In the entanglement PNJL (EPNJL) model which was proposed by Sakai, Sasaki, Kouno and Yahiro [89–91], the coupling is a function of the expectation value of the Polyakov loop Φ, so that it indirectly depends on the temperature through the Polyakov loop. This coupling corresponds to the entanglement vertex between the chiral condensate and the Polyakov loop. They have shown that the pseudo critical temperature calculated in the EPNJL model becomes smaller than that in the original PNJL model, and that the critical temperature of the chiral transition can take the same value as that of the de-confinement transition by tuning the parameters of the model. The (P)NJL model with multi-quark interactions [92, 93] proposed first by Osipov, Hiller and da Providencia is also a variation of the (P)NJL model. Since they consider the three-flavour case, the Lagrangian has a four-point interaction and a six point interaction which breaks the axial $U(1)$ symmetry. In addition, they have introduced an eight point interaction between quarks and antiquarks in the Lagrangian in order to make the potential stable.

In this work, we simply neglect both the temperature dependence and the chemical potential dependence of the coupling. We fix the coupling at the same time as all other parameters in the vacuum.

Chapter 3

Useful techniques in field theory at finite temperature

In this chapter, some useful techniques for studying many body systems at finite temperature are summarised. The canonical operator method [94, 95], the functional integral formalism [96] and the stochastic formalism [97] may be used for the second quantisation of a many body system. Here we will present only the functional integral method since this will be used later in the calculations performed in Chapters 4 to 7.

3.1 The path integral method

The path integral method is one of the formulations of quantum mechanics. The transition amplitude in the path integral method is obtained by adding all the virtual paths of the transitions from $t = t_i$ to $t = t_f$. We will show in this section how to express the transition amplitude in the path integral by using a boson field ϕ as an example.

For an arbitrary Hamiltonian H given as,

$$H = \int d^3x \; \mathcal{H}(\hat{\pi}, \hat{\phi}), \tag{3.1}$$

where $\hat{\phi}$ is a field operator and $\hat{\pi}$ is the conjugate operator of $\hat{\phi}$, the transition amplitude from a state $|\phi_a\rangle$ to another state $|\phi_b\rangle$ is written by

$$\langle \phi_b | e^{-iHt} | \phi_a \rangle. \tag{3.2}$$

Let us consider more specifically the case where the system goes back to the original state after a time t, so that the transition amplitude reads,

$$\langle \phi_a | e^{-iHt} | \phi_a \rangle. \tag{3.3}$$

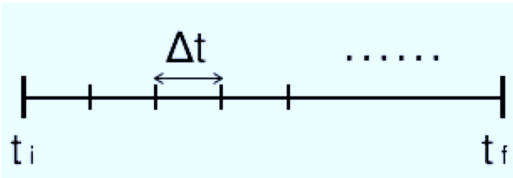

Figure 3.1: Elementary time interval

In order to define the path integral, we discretise the time interval (t_i, t_f) into N slices, as shown in Fig3.1, namely

$$\Delta t = \frac{t_f - t_i}{N}. \tag{3.4}$$

The transition amplitude can be rewritten in terms of N and Δt as

$$\begin{aligned}\langle\phi_a|e^{-iH(t_f-t_i)}|\phi_a\rangle &= \lim_{N\to\infty}\int(\prod_{i=1}^{N}\frac{d\pi_i d\phi_i}{2\pi})\langle\phi_a|\pi_N\rangle\langle\pi_N|e^{-iH\Delta t}|\phi_N\rangle\langle\phi_N|\pi_{N-1}\rangle \\ &\times \langle\pi_{N-1}|e^{-iH\Delta t}|\phi_{N-1}\rangle\cdots\langle\phi_2|\pi_1\rangle\langle\pi_1|e^{-iH\Delta t}|\phi_1\rangle\langle\phi_1|\phi_a\rangle.\end{aligned} \tag{3.5}$$

In this formula, we have introduced the identity operator at the intermediate times, written as a sum over a complete set of states $|\phi\rangle$ and $|\pi\rangle$:

$$\int d\phi(x)\ |\phi\rangle\langle\phi| = 1 \tag{3.6}$$

$$\int \frac{d\pi(x)}{2\pi}\ |\pi\rangle\langle\pi| = 1. \tag{3.7}$$

Note that these states satisfy the following orthogonality relations:

$$\langle\phi_a|\phi_b\rangle = \prod_x \delta\big(\phi_a(x) - \phi_b(x)\big) \tag{3.8}$$

$$\langle\pi_a|\pi_b\rangle = \prod_x \delta\big(\pi_a(x) - \pi_b(x)\big). \tag{3.9}$$

Eq.(3.5) corresponds to approximating the path by a polygonal line with ϕ_i at each intermediate time t_i. Using the relations

$$\langle\phi_1|\phi_a\rangle = \delta(\phi_1 - \phi_a) \tag{3.10}$$

and

$$\langle\phi_{i+1}|\pi_i\rangle = \exp\Big(i\int d^3x\ \pi_i(\boldsymbol{x})\phi_{i+1}(\boldsymbol{x})\Big), \tag{3.11}$$

and taking the limit $\Delta t \to 0$, we obtain

$$\begin{aligned}\langle\phi_a|e^{-iH(t_f-t_i)}|\phi_a\rangle &= \lim_{N\to\infty}\int(\prod_{i=1}^{N}\frac{d\pi_i d\phi_i}{2\pi})\delta(\phi_1-\phi_a)\\ &\times \exp\Big(-i\Delta t\sum_{j=1}^{N}\int d^3x\big[\,\mathcal{H}(\pi_j,\phi_j)-\frac{\pi_j(\phi_{j+1}-\phi_j)}{\Delta t}\big]\Big).\end{aligned} \tag{3.12}$$

Note that when $\Delta t \to 0$,

$$\langle\pi_i|e^{-iH_i\Delta t}|\phi_i\rangle \approx (1-iH_i\Delta t)\exp\big(-i\int d^3x\pi_i(x)\phi_i(x)\big). \tag{3.13}$$

After taking the continuum limit $N \to \infty$, we obtain the transition amplitude in path integral form

$$\begin{aligned}&\langle\phi_a|e^{-iHt}|\phi_a\rangle\\ &=\int[d\pi]\int[d\phi]\,\exp\Big[i\int_{t_i}^{t_f}dt\int d^3x\,\big(\pi(\boldsymbol{x},t)\frac{\partial\phi(\boldsymbol{x},t)}{\partial t}-\mathcal{H}(\pi,\phi)\big)\Big].\end{aligned} \tag{3.14}$$

3.2 Imaginary time formalism

In this section, we write the partition function in terms of a transition amplitude which has been obtained in the previous section. The partition function is introduced as,

$$Z = \mathrm{Tr}\ e^{-\beta H} = \int d\phi_a\langle\phi_a|e^{-\beta H}|\phi_a\rangle, \tag{3.15}$$

where β is the inverse temperature $1/T$. As we have seen in the previous section, the transition amplitude from an initial state $|\phi\rangle$ at $t = t_i$ to a final state which is the same state as the initial state at $t = t_f$ is

$$\langle\phi_i|e^{-iH(t_f-t_i)}|\phi_i\rangle. \tag{3.16}$$

In order to simplify the notations, we set $t_i = 0$ and $t_f = t$, and we consider the amplitude,

$$\langle\phi_i|e^{-iHt}|\phi_i\rangle. \tag{3.17}$$

Compared to Eqs.(3.15) and (3.17), the partition function corresponds to the transition amplitude provided that $\beta = it$. From the evolution operator $\exp(-iH(-i\beta))$, a periodic boundary condition appears for ϕ as

$$\phi(-i\beta) = \phi(0). \tag{3.18}$$

Therefore, the partition function can be expressed in terms of an imaginary time $\tau = it$,

$$Z = \int [d\pi] \int [d\phi] \exp\Big[\int_0^\beta d\tau \int d^3x \big(i\pi \frac{\partial \phi}{\partial \tau} - \mathcal{H}(\pi, \phi)\big)\Big]. \tag{3.19}$$

Note that the integral over ϕ must obey the periodic boundary condition Eq.(3.18). This replacement from a real time t to an imaginary time τ is illustrated in Fig.3.2.

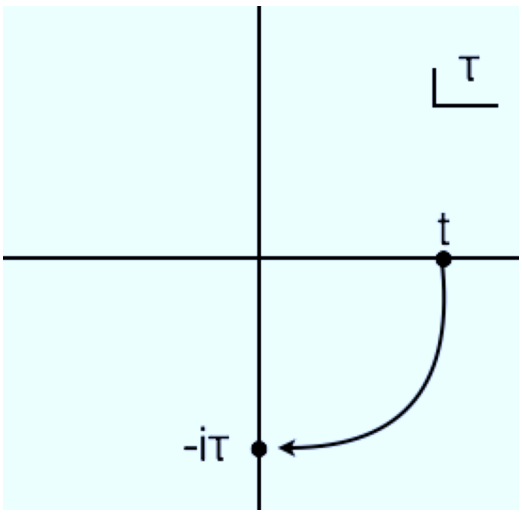

Figure 3.2: A real time is replaced by an imaginary time.

In the case where there is a finite chemical potential, the Hamiltonian density $\mathcal{H}(\hat{\pi}, \hat{\phi})$ is modified to $\mathcal{H}(\hat{\pi}, \hat{\phi}) - \mu\mathcal{N}(\hat{\pi}, \hat{\phi})$, and the partition function is given as,

$$Z = \int [d\pi] \int [d\phi] \exp\Big[\int_0^\beta d\tau \int d^3x \big(i\pi \frac{\partial \phi}{\partial \tau} - \mathcal{H}(\pi, \phi) + \mu\mathcal{N}(\pi, \phi)\big)\Big]. \tag{3.20}$$

3.3 Sum over the Matsubara frequencies

When we calculate the partition function which has been introduced in the previous section, it is convenient to represent the path integral in momentum space. From a Fourier transformation of the field $\phi(\boldsymbol{x}, \tau)$,

$$\phi(\boldsymbol{x}, \tau) = \sqrt{\frac{\beta}{V}} \sum_{n=-\infty}^{+\infty} \sum_{\boldsymbol{p}} e^{i(\boldsymbol{p}\cdot\boldsymbol{x} + \omega_n \tau)} \phi_n(\boldsymbol{p}), \tag{3.21}$$

the discrete Matsubara frequencies ω_n appear. For bosons, $\omega_n = 2n\pi T$ because of the periodic boundary condition $\phi(\boldsymbol{x}, 0) = \phi(\boldsymbol{x}, \beta)$, while for fermions $\psi(\boldsymbol{x}, \tau)$, $\omega_n = (2n+1)\pi T$ because their boundary condition are anti periodic: $\psi(\boldsymbol{x}, 0) = -\psi(\boldsymbol{x}, \beta)$.

Considering a sum over the index n for a arbitrary function $f(\omega_n)$,

$$T \sum_{n=-\infty}^{+\infty} f(\omega_n), \tag{3.22}$$

where $i\omega_n = 2\pi n T i$ for bosons, and $i\omega_n = (2n+1)\pi T i$ for fermions. We can rewrite this discrete sum as an integral by introducing another function $F(p_0)$ which has poles on the imaginary axis precisely at the location of the Matsubara frequencies, and which has a residue T at these poles. To achieve this, we can choose $F(p_0)$ as

$$F(p_0) = \frac{1}{e^{\beta p_0} + 1} \tag{3.23}$$

for fermions, and

$$F(p_0) = \frac{1}{e^{\beta p_0} - 1} \tag{3.24}$$

for bosons. This difference between the $F(p_0)$ for fermions and for bosons comes from the difference of their Matsubara frequencies. Thanks to this function $F(p_0)$ the sum over the Matsubara frequencies can be replaced by

$$T \sum_n f(\omega_n) = \frac{1}{2\pi i} \int_C dp_0 \; f(p_0) \; \frac{1}{e^{\beta p_0} \pm 1}, \tag{3.25}$$

where the integration path C is shown in (a) of Fig.3.3. Only when the integrand has no other singularities on the vicinity of the imaginary axis, except the poles at $p_0 = i\omega_n$, the integration path can be changed to (b) in Fig.3.3. In this case, the poles of $f(p_0)$ may appear in the region where $\mathrm{Re}(p_0) < -\epsilon$ or $\mathrm{Re}(p_0) > \epsilon$, so that the integration can be performed by the residue theorem provided that it is possible to add a semicircle at infinity to the path.

We present two examples in order to show how to calculate the sum over the Matsubara frequencies of bosons and fermions. Firstly, we consider a function written in terms of the bosonic Matsubara frequencies,

$$f(\omega_n) = \frac{1}{\omega_n^2 + \omega^2}, \tag{3.26}$$

where $\omega_n = 2n\pi T$, and ω is real. From Eq.(3.25), the sum over the bosonic Matsubara frequencies can be replaced by the integration

$$T \sum_n f(\omega_n) = -\frac{1}{2\pi i} \int_C dp_0 \; \frac{1}{p_0^2 - \omega^2} \; \frac{1}{e^{\beta p_0} - 1}. \tag{3.27}$$

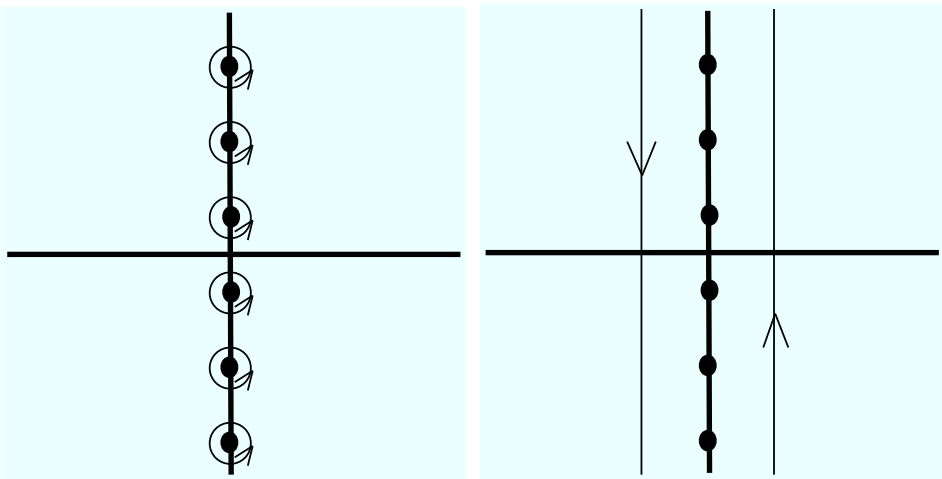

(a) (b)

Figure 3.3: The integration paths in Eq.(3.25).

The negative sign in the left-hand side comes from the replacement of $\omega_n = -ip_0$. Since $f(p_0)$ has two poles, $p_0 = \pm\omega$, on the real p_0 axis, the integration in Eq.(3.27) can be performed by picking these poles based on the residue theorem. Then, we obtain

$$T\sum_n f(\omega_n) = \frac{1}{\omega}\Big(\frac{1}{2} + \frac{1}{e^{\beta\omega}-1}\Big). \tag{3.28}$$

Note that in this expression, the temperature-dependent term and the temperature-independent term are completely separated.

Next, we consider a function written in terms of the fermionic Matsubara frequencies,

$$f(\omega_n) = \frac{1}{(\omega_n + i\mu)^2 + \omega^2}, \tag{3.29}$$

where $\omega_n = (2n+1)\pi T$ and μ is the chemical potential. From Eq.(3.25), we can write the sum over the fermionic Matsubara frequencies as the integration

$$T\sum_n f(\omega_n) = -\frac{1}{2\pi i}\int_C dp_0\ \frac{1}{(p_0-\mu)^2-\omega^2}\ \frac{1}{e^{\beta p_0}+1}. \tag{3.30}$$

In this case, $f(p_0)$ has two poles also, $\pm\omega + \mu$, on the real p_0 axis. By using the same method as the first example, we obtain

$$T\sum_n f(\omega_n) = \frac{1}{2\omega}\Big(1 - \frac{1}{e^{\beta(\omega-\mu)}+1} - \frac{1}{e^{\beta(\omega+\mu)}+1}\Big). \tag{3.31}$$

Note that the first term does not depend on both the temperature and the chemical potential, while the second and the third terms depend on them. The relative sign of the chemical potential with respect to ω corresponds to particles and antiparticles.

Chapter 4

Review of the Nambu-Jona-Lasinio model

In this chapter, we give a brief review of the Nambu-Jona-Lasinio (NJL) model which has been the basis of the PNJL model. The NJL model was originally designed by Nambu and Jona-Lasinio to describe profound consequences of the presumed underlying chiral symmetry in hadron dynamics, based on an analogy with the BCS theory of superconductivity [40, 41]. It has later been transcribed in order to describe the effect of chiral symmetry in an effective theory of the dynamics of quarks [28, 29]. Although there is no mechanism of the colour confinement since this model was not originally made for QCD, it has achieved some successes in predicting hadron masses in the vacuum that agree with experiments, and also the chiral crossover at finite temperatures and zero chemical potential that agrees with lattice QCD simulations. In addition, this model has predicted a phase transition at finite chemical potential, and the existence of a critical point as a merging point of the crossover line and the first order transition line was indicated by Asakawa and Yazaki [33], but it has not been established in experiments yet. Regarding this critical point, some works have considered the possibility of "inhomogenous chiral condensates" [98–103]. They assume that the chiral condensate can depend on space-time, and that this dependence is periodic. In this method, the critical point does not appear on the phase diagram. Thus the theoretical discussion for the critical point has not been settled yet.

The colour superconductor (CSC) phase has also been discussed in the NJL model [20, 22, 46, 48, 50, 104–106]. To make a diquark condensate, a quark-quark four-point interaction is introduced in the NJL Lagrangian in adding to the quark-antiquark four-point interaction. The two condensates, the chiral and the diquark condensates, are determined by solving self consistent equations called gap equations. If the gap equations have several solutions, the one that makes the thermodynamic potential minimal is the

true solution. Based on this, a phase where the chiral condensate is finite but the diquark condensate is zero appears in the region of low temperature and low density. On the other hand, a phase where the chiral condensate is zero and the diquark condensate has a finite value appears in the region of low temperature and high density. However, this discussion breaks down when the chemical potential becomes comparable or larger than the cutoff scale which is required for regularising the divergence of quark-momentum integrations, as a consequence of a non-renormalisabielity of the NJL model. One of the good examples to see this limit of applicability at large chemical potential is the phase diagram shown by Vanderheyden and Jackson [107]. Their result tells that the CSC phase disappear in favour of the normal phase at large chemical potential. Especially focusing on $T = 0$, the CSC phase disappears when the chemical potential becomes 1.75 times the cutoff. This is clearly in contradiction with the prediction of perturbative QCD; the CSC phase is predicted by QCD at arbitrarily large chemical potential, while the NJL model calculation shows that the CSC phase disappears at large chemical potential. This means that the model is not reliable in this region.

Thus, effective theories with a cutoff demand attention in its applications. The value of the cutoff parameter in the NJL model is usually 600 MeV to 900 MeV, although it depends on the values of the other parameters. Since the chiral transition temperature at zero chemical potential is around 200MeV which is smaller enough compared to the cutoff scale, it should be fine to apply this model to the chiral phase transition.

The rest of this chapter is organised as follows. In Section 4.1, we introduce a basic two-flavour NJL model and explain how to calculate physical quantities with the path integral method. This will be useful when we extend this model to the PNJL model in Chapter 5 to Chapter 7, since we can use the same method for the PNJL model. In Section 4.2, the mean-field approximation is applied to obtain the equation of state and the gap equation. In this approximation, we show a behaviour of the chiral condensate which is an order parameter of the chiral transition. When the bare quark mass is zero, the chiral transition is a second order transition at zero chemical potential. On the other hand, it becomes a crossover with a finite bare quark mass. We also show the phase diagram with zero and non-zero bare quark mass. In Section 4.3, we briefly describe how the mesonic excitations can be taken into account. In Section 4.4, we summarise the two-flavour NJL model with diquark interaction. For this diquark interaction, we only introduce a scalar diquark which has colour anti-triplet and flavour singlet states. Then we obtain the thermodynamic potential in the mean-field approximation.

4.1 The two-flavour NJL model

4.1.1 Chiral symmetry of the NJL Lagrangian

The Lagrangian of the two-flavour NJL model is given by

$$\mathcal{L} = \bar{q}(i\gamma^\mu\partial_\mu - m_0)q + G\big[(\bar{q}q)^2 + (\bar{q}i\gamma_5\boldsymbol{\tau}q)^2\big], \tag{4.1}$$

where q and $\bar{q}$ are quark and antiquark fields, m_0 is a bare quark mass and G is a coupling constant. The second term represents the quark-antiquark four-point interaction shown in Fig.4.1. We first check that this Lagrangian

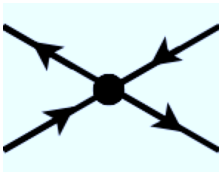

Figure 4.1: The four-point interaction of the NJL model.

has the chiral symmetry when the bare quark mass is equal to zero. As we have seen in Chapter 2, the kinetic term in Eq.(4.1) has the chiral symmetry, while the mass term does not. For the interaction term, let us consider an axial transformation,

$$q \to \exp(i\frac{\gamma_5\tau^i\theta^i}{2})q, \tag{4.2}$$

where τ^i is the Pauli matrix and i runs 1 to 3. Under this transformation, $\bar{q}q$ and $\bar{q}i\gamma_5\tau^i q$ are transformed as follows (for θ^i infinitesimal)

$$\begin{aligned} \bar{q}q &\to \big(q^\dagger e^{-i\frac{\gamma_5\tau^i\theta^i}{2}}\gamma_0 e^{i\frac{\gamma_5\tau^i\theta^i}{2}}q\big) \\ &\approx \Big(q^\dagger\big(1-\frac{i\tau^i\theta^i}{2}\gamma_5\big)\gamma_0\big(1+\frac{i\tau^i\theta^i}{2}\gamma_5\big)q\Big) \\ &= \bar{q}q + \bar{q}(i\tau^i\theta^i\gamma_5)q + \mathcal{O}(\theta^2) \end{aligned} \tag{4.3}$$

and

$$\begin{aligned} \bar{q}i\gamma_5\tau^i q &\to q^\dagger e^{-i\frac{\gamma_5\tau^i\theta^i}{2}}\gamma_0 i\gamma_5\tau^i e^{i\frac{\gamma_5\tau^i\theta^i}{2}}q \\ &\approx q^\dagger\big(1-\frac{i\tau^i\theta^i}{2}\gamma_5\big)\gamma_0 i\tau^i\gamma_5\big(1+\frac{i\tau^i\theta^i}{2}\gamma_5\big)q \\ &= \bar{q}i\tau^i\gamma_5 q - \theta^i\bar{q}q + \mathcal{O}(\theta^2). \end{aligned} \tag{4.4}$$

Therefore, $(\bar{q}q)^2 + (\bar{q}i\gamma_5\tau^i q)^2$ is invariant under the axial transformation. Similarly, the invariance under a vector transformation,

$$q \to \exp(i\frac{\tau^i\theta^i}{2})q, \tag{4.5}$$

can also be checked, so that the Lagrangian Eq.(4.1) has the chiral symmetry when $m = 0$.

4.1.2 Method of auxiliary fields

The partition function is given by

$$Z = \int [d\bar{q}][dq] \exp \int_0^\beta d\tau \int d^3x \mathcal{L} \tag{4.6}$$

with the NJL Lagrangian Eq.(4.1). The four-point interaction term in this Lagrangian prevents us from performing the integration on the fermion fields because the only Grasmann integrals that can be performed analytically are those with a Lagrangian which is quadratic in the fermion fields. We can rewrite the interaction term by the Hubbard-Stratonovich transformation [108, 109], which gives a Yukawa interaction . For this, we insert a dummy integral over an auxiliary boson fields $\phi_i = (\sigma, \boldsymbol{\pi})$, as a constant Gaussian integral multiplying the partition function,

$$\int [d\phi] \exp\left[-\frac{1}{4G} \int_0^\beta d\tau \int d^3x \left((\sigma + 2G\bar{q}q - m_0)^2 + (\boldsymbol{\pi} + 2Gi\bar{q}\gamma_5 \boldsymbol{\tau} q)^2 \right) \right]. \tag{4.7}$$

Then, the partition function is rewritten in terms of the integrations over the quark, antiquark and boson fields with an effective Lagrangian.

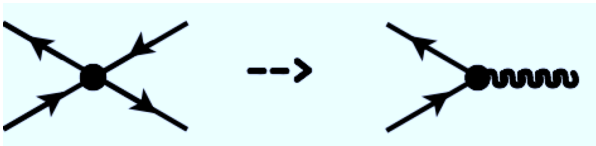

Figure 4.2: The original four-point interaction between quarks and antiquarks is replaced by a Yukawa interaction by the Hubbard-Stratonovich transformation.

$$Z = \int [d\bar{q}][dq][d\phi] \exp\Big[\int_0^\beta d\tau \int d^3x \mathcal{L}_{\text{eff}} \Big], \tag{4.8}$$

where

$$\mathcal{L}_{\text{eff}}(q, \bar{q}, \phi) = \bar{q} \left[i\gamma^\mu \partial_\mu - \sigma - i\gamma_5 \boldsymbol{\tau} \cdot \boldsymbol{\pi} \right] q - \frac{1}{4G} ((\sigma - m_0)^2 + \pi_i^2). \tag{4.9}$$

This replacement is illustrated in Fig.4.2.

Now we can perform the fermion integration since the Lagrangian in Eq.(4.9) is quadratic in the quark fields after this procedure. Based on the Grasmann integral,

$$\int d\eta_1^\dagger d\eta_1 \cdots d\eta_N^\dagger d\eta_N \; e^{\eta^\dagger D \eta} = \det D, \tag{4.10}$$

where D is $N \times N$ matrix, the quark integration in Eq.(4.8) leads to

$$\begin{aligned} &\int [d\bar{q}][dq] \exp\Big[\int_0^\beta d\tau \int d^3x \{q^\dagger (i\gamma^0\gamma^\mu\partial_\mu - \gamma^0\sigma - i\gamma^0\gamma_5 \boldsymbol{\tau}\cdot\boldsymbol{\pi})q\Big] \\ &= \mathrm{Det}[i\gamma^0\gamma^\mu\partial_\mu - \gamma^0\sigma - i\gamma^0\gamma_5\boldsymbol{\tau}\cdot\boldsymbol{\pi}] \end{aligned} \tag{4.11}$$

then we get the partition function as a function of the auxiliary boson fields

$$\begin{aligned} Z = &\int [d\phi] \mathrm{Det}[i\gamma^0\partial\!\!\!/ - \gamma^0(\sigma + i\gamma_5\gamma_5\boldsymbol{\tau}\cdot\boldsymbol{\pi})] \\ &\times \exp\Big[-\int_0^\beta d\tau \int d^3x \; \frac{1}{4G}((\sigma - m_0)^2 + \pi_i^2) \qquad (4.12) \\ = &\int [d\phi] \exp\Big[\mathrm{Tr}\ \ln[i\gamma^0\partial\!\!\!/ - \gamma^0(\sigma + i\gamma_5\gamma_5\boldsymbol{\tau}\cdot\boldsymbol{\pi})] \\ &- \int_0^\beta d\tau \int d^3x \; \frac{1}{4G}((\sigma - m_0)^2 + \pi_i^2)\Big], \qquad (4.13) \end{aligned}$$

where the trace is taken over the space-time coordinates with anti-periodic boundary condition in the imaginary time axis, Dirac gamma matrices, the colour indices and flavour indices. Therefore, the partition function can be obtained from an effective action that depends only on the auxiliary boson fields,

$$Z = \int [d\phi] e^{-I[\phi]}, \tag{4.14}$$

where

$$I[\phi] = -\mathrm{Tr}\ \ln\ D + \int_0^\beta d\tau \int d^3x \; \frac{1}{4G}((\sigma - m_0)^2 + \pi_i^2) \tag{4.15}$$

with

$$D = i\gamma^0\partial\!\!\!/ - \gamma^0(\sigma + i\gamma_5\boldsymbol{\tau}\cdot\boldsymbol{\pi}). \tag{4.16}$$

4.2 Mean field approximation

In this section, we derive an approximate effective action using the mean-field approximation. The meson fields which have been introduced as auxiliary fields do not have any fluctuations in this approximation. In other

words, the mean-field approximation is a classical approximation for the meson fields. This would be clear if we reintroduced the Planck constant $\hbar$ that was set to 1 so far. From the dimensional analysis, $\hbar$ would enter in the partition function as follows

$$Z = \int [d\phi] \exp\Big[\mathrm{Tr}\ \ln(-i\gamma^0\partial\!\!\!/ + \gamma^0(\sigma + i\gamma_5\gamma_5\boldsymbol{\tau}\cdot\boldsymbol{\pi})) - \int_0^{\beta\hbar} d\tau \int d^3x\ \frac{1}{4G}((\sigma - m_0)^2 + \pi_i^2)\Big]/\hbar. \tag{4.17}$$

Since the space-time dependence of ϕ is neglected in the mean-field approximation, the second term in the argument of the exponential in Eq.(4.17) corresponding to the mass term of the mesons can be written as

$$\begin{aligned} &\int_0^{\beta\hbar} d\tau \int d^3x\ \frac{1}{4G}((\sigma - m_0)^2 + \pi_i^2)/\hbar \\ &= \frac{\beta\hbar V}{4G}((\sigma - m_0)^2 + \pi_i^2)\frac{1}{\hbar} \\ &= \frac{\beta V}{4G}((\sigma - m_0)^2 + \pi_i^2), \end{aligned} \tag{4.18}$$

so that $\hbar$ disappears in Eq.(4.18). This means that mesons do not have quantum fluctuations in this approximation. On the other hand, the first term corresponding to the fermion propagator still has $\hbar$. Therefore, we see that there are fermionic fluctuations in this approximation. Since the fluctuations of ϕ are neglected in the mean-field approximation, one can say that this approximation is the zeroth order in the expansion of the action around the stationary point for ϕ. In this sense, when we consider the fluctuations of ϕ, the second order of the expansion is taken into account. We will explain more about it later. Denoting the stationary point ϕ_0, the effective action under the mean-field approximation is $I[\phi_0]$.

4.2.1 Deriving the effective action

We let $\phi_0 = (\sigma_0, \boldsymbol{\pi}_0)$ be a point that gives a local minimum of the effective action, obtained from the stationarity condition,

$$\left.\frac{\delta I}{\delta\phi_i}\right|_{\phi=\phi_0} = 0, \tag{4.19}$$

where we choose $\boldsymbol{\pi}_0 = 0$ and $\sigma_0 = -M_0$, which obviously satisfy stationarity conditions for effective pion fields. The action reads:

$$\begin{aligned} I_0 = \beta V \frac{1}{4G}(M_0 - m_0)^2 \\ -2V\mathrm{tr}\sum_n \int \frac{d^3p}{(2\pi)^3} \ln[-i\beta(-i\epsilon_n - \gamma^0\gamma\cdot p - \gamma^0 M_0)], \end{aligned} \tag{4.20}$$

where $p_0 = i\epsilon_n$, ϵ_n are Matsubara frequencies for fermion $\epsilon_n = (2n+1)\pi T$. The trace is taken over the colour, flavour and spin indices. After performing the trace of the Gamma matrices (See Appendix A), we obtain the effective action I_0

$$\begin{aligned} I_0 = \beta V \frac{1}{4G}(M_0 - m_0)^2 \\ -4VN_fN_cT \sum_{n=-\infty}^{+\infty} \int \frac{\mathrm{d}^3p}{(2\pi)^3} \ln[\beta^2(\epsilon_n^2 + E_p^2)], \end{aligned} \tag{4.21}$$

where E_p is the energy constituent quarks

$$E_p = \sqrt{\boldsymbol{p}^2 + M_0^2}.$$

Using the following relations,

$$\begin{aligned} &\ln((2n+1)^2\pi^2 + \beta^2(E_p \pm \mu)^2) \\ &= \int_1^{\beta^2(E_p\pm\mu)^2} d\theta^2 \frac{1}{(2n+1)^2\pi^2 + \theta^2} + \ln((2n+1)^2\pi^2 + 1) \end{aligned} \tag{4.22}$$

and

$$\sum_{n=-\infty}^{+\infty} \frac{1}{(2n+1)^2\pi^2 + \theta^2} = \frac{1}{\theta}\Big(\frac{1}{2} - \frac{1}{e^\theta + 1}\Big), \tag{4.23}$$

and performing the sum over the Matsubara frequencies for quarks, we get the effective action in the mean-field approximation,

$$\begin{aligned} I_0 = \beta V \frac{1}{4G}(M_0 - m_0)^2 \\ -2N_cN_fV \int \frac{\mathrm{d}^3p}{(2\pi)^3} \big[\beta E_p + 2\ln(1 + e^{-\beta E_p})\big], \end{aligned} \tag{4.24}$$

where N_c is the number of colours and N_f is the number of flavours.

With a finite chemical potential, the partition function is given by

$$Z = \int [d\bar{q}][dq] \exp\Big[\int_0^\beta d\tau \int d^3x \big(\mathcal{L} - i\mu\bar{q}\gamma_0 q\big)\Big] \tag{4.25}$$

instead of Eq.(4.6). By the same method as the one we have used for zero chemical potential, Eq.(4.16) is replaced by

$$D = i\gamma^0\partial\!\!\!/ - \gamma^0(\sigma + i\gamma_5\boldsymbol{\tau}\cdot\boldsymbol{\pi}) + \mu. \tag{4.26}$$

Then we get the effective action with chemical potential,

$$I_0 = \beta V \frac{1}{4G}(M_0 - m_0)^2$$
$$-2N_c N_f V \int \frac{\mathrm{d}^3 p}{(2\pi)^3} \left[\beta E_p + \ln(1 + e^{-\beta(E_p - \mu)}) + \ln(1 + e^{-\beta(E_p + \mu)})\right]. \tag{4.27}$$

μ appears in the argument of the exponentials with the quark energy. The relative sign with respect to the quark energy corresponds to particles and antiparticles.

4.2.2 Gap equation

The constituent quark mass M_0 is obtained from the stationarity condition that gives a local minimum of the potential;

$$\left.\frac{\delta I(\phi)}{\delta \phi}\right|_{M_0} = 0. \tag{4.28}$$

In this condition, we have assumed that only the sigma meson has a condensate in the vacuum and that the pions do not have condensate. Under this assumption, we obtain the following self consistent equation called a "gap equation":

$$M_0 - m_0 = 2GT \mathrm{tr} \sum_n \int \frac{d^3 p}{(2\pi)^3} \frac{-1}{\not{p} - M_0}, \tag{4.29}$$

where the trace is taken over the gamma matrices, colour, flavour, spin indices, and the sum is taken over the fermionic Matsubara frequencies $p_0 = i\epsilon_n = (2n+1)\pi T i$. This gap equation corresponds to the diagram shown in Fig.4.3. The big circle in Fig.4.3 represents the constituent quark mass

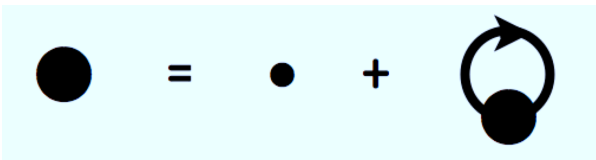

Figure 4.3: Diagrammatical representation of the gap equation.

M_0 and the small circle is the bare quark mass m_0. The constituent quark mass is obtained by the sum of the bare quark mass and the dressed quark loop. Performing the trace over all indices and the sum over the Matsubara frequencies, the gap equation becomes

$$M_0 - m_0 = 8GN_c N_f \int \frac{d^3 p}{(2\pi)^3} \frac{M_0}{E_p} \Big(\frac{1}{2} - f(E_p)\Big), \tag{4.30}$$

where

$$f(E_p) = \frac{1}{e^{\beta E_p} + 1} \tag{4.31}$$

is the quark distribution function. The first term in the right-hand side does not depend on the temperature, and it determines the constituent quark mass in the vacuum. We note that the quark momentum integration in this term requires a cutoff Λ_f in order to suppress the ultraviolet divergence since $(3+1)$ dimensional NJL type models are nonrenormalizable. (The $(1+1)$ dimensional NJL model is renormalizable so that the cutoff is not necessary. This model is called the Gross-Neveu model [110].) The way to introduce the cutoff is not unique: there are some variations, for instance the 3-momentum cutoff scheme, the proper-time regularisation [42, 43, 111, 112], the Pauli-Villars scheme [113]. Here we use the 3-momentum cutoff scheme. The second term depends on the temperature through the quark distribution function. It is not necessary to use the cutoff in the momentum integral in this term since the contribution from high momentum is automatically suppressed by the quark distribution function. Fig.4.4 shows the quark distribution as a function of the quark momentum with fixed temperature. Since the constituent quark mass is determined at each temperature through the gap equation, M_0 is uniquely fixed once T is fixed. The distribution becomes small as the momentum becomes large, then it approaches zero exponentially as $p \gg T$. Therefore, the contribution to the gap equation from the high momentum part of the integral does not dominate.

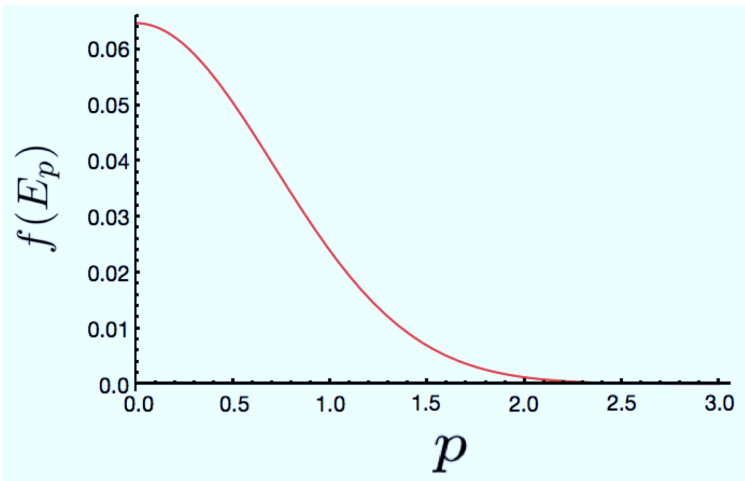

Figure 4.4: Quark distribution function as a function of the quark momentum.

Once the constituent quark mass is obtained by solving the gap equation, the chiral condensate which is an order parameter of the chiral phase

transition can also be obtained based on the following relation;

$$\langle \bar{q}q \rangle = -\frac{M_0 - m_0}{2G}. \tag{4.32}$$

The behaviour of the order parameter at zero chemical potential is shown in Fig.4.5. The vertical axis is the chiral condensate scaled by its value at zero temperature, and the horizontal axis is the temperature scaled by the critical temperature in the chiral limit (zero bare quark mass limit). The red line is calculated in the chiral limit, which shows a second order phase transition. On the other hand, the blue line which is calculated with finite bare quark mass shows only a crossover transition.

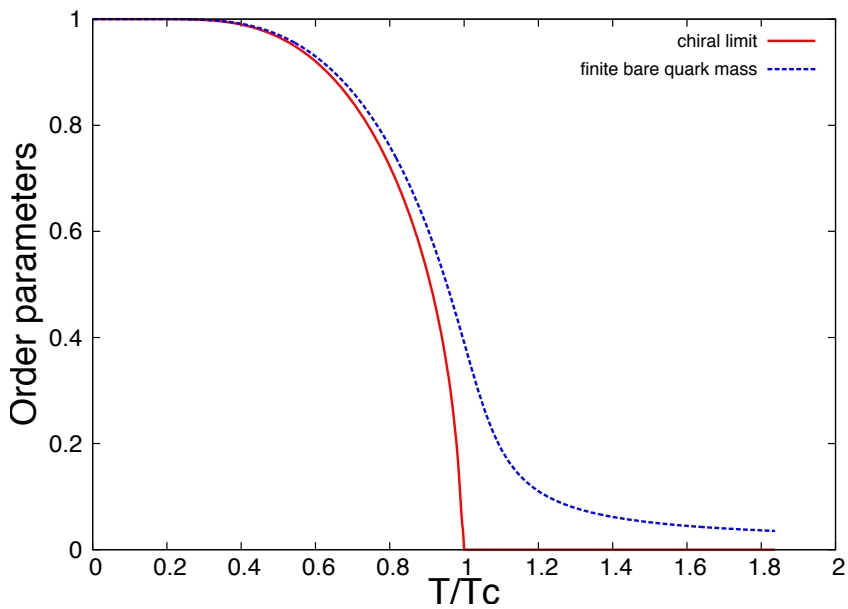

Figure 4.5: Behaviour of the order parameter. In the calculation of the blue line, the bare quark mass is set to 5.5 MeV.

The two-flavour NJL model has three parameters and these parameters are determined in the vacuum in order to reproduce the pion mass m_π, the pion decay constant f_π and the chiral condensate in the vacuum obtained in lattice calculations. The parameter set that we use [58] is shown in Table 4.1.

In the case of a finite chemical potential, the gap equation is modified into

$$M_0 - m_0 = 8GN_cN_f \int \frac{d^3p}{(2\pi)^3} \frac{M_0}{2E_p} \left(1 - \frac{1}{e^{\beta(E_p+\mu)}+1} - \frac{1}{e^{\beta(E_p-\mu)}+1}\right). \tag{4.33}$$

Table 4.1: Parameters

Λ_f[MeV]	G[MeV^{-2}]	m[MeV]
0.651	10.08	5.5
$\langle\bar{q}q\rangle^{1/3}$[MeV]	f_π[MeV^{-2}]	m_π[MeV]
251	92.3	139.3

4.2.3 Equation of state

It is known that there is a relation between the temperature and the other variables that characterise a thermal equilibrium state of the system, and this relation can generally be written as

$$pV = g(T), \tag{4.34}$$

where p is the pressure, V is the volume and T is the temperature. By the definition of the partition function, we have

$$p = \frac{\partial(T\ln Z)}{\partial V}. \tag{4.35}$$

If the volume is large enough, $\ln Z$ is proportional to V, so that

$$\frac{\partial(\ln Z)}{\partial V} = \frac{\ln Z}{V}. \tag{4.36}$$

Then, we get

$$pV = T\ln Z. \tag{4.37}$$

Since $-\ln Z$ is the effective action, one can obtain the pressure from the effective action;

$$p = -\frac{T}{V}I. \tag{4.38}$$

From the effective action we have obtained in Eq.(4.27), we obtain the pressure under the mean-field approximation.

$$\begin{aligned} p_{MF} = &-\frac{1}{4G}(M_0 - m_0)^2 \\ &+2N_cN_f\int\frac{\mathrm{d}^3p}{(2\pi)^3}\left[E_p + T\ln(1+e^{-\beta(E_p-\mu)}) + T\ln(1+e^{-\beta(E_p+\mu)})\right]. \end{aligned} \tag{4.39}$$

The first term does not depend explicitly on the temperature and on the chemical potential, but indirectly trough the constituent quark mass which

is determined by the gap equation. The first term in the square bracket in Eq.(4.39) does not have an explicit temperature or chemical potential dependence. This term needs to have a cutoff for the quark integral so that we use the same cutoff Λ_f which has been introduced in Section 4.2.2. The second and third terms in the square bracket depend on the temperature and the chemical potential explicitly. The quark excitations are described by these terms.

The mean-field pressure is shown in Fig.4.6. The vertical axis is the pressure scaled by T^4 so that this is dimensionless. The horizontal axis is the temperature scaled by the pseudo-critical temperature. Noting that we have only quark excitations in the mean-field approximation, namely the mesonic excitations are neglected so that the quarks dominate the system even in the low temperature phase where hadrons are expected. In Fig.4.6, the pressure is zero at $T \sim 0$ because the constituent quark mass prevents quark excitations. However, quarks start to be excited before T reaches the transition temperature. This means that there are quark excitations in the hadronic phase, even though it is a confined phase. This unphysical situation cannot be solved in the NJL framework because of the lack of colour confinement. At high temperatures, the constituent quark mass gets close to zero, and the quarks become nearly free. Therefore, p/T^4 approaches the Stefan-Boltzmann constant $\sigma = 3 \times 2 \times 2 \times 2 \times 7/8 \times \pi^2/90 \sim 2.3$.

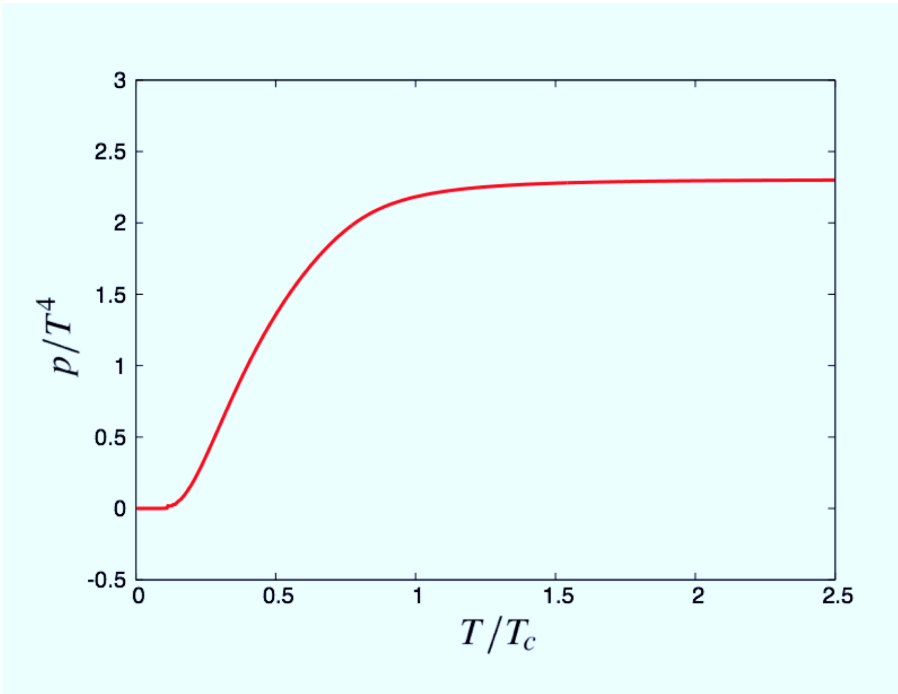

Figure 4.6: The pressure calculated in the two-flavour NJL model.

4.3 Mesonic excitations

We have seen in Section 4.2 a method to obtain the gap equation, the equation of state and the phase diagram in the mean-field approximation. In this section, we summarise the basic ideas for describing the mesonic excitations in the NJL model. As we have already seen in Section 4.2, the NJL model does not have colour confinement so that quark excitations exist even in the low temperature hadronic phase in the mean-field approximation. To make matters worse, hadronic excitations do not exist at low temperatures. Therefore, we need to do two things for a more realistic description of the hadronic phase; the first thing is to suppress the unphysical quark excitations at low temperatures, and the second one is to take into account the hadronic excitations. The first one is achieved in the PNJL model, which will be presented in Chapter 5 to Chapter 7. The second of these requirements may be realised by considering the mesonic fluctuations which are neglected in the mean-field approximation.

The mesonic fluctuations are included by expanding the effective action around the stationary point that was obtained in the previous section after performing the fermion integration. Since the effective action is a function of the auxiliary mesonic fields, we expand it up to the second order in the fluctuations around the stationary point ϕ_0. If we keep only quadratic terms in the fluctuations, we can perform the Gaussian integral over the meson field. Recalling the following integral for an arbitrary matrix D,

$$\int_{-\infty}^{+\infty} dx_1 \cdots dx_n e^{-x_i D_{ij} x_j} = \pi^{n/2} (\mathrm{Det} D)^{-1/2}, \tag{4.40}$$

the partition function is given by

$$\begin{aligned} Z &= \int [d\phi] \exp\Big[-I[\phi_0] - \frac{1}{2}\frac{\delta^2 I}{\delta\phi_a \delta\phi_b}(\phi-\phi_0)^2\Big] \\ &= \exp\Big[-I[\phi_0]\Big] \int [d\phi] \exp\Big[-\frac{1}{2}\frac{\delta^2 I}{\delta\phi_a \delta_b \phi_b}(\phi-\phi_0)^2\Big] \\ &= \exp\Big[-I[\phi_0] - \frac{1}{2}\mathrm{Tr}\ \ln\frac{\delta^2 I}{\delta\phi_a\delta\phi_b}\Big]. \end{aligned} \tag{4.41}$$

Let us denote I' the effective action containing the mesonic fluctuations,

$$I' = I[\phi_0] + \frac{1}{2}\mathrm{Tr}\ \ln\frac{\delta^2 I}{\delta\phi_a\delta\phi_b}. \tag{4.42}$$

Then from the relation between the pressure and the effective action, we get the following pressure

$$p = -\frac{T}{V}\Big(I[\phi_0] + \frac{1}{2}\mathrm{Tr}\ \ln\frac{\delta^2 I}{\delta\phi_a\delta\phi_b}\Big). \tag{4.43}$$

In Eq.(4.43), the first term is the contribution from the mean-field approximation and the second term is due to the mesonic excitations. In this approach, we have neglected the higher order terms in the fluctuations than would appear beyond the second order, so that meson-meson correlations are neglected. If one wants to include these correlations, it is necessary to take higher order fluctuations into account.

4.4 NJL model with diquark interaction

In this section we consider another extension of the NJL model that includes a diquark interaction. The basic NJL Lagrangian has only the four-point interaction between quarks and antiquarks, which generates a $\langle \bar{q}q \rangle$ condensate at low temperatures. To describe the colour superconductor phase at high densities and low temperatures, the quark-quark interaction is also required. There are many works related to colour superconductors and diquark condensates in the NJL framework [20, 22, 46, 48, 50, 104–106]. The diquark interaction is important not only for making diquark condensates, but also for considering quark-quark correlations. From the perturbative QCD analysis, a diquark condensate can exist only in the high density region because in the low density (and low temperature) region the colour confinement prevents the existence of the diquark condensate which is not a colour singlet state. However, the correlations can exist even in baryons in the hadronic phase; a quark pair among the three quarks composing a baryon may be correlated. We will discuss this in more detail in Chapter 7.

A diquark is composed by two quarks which have a colour, a flavour, a spin and a parity. From the Pauli principle, two quarks should be in a totally antisymmetric state, so that 16 combinations of a quark pair are possible, as shown in Fig.4.7. Among these 16 combinations, diquarks which have odd parity do not appear in a single mode configuration [114, 115], and the colour should be antisymmetric. Therefore, only two diquarks are allowed in baryons;

$$\left|\{qq\}\bar{\mathbf{3}}_c(A)\mathbf{1}_f(A)0^+\right\rangle \tag{4.44}$$

which is called a "scalar diquark" or a "good diquark" since it is light and stable, and

$$\left|\{qq\}\bar{\mathbf{3}}_c(A)\mathbf{6}_f(S)1^+\right\rangle \ . \tag{4.45}$$

which is called a "vector diquark" or a "bad diquark". In this section, we only consider the scalar good diquark.

4.4.1 NJL Lagrangian with diquark interaction

The two-flavour NJL model with the diquark interaction is given by

$$\mathcal{L}(\bar{q}, q) = \bar{q}(i\partial\!\!\!/ - m_0)q + \mathcal{L}_{\bar{q}q} + \mathcal{L}_{qq}, \tag{4.46}$$

spin, parity	(flavour, colour)
0^+	$(\mathbf{3}, \mathbf{6})$
	$(\mathbf{1}, \overline{\mathbf{3}})$
0^-	$(\mathbf{3}, \mathbf{6})$
	$(\mathbf{1}, \overline{\mathbf{3}})$
1^+	$(\mathbf{3}, \mathbf{6})$
	$(\mathbf{1}, \overline{\mathbf{3}})$
1^-	$(\mathbf{3}, \mathbf{6})$
	$(\mathbf{1}, \overline{\mathbf{3}})$

Figure 4.7: Allowed combinations for two quarks.

where $\mathcal{L}_{\bar{q}q}$ is a four-point interaction between quarks and antiquarks,

$$\mathcal{L}_{\bar{q}q} = G\big[(\bar{q}q)^2 + (\bar{q}i\gamma_5\tau q)^2\big] \tag{4.47}$$

with a coupling constant G , and $\mathcal{L}_{qq}$ is another four-point interaction which makes diquarks,

$$\mathcal{L}_{qq} = H \sum_{A=2,5,7} \big[(\bar{q}i\gamma_5\tau_2\lambda_A C\bar{q}^T)(q^T C i\gamma_5\tau_2\lambda_A q)\big] \tag{4.48}$$

with a coupling constant H. For the diquark interaction, only the scalar diquark is taken into account. The spin parity of the scalar diquark is antisymmetric, the flavour is antisymmetric and the colour is also antisymmetric. To achieve this, we need $C\gamma_5$ for a Dirac operator, τ_2 for the $U(2)$ generator since we consider the two-flavour case, and λ_2, λ_5, λ_7 for the $U(3)$ generator. When one extends it to the three-flavour case, τ_2 is replaced by λ_2, λ_5, λ_7. The coupling constant H in $\mathcal{L}_{qq}$ is related to G in $\mathcal{L}_{\bar{q}q}$ by the Fierz transformation [116];

$$G : H = \frac{(N_c^2 - 1)}{N_c^2} : \frac{N_c + 1}{2N_c} \tag{4.49}$$

for three colour,

$$G : H = 3 : 4 \ . \tag{4.50}$$

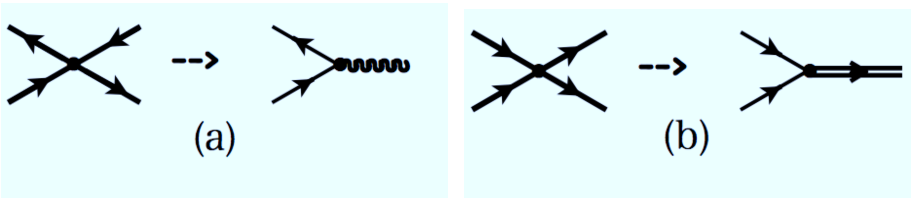

Figure 4.8: (a) $\mathcal{L}_{\bar{q}q}$ is replaced by a dummy integral over meson fields. (b) $\mathcal{L}_{qq}$ is replaced by a dummy integral over a diquark field.

4.4.2 Thermodynamic potential

We now calculate the partition function with the Lagrangian Eq.(4.46) from the path integral in order to get the thermodynamic potential, like in the previous section.

$$Z = \int [d\bar{q}][dq] \exp\Big[\int_0^\beta d\tau \int d^3x \ \big(\mathcal{L}(\bar{q}, q) - i\mu\bar{q}\gamma_0 q\big)\Big]. \tag{4.51}$$

To remove the four-point interactions in Eq.(4.46), we insert dummy integrals over auxiliary boson fields and auxiliary diquark fields by the Hubbard-Stratonovich transformation:

$$\int [d\phi][d\bar{\Delta}][d\Delta] \exp\Big(\int_0^\beta d\tau \int d^3x \mathcal{L}_{\text{aux}}(\phi, \bar{\Delta}, \Delta)\Big) \tag{4.52}$$

with

$$\begin{aligned} \mathcal{L}_{\text{aux}} = &-\frac{1}{4G}\big((\sigma - 2G\bar{q}q)^2 + (\boldsymbol{\pi} - 2iG\bar{q}\gamma_5\boldsymbol{\tau}q)^2\big) \\ &-\frac{1}{4H}\sum_i (\bar{\Delta}_i - 2H\bar{q}\gamma_5\tau_2\zeta_i C\bar{q}^T)(\Delta_i - 2Hq^T C\gamma_5\tau_2\zeta_i q). \end{aligned} \tag{4.53}$$

In this equation, the mesons $\phi = (\sigma, \boldsymbol{\pi})$ and the diquarks (antidiquarks) Δ ($\bar{\Delta}$) are boson fields. The first term in Eq.(4.53) is used for replacing the four-point Fermi interaction in $\mathcal{L}_{\bar{q}q}$ by a Yukawa interaction which is shown in (a) of Fig.4.8. The second term in Eq.(4.53) works in the same way for $\mathcal{L}_{qq}$, which corresponds to (b) in Fig.4.8. After inserting the dummy integrals, the partition function is written in terms of the integrals over quark, antiquark, meson, diquark and antidiquark fields,

$$Z = \int d\bar{q}dqd\phi d\bar{\Delta}d\Delta e^{-I(\bar{q},q,\phi,\bar{\Delta},\Delta)}, \tag{4.54}$$

and the effective action becomes a function of the quark and antiquark fields and of the auxiliary fields,

$$
\begin{aligned}
&I(\bar{q}, q, \phi, \bar{\Delta}, \Delta) \\
&= \int d\tau \int d^3x \big[\bar{q}(i\partial\!\!\!/ - m_0 - i\mu\gamma_0 + \sigma + i\gamma_5 \boldsymbol{\tau}\cdot\boldsymbol{\pi})q \\
&+\frac{1}{2}\bar{\Delta}_i(q^T C\gamma_5\tau_2\zeta_i q) + \frac{1}{2}(\bar{q}\gamma_5\tau_2\zeta_i C\bar{q}^T)\Delta_i \\
&-\frac{1}{4G}\big(\sigma^2 + \boldsymbol{\pi}^2\big) - \frac{1}{4H}\bar{\Delta}\Delta\big].
\end{aligned}
\tag{4.55}
$$

The effective action contains terms which are proportional to $\bar{q}\bar{q}$ and qq, not only $\bar{q}q$, so that we cannot use the same Grassmann integral technique as in the previous section.

Going back to a general situation, we consider a partition function written in terms of the integration of fermion fields,

$$
Z = \int d\psi^\dagger d\psi \exp\Big[\int_0^\beta d\tau \int d^3x\big(\psi^\dagger(\partial + \Omega)\psi + \frac{1}{2}\Delta^*\psi^2 + \frac{1}{2}\Delta\psi^{\dagger 2}\big)\Big], \tag{4.56}
$$

where ψ is a fermion field and Δ is a complex field. To perform the fermion integral, it is useful to introduce a fermion doublet $\boldsymbol{\Psi}$,

$$
\boldsymbol{\Psi} = \begin{pmatrix} \psi \\ \psi^\dagger \end{pmatrix}. \tag{4.57}
$$

By using the fermion basis $\boldsymbol{\Psi}$, the partition function can be written as

$$
Z = \int d\boldsymbol{\Psi}^\dagger d\boldsymbol{\Psi} e^{-\boldsymbol{\Psi}^\dagger \boldsymbol{M}\boldsymbol{\Psi}}, \tag{4.58}
$$

where the matrix M is

$$
\boldsymbol{M} = \begin{pmatrix} \partial + \Omega & \frac{1}{2}\Delta \\ \frac{1}{2}\Delta^* & -\partial + \Omega \end{pmatrix}. \tag{4.59}
$$

Since the terms $\bar{\boldsymbol{\Psi}}\bar{\boldsymbol{\Psi}}$ and $\boldsymbol{\Psi}\boldsymbol{\Psi}$ do not appear in Eq.(4.58), the Grassmann integral can be performed, then we obtain the "fermion determinant",

$$
Z = \det \begin{pmatrix} \partial + \Omega & \frac{1}{2}\Delta \\ \frac{1}{2}\Delta^* & -\partial + \Omega \end{pmatrix}^{1/2}. \tag{4.60}
$$

Let us now come back to the partition function of the NJL model. To deal with the quark integral, we use the same trick by introducing the following doublet of quark fields,

$$
\boldsymbol{q} = \begin{pmatrix} q \\ C\bar{q}^T \end{pmatrix}, \bar{\boldsymbol{q}} = \left(\bar{q}, q^T C\right), \tag{4.61}
$$

and the Nambu-Gorkov propagator

$$\boldsymbol{G}^{-1} = \begin{pmatrix} i\partial\!\!\!/ + \Sigma & \frac{1}{2}\gamma_5\tau_2\zeta\Delta \\ \frac{1}{2}\bar{\Delta}\zeta\gamma_5\tau_2 & -i\partial\!\!\!/ + \Sigma \end{pmatrix}, \tag{4.62}$$

where

$$\Sigma = -m_0 - i\mu\gamma_0 + \sigma + i\gamma_5\boldsymbol{\tau}\cdot\boldsymbol{\pi}. \tag{4.63}$$

By performing the fermion integral in Eq.(4.54), we get the effective action as a function of the meson and diquark fields,

$$I(\phi,\bar{\Delta},\Delta) = -\int d\tau \int d^3x \Big(\frac{1}{4G}(\sigma^2+\boldsymbol{\pi}^2) + \frac{1}{4H}\bar{\Delta}\Delta\Big) - \frac{1}{2}\ln(\mathrm{Det}\boldsymbol{G}^{-1}). \tag{4.64}$$

4.4.3 Mean-field approximation

In the mean-field approximation, fluctuations of the meson fields and the diquark fields are neglected. As we have seen in the previous section, we have obtained the stationary point by solving a gap equation in order to get the thermodynamic potential and the pressure in the mean-field approximation. Unlike the previous section, we now have not only the meson fields but also the diquark fields, so that two gap equations are required in order to obtain stationary values for meson and diquark. From the conditions that give a local minimum of the potential,

$$\left.\frac{\delta I}{\delta\phi}\right|_{\phi_0} = 0, \qquad \left.\frac{\delta I}{\delta\bar{\Delta}}\right|_{\Delta_0} = \left.\frac{\delta I}{\delta\bar{\Delta}}\right|_{\Delta_0} = 0, \tag{4.65}$$

we get two gap equations, for the mesons

$$\begin{aligned} M_0 - m_0 = 4N_cN_fG\int \frac{d^3p}{(2\pi)^3}\frac{M_0}{2E_p} \\ \times\Big(\frac{E_p+\mu}{E^+_{\Delta_0}}\big(1-2f(E^+_{\Delta_0})\big) + \frac{E_p-\mu}{E^-_{\Delta_0}}\big(1-2f(E^-_{\Delta_0})\big)\Big), \end{aligned} \tag{4.66}$$

and for the diquarks

$$\begin{aligned} \Delta_0 = 4N_fN_cH\Delta_0\int\frac{d^3p}{(2\pi)^3} \\ \times\Big(\frac{1}{E^+_{\Delta_0}}\big(\frac{1}{2}-f(E^+_{\Delta_0})\big) + \frac{1}{E^-_{\Delta_0}}\big(\frac{1}{2}-f(E^-_{\Delta_0})\Big), \end{aligned} \tag{4.67}$$

where

$$E^{\pm}_{\Delta_0} = \sqrt{(E_p \pm \mu)^2 + \Delta_0^2}. \tag{4.68}$$

Note that Eq.(4.66) agrees with Eq.(4.30) when $\Delta_0 = 0$ and $\mu = 0$. The stationary points for mesons and diquarks at each temperature and chemical potential are obtained by solving these self consistent gap equations simultaneously. In the mean-field approximation, the mesons and diquarks in the thermodynamic potential are simply represented by the values of the stationary points since the quantum fluctuations of mesons and diquarks are neglected in this approximation.

The thermodynamic potential in the mean-field approximation is obtained from the effective action Eq.(4.64).

$$\begin{aligned}\Omega_{MF} &= \frac{V}{4G}(M_0 - m_0)^2 + \frac{V}{4H}\Delta_0^2 \\ &-\gamma_q V \int \frac{d^3p}{(2\pi)^3}\Big[\frac{E^+_{\Delta_0} + E^+_{\Delta_0}}{2} + T\ln(1 + e^{-\beta E^-_{\Delta_0}}) + T\ln(1 + e^{-\beta E^+_{\Delta_0}})\Big],\end{aligned} \tag{4.69}$$

where $\gamma_q = 2\times 2\times 3\times N_f$ counts spin, particle-antiparticle space, colour, and flavour degeneracy. From the relation between the thermodynamic potential and the pressure,

$$\Omega_{MF} = -p_{MF}V, \tag{4.70}$$

we immediately obtain the pressure,

$$\begin{aligned}p_{MF} &= -\frac{1}{4G}(M_0 - m_0)^2 + \frac{1}{4H}\Delta_0^2 \\ &+\gamma_q \int \frac{d^3p}{(2\pi)^3}\Big[\frac{E^+_{\Delta_0} + E^+_{\Delta_0}}{2} + T\ln(1 + e^{-\beta E^-_{\Delta_0}}) + T\ln(1 + e^{-\beta E^+_{\Delta_0}})\Big].\end{aligned} \tag{4.71}$$

If the diquark condensate Δ_0 is equal to zero, Eq.(4.71) agrees with the pressure calculated in Section 4.2.

Chapter 5

Quark-hadron phase transition in the 2-flavour PNJL model at zero chemical potential

In this chapter, we discuss the quark-hadron phase transition by using a 2-flavour PNJL model with mesonic excitations. One of the advantages of the PNJL model is that this model contains the Polyakov loop which is an order parameter of the deconfinement phase transition, so that one can calculate this transition as well as the chiral phase transition. In addition, since the Lagrangian of this model is written in terms of quark and antiquark fields, we can describe the change of the degrees of freedom from hadrons to quarks by forming hadrons from quarks. However, there are still insufficiencies in this model. For instance, dynamical gluons are not treated in this model because a contribution of gluons to the equation of state is considered through an effective potential.

In this chapter, we consider only the case of zero chemical potential. Even though it is necessary to study the phase transition at finite chemical potential in order to determine the QCD phase diagram, the case of a vanishing chemical potential is an important first step in order to establish a scheme for describing the change of degrees of freedom from hadrons to quarks, before applying the same method with a non-zero chemical potential. Therefore, we concentrate on zero chemical potential in this chapter.

We calculate the partition function with the 2-flavour PNJL model Lagrangian in the path integral method. In order to describe more realistic hadronic phase where hadrons dominate the system, we take mesonic excitations into account by considering the second order in the fluctuations of the auxiliary meson fields which are introduced in the partition function. This analysis therefore goes beyond the mean-field approximation. The equa-

tion of state is obtained as a sum of a contribution from quarks and gluons which appears in the mean-field approximation, and the meson gas contribution which comes from the mesonic fluctuations. At low temperatures, the quark excitations are not allowed by the Polyakov loop, and the gluons given by the effective potential are prevented from appearing in the confined phase, so that only mesonic excitations contribute to the equation of state. On the other hand, at high temperatures, the Polyakov loop does not suppress quarks anymore, and their excitations are allowed to exist. Gluons also appear at high temperatures because of the effective potential whose parameters are determined to realise this. On the other hand, the mesonic excitations which dominate at low temperatures becomes weaker as the temperature increases. When the temperature is sufficiently above the pseudo-critical temperature, mesonic excitations disappear completely and only quarks and gluons contribute to the pressure.

The rest of this chapter is organised as follows. In Section 5.1, we consider the validity of the approximation that we use in this chapter. In Section 5.2, we present the PNJL model in uniform colour gauge fields. Bosonic fields are introduced as auxiliary fields in order to describe the chiral condensate and mesonic correlations. This procedure changes the four-point NJL interaction into a Yukawa interaction. In Section 5.3, the mean-field approximation is reviewed. Under the mean-field approximation, the fluctuations of the meson fields are neglected. Therefore, the pressure is written in terms of constant auxiliary meson fields and thermalised quark quasiparticles. However, these quark quasiparticles are not actually excited at low temperatures because the small expectation value of the Polyakov loop prohibits excitations of coloured states. We discuss this mechanism by focusing on the modification of the quark distribution function. In this section, we also discuss the behaviour of the order parameters for the chiral and the confinement phase transitions. In Section 5.4, we calculate the contribution of mesonic correlations to the equation of state and we show that they are decomposed into collective meson excitations and non-collective individual excitations of quarks or quark-triads. Especially in the chiral limit, where the bare quark mass vanishes, the contribution from collective modes is separated from that of non-collective modes. The collective modes give the pressure of the free pion gas and the free sigma meson gas. We present our numerical results in the last part of this section. It is shown that the pressure of the free pion gas is gradually converted into that of the free quark-gluon gas as the temperature increases, exhibiting a cross-over transition from a hadron gas to the quark-gluon plasma. We also examine in detail the role of collective and non-collective degrees of freedom in the low temperature confined phase and how they change as the temperature increases, both in the chiral limit with massless pions and in the more realistic situation of a non-zero pion mass, by studying the modification of the dispersion relations. It will be shown that the collective meson poles are absorbed into

the continuum of quark-antiquark excitations at high temperatures and that individual excitations do not contribute significantly to the pressure of the system at all temperatures.

5.1 Validity of the approximation

In order to take the mesonic correlations into account, we go beyond the mean-field approximation by considering the second order in the fluctuations of meson fields. This is known as the saddle point approximation. In the NJL model, it corresponds to the $1/N_c$ expansion [117] where N_c is the number of colours. The coupling constant of the NJL model, G, is of order $1/N_c$, while a quark line is $\mathcal{O}(1)$ and a quark loop is $\mathcal{O}(N_c)$. Based on this counting rule, the pressure at leading order (mean-field approximation) is of order $\mathcal{O}(N_c)$, and the next to leading order is of order $\mathcal{O}(1)$. In the PNJL model, we explicitly use the fact that the number of colours is three in order to obtain the distribution function modified by the Polyakov loop. Therefore, it is not clear whether the saddle point approximation in the PNJL model corresponds exactly to the $1/N_c$ expansion. At least in the vacuum, the Polyakov loop does not appear in the PNJL model so that the PNJL model becomes equivalent to the NJL model.

In this approximation, we only take the mesonic correlations between quarks and anti-quarks, and we neglect the correlations between mesons. This may not be justified in the region where the critical fluctuations become large, namely around the critical point. In the chiral limit, where the bare quark mass is zero, it has been shown that the chiral transition at zero chemical potential is a second order transition. In this case, the fluctuations near the transition region are large, so that this approximation around the critical region will break down. However, in the case with a finite bare quark mass, where the chiral transition at zero chemical potential is a crossover, the critical fluctuations become weaker. In this case, the situation is better than in the chiral limit. We are interested in the case with non-zero bare quark mass, since it corresponds to the situation realised in Nature. Therefore, we will perform this approximation to calculate the equation of state.

5.2 Model set up

We begin with the partition function of the 2-flavour PNJL model in an the external temporal colour gauge field, in the path integral method:

$$Z = \int [dq][d\bar{q}] \exp\left[\int_0^\beta d\tau \int d^3x \mathcal{L}\right], \tag{5.1}$$

where the Lagrangian is given by

$$\mathcal{L} = \bar{q}(i\gamma^\mu D_\mu - m_0)q + G\left[(\bar{q}q)^2 + (i\bar{q}\gamma_5\tau q)^2\right] - \mathcal{U}[\bar{\Phi}, \Phi, T] \tag{5.2}$$

for 2-flavour light quarks, $\bar{q} = (\bar{u}, \bar{d})$ in an external temporal colour gauge field. The covariant derivative is $D_\mu = \partial_\mu + gA_0\delta_{\mu,0}$ and m_0 is the bare quark mass, which breaks the chiral symmetry explicitly when it differs from zero. Here we have used a standard Minkovski metric notation with the real time being replaced by the imaginary time $\tau = ix_0$ and the time component of the gauge field replaced by $A_4 = iA_0$. We note here that only the quark fields are dynamical variables which describe thermal excitations of the system, while the temporal component of the SU(3) gauge fields, $A_4 = \frac{1}{2}\lambda^a \mathcal{A}_4^a$ (λ^a being the 3×3 Gell-Mann matrices), only plays a side role by imposing constraints on the colour configurations of the thermal quark excitations. In the following calculation, we use the diagonal representation Ansatz for A_4, following some earlier works [54, 58, 63, 118]. $\mathcal{U}[\bar{\Phi}, \Phi, T]$ is the effective potential as a function of the expectation value of the Polyakov loop Φ and its conjugate $\bar{\Phi}$, defined by

$$\Phi = \frac{1}{3}\langle \mathrm{tr}_c L\rangle, \qquad \bar{\Phi} = \frac{1}{3}\langle \mathrm{tr}_c L^\dagger\rangle \ , \tag{5.3}$$

where L is the Polyakov loop:

$$L(\mathbf{r}) = P\exp\left[ig\int_0^\beta d\tau A_4(\mathbf{r}, \tau)\right]. \tag{5.4}$$

Taking the diagonal representation $L = (e^{\phi_1}, e^{i\phi_2}, e^{-i(\phi_1+\phi_2)})$, the expectation values of the Polyakov loop Φ and $\bar{\Phi}$ become

$$\Phi = \frac{1}{3}\left\langle \left(e^{i\phi_1} + e^{i\phi_2} + e^{-i(\phi_1+\phi_2)}\right)\right\rangle \tag{5.5}$$

$$\bar{\Phi} = \frac{1}{3}\left\langle \left(e^{-i\phi_1} + e^{-i\phi_2} + e^{i(\phi_1+\phi_2)}\right)\right\rangle. \tag{5.6}$$

The form of the effective potential $\mathcal{U}[\bar{\Phi}, \Phi, T]$ is fixed by the following principles;

1. $\mathcal{U}[\bar{\Phi}, \Phi, T]$ satisfies the $SU(3)$ centre symmetry, like the pure gauge Lagrangian

2. $\mathcal{U}[\bar{\Phi}, \Phi, T]$ has a single minimum at $\Phi = 0$ at $T \ll T_c$

3. $\mathcal{U}[\bar{\Phi}, \Phi, T]$ gets close to unity at $T \gg T_c$.

One of the simplest forms that fulfils these requirements is a Ginzburg-Landau potential [118]:

$$\mathcal{U}[\bar{\Phi}, \Phi, T]/T^4 = -\frac{1}{2}b_2(T)\bar{\Phi}\Phi - \frac{1}{6}b_3(\Phi^3 + \bar{\Phi}^3) + \frac{1}{4}b_4(\bar{\Phi}\Phi)^2 \tag{5.7}$$

with

$$b_2(T) = a_0 + a_1\left(\frac{T_0}{T}\right) + a_2\left(\frac{T_0}{T}\right)^2 + a_3\left(\frac{T_0}{T}\right)^3. \tag{5.8}$$

This potential has 7 parameters and they are chosen in order to reproduce lattice data calculated in the pure gauge sector. We show the values of these 7 parameters fixed in this way by [58] in Table 5.2.

Table 5.1: Parameters

a_0	a_1	a_2	a_3	b_3	b_4	T_0
6.75	-1.95	2.625	-7.44	0.75	7.5	270 MeV

We note here that, although the gluon fields are not treated as dynamical variables, gluon excitations can be included in a phenomenological fashion through the effective potential by setting,

$$\mathcal{U}[\bar{\Phi} = \Phi = 1, T] = \left(-a_0 - \frac{1}{3}b_3 + \frac{1}{4}b_4\right)T^4 \sim -\frac{16\pi^2}{90}T^4, \tag{5.9}$$

so that the equation of state approaches that of a free quark-gluon plasma at asymptotic high temperatures.

The partition function, Eq.(5.1), contains the fourth power of the quark fields, so that it is impossible to perform analytically the integration over the fermion fields. To circumvent this problem, we introduce four auxiliary bosonic fields $\phi_i = (\sigma, \boldsymbol{\pi})$ coupled to the quark densities $(\bar{q}q, i\bar{q}\gamma_5\boldsymbol{\tau}q)$ by multiplying $Z(T, A_4)$ by a constant Gaussian integral:

$$\int [d\phi] \exp\left[-\frac{1}{4G}\int_0^\beta d\tau \int d^3x \left((\sigma + 2G\bar{q}q - m_0)^2 + (\boldsymbol{\pi} + 2Gi\bar{q}\gamma_5\boldsymbol{\tau}q)^2\right)\right], \tag{5.10}$$

where periodic boundary conditions are applied for each of the auxiliary fields in the imaginary temporal direction: $\phi_i(\beta) = \phi_i(0)$. The integration measure is normalised so that the integral gives unity. This procedure, known as the Hubbard-Stratonovich transformation [108, 109], converts the four-point quark-antiquark interaction into a Yukawa interaction with the bosonic fields ϕ_i.

$$Z(T, A_4) = \int [dq][d\bar{q}][d\phi] \exp\left[\int_0^\beta d\tau \int d^3x \mathcal{L}_{\rm eff}(q, \bar{q}, \phi, A_4)\right], \qquad (5.11)$$

where

$$\begin{aligned} \mathcal{L}_{\rm eff}(q, \bar{q}, \phi, A_4) = \bar{q}\left[i\gamma^\mu D_\mu + \sigma + i\gamma_5 \boldsymbol{\tau}\cdot\boldsymbol{\pi}\right] q \quad &- \quad \frac{1}{4G}((\sigma - m_0)^2 + \pi_i^2) \\ &- \quad \mathcal{U}[\bar{\Phi}, \Phi, T]. \end{aligned} \qquad (5.12)$$

Performing the Grassmann integral over the quark Dirac fields, the partition function becomes

$$Z(T, A_4) = \int [d\phi] e^{-I(\phi, A_4)}, \qquad (5.13)$$

where the exponent is given by

$$\begin{aligned} I(\phi, A_4) \quad &= \quad \frac{1}{4G}\int_0^\beta d\tau \int d^3x \ \left((\sigma - m_0)^2 + \boldsymbol{\pi}^2\right) \\ &- \quad \mathrm{Tr}\ \ln\left[\beta\left(\mathrm{i}\gamma^\mu \mathrm{D}_\mu + \sigma + \mathrm{i}\gamma_5 \boldsymbol{\tau}\cdot\boldsymbol{\pi}\right)\right] + \int_0^\beta \mathrm{d}\tau \int \mathrm{d}^3\mathrm{x}\ \mathcal{U}[\bar{\Phi}, \Phi, \mathrm{T}], \end{aligned} \qquad (5.14)$$

where the trace in the second term is taken over the arguments of quark fields, including the space-time coordinates with anti-periodic boundary condition in the imaginary time axis, Dirac gamma matrices and the isospin and colour indices. For constant auxiliary meson fields ($(\sigma, \boldsymbol{\pi}) =$ constants), the trace can be expressed as a sum over the fermionic (quark) Matsubara frequencies $\epsilon_n = (2n+1)\pi T$ and integrals over the spatial momenta:

$$\begin{aligned} I(\phi, A_4) \quad &= \quad \frac{\beta V}{4G}\left((\sigma - m_0)^2 + \boldsymbol{\pi}^2\right) \qquad (5.15) \\ &\quad -2VN_f \sum_n \int \frac{d^3p}{(2\pi)^3} \mathrm{tr}_c \ln\left[\beta^2\left((\epsilon_n - gA_4)^2 + \mathbf{p}^2 + \sigma^2 + \boldsymbol{\pi}^2\right)\right] \\ &\quad +\beta V \mathcal{U}[\bar{\Phi}, \Phi, T] \end{aligned}$$

leaving only the trace over the colour indices. Here we have performed the flavour sum with $N_f = 2$, assuming a perfect degeneracy of the up and down quarks ($m_u = m_d = m_0$).

We evaluate the functional integral over the mesonic auxiliary fields by the method of steepest descent. Let $\phi_0 = (\sigma_0, \boldsymbol{\pi}_0)$ give a local minimum value of the integrand, so that

$$\left.\frac{\delta I}{\delta \phi_i}\right|_{\phi=\phi_0} = 0. \qquad (5.16)$$

Hereafter we choose $\boldsymbol{\pi}_0 = 0$, along with $\sigma_0 = -M_0$, which obviously satisfy the stationarity conditions for effective pion fields. Shifting the integration variables by $\varphi_i = \phi_i - \phi_0$, we expand the integral as a power series in φ:

$$I(\phi, A_4) = I_0 + \frac{1}{2} \left. \frac{\delta^2 I}{\delta\phi_i \delta\phi_j} \right|_{\phi=\phi_0} \varphi_i \varphi_j + \cdots . \tag{5.17}$$

The first order term in φ becomes zero because the expansion is done around a local minimum. Keeping only terms up to the quadratic order in the expansion, we have

$$Z(T, A_4) \simeq e^{-I_0} \int [d\varphi] \exp\left[-\frac{1}{2} \left. \frac{\delta^2 I}{\delta\phi_i \delta\phi_j} \right|_{\phi=\phi_0} \varphi_i \varphi_j \right]. \tag{5.18}$$

The remaining Gaussian integrals can be easily performed, giving

$$Z(T, A_4) = e^{-I_0} \left[\mathrm{Det}\ \frac{\delta^2 I}{\delta\phi_i \delta\phi_j} \right]^{-\frac{1}{2}} \tag{5.19}$$

$$= e^{-I_0 - \frac{1}{2}\mathrm{Tr_M} \ln \frac{\delta^2 I}{\delta\phi_i \delta\phi_j}} . \tag{5.20}$$

This gives the thermodynamic potential:

$$\Omega(T, A_4) = T \left(I_0 + \frac{1}{2} \mathrm{Tr_M} \ln \frac{\delta^2 I}{\delta\phi_i \delta\phi_j} \right) \tag{5.21}$$

accurate up to one-loop fluctuations of the collective meson fields. The trace is to be performed over the space-time coordinates of the auxiliary meson fields with a periodic boundary condition in the imaginary time direction.

The first term of Eq.(5.21) represents the thermodynamic potential in the mean-field approximation and the second term represents the contribution of the mesonic fluctuations to the thermodynamic potential. These mesons are free because we have stopped the expansion of $I(\phi, A_4)$ at the quadratic term in Eq.(5.17). If one wishes to take meson-meson interactions into account, higher order terms in the expansion of $I(\phi, A_4)$ should be kept. In this case, it is impossible to perform exactly the integrals in the partition function, because of the terms of degree 3 in φ or higher. Therefore, one would have to calculate the partition function in a perturbative way. In this work, we ignore the interactions between mesons.

5.3 Mean-field approximation

5.3.1 Pressure in the mean-field approximation

The thermodynamic potential in the mean-field approximation, $\Omega_{\mathrm{MF}}(T, A_4)$, or the corresponding pressure $p_{\mathrm{MF}}(T, A_4)$, can be retrieved from the leading term I_0 by the relation:

$$\Omega_{\mathrm{MF}}(T, A_4) = T I_0 = -p_{MF} V.$$

The explicit form of the leading term I_0 is given by

$$
\begin{aligned}
I_0 &= \beta V \frac{1}{4G}(M_0 - m_0)^2 \\
&-2VN_f \sum_n \int \frac{d^3p}{(2\pi)^3} \mathrm{tr}_c \ln\left[\beta^2\left((\epsilon_n - gA_4)^2 + \mathbf{p}^2 + M_0^2\right)\right] \\
&+\beta V \mathcal{U}[\bar{\Phi}, \Phi, T]. \qquad (5.22)
\end{aligned}
$$

This leads to

$$
\begin{aligned}
p_{\mathrm{MF}}(T, A_4) &= -\frac{1}{4G}(M_0 - m_0)^2 \qquad (5.23) \\
&+2TN_f \sum_n \int \frac{d^3p}{(2\pi)^3} \mathrm{tr}_c \ln\left[\beta^2\left((\epsilon_n - gA_4)^2 + \mathbf{p}^2 + {M_0}^2\right)\right] \\
&-\mathcal{U}[\bar{\Phi}, \Phi, T],
\end{aligned}
$$

where the ϵ_n are the fermionic Matsubara frequencies, $\epsilon_n = (2n+1)\pi T$. The trace is to be performed over the 3×3 colour matrix A_4. The sum is taken over the Matsubara frequencies. Evaluating the discrete sum over the Matsubara frequencies by the standard method of contour integration [119, 120], we find

$$
\begin{aligned}
p_{\mathrm{MF}}(T, A_4) &= p^0_{\mathrm{MF}}(M_0) \qquad (5.24) \\
&+2N_f T \int \frac{d^3p}{(2\pi)^3} \mathrm{tr}_c \left[\ln\left(1 + e^{-\beta(E_p + igA_4)}\right) + \ln\left(1 + e^{-\beta(E_p - igA_4)}\right)\right] \\
&-\mathcal{U}[\bar{\Phi}, \Phi, T],
\end{aligned}
$$

where

$$
p^0_{\mathrm{MF}}(M_0) \;=\; 3 \times 2N_f \int^{\Lambda_f} \frac{d^3p}{(2\pi)^3} E_p - \frac{1}{4G}(M_0 - m_0)^2 \qquad (5.25)
$$

is the pressure exerted by the zero point motion of the quark quasiparticles with energy $E_p = \sqrt{p^2 + M_0^2}$ in the "Dirac sea". The factor 3 in the first term of Eq.(5.25) accounts for colour and the factor 2 for spin degeneracies. The second term in Eq.(5.25) is the pressure due to the chiral condensate which shifts the quark mass from m_0 to M_0 and hence reduces the Dirac sea pressure. This term can be understood as a subtraction of the double counting of the mean-field effect in the Hartree approximation. Note that this "vacuum pressure" does not depend on the external background gauge potential due to the cancellation of the effects of the potential on particles and antiparticles. It does not depend on the temperature directly, but indirectly through the constituent quark mass M_0 which depends on the temperature. The last term in Eq.(5.25) is equal to the entropy of the system carried by the thermal excitations of quasiparticles, multiplied by the temperature.

This form of the pressure Eq.(5.25) can be further simplified into a more familiar form by partial integration,

$$
\begin{aligned}
&p_{\rm MF}(T, A_4) = p^0_{\rm MF}(M_0) \\
&+2N_f \int \frac{d^3p}{(2\pi)^3} \frac{p^2}{3E_p} {\rm tr}_c \left[f(E_p + igA_4) + f(E_p - igA_4) \right] \\
&-\mathcal{U}[\bar{\Phi}, \Phi, T],
\end{aligned}
\tag{5.26}
$$

where

$$
f(E_p \pm igA_4) = \frac{1}{e^{\beta(E_p \pm igA_4)} + 1} \tag{5.27}
$$

is the quark (anti-quark) quasiparticle distribution function in an external gauge field potential. Note that quarks and antiquarks have an opposite sign in front of the gauge potential: $+igA_4$ and $-igA_4$ respectively. The second term in Eq.(5.27) corresponds to the pressure exerted by quark and anti-quark quasiparticles in an external gauge potential. The factor 2 accounts for the spin degrees of freedom. The first term in Eq.(5.25) exists even in the vacuum at zero temperature, so that it can be removed because the pressure is defined as the gap from the vacuum pressure. The second term describes the pressure exerted by thermally excited quark quasi-particles which carry entropy. This term should also be removed in the low temperature phase where quarks and antiquarks are confined into hadrons. This can be done by choosing a specific form of A_4 as will be described in the next subsection.

In the mean-field approximation, the value of the quark quasiparticle mass M_0 is determined by the condition that the term linear in the fluctuation $\delta\phi$ vanishes owing to the stationarity condition Eq.(5.16). Written explicitly, for $\sigma_0 = M_0$, it reads

$$
M_0 - m_0 = 8GN_f \sum_n \int \frac{{\rm d}^3p}{(2\pi)^3} \frac{M_0}{(\epsilon_n - gA_4)^2 + p^2 + M_0^2}, \tag{5.28}
$$

which can be reduced to

$$
\begin{aligned}
&M_0 - m_0 = 8GN_f {\rm tr}_c \int \frac{{\rm d}^3p}{(2\pi)^3} \frac{M_0}{E_p} \\
&\times \left(1 - f(E_p + igA_4) - f(E_p - igA_4)\right).
\end{aligned}
\tag{5.29}
$$

5.3.2 Modified quark distributions

In the above calculations, the constant temporal gauge field A_4 appears as a phase factor together with the quark quasiparticle energy in the single particle distribution function Eq.(5.27). This connection was first emphasised in the construction of the model by Fukushima [54] and was developed by Weise et al. [58, 63] based on the assumption that quarks are moving in a

uniform background gauge field, not fluctuating either in space or in imaginary time. Taking diagonal representation $L = (e^{\phi_1}, e^{i\phi_2}, e^{-i(\phi_1+\phi_2)})$, one finds [118]

$$\langle \frac{1}{3}\mathrm{tr}_c f(E_p + igA_4)\rangle \to \frac{\bar{\Phi}e^{2\beta E_p} + 2\Phi e^{\beta E_p} + 1}{e^{3\beta E_p} + 3\bar{\Phi}e^{2\beta E_p} + 3\Phi e^{\beta E_p} + 1} \equiv f_\Phi(E_p), \quad (5.30)$$

where

$$\Phi = \frac{1}{3}\langle \mathrm{tr}_c L\rangle = \frac{1}{3}\langle \Big(e^{i\phi_1} + e^{i\phi_2} + e^{-i(\phi_1+\phi_2)}\Big)\rangle \quad (5.31)$$

$$\bar{\Phi} = \frac{1}{3}\langle \mathrm{tr}_c L^\dagger\rangle = \frac{1}{3}\langle \Big(e^{-i\phi_1} + e^{-i\phi_2} + e^{i(\phi_1+\phi_2)}\Big)\rangle. \quad (5.32)$$

The anti-quark distribution, $\bar{f}_\Phi(E_p) \equiv \langle \frac{1}{3}\mathrm{tr}_c f(E_p - igA_4)\rangle$, is obtained from the quark distribution by the exchange of Φ and $\bar{\Phi}$. At zero chemical potential, the two distributions are identical and Φ is real so that $\Phi = \bar{\Phi}$. We note that this replacement corresponds to a Gaussian approximation in the statistical average, ignoring statistical correlations between the Polyakov loops, in the same spirit as in the mean-field approximation.

A very interesting observation here is that in the de-confined phase where $\Phi = \bar{\Phi} = 1$, one would simply recover the ordinary quark distribution,

$$f_\Phi(E_p)|_{\Phi=1} = \frac{1}{e^{\beta E_p} + 1}. \quad (5.33)$$

In the confined phase, where $\Phi = \bar{\Phi} = 0$, we have instead,

$$f_\Phi(E_p)|_{\Phi=0} = \frac{1}{e^{3\beta E_p} + 1} \quad (5.34)$$

which can be interpreted as a triad of three quark quasiparticles excited together in a colour singlet configuration. It looks somewhat like a baryon, although no effect of interactions is taken into account between the three quarks to form a baryon, as reflected by the same value of momentum for all three quarks. We note that the degrees of freedom of the excitations is not reduced to 1/3 of the colour triplet free quark excitations. They do not completely disappear. This becomes clear when we write the mean-field pressure in terms of the momentum, the energy and the mass of quark triads: The "triad" carries the energy $E_{\mathrm{tri}} = 3E_p$, the momentum $p_{\mathrm{tri}} = 3p$ and the mass $M_{\mathrm{tri}} = 3M_0$. This implies that the Lorentz invariant phase space integral over the quark momentum is reduced when written in term of the triad momentum, e.g.

$$\int \frac{d^3p}{E_p} \to \frac{1}{9}\int \frac{d^3p_{\mathrm{tri}}}{E_{\mathrm{tri}}}. \quad (5.35)$$

With all these prescriptions, the equation of state in the mean-field approximation of the PNJL model can be written as

$$\begin{aligned} p_{\rm MF}(T,\Phi,M_0) &= p^0_{\rm MF}(M_0) - \Delta p_{\rm vac} \\ &+ 4\times 3\times \int \frac{d^3p}{(2\pi)^3}\frac{p^2}{3E_p} f_\Phi(E_p) - \mathcal{U}[\bar\Phi,\Phi,T], \end{aligned} \tag{5.36}$$

and the constituent quark mass M_0 is determined by the gap equation written in terms of the modified quark distribution function

$$M_0 - m_0 = 12GN_f\Big[\int^{\Lambda_f}\frac{d^3p}{(2\pi)^3}\frac{M_0}{E_p} - \int\frac{d^3p}{(2\pi)^3}\frac{M_0}{E_p}\left(f_\Phi(E_p)+\bar f_\Phi(E_p)\right)\Big]. \tag{5.37}$$

The constant $\Delta p_{\rm vac}$ is chosen to make the pressure vanish at zero temperature. In the confined phase, this equation could be interpreted as a gap equation for the quark triad mass by using $E_{\rm tri} = 3E_p$, $p_{\rm tri} = 3p$ and $M_{\rm tri} = 3M_0$,

$$M_{tri} - 3m_0 = 3\times 12GN_f\times\frac{1}{27}\int\frac{d^3p_{tri}}{(2\pi)^3}\frac{M_{tri}}{E_{tri}}(1-f(E_{tri})-\bar f(E_{tri})). \tag{5.38}$$

If we use a rescaled coupling $G' = G/3$, this equation indeed looks more like the original Nambu-Jona-Lasinio gap equation for baryons. This interpretation however meets difficulty when we try to interpret the quark quasiparticle pressure Eq.(5.36) as a pressure from thermal excitations of baryons and anti-baryons. By rescaling the momentum of the quarks, the second term of Eq.(5.36) may be rewritten in the limit $\Phi = 0$ as

$$4\times 3\times\frac{1}{3^4}\int\frac{d^3p_{tri}}{(2\pi)^3}\frac{p^2_{tri}}{3E_{tri}}f(E_{tri}). \tag{5.39}$$

The reduction of the degrees of freedom is by a factor 1/27, more than what we need for the compensation of the remaining colour factor 3.

5.3.3 Behaviour of the order parameters as a function of temperature

To see the temperature dependence of the order parameters, we solve the gap equations for M_0 and Φ obtained by stationarity conditions;

$$\left.\frac{\delta I}{\delta\phi_i}\right|_{M_0} = 0 \tag{5.40}$$

and

$$\frac{\delta I}{\delta\bar\Phi} = \frac{\delta I}{\delta\Phi} = 0. \tag{5.41}$$

As we have seen in Subsection 5.2.2, we get the gap equation for M_0 Eq.(5.37) from Eq.(5.40). For Φ and $\bar{\Phi}$, we obtain the following equations from Eq.(5.41);

$$\begin{aligned} & b_2(T)\bar{\Phi} + b_3\Phi^2 - b_4(\bar{\Phi}\Phi)\bar{\Phi} \\ & = -\frac{24}{T^3}N_f \int \frac{d^3p}{(2\pi)^3}\Big[\frac{e^{\beta E_p}}{e^{3\beta E_p} + 3\bar{\Phi}e^{2\beta E_p} + 3\Phi e^{\beta E_p} + 1} + \frac{e^{2\beta E_p}}{e^{3\beta E_p} + 3\Phi e^{2\beta E_p} + 3\bar{\Phi}e^{\beta E_p} + 1}\Big] \end{aligned} \tag{5.42}$$

and

$$\begin{aligned} & b_2(T)\Phi + b_3\bar{\Phi}^2 - b_4\Phi(\bar{\Phi}\Phi) \\ & = -\frac{24}{T^3}N_f \int \frac{d^3p}{(2\pi)^3}\Big[\frac{e^{\beta E_p}}{e^{3\beta E_p} + 3\Phi e^{2\beta E_p} + 3\bar{\Phi}e^{\beta E_p} + 1} + \frac{e^{2\beta E_p}}{e^{3\beta E_p} + 3\bar{\Phi}e^{2\beta E_p} + 3\Phi e^{\beta E_p} + 1}\Big]. \end{aligned} \tag{5.43}$$

Setting $\bar{\Phi} = \Phi$, we show in Fig.5.1 the temperature dependence of Φ and M_0 obtained from the mean-field approximation. In the chiral limit $m_0 = 0$, the gap equation Eq.(5.37) possesses a nontrivial solution $M_0 \neq 0$ only at temperatures below a critical temperature T_c. In the ordinary NJL model, with no Polyakov loop prescription, the chiral transition takes place at a relatively low temperature, while the confinement-deconfinement transition takes place at a higher temperature, and is a first order transition with a discontinuous change in the value of Φ. In the PNJL model, these two distinct transitions interfere with each other through the quark quasiparticle loops. As a result, the two transitions take place at similar temperatures: the critical temperature for de-confinement transition becomes lower and it becomes a smooth crossover transition, while the chiral transition takes place at a higher temperature, since the quark excitations are suppressed at low temperatures by a small expectation value of the Polyakov loop. This important observation was first made by Fukushima [54]. With a finite bare quark mass m_0, the chiral symmetry is broken explicitly and the chiral transition also becomes a smooth crossover transition.

In these calculations, we have assumed that the coupling G is a constant. However, there is no reason for it to be independent of temperature. Indeed Bernard, Meissner and Zahed have investigated the change of the critical temperature with a temperature dependent coupling $G(T)$, compared to the case of a temperature independent G by using the NJL model [84]. They assumed a temperature dependence of the coupling G based on the parametrisation of Alvarez and Pisarski [85] :

$$\frac{G}{G_0} = \Big[1 - \Big(\frac{T}{T_0}\Big)^2\Big]^{1/2}, \tag{5.44}$$

where G_0 is the coupling determined at zero temperature and T_0 is some temperature which is connected to the critical temperature T_c. They have shown that the critical temperature becomes smaller as T_0 becomes smaller.

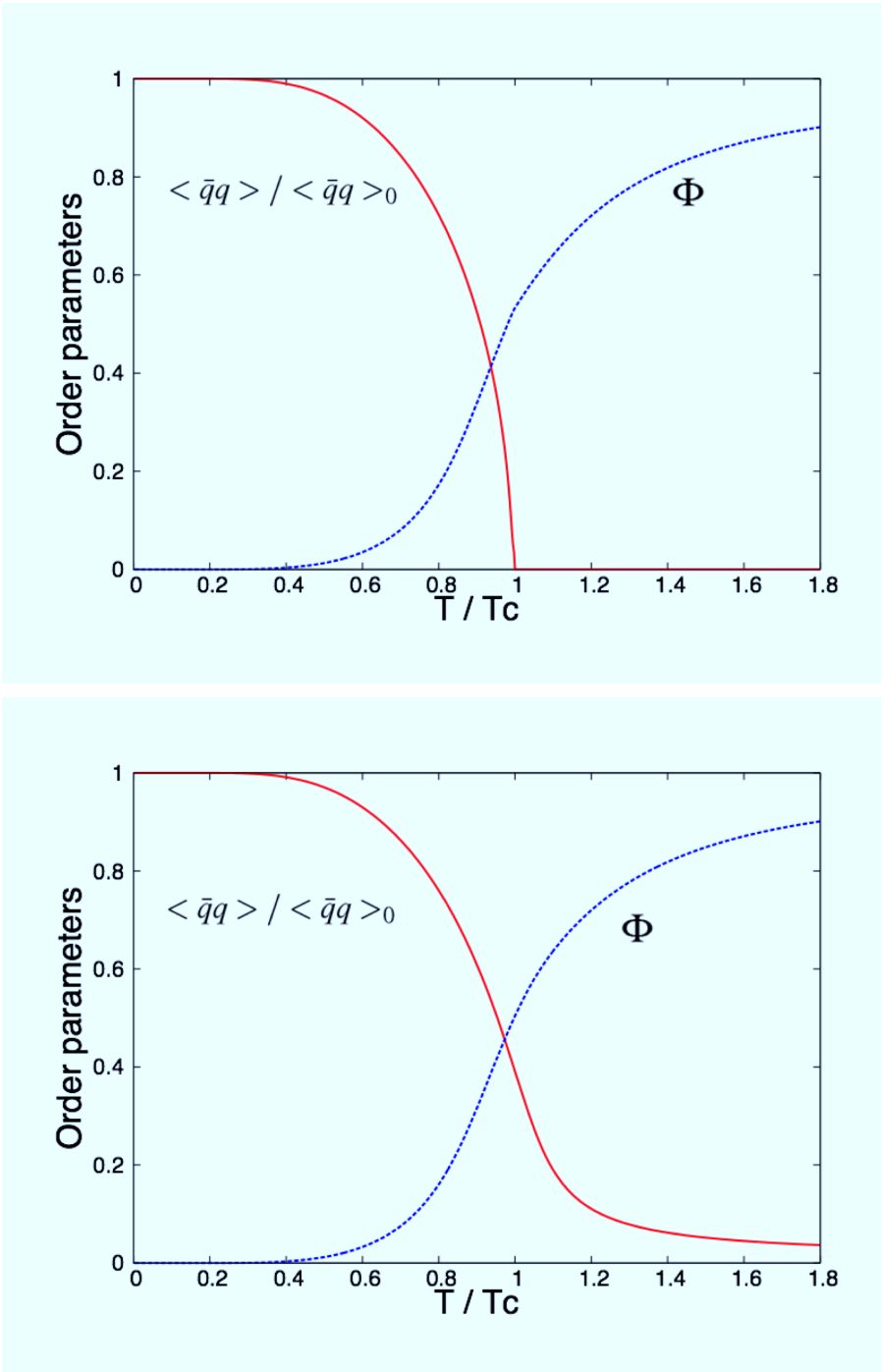

Figure 5.1: Temperature dependence of the effective quark mass M_0 and the expectation value of the Polyakov loop: the top panel is for a vanishing bare quark mass (the chiral limit) and the bottom panel is with a finite bare quark mass m_0 which is chosen in order to reproduce the pion mass $m_\pi = 140$MeV.

We have done a similar calculation by using the PNJL model instead of the NJL model, and we have obtained the behaviour of the order parameters as functions of temperature shown in Fig.5.2. The two red lines in Fig.5.2 show the constituent quark mass and the expectation value of the Polyakov loop with a fixed coupling constant $G = G_0$. The blue and pink lines correspond to $T_0 = 0.3\Lambda_f$ and $0.22\Lambda_f$ where Λ_f is the cutoff parameter introduced for regularising the vacuum pressure in Eq.(5.25). This result for the chiral condensate agrees with the NJL calculation of Bernard, Meissner and Zahed. The critical temperature determined from the Polyakov loop also goes down as T_0 becomes small, but not as much as the critical temperature determined from the chiral condensate, so that the two critical temperatures split at small T_0.

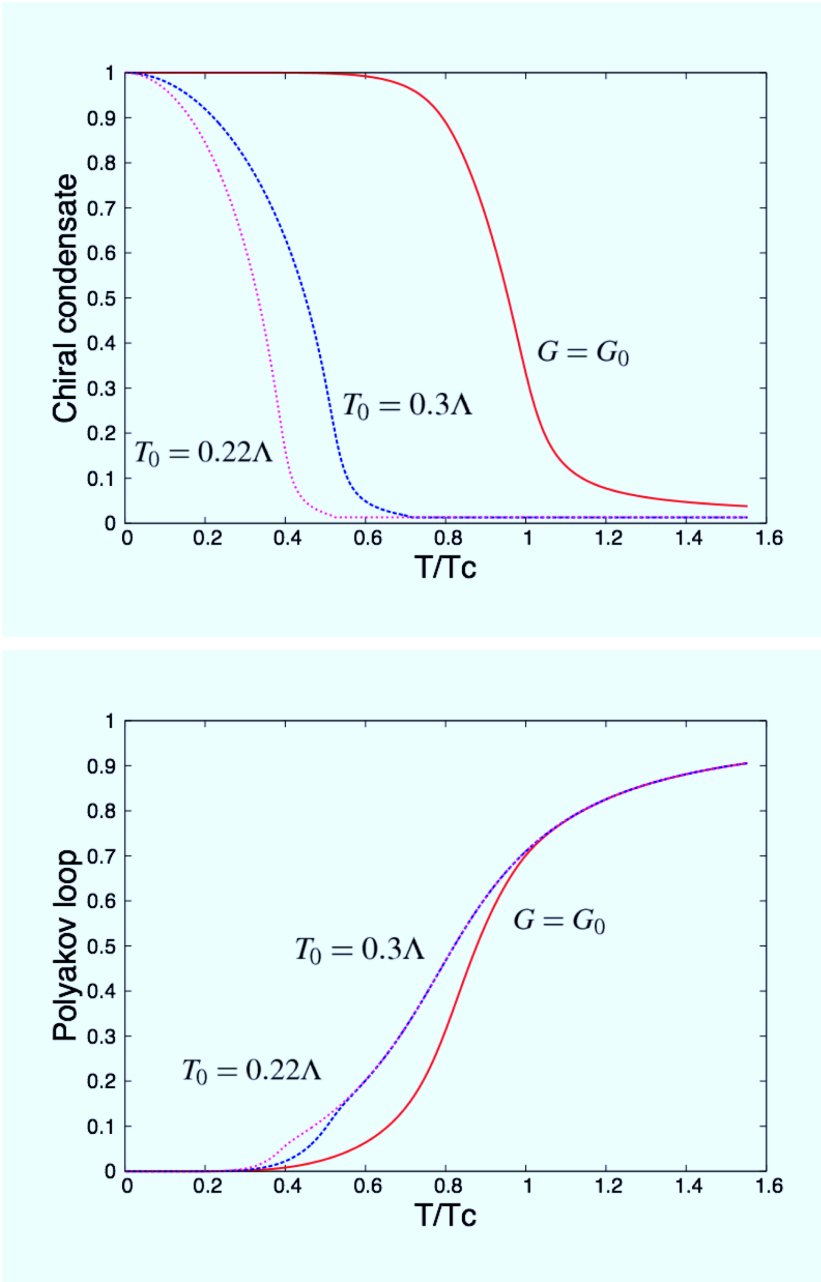

Figure 5.2: Temperature dependence of the order parameters M_0 and Φ with a temperature dependent coupling $G(T)$. The red lines are calculated by using the coupling constant which is determined at zero temperature so that these lines are the same as in the bottom panel of Fig.5.1. The blue and pink lines correspond to $T_0 = 0.3\Lambda_f$ and $0.22\Lambda_f$.

5.4 Mesonic fluctuations

Now we come to our main task of evaluating the mesonic correlation energy. The contribution of the mesonic correlation energy to the free energy, Ω_M, or the corresponding pressure $p_M = -\Omega_M/V$, is given by

$$\Omega_M(T, A_4) = \frac{T}{2}\mathrm{Tr}_M \ln \left.\frac{\delta^2 I}{\delta\phi_i \delta\phi_j}\right|_{\phi=\phi_0} \tag{5.45}$$

and

$$p_M(T, A_4) \quad = \quad -\frac{T}{2V}\mathrm{Tr}_M \ln \left.\frac{\delta^2 I}{\delta\phi_i \delta\phi_j}\right|_{\phi=\phi_0}, \tag{5.46}$$

where the trace is taken over the arguments of the shifted auxiliary fields ϕ_i with a periodic boundary condition along the imaginary time axis. Using Eq.(5.14) and Eq.(5.16), we find that the mesonic pressure is given by

$$\begin{aligned} p_M(T, A_4) &= -\frac{T}{2}\sum_n \int \frac{d^3q}{(2\pi)^3} \\ &\times \left\{ \ln\left[\beta^2\left((2G)^{-1} - \Pi_\sigma(\omega_n, q, A_4)\right)\right] + 3\ln\left[\beta^2\left((2G)^{-1} - \Pi_\pi(\omega_n, q, A_4)\right)\right]\right\}, \end{aligned} \tag{5.47}$$

where the $\omega_n = 2n\pi T$ are the bosonic Matsubara frequencies. The quantities

$$\Pi_\sigma(\omega_n, q, A_4) \quad = \quad \Pi_\sigma^1(A_4) + \Pi_\sigma^2(\omega_n, q, A_4) \tag{5.48}$$

$$\Pi_\pi(\omega_n, q, A_4) \quad = \quad \Pi_\pi^1(A_4) + \Pi_\pi^2(\omega_n, q, A_4) \tag{5.49}$$

are the meson self-energies, with

$$\Pi_\sigma^1 = \Pi_\pi^1 = -2T\sum_n \mathrm{tr}_c \int \frac{\mathrm{d}^3p}{(2\pi)^3}\frac{1}{(\epsilon_n + gA_4)^2 + E_p^2} \tag{5.50}$$

and

$$\Pi_\sigma^2(\omega_n, q, A_4) \quad = \quad \left(\omega_n^2 + \mathrm{q}^2 + 4M_0^2\right) F(\omega_n, \mathrm{q}, A_4) \tag{5.51}$$

$$\Pi_\pi^2(\omega_n, q, A_4) \quad = \quad \left(\omega_n^2 + \mathrm{q}^2\right) F(\omega_n, \mathrm{q}, A_4). \tag{5.52}$$

We have introduced a common dimensionless multiplicative factor

$$\begin{aligned} F(\omega_n, \mathrm{q}, A_4) &= 2T\sum_{n'} \mathrm{tr}_c \int \frac{\mathrm{d}^3p}{(2\pi)^3} \\ &\times \frac{1}{\left[(\epsilon_{n'} + gA_4)^2 + E_p^2\right]\cdot\left[(\epsilon_{n'} + gA_4 + \omega_n)^2 + E_{p+q}^2\right]}. \end{aligned} \tag{5.53}$$

We now show that the contribution of the mesonic correlations to the free energy Eq.(5.45) or the pressure Eq.(5.46) indeed contains that of a

free meson gas composed of massless pions and massive sigma mesons. For this purpose we first eliminate the "tadpole" terms Π^1_σ and Π^1_π by using the stationarity condition, or the "gap equation" Eq.(5.28) which determines the quark quasiparticle mass M_0 in the symmetry broken phase. We then find,

$$(2G)^{-1} - \Pi_\sigma(\omega_n, q, A_4) = (\omega_n^2 + \mathrm{q}^2 + 4M_0^2)F(\omega_n, q, A_4) + \frac{m_0}{2GM_0} \tag{5.54}$$

and

$$(2G)^{-1} - \Pi_\pi(\omega_n, q, A_4) = (\omega_n^2 + \mathrm{q}^2)F(\omega_n, q, A_4) + \frac{m_0}{2GM_0}. \tag{5.55}$$

5.4.1 Chiral limit: $m_0 = 0$

We first consider the chiral limit, $m_0 = 0$. In this limiting case, we have

$$(2G)^{-1} - \Pi_\sigma(\omega_n, q, A_4) = (\omega_n^2 + \mathrm{q}^2 + 4M_0^2)F(\omega_n, q, A_4) \tag{5.56}$$
$$(2G)^{-1} - \Pi_\pi(\omega_n, q, A_4) = (\omega_n^2 + \mathrm{q}^2)F(\omega_n, q, A_4) \tag{5.57}$$

and we can separate the contributions of the collective bare meson modes from non-collective individual excitations:

$$p_M(T, A_4) = -\frac{1}{2}T\sum_n \int \frac{d^3q}{(2\pi)^3}$$
$$\times \left[\ln\left(\beta^2(\omega_n^2 + \mathrm{q}^2 + 4M_0^2)\right) + 3\ln\left(\beta^2(\omega_n^2 + \mathrm{q}^2)\right) + 4\ln F(\omega_n, q, A_4)\right]. \tag{5.58}$$

The first two terms are respectively the contributions to the pressure of a gas of free sigma mesons with mass $m_\sigma = 2M_0$ and of a gas of free massless pions with 3-fold isospin degeneracy. Indeed, one can perform all the bosonic Matsubara frequency sums by contour integration and find,

$$p_M^{\text{free}}(T) = p_M^0 + \int \frac{d^3q}{(2\pi)^3}\left[\frac{q^2}{3\omega_q}f_B(\omega_q) + 3 \times \frac{q}{3}f_B(q)\right], \tag{5.59}$$

where $\omega_q = \sqrt{\mathrm{q}^2 + 4M_0^2}$ is the sigma meson energy and $f_B(\omega) = 1/(e^{\beta\omega} - 1)$ is a bosonic single particle distribution function. The first term is the mesonic vacuum pressure p_M^0,

$$p_M^0 = -\frac{1}{2}\int^{\Lambda_b} \frac{d^3q}{(2\pi)^3}\left[3q + \omega_q\right], \tag{5.60}$$

where we have indicated an additional cutoff Λ_b which needs to be introduced to regularise the divergence in the momentum integral for mesons.

This vacuum mesonic pressure needs to be removed by renormalisation. The momentum integral for the pressure of the massless pion gas can be evaluated analytically and one finds a familiar Stefan-Boltzmann pressure with three-fold isospin degeneracy:

$$p_{\rm pion}^{\rm free} = \int \frac{d^3q}{(2\pi)^3} 3 \times \frac{q}{3} f_B(q) = 3 \times \frac{\pi^2}{90} T^4. \tag{5.61}$$

Now we evaluate the correction to the free meson gas due to underlying quark substructure of the mesons. This is contained in the additional contribution,

$$\Delta p_M(T, A_4) = -2T \sum_n \int \frac{d^3q}{(2\pi)^3} \ln F(\omega_n, q, A_4), \tag{5.62}$$

where the ω_n are the bosonic Matsubara frequencies, $\omega_n = 2\pi n T$. The function F defined by Eq.(5.53) also contains a sum over the fermionic Matsubara frequencies $\epsilon_n = (2n+1)\pi T$. These sums are computed via a contour integration in the complex z plane, with a multiplicative complex function $\pm 1/(\exp(z\beta) \pm 1)$ which has poles on the imaginary z-axis at ϵ_n (ω_n). We find

$$\Delta p_M(T, A_4) \quad = \quad -2 \int_C \frac{dz}{2\pi i} \int \frac{d^3q}{(2\pi)^3} \frac{1}{e^{z\beta} - 1} \ln \mathcal{F}(z, q, A_4), \tag{5.63}$$

where

$$\mathcal{F}(z, q, A_4) = F(-iz, q, A_4). \tag{5.64}$$

The contour $\mathcal{C}$ is shown in Fig.5.3 . We note that the function $\mathcal{F}$ has

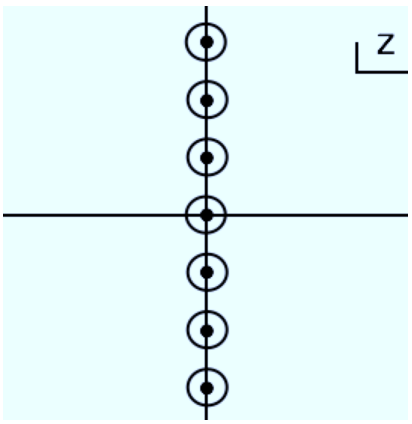

Figure 5.3: The contour in Eq.(5.63).

poles only on the real $z-$axis. We continuously rotate the integration path clockwise to the one that encloses the real $z-$axis. Rewriting the real value of z by ω, we obtain

$$\begin{aligned}\Delta p_M(T,A_4) &= -2\int_{-\infty}^{\infty}\frac{d\omega}{2\pi i}\int\frac{d^3q}{(2\pi)^3}\frac{1}{e^{\omega\beta}-1}\ln\frac{\mathcal{F}(\omega+i\epsilon,q,A_4)}{\mathcal{F}(\omega-i\epsilon,qA_4)}\\ &= -2\int_{0}^{\infty}\frac{dz}{2\pi i}\int\frac{d^3q}{(2\pi)^3}(1+\frac{2}{e^{\omega\beta}-1})\ln\frac{\mathcal{F}(\omega+i\epsilon,q,A_4)}{\mathcal{F}(\omega-i\epsilon,qA_4)},\end{aligned} \tag{5.65}$$

where we have used the fact that the function $\mathcal{F}(\omega,q,A_4)$ is an even function of ω and

$$-\frac{1}{e^{-\omega\beta}-1}=1+\frac{1}{e^{\omega\beta}-1}. \tag{5.66}$$

Similarly, the sum over the fermionic Matsubara frequency in Eq.(5.53) can also be performed by contour integration:

$$\begin{aligned}\mathcal{F}(\omega,q,A_4) &= \mathrm{tr}_c\int\frac{\mathrm{d}^3p}{(2\pi)^3}\int_{\mathcal{C}}\frac{dz}{2\pi i} \qquad (5.67)\\ &\times \frac{1}{e^{z\beta}+1}\frac{1}{\left[(-(z+igA_4)^2+E_p^2\right]\cdot\left[-(z+igA_4+\omega)^2+E_{p+q}^2\right]}\\ &= \mathrm{tr}_c\int\frac{\mathrm{d}^3p}{(2\pi)^3}\frac{1}{2E_p2E_{p+q}}\\ &\times \Big\{\left(\frac{1}{\omega+E_p-E_{p+q}}-\frac{1}{\omega-E_p+E_{p+q}}\right)\\ &\times \big(f(E_p-igA_4)-f(E_{p+q}-igA_4)\big) \qquad (5.68)\\ &+ \left(\frac{1}{\omega+E_p+E_{p+q}}-\frac{1}{\omega-E_p-E_{p+q}}\right)\\ &\times \big(1-f(E_p-igA_4)-f(E_{p+q}-igA_4)\big)\Big\},\end{aligned}$$

where

$$f(E-igA_4)=\frac{1}{e^{\beta(E-igA_4)}+1}. \tag{5.69}$$

We have performed the contour integration by modifying the path to the paths encircling the poles on the real $z-$axis, showing only one of four terms. Again, the external gauge field appears as a phase factor in the quark distribution function in $\mathcal{F}(\omega_n,q,A_4)$, like in the mean-field approximation. We therefore replace these phase factors by the Polyakov loops and then substitute them by a statistical average as in Eq.(5.30). Performing the sum over the bosonic Matsubara frequencies by contour integration, we find

$$\mathcal{F}(\omega,q) \equiv \langle\mathcal{F}(\omega,q,A_4)\rangle=\mathcal{F}_{\mathrm{scat}}(\omega,q)+\mathcal{F}_{\mathrm{pair}}(\omega,q), \tag{5.70}$$

where

$$\mathcal{F}_{\rm scat}(\omega,q) = 3\int \frac{d^3p}{(2\pi)^3}\frac{1}{2E_p 2E_{p+q}}\left(\frac{1}{\omega+E_p-E_{p+q}}-\frac{1}{\omega-E_p+E_{p+q}}\right) \times (f_\Phi(E_p)-f_\Phi(E_{p+q})) \quad (5.71)$$

$$\mathcal{F}_{\rm pair}(\omega,q) = 3\int \frac{d^3p}{(2\pi)^3}\frac{1}{2E_p 2E_{p+q}}\left(\frac{1}{\omega+E_p+E_{p+q}}-\frac{1}{\omega-E_p-E_{p+q}}\right) \times (1-f_\Phi(E_p)-f_\Phi(E_{p+q}))\,. \quad (5.72)$$

The detail of this computation is given in the appendix B. We can interpret these correlation energies as non-collective fluctuations of a system carrying mesonic quantum numbers with modified quark distributions.

For the computation of the correlation energy or pressure, it is convenient to decompose the function $\mathcal{F}(\omega \pm i\epsilon, q)$ into a real part $\mathcal{F}_1(\omega,q)$ and an imaginary part $\mathcal{F}_2(\omega,q)$:

$$\mathcal{F}(\omega\pm i\epsilon,q) = \mathcal{F}_1(\omega,q)\pm i\mathcal{F}_2(\omega,q) \quad (5.73)$$

$$= \sqrt{\mathcal{F}_1(\omega,q)^2+\mathcal{F}_2(\omega,q)^2}\,e^{\pm i\phi(\omega,q)}, \quad (5.74)$$

where the argument ϕ is given by

$$\phi(\omega,q) = \tan^{-1}\frac{\mathcal{F}_2(\omega,q)}{\mathcal{F}_1(\omega,q)}\quad . \quad (5.75)$$

The pressure arising from the non-collective or individual excitations of the system is given by

$$\Delta p_M(T) = \langle \Delta p_M(T,A_4)\rangle = -2\int^{\Lambda_b}\frac{d^3q}{(2\pi)^3}\int_0^\infty \frac{d\omega}{2\pi}\left[1+\frac{2}{e^{\beta\omega}-1}\right]2\phi(\omega,q). \quad (5.76)$$

5.4.2 Breaking the chiral symmetry with $m_0 \neq 0$

The previous analysis applies only to the chiral limit ($m_0 = 0$) and to the symmetry broken phase. For a non-zero value of m_0, the separation of the collective modes and the individual excitations is not as simple as in the above analysis due to the term $m_0/(2GM_0)$ in the dispersion relations Eq.(5.54) and Eq.(5.55) for the various species of mesons. In this case, we expect that the pions, as Nambu-Goldstone modes associated with spontaneous symmetry breaking of the chiral symmetry, acquire non-zero mass m_π. To calculate the contribution to the thermodynamic potential of such modes, we need to go back to the original formula Eq.(5.47) for the pressure from mesonic correlations. It is convenient to write

$$M_\sigma(\omega_n,q) = (2G)^{-1} - \langle \Pi_\sigma(\omega_n,q,A_4)\rangle \quad (5.77)$$

$$M_\pi(\omega_n,q) = (2G)^{-1} - \langle \Pi_\pi(\omega_n,q,A_4)\rangle \quad (5.78)$$

or, using the gap equation,

$$M_\sigma(\omega_n, q) = (\omega_n^2 + \mathrm{q}^2 + 4M_0^2)\langle F(\omega_n, q, A_4)\rangle + \frac{m_0}{2GM_0} \tag{5.79}$$

$$M_\pi(\omega_n, q) = (\omega_n^2 + \mathrm{q}^2)\langle F(\omega_n, q, A_4)\rangle + \frac{m_0}{2GM_0}. \tag{5.80}$$

Performing again the bosonic-Matsubara frequency sum by contour integration, we obtain

$$\begin{aligned} p_M(T) &= -\frac{1}{2}\int \frac{d^3q}{(2\pi)^3}\frac{1}{2\pi i}\int_0^\infty d\omega \left[1 + \frac{2}{e^{\beta\omega}-1}\right] \\ &\quad \times \left\{3\ \ln\left[\frac{\mathcal{M}_\pi(\omega+i\epsilon, q)}{\mathcal{M}_\pi(\omega-i\epsilon, q)}\right] + \ln\left[\frac{\mathcal{M}_\sigma(\omega+i\epsilon, q)}{\mathcal{M}_\sigma(\omega-i\epsilon, q)}\right]\right\}, \end{aligned} \tag{5.81}$$

where we have written

$$\mathcal{M}_{\pi/\sigma}(\omega, q) = M_{\pi/\sigma}(-i\omega_n, q) \tag{5.82}$$

with $\langle F(\omega_n, q, A_4)\rangle$ in $M_{\pi/\sigma}(-i\omega_n, q)$ replaced by Eq.(5.70). Expressing the integrand of Eq.(5.81) in terms of the arguments of the complex $\mathcal{M}_{\pi/\sigma}(\omega \pm i\epsilon, q)$, we have

$$p_M(T) = -\int^{\Lambda_b} \frac{d^3q}{(2\pi)^3}\int_0^\infty \frac{d\omega}{2\pi}\Big[1 + \frac{2}{e^{\omega\beta}-1}\Big]\left[3\phi_\pi(\omega, q) + \phi_\sigma(\omega, q)\right], \tag{5.83}$$

where

$$\phi_{\pi/\sigma}(\omega, q) = \tan^{-1}\frac{\mathcal{M}_{\pi/\sigma,2}(\omega, q)}{\mathcal{M}_{\pi/\sigma,1}(\omega, q)} \tag{5.84}$$

with

$$\mathcal{M}_{\pi/\sigma}(\omega \pm i\epsilon, q) = \mathcal{M}_{\pi/\sigma,1}(\omega, q) \pm i\mathcal{M}_{\pi/\sigma,2}(\omega, q). \tag{5.85}$$

We note that unlike in the case of the chiral limit, ϕ_π and ϕ_σ defined as Eq.(5.84) contain contributions not only from non-collective modes but also from collective modes. Here, we call a meson mode collective only when it appears as an isolated pole on the real ω axis: it requires the condition that both real and imaginary parts of $\mathcal{M}_{\pi/\sigma}(\omega, q)$ vanish for a certain combination of ω and q determining the mesonic dispersion relation. In this case, the argument $\phi(\omega, q)$ becomes a δ function, $\delta(\omega - \omega_q)$ with the mesonic dispersion relation, $\omega_q \simeq \sqrt{q^2 + m^2}$, with $m = m_\pi(m_\sigma)$.

On the other hand, if only the real part of $\mathcal{M}(\omega, q)$ vanishes while the imaginary part is non-vanishing, the corresponding mode decays by Landau-damping into non-collective excitations. We refer to these modes as the non-collective individual excitations As the temperature increases, the low energy boundary of the continuum of the particle-antiparticle excitations

moves down and eventually absorbs the meson poles. Hence no isolated meson poles remain. In the chiral limit, this happens at $T = T_c$ where the chiral symmetry is restored and where the pions, the Nambu-Goldstone modes, disappear. In this case, there is no meson pole contribution and only contributions from cuts remain in the mesonic correlation energy. With explicit chiral symmetry breaking by the bare quark mass, we have to go back to the original expression Eq.(5.47) in order to compute the mesonic correlation energy in a similar way to what is done in [118]. We found numerically that the real part of $\mathcal{M}(\omega, q)$ does not vanish at high temperatures for all values of (ω, q), showing no sign of persistence of the mesonic modes, as shown in Section 6.

5.4.3 Entropy including mesonic fluctuations

The total entropy is a sum of the mean-field quark entropy, s_{MF}, which changes continuously with temperature through the transition region, and the entropy of the collective mesonic-like excitations at low temperature. To include the latter excitations, we need to go one step beyond the mean-field approximation. The low energy excitations we consider here are pion-like and sigma-like. For simplicity, we refer to such excitations as "mesons" in the following.

In the hadronic phase, pions, which are massless in the chiral limit ($m_0 = 0$), and sigma mesons give a contribution to the pressure,

$$p_{\text{meson}}(T) = \sum_{\nu} \gamma_\nu \int \frac{d^3q}{(2\pi)^3} \frac{q^2}{3\omega_q} \left(\frac{1}{2} + f_B(\omega_q) \right), \tag{5.86}$$

where the index ν denotes the meson type; $\gamma = 3$, $\omega_q = q$ for pions, and $\gamma = 1$, $\omega_q = \sqrt{q^2 + m_\sigma^2}$ for sigma mesons. The $\frac{1}{2}$ term is the divergent vacuum pressure, which should be removed by renormalisation. The entropy of the meson gas, $s_{\text{meson}}(T) = \partial p_{\text{meson}}(T)/\partial T$, takes the canonical form

$$s_{\text{meson}}(T) \quad = \quad \sum_{\nu} \gamma_\nu \int \frac{d^3q}{(2\pi)^3} \sigma_{B\nu}(\omega_q), \tag{5.87}$$

where

$$\sigma_B(\omega) = (1 + f_B(\omega))\ln(1 + f_B(\omega)) - f_B(\omega)\ln f_B(\omega) \tag{5.88}$$

with $f_B(\omega) = 1/(e^{\beta\omega} - 1)$ the bosonic distribution function.

In general, the mesonic modes appear as collective modes of the quarks. We derive the mesonic entropy from the mesonic correlation pressure, $p_{\text{corr}} \equiv p(G) - p_{\text{MF}}^{\text{ren}}(G)$, where $p(G)$ is the full pressure at coupling constant G. The

correlation pressure is given, in the random phase approximation, in terms of Matsubara frequencies by

$$p_{\rm corr}(T) = \frac{1}{2\beta}\sum_{\nu}\sum_{{\rm q},n}\ln\left(1-2G\Pi_{\nu}(\omega_n,q)\right), \tag{5.89}$$

where the index ν runs over the four pion and sigma degrees of freedom. Here $\Pi_\nu(\omega,q)$ is the quark polarisation of the mean-field distribution:

$$\begin{aligned}\Pi_\nu(\omega_n,q) &= -\frac{1}{\beta}\int\frac{d^3p}{(2\pi)^3}\\ &\times\sum_{m,i}{\rm Tr}\left[\Gamma_\nu S_i(\epsilon_m+\omega_n,p+q)\Gamma_\nu S_i(\epsilon_m,p)\right],\end{aligned} \tag{5.90}$$

where $S_i(\epsilon,p) = [(\epsilon - i\phi_i T)\gamma_0 - \mathbf{p}\cdot\boldsymbol{\gamma} - M]^{-1}$ is the quark quasiparticle propagator. The trace is over Dirac as well as flavour indices and the sum is over the quark colour index i and the Matsubara frequencies. The sum over the Matsubara frequencies yields

$$\begin{aligned}\Pi_\nu(\omega,q) &= -\int\frac{d^3p}{(2\pi)^3}\int_C\frac{d\epsilon}{2\pi i}f_F(\epsilon)\\ &\times\sum_i{\rm Tr}\left[\Gamma_\nu S_i(\epsilon+\omega,p+q)\Gamma_\nu S_i(\epsilon,p)\right],\end{aligned} \tag{5.91}$$

where $\Gamma_\pi = i\gamma_5\tau_\nu$, $\Gamma_\sigma = 1$, and $f_F(\epsilon) = 1/(e^{\beta\epsilon}+1)$.

The correlation pressure Eq.(5.89) can be derived in several equivalent ways. Reference [1] evaluated the path integral of the effective mesonic action, obtained by integrating out the Grassmann quark fields variables, then integrating over the remaining auxiliary mesonic fields, by making a Gaussian approximation around the saddle point (which amounts to neglecting meson-meson interactions). This result can be equivalently obtained by differentiating the total pressure $P = (T/V){\rm ln}{\rm Tr}e^{-\beta\hat{H}}$, with respect to the coupling constant G. Schematically, with $\hat{H} = \hat{H}_0 - G\int d^3x q(x)\bar{q}(x)\hat{\tau}q(x)$ in terms of Dirac quark field operators $q(x)$,

$$\frac{\partial P}{\partial G} = \frac{1}{V}\int d^3x\langle\bar{q}(x)q(x)\bar{q}(x)q(x)\rangle, \tag{5.92}$$

where for simplicity we focus on the scalar field. (Including the pseudo scalar interaction in the NJL model, $-G\int d^3x\bar{q}(x)\gamma_5\hat{\tau}q(x)\bar{q}(x)\gamma_5\hat{\tau}q(x)$, the right side of Eq.(5.92) would acquire an additional term, $-\langle\bar{q}(x)\gamma_5\hat{\tau}q(x)\bar{q}(x)\gamma_5\hat{\tau}q(x)\rangle$.) The right hand side of Eq. (5.92) can be expressed, in the presence of a uniform scalar condensate $\langle\bar{q}q\rangle \neq 0$, as the sum of the condensate pressure

and the pressure due to scalar density fluctuations. In terms of the Fourier components of the scalar density propagator,

$$D_s(x,\tau) = -i\langle T\left(n_s(x,\tau)n_s(0,0)\right)\rangle\,, \tag{5.93}$$

where $n_s(x,\tau) = e^{\hat{H}\tau}\bar{q}(x)q(x)e^{-\hat{H}\tau} - \langle\bar{q}q\rangle$, one has

$$\frac{1}{V}\int d^3x\langle\bar{q}(x)q(x)\bar{q}(x)q(x)\rangle = \langle\bar{q}q\rangle^2 - \tfrac{1}{\beta}\textstyle\sum_{\mathrm{q},n} D_s(\omega_n,q). \tag{5.94}$$

Calculating the scalar density propagator in the random phase approximation by summing the Dyson series with the quark polarization taken to be the lowest order scalar density fluctuation, we have

$$D_s(\omega_n,q) = \frac{\Pi_\sigma(\omega_n,q)}{1-2G\Pi_\sigma(\omega_n,q)}. \tag{5.95}$$

Then the sigma term in the derivative of Eq. (5.89) with respect to G, at fixed M (since M is determined by extremizing the pressure) is simply Eq.(5.94) – namely the right hand side of Eq. (5.92), with the propagator given in Eq.(5.95)) – while the first term is just the derivative of the first term on the right side of the mean-field pressure, Eq. (5.36), at fixed M.

Carrying out the Matsubara sum in Eq. (5.89), one obtains

$$\begin{aligned} p_{\mathrm{corr}}(T) &= \frac{i}{2}\int\frac{d^3q}{(2\pi)^3}\int_{-\infty}^{\infty}\frac{d\omega}{2\pi}f_B(\omega) \\ &\times\left\{3\ln\left[\frac{\mathcal{M}_\pi(\omega-i\epsilon,q)}{\mathcal{M}_\pi(\omega+i\epsilon,q)}\right]+\ln\left[\frac{\mathcal{M}_\sigma(\omega-i\epsilon,q)}{\mathcal{M}_\sigma(\omega+i\epsilon,q)}\right]\right\}, \end{aligned} \tag{5.96}$$

where

$$\mathcal{M}_\nu(\omega,q) \equiv 1-2G\Pi_\nu(\omega,q). \tag{5.97}$$

The arguments of the logarithms in Eq. (5.96) can be interpreted as the phase shifts of the scattering of the $q\bar{q}$ pair in the time-like ($\omega > q$) region. Contributions from the mesonic excitations arise from the zeros of $\mathcal{M}_{\pi/\sigma}$ in the complex ω plane.

Integrating by parts with respect to ω in Eq.(5.96), we derive the following useful expression,

$$\begin{aligned} p_{\mathrm{corr}}(T) &= -\int\frac{d^3q}{(2\pi)^3}\int_0^\infty d\omega\left(\frac{\omega}{2}+T\ln(1-e^{-\beta\omega})\right) \\ &\quad\times\left[3\rho_\pi(\omega,q;T)+\rho_\sigma(\omega,q;T)\right], \end{aligned} \tag{5.98}$$

where we have introduced the spectral weights

$$\rho(\omega, q; T) = \frac{1}{2\pi i}\left[\frac{1}{\mathcal{M}_-}\frac{\partial \mathcal{M}_-}{\partial \omega} - \frac{1}{\mathcal{M}_+}\frac{\partial \mathcal{M}_+}{\partial \omega}\right] \tag{5.99}$$

of π and σ mesons, with $\mathcal{M}_\pm(\omega, q) \equiv \mathcal{M}(\omega \pm i\epsilon, q)$. The spectral weights are real and can be written in terms of the real and imaginary parts of $\mathcal{M}(\omega \pm i\epsilon, q) = \mathcal{M}_1(\omega, q) \pm i\mathcal{M}_2(\omega, q)$ as

$$\rho(\omega, q; T) = \frac{1}{\pi}\frac{\mathcal{M}_2 \partial \mathcal{M}_1/\partial\omega - \mathcal{M}_1 \partial \mathcal{M}_2/\partial\omega}{\mathcal{M}_1(\omega, q)^2 + \mathcal{M}_2(\omega, q)^2}. \tag{5.100}$$

The $\omega/2$ term in Eq.(5.98) is the vacuum pressure, whose divergent part is removed by renormalisation at $T = 0$, leaving only a finite contribution to the pressure at finite temperature.

We differentiate the correlation pressure Eq.(5.98) with respect to T and use the relation $\partial\left(T\ln(1 - e^{-\beta\omega})\right)/\partial T = \sigma_B(\omega)$, to find the entropy,

$$\begin{aligned} s_{\rm corr} &= -\int \frac{d^3q}{(2\pi)^3}\int_0^\infty d\omega \sigma_B(\omega)\left[3\rho_\pi(\omega, q; T) + \right. \\ &\quad \left. + \rho_\sigma(\omega, q; T)\right] + \Delta s_{\rm corr}, \end{aligned} \tag{5.101}$$

where

$$\begin{aligned} \Delta s_{\rm corr} = &-\int \frac{d^3q}{(2\pi)^3}\int_0^\infty d\omega \left(\frac{\omega}{2} + T\ln(1 - e^{-\beta\omega})\right) \\ &\times \left[3\frac{\partial}{\partial T}\rho_\pi(\omega, q; T) + \frac{\partial}{\partial T}\rho_\sigma(\omega, q; T)\right]. \end{aligned} \tag{5.102}$$

The values of the quark mass M and the Polyakov loop parameter Φ contained in Π_π and Π_σ minimise the free energy, and therefore, when calculating the entropy from the mesonic correlation pressure, both M and Φ can be held fixed. The temperature dependence of $p_{\rm corr}$ is contained in $f_B(\omega)$ as well as in the modified quark distribution functions $f_\Phi(E_p)$ in the quark bubbles, Π_π and Π_σ.

To proceed with the calculation of the correlation entropy, we write the explicit forms of the quark polarisation:

$$\begin{aligned} &\mathrm{Tr}\left[\Gamma_\nu S_i(\epsilon + \omega, p + q)\Gamma_\nu S_i(\epsilon, p)\right] \\ &= \frac{N_\nu}{\left[(\epsilon + \omega + i\phi_i T)^2 - E_{p+q}^2\right]\left[(\epsilon + i\phi_i T)^2 - E_p^2\right]}, \end{aligned} \tag{5.103}$$

where

$$\begin{aligned} N_\pi &= \mathrm{Tr}\left\{i\gamma_5\left[(\epsilon + \omega + i\phi T)\gamma_0 + (\mathbf{p} + \mathrm{q})\cdot\boldsymbol{\gamma} + M\right]\right. \\ &\qquad \left. \times i\gamma_5\left[(\epsilon + i\phi T)\gamma_0 + \mathbf{p}\cdot\boldsymbol{\gamma} + M\right]\right\} \\ &= 2\left(\left[(\epsilon + \omega + i\phi_i T)^2 - E_{p+q}^2\right]\right. \\ &\qquad \left. + \left[(\epsilon + i\phi_i T)^2 - E_p^2\right] - (\omega^2 - q^2)\right), \end{aligned} \tag{5.104}$$

and

$$
\begin{aligned}
N_\sigma &= \mathrm{Tr}\left\{[(\epsilon+\omega+i\phi T)\gamma_0+(\mathbf{p}+\mathrm{q})\cdot\boldsymbol{\gamma}+M]\right. \\
&\qquad\qquad \left.\times[(\epsilon+i\phi T)\gamma_0+\mathbf{p}\cdot\boldsymbol{\gamma}+M]\right\} \\
&= 2\left(\left[(\epsilon+\omega+i\phi_i T)^2-E_{p+q}^2\right]+(\epsilon+i\phi_i T)^2\right. \\
&\quad \left.-E_p^2-(\omega^2-q^2-4M^2)\right). \qquad (5.105)
\end{aligned}
$$

Inserting Eq.(5.103)-Eq.(5.105) into Eq.(5.90), and performing the integral over ϵ, we pick up the residues of the poles at $\epsilon=\pm E_{p+q}-\omega-i\phi_i T$ and at $\epsilon=\pm E_p-i\phi_i T$, and we find

$$
\Pi_\pi(\omega,q)=\mathcal{T}+(\omega^2-q^2)\mathcal{F}(\omega,q), \qquad (5.106)
$$

and

$$
\Pi_\sigma(\omega,q)=\mathcal{T}+(\omega^2-q^2-4M^2)\mathcal{F}(\omega,q), \qquad (5.107)
$$

where the constant tadpole term $\mathcal{T}$ equals $\langle\bar{q}q\rangle/M$. Moreover,

$$
\mathcal{F}(\omega,q)=\mathcal{F}_{\mathrm{scatt}}(\omega,q)+\mathcal{F}_{\mathrm{pair}}(\omega,q), \qquad (5.108)
$$

with the quark particle-hole bubble,

$$
\begin{aligned}
\mathcal{F}_{\mathrm{scatt}}(\omega,q) &= \gamma_q\int\frac{d^3p}{(2\pi)^3}\frac{f_\Phi(E_p)-f_\Phi(E_{p+q})}{2E_p\;2E_{p+q}} \\
&\quad\times\left(\frac{1}{\omega+E_p-E_{p+q}}-\frac{1}{\omega-E_p+E_{p+q}}\right), \qquad (5.109)
\end{aligned}
$$

and the quark-antiquark bubble,

$$
\begin{aligned}
\mathcal{F}_{\mathrm{pair}}(\omega,q) &= \gamma_q\int\frac{d^3p}{(2\pi)^3}\frac{1-f_\Phi(E_p)-f_\Phi(E_{p+q})}{2E_p\;2E_{p+q}} \qquad (5.110) \\
&\times\left(\frac{1}{\omega+E_p+E_{p+q}}-\frac{1}{\omega-E_p-E_{p+q}}\right). \qquad (5.111)
\end{aligned}
$$

We see explicitly that the selff-energy Π_ν and hence the $\mathcal{M}_\nu$ are even functions of ω.

The function $\mathcal{F}_{\mathrm{scat}}(\omega-i\epsilon,q)$ has a non-zero imaginary part in the space-like region $\omega<q$, while $\mathcal{F}_{\mathrm{pair}}(\omega-i\epsilon,q)$ has a non-zero imaginary part in the time-like region $\sqrt{q^2+4M^2}<\omega$. The effect of the Polyakov loop appears in the suppression of the continuum due to the suppression of the quark distribution functions; the kinematical conditions for the location of the continua are unchanged by a uniform temporal colour gauge field, since the

complex chemical potentials for quark and holes or antiquarks generated by the uniform gauge field cancel each other due to the colour neutrality of the pair. The quark continuum contributions to the correlation pressure and entropy are strongly suppressed in the confined phase, and the mesonic entropy is essentially that of free mesons.

In the chiral limit ($m_0 = 0$) the gap equation Eq.(5.28) implies that for $M \neq 0$ below T_c, $\mathcal{T} = 1/2G$, so that $\mathcal{M}$ contains only the quark bubble terms, and the entropy from the free meson gas is readily isolated from the non-collective quark pair excitations. To recover the free meson results in the chiral limit below T_c, we note that since $\mathcal{M}_\nu(\omega, q)$ factors into $(-\omega^2 + \omega_q \nu^2)\mathcal{F}$, we can extract the piece in $\rho(\omega, q)$,

$$\rho_{\text{meson}}(\omega, q) = \delta(\omega - \omega_q) - \delta(\omega + \omega_q), \tag{5.112}$$

which with Eq. (5.98) leads immediately to Eq. (5.86). While the upper edge of the scattering continuum at the light cone coincides with the location of the pion pole, and the lower edge of pair excitation continuum coincides with the σ meson pole in the chiral limit, the meson poles decouple from the continuum owing to the factorisation of $\mathcal{M}_\nu(\omega, q)$.

On the other hand, for $T > T_c$, the gap equation has only the solution $M = 0$, and rather

$$1 - 2G\mathcal{T} \simeq c(T - T_c). \tag{5.113}$$

Furthermore, the gap in the time-like continuum vanishes above T_c since $M = 0$, closing the window between two continua. There is no room where the collective mesonic excitations could appear as isolated poles.

More generally, with a non-vanishing bare quark mass m_0, explicitly breaking the chiral symmetry, $\mathcal{M}(\omega, q)$ does not simply factorise, even at low temperatures. However, since the gap equation always has solutions with non-vanishing M, there will be a gap in the continuum excitation spectrum, and an isolated meson pole can exist in such a window. At temperatures below T_c, $\mathcal{M}(\omega, q)$ still contains an isolated zero, corresponding to mesons with spectra shifted from those in the chiral limit, in the region $q < \omega < \sqrt{q^2 + 4M^2}$ where the imaginary part of $\mathcal{F}(\omega \pm i\epsilon, q)$ vanishes [1]. In this case, we can still extract the meson pressure and entropy from the ω-integral over this region.

Assume that $\mathcal{M}_\nu(\omega, q)$ has a zero at $\omega = \omega_q$; owing to $\mathcal{M}_\nu(\omega, q)$ being even in ω, there is also a zero at $\omega = -\omega_q$. (We do not need to assume that $\omega_q = \sqrt{q^2 + m^2}$ here). In the vicinity of each of these zeros, $\mathcal{M}(\omega, q) = c_q(\omega^2 - \omega_q^2)$, where c_q is a non-vanishing function of q. Then the

[1] This is the case for pions up to a certain melting temperature above T_c, while the σ meson pole is absorbed into the pair excitation continuum; the signature of the pole remains a strong peak since the continuum is suppressed by the Polyakov loop in the confined phase.

square bracket in Eq.(5.98) reduces in the vicinity of $\pm\omega_q$ to the δ-function form of Eq.(5.112) which upon integration over ω in Eq. (5.98) indeed gives the meson pressure in the form Eq.(5.86) with a modified spectrum ω_q obtained from $\mathcal{M}(\omega_q, q) = 0$. The corresponding meson entropy approximately takes the canonical form Eq.(5.87), with a small correction $\Delta s_{\rm corr}$ originating from the temperature dependence of the meson spectrum $\rho(\omega_q, q)$; this dependence arises via the temperature dependence of ω_q as well as the more explicit temperature dependence of the distribution function.

Additional contributions to the pressure and entropy arise from (non-collective) fluctuations of thermal quark quasiparticle excitations, due to scattering for $\omega < q$ and pair creation for $\omega > \sqrt{q^2 + 4M^2}$, as indicated by the appearance of a non-vanishing imaginary part of $\mathcal{F}(\omega \pm i\epsilon, q)$. As the temperature increases, isolated meson poles become absorbed into the continuum of quark quasiparticle excitations, and no singularity appears in the pressure or entropy as a function of temperature. This non-collective correlation contains the remnants of the meson poles as resonance peaks in $\rho(\omega, q)$. As found numerically, the contribution of these non-collective quark fluctuations to the pressure is actually small compared to the mean-field pressure of the quark quasiparticles [1]. In the chiral limit, the coupling between mesonic modes, both pions and sigma mesons, and quark-pair excitations turns on suddenly at the critical temperature as the temperature is raised from below, causing a singularity in the derivative of the entropy density with respect to the temperature, and changing the transition to the second order one, as in the mean-field approximation.

5.4.4 Cutoff parameters

Since our model contains some ultraviolet divergences, we have to introduce cutoff parameters in order to suppress these divergences. For calculating the pressure of mesonic correlations, we need two cutoff parameters. A first divergence appears in the mean-field approximation, for which cutoff parameter has been introduced in Eq.(5.25). This is the vacuum pressure in the mean-field approximation. The first term of Eq.(5.25) diverges because of the momentum integral. We remove the higher momentum modes by the cutoff Λ_f already introduced earlier in this chapter. The thermal excitation term, the third term on the right hand side of Eq.(5.36), does not need any cutoff because the quark distribution functions suppress the excitations of high momentum modes. Hence, after Λ_f has been introduced in the vacuum term, we can calculate the pressure in the mean-field approximation without any further divergence.

However, when we calculate the pressure of the mesonic correlations, an additional divergence appears in the momentum integral in the first term in the bracket of Eq.(5.76). This divergence arises from the meson momentum integral and we cannot eliminate it by the quark momentum cutoff Λ_f

alone. This problem arises because NJL models are non-renormalise: even if we suppress the divergences from a calculation of some order, additional divergences may appear in the next order calculation. For this reason, we have to introduce a second cutoff parameter Λ_b in order to suppress the divergence from the bosonic loop calculation [42, 43]. The total pressure does not depend on the value on the cutoff Λ_b because of the subtraction of the vacuum pressure.

The integral in the second term in the bracket of Eq.(5.76) does not diverge. Since the bosonic distribution function as a function of ω suppresses excitation modes in the large ω region, no divergence appears in the ω integral. Regarding the q integral, it seems at first sight that it may diverge because the bosonic distribution function is only a function of ω. However since ϕ becomes very small at large q, such a divergence does not appear. One can see this from Eq.(C.12). When we fix ω and consider the large q region, it is always a space-like region so that the behavior of $\mathcal{F}_2$ corresponds to $\mathcal{F}_{scat,2}$. From Eq.(C.12), we see that $N_{scat}(\epsilon)$ becomes exponentially small in the large q region. As a result $\mathcal{F}_{scat,2}$ also gets close to zero from Eq.(C.18). Although Eq.(C.12) is an approximation under the condition of small ϵ, this approximation is justified as long as q becomes large for fixed ω in the q integral of Eq.(5.76).

5.5 Numerical results

5.5.1 Pressure

We display in Fig. 5.4 the pressure calculated by the present method. The top panel is the result computed in the chiral limit $m_0 = 0$. At low temperatures below the second order chiral transition temperature T_c, the pressure from quark quasiparticle excitations is suppressed by the modification of the distribution function: excitations of triad of quarks in a colour singlet configuration are only allowed with effective excitation energy at least three times that of a massive quark excitation, and this contribution to the pressure is hence suppressed. The dominant excitation modes which determine the pressure are massless pion excitations with 3 isospin degeneracy as shown in the red solid curve. We found that the contribution from massive sigma meson excitations and non-collective individual excitations of the quark triads and antiquark triads are also negligible at low temperature. At high temperatures, massless quark excitations in the mean-field approximation dominate the pressure, with comparable contributions of the gluon pressure phenomenologically introduced in the construction of the effective potential. The contribution from the mesonic correlations becomes negligible at high temperatures, and the pressure approaches that of an ideal gas of massless quarks and gluons in our model. We note that at large temperatures the cutoff Λ_f in the quark momentum integration reduces the pressure compared to

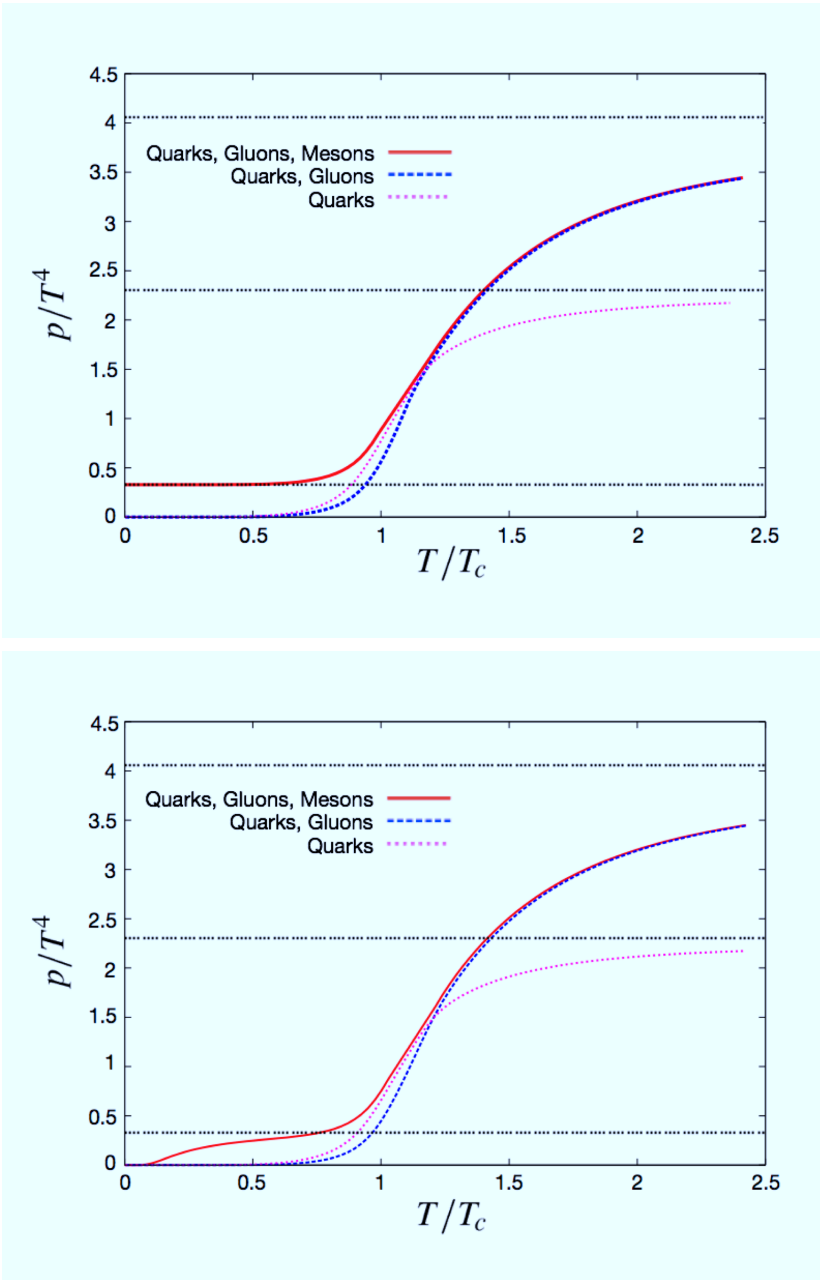

Figure 5.4: Pressure scaled by T^4 as a function of temperature: the top panel is for vanishing bare quark mass (chiral limit) and the bottom panel is with a finite bare quark mass m_0 which is chosen in order to reproduce the pion mass $m_\pi = 140$MeV. In comparison, the pressures calculated in the mean-field approximation are shown with (blue dotted line) and without (red dotted line) gluon contributions. The pressures of the massless pion gas, the quark gas and the gas of quarks and gluons are indicated by the horizontal dashed lines, going from bottom to top respectively.

that of free quark-gluon gas, as seen in the effective reduction of the Stefan-Boltzmann constant p/T^4 from $\sigma = 3 \times 2 \times 2 \times 2 \times 7/8 \times \pi^2/90 \approx 2.3$. With a symmetry breaking finite bare quark mass (bottom panel of Fig.5.4), the pion becomes massive and its contribution to the pressure decreases exponentially at very low temperature, otherwise the behaviour of its pressure at higher temperatures is qualitatively unchanged.

5.5.2 Entropy

We display in Fig. 5.5 the entropy calculated by the present method.

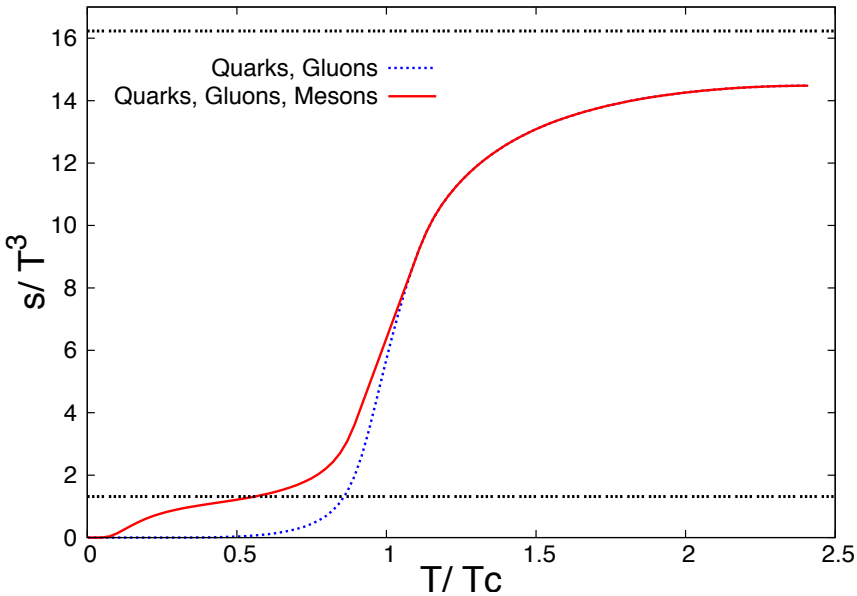

Figure 5.5: Temperature dependence of the entropy scaled by T^3: the dotted line is the entropy carried by quarks and gluons in the mean-field approximation, while the solid curve also includes the entropy carried by the collective excitations. The entropies of the massless pion gas and the gas of massless quarks and gluons are indicated by the lower and upper horizontal dashed lines, respectively. The temperature axis is scaled by the critical temperature T_c taken here to be 230 MeV, i.e. roughly the temperature determined from the chiral susceptibility in the mean-field approximation.

5.5.3 Collective modes and non-collective modes

Since mesonic excitations contain two types of modes, collective meson modes and non-collective individual excitations, we consider in this subsection the two contributions separately, in the chiral limit where the separation

is manifest, and in the case with an explicit chiral symmetry breaking term, where we need to separate them carefully due to the mixing via the bare quark mass term.

Chiral limit

As shown in Fig.5.4, the pressure at low temperatures satisfies the Stefan-Boltzmann relation $p/T^4 \simeq 0.33$. This means that the pressure at low temperatures comes only from pion collective modes, Eq.(5.61), and that the contributions from sigma meson collective modes and non-collective modes are both very small. The contribution from the thermal excitations of the sigma meson is suppressed compared to that of pions due to the large sigma meson mass, $m_\sigma = 2M_0$. The contribution from the non-collective modes is also expected to be suppressed for the same reason: the effective mass of a quark triad is $3M_0$ as it appears in the modified quark distribution. Since the contribution of non-collective modes to the pressure comes from the phase space integral of the argument $\phi(\omega, q)$ of $\mathcal{F}(\omega + i\epsilon, q)$, we should inspect in detail the behaviour of $\mathcal{F}(\omega + i\epsilon, q)$.

We show first the region where the imaginary part of the function $\mathcal{F}(\omega + i\epsilon, q)$, $\mathcal{F}_2$, becomes non-zero in Fig. 5.6. It consists of two regions, one in the space-like region ($\omega < q$) corresponding to the scattering, and the other in the time-like region ($\omega > q$) where pair excitations contribute. The upper boundary of the scattering region is at the light cone ($\omega = q$) and the lower boundary of the pair excitation region is given by $\omega = \sqrt{q^2 + (2M_0)^2}$ where q is the momentum of the mesonic excitation and M_0 is the constituent quark mass determined from the gap equation Eq.(5.29). In the region between the two boundaries, $\mathcal{F}_2$ is equal to zero. There are no physically allowed excitations in the kinematical region between these boundaries, besides meson poles which are not shown here. As the temperature increases, the upper boundary goes down, because the increase of temperature causes the decrease of the constituent quark mass M_0 as a result of the restoration of chiral symmetry. Hence, there are eventually individual excitations filling all this region at high temperature, as shown in the bottom panel of Fig. 5.6.

Next we display $\mathcal{F}_1$ and $\mathcal{F}_2$ as a function of ω/q for a fixed value of $q = \Lambda_f$ at two characteristic temperatures, in Fig. 5.7 ($T = 0.7T_c$) and Fig. 5.8 ($T = 1.4T_c$). Below T_c, $\mathcal{F}_1$ crosses the horizontal axis and there are two valleys at $\omega/q = 1$ and $\omega/q \simeq 1.6$. On the other hand, above T_c, $\mathcal{F}_1$ does not cross the horizontal axis and the valley at $\omega/q \simeq 1.6$ goes down and is absorbed into the continuum.

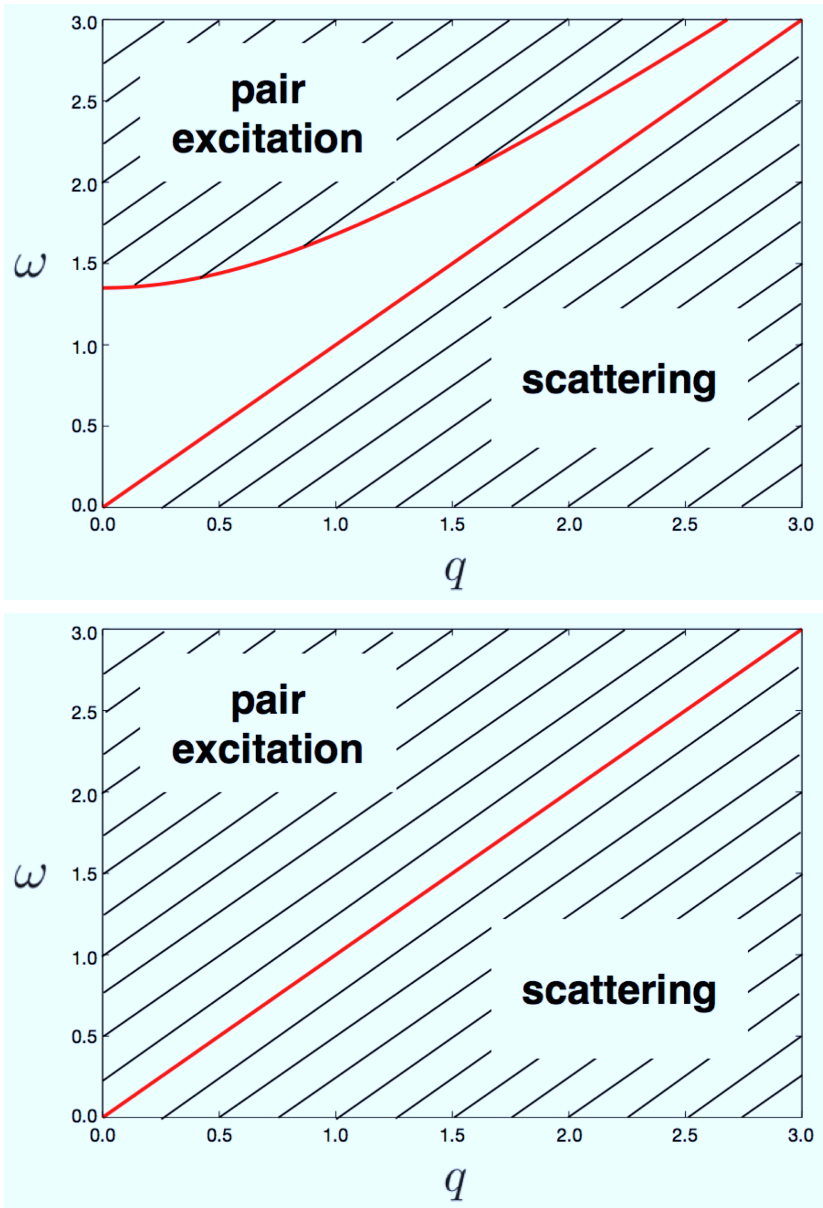

Figure 5.6: The kinematical regions where $\mathcal{F}_2$ is non-vanishing is shown by shaded areas: (1) $\omega < q$ (scattering), (2) $\omega > \sqrt{q^2 + (2M_0^2)}$ (pair excitation). The top panel is for $T = 0.7T_c$, while the bottom panel is for $T = 1.4T_c$.

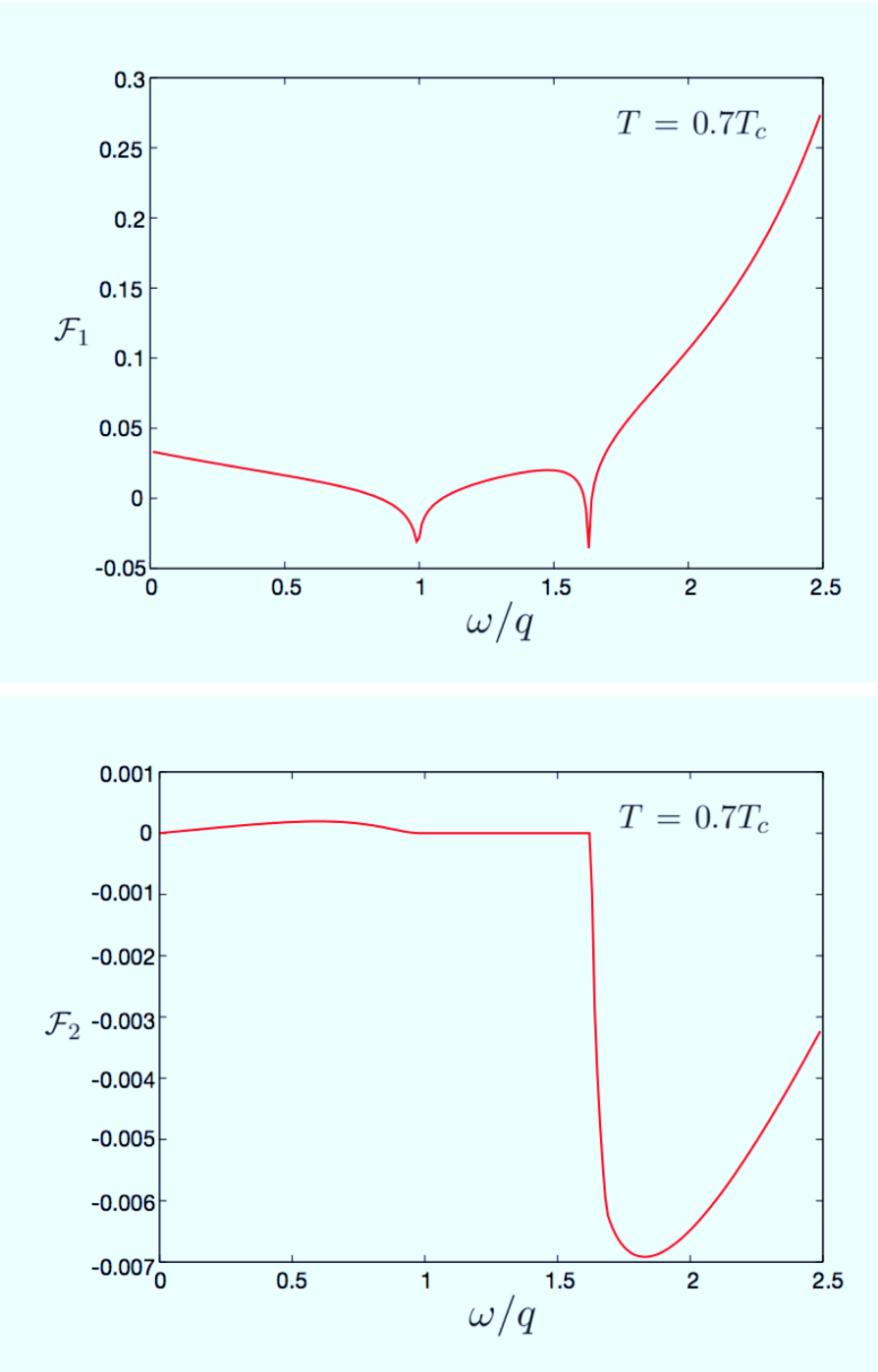

Figure 5.7: Top: $\mathcal{F}_1$ as a function of ω/q at $T = 0.7T_c$. Bottom: $\mathcal{F}_2$ as a function of ω/q at $T = 0.7T_c$.

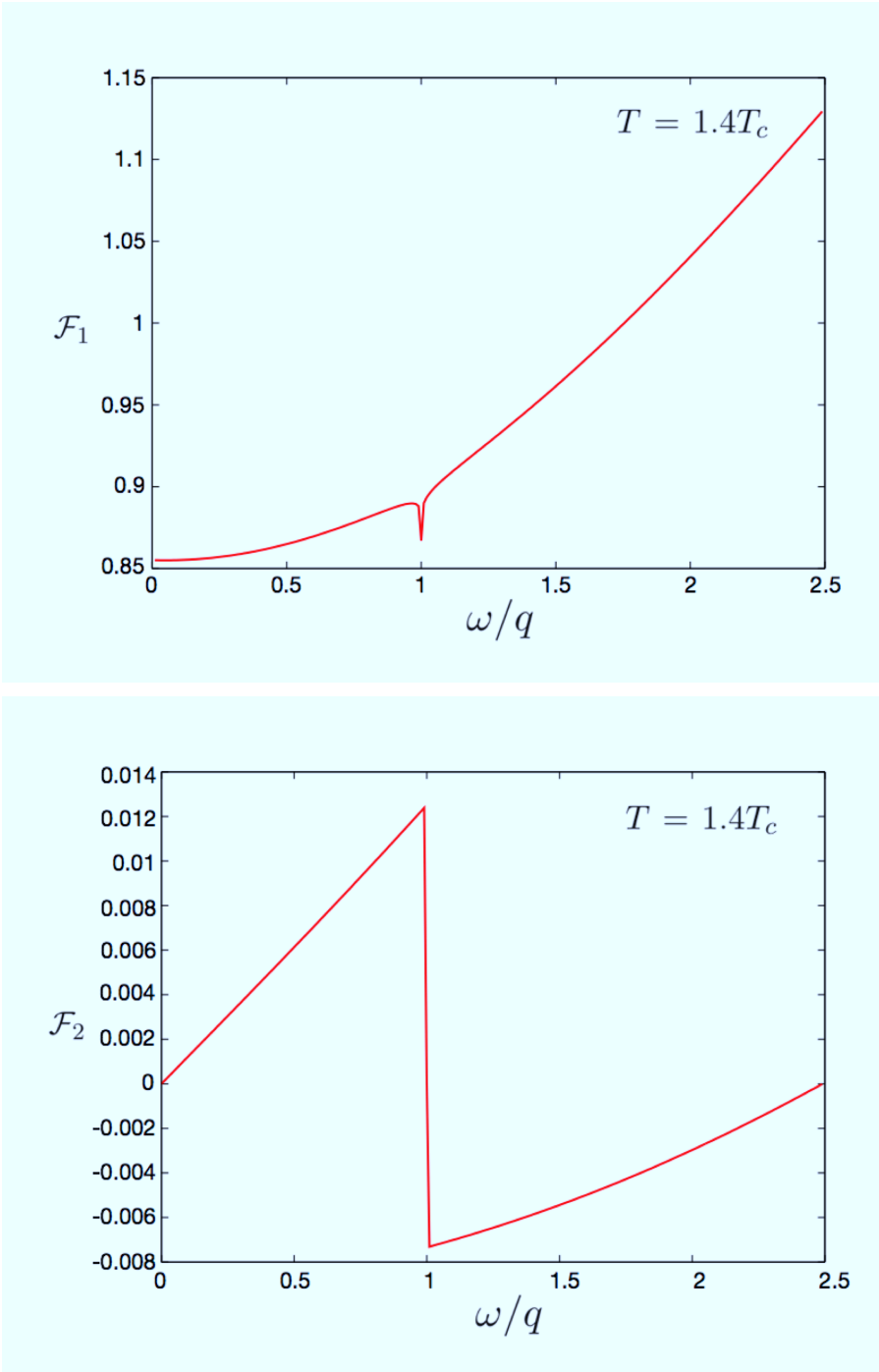

Figure 5.8: Top: $\mathcal{F}_1$ as a function of ω/q at $T = 1.4T_c$. Bottom: $\mathcal{F}_2$ as a function of ω/q at $T = 1.4T_c$.

The case with $m_0 \neq 0$

In the case of the chiral limit, we have found that the contribution from the collective modes among mesonic excitations is much larger than that of the non-collective modes. We anticipate that this conclusion remains unchanged when quarks have a finite bare mass, violating the chiral symmetry explicitly. In this subsection, we show that even if quarks have a finite mass, the collective modes also exist at low temperatures and disappear at high temperatures. In addition, we show that the largest contribution at low temperatures still comes from the collective modes, and that the contribution from the non-collective modes remains negligible, by calculating the integral of the argument of the complex function $\mathcal{M}(\omega \pm i\epsilon, q)$.

When quarks have a finite mass, we cannot separate the collective modes from the non-collective modes easily by factorisation as in Eqs.(5.56) and (5.57). In this case, we first need to determine whether collective modes exist or not. For this reason we calculate the real and imaginary parts of $\mathcal{M}(\omega \pm i\epsilon, q)$ separately given by Eq.(5.85). The condition of isolated meson poles is that both $\mathcal{M}_1$ and $\mathcal{M}_2$ vanish; in particular the condition $\mathcal{M}_1(\omega, q) = 0$ determines the dispersion relation of the collective meson modes.

We show plots of $\mathcal{M}_1$ and $\mathcal{M}_2$ of the pion as a function of ω/q at $q = 240$ MeV in Fig.5.9. At low temperatures, $\mathcal{M}_1$ crosses the horizontal axis in the time-like region, and $\mathcal{M}_2$ is also zero at the value of ω/q where $\mathcal{M}_1$ vanishes. This means that a collective pion mode exists at this point. Furthermore, there are no individual excitations in the region where $\mathcal{M}_2 = 0$, since $\mathcal{M}_2$ is proportional to $\mathcal{F}_2(\omega, q)$, so that the collective pion mode appears in this region as a stable excitation with infinite lifetime. On the other hand, at high temperatures, the region where $\mathcal{M}_2 = 0$ disappears. This means that there are no isolated pion poles with infinite lifetime at high temperatures, even though $\mathcal{M}_1$ becomes zero. The pion would appear as a resonance with a finite decay width, decaying into individual excitations, a phenomenon known as Landau damping.

We also show $\mathcal{M}_1$ and $\mathcal{M}_2$ for the sigma meson as a function of ω/q in Fig. 5.10. The situation is same as the case of the pion. At low temperatures there is an isolated sigma meson pole in the time-like region, while there are no poles at high temperatures.

As shown in the figures both the collective meson modes exist as isolated poles even at T_c which is defined by the maximum of the second derivative of the chiral condensate, or the effective quark mass, with respect to temperature. The pion and the sigma meson spectra become almost degenerate near T_c so that they are absorbed into the continuum almost at the same temperature slightly above T_c. We found no significant q-dependence of the dissociation of the meson poles.

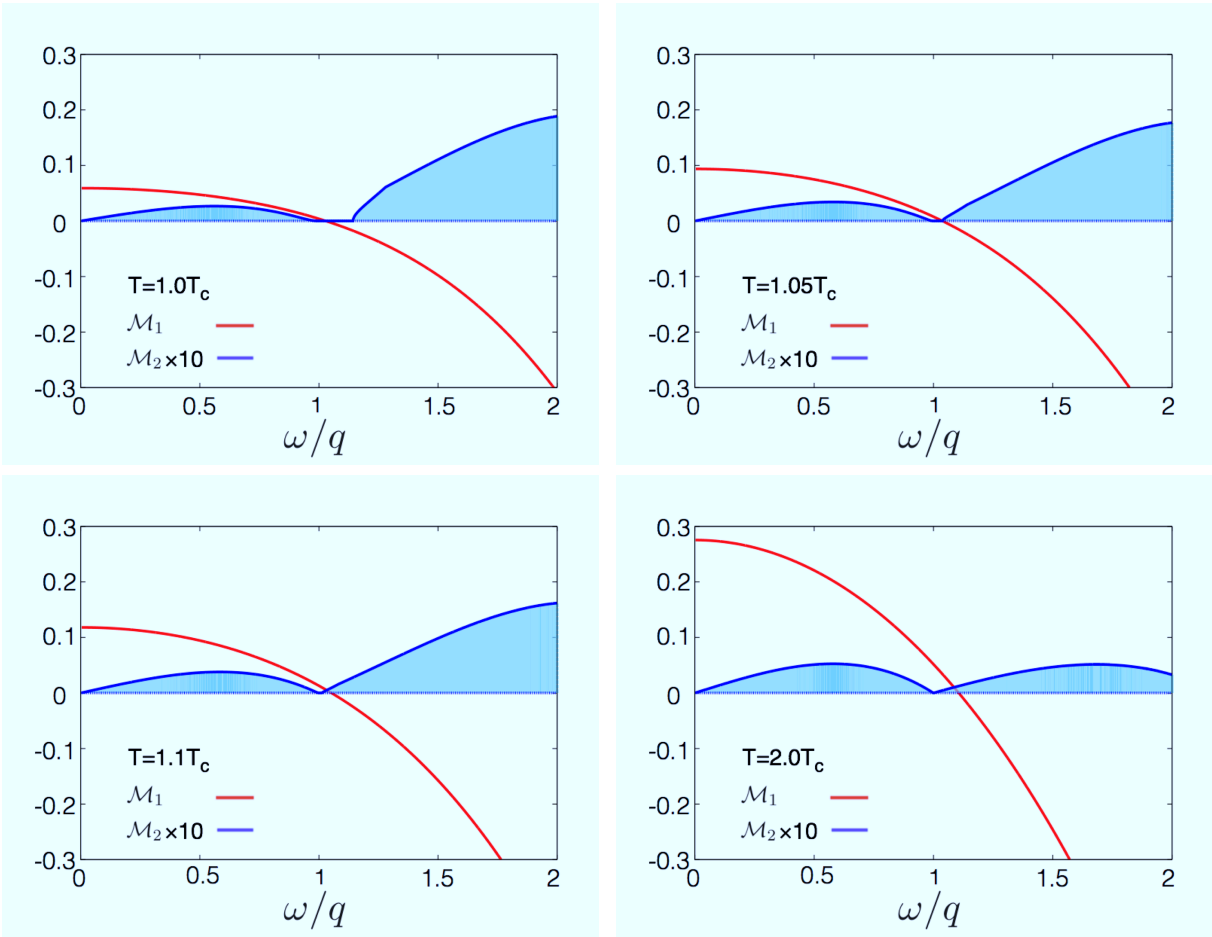

Figure 5.9: $\mathcal{M}_1$ and $\mathcal{M}_2$ of the pion as a function of ω/q at $q = 240$MeV calculated at four different values of the temperature $T/T_c = 1.0, 1.05, 1.1, 2.0$ respectively. The location of the zeros of $\mathcal{M}_1$ are indicated by a cross on the $\mathcal{M}_2$ plots.

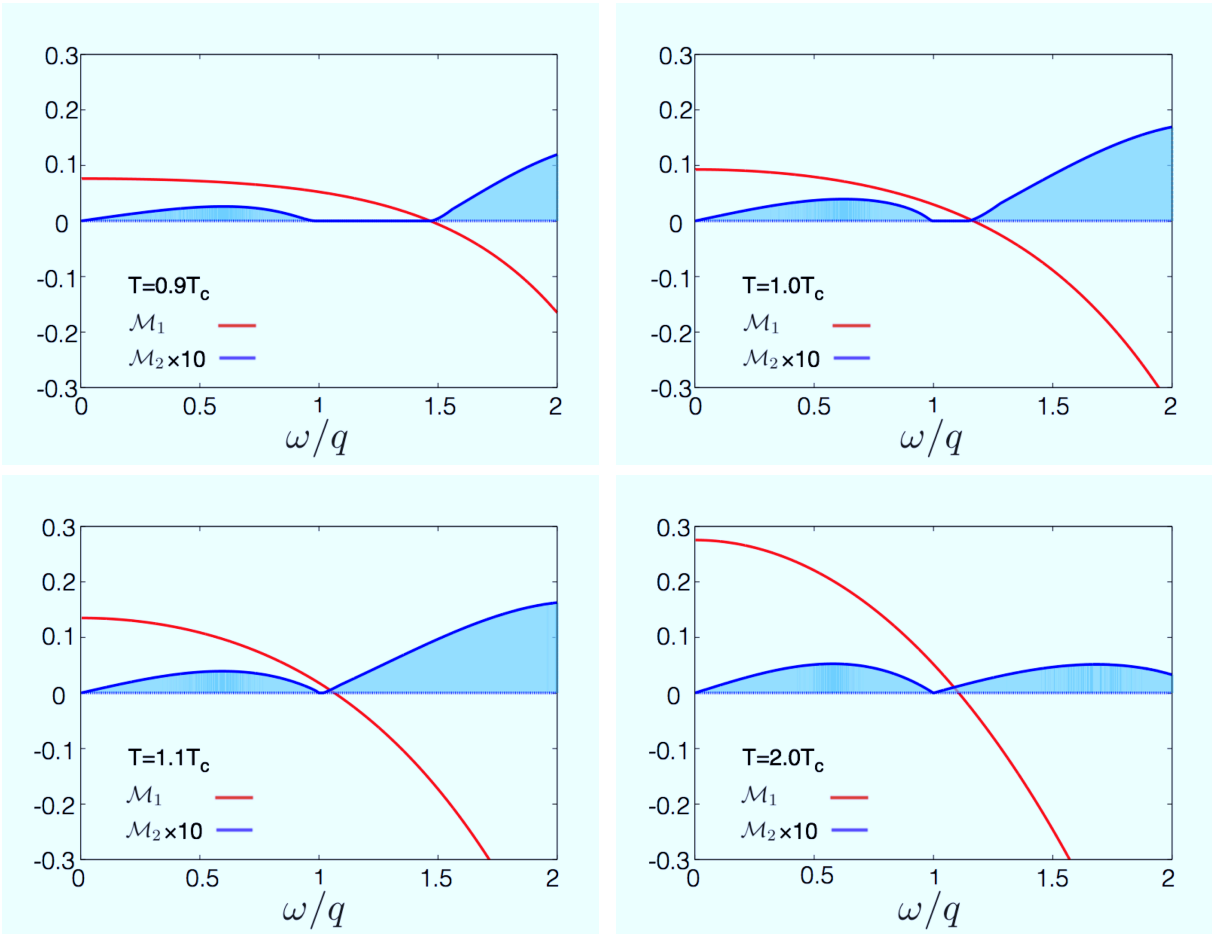

Figure 5.10: $\mathcal{M}_1$ and $\mathcal{M}_2$ for the sigma meson as a function of ω/q at $q = 240$MeV at four different values of the temperature $T/T_c = 0.9, 1.0, 1.1, 2.0$ respectively. The location of the zeros of $\mathcal{M}_1$ are indicated on the $\mathcal{M}_2$ plots.

Chapter 6

Quark-hadron phase transition in the 3-flavour PNJL model at zero chemical potential

In this chapter, we extend our previous study of the quark-hadron phase transition in the two-flavour PNJL model exposed in Chapter 5 to the three-flavour case. As we have seen in chapter 5, the two-flavour PNJL model including mesonic excitations describes the phase transition between the hadronic phase where mesons, especially pions, dominate, to the deconfined phase where the quarks (and gluons added by hand) dominate. However, if we wish to compare the results with experimental data, it is necessary to consider also the role of the strangeness degrees of freedom. Therefore, we extend the two-flavour model to three-flavours along the line of the NJL model without the Polyakov loop [31, 32, 34, 36, 39]. By going from quark fields with two-flavour components to three-flavours, the number of mesons that appear in the effective action also changes. While the two-flavour model contains only four mesons (three pions and a sigma meson), nine pseudo-scalar mesons (3π, $4K$, η and η') and nine scalar mesons (σ, 4κ, f_0 and $3a_0$) appear in the three-flavour model. Regarding the scalar mesons, not all of them have been established by experiments [121] due to their large decay widths. However, some analyses support the existence of the scalar nonet [122–124]. In addition to the change in the quark fields, it is necessary to include a six-point interaction called the Kobayashi-Maskawa-'t Hooft interaction [66,67]. This interaction breaks the axial $U(1)$ symmetry, ensuring the observed mass splitting of the η and the η'.

The extension of the number of flavours has also been performed in the PNJL model [125–128]. However, all of these works have been done in the mean-field approximation, so that the mesonic excitations are absent in these

calculations. In this work, we take mesonic correlations into account in the equation of state and we describe how the degrees of freedom of thermal excitations change from hadrons to quarks and gluons.

In Section 6.1, we introduce a three-flavour PNJL model, that we use in the evaluation of the path integral expression of the partition function. All the NJL type models contain four-point interactions of fermion fields. These four-point quark interactions can be eliminated by a standard Hubbard-Stratonovich transformation in favour of integrable quadratic terms. Three-flavour NJL models have an additional six-point interaction. To eliminate this six-point interaction, we need to introduce "counter terms" generated by the third power of bosonic auxiliary fields, each shifted by the quark bilinear terms with an appropriate normalisation. Intuitively, this procedure can be regarded as reducing the six-point interaction to an effective four-point interactions by replacing one set of quark bilinear terms by its expectation value [34]. In Section 6.2, we summarise the results of the mean-field approximation which freezes the meson fields as background fields. We also show how the effect of the Polyakov loop appears in the equation of state. In Section 6.3, we calculate the contribution of mesonic correlations to the equation of state and we show that the pressure is dominated by the low mass mesons as pseudo-Nambu-Goldstone modes, pions and kaons, at low temperatures, while it is dominated by quarks and gluons at high temperatures. In order to explore what is happening at intermediate temperatures, we also calculate at which temperature the collective mesonic excitations melt into quarks and antiquarks.

6.1 Model set up

In this section, we set the three-flavour PNJL model and derive the thermodynamic potential by calculating the partition function via the path integral. Let us first introduce the Lagrangian of the three-flavour PNJL model:

$$\mathcal{L} = \sum_{i,j=1}^{3} \bar{q}_i (i\not{D} - \hat{m})_{ij} q_j + \mathcal{L}_4 + \mathcal{L}_6 - \mathcal{U}[\bar{\Phi}, \Phi, T], \tag{6.1}$$

where

$$\mathcal{L}_4 = G \sum_{a=0}^{8} \big[(\bar{q}\lambda^a q)^2 + (\bar{q} i\gamma_5 \lambda^a q)^2 \big] \tag{6.2}$$

and

$$\mathcal{L}_6 \;=\; -K \big[\det \bar{q}(1+\gamma_5)q + \det \bar{q}(1-\gamma_5)q \big] \tag{6.3}$$

for three-flavour light quarks, $\bar{q} = (\bar{q}_1, \bar{q}_2, \bar{q}_3) = (\bar{u}, \bar{d}, \bar{s})$. The covariant derivative is $D_\mu = \partial_\mu + g A_0 \delta_{\mu,0}$ where A_0 is the temporal component of the

gauge fields, $A_0 = -iA_4$. Here the gauge field is not treated as a dynamical variable, but as an external parameter like an imaginary chemical potential which depends on the colour of the quarks. $\hat{m}$ is a 3×3 mass matrix, giving the bare quark masses m_u, m_d and m_s for u, d and s quarks, respectively. In the subsequent calculations, we set $m_u = m_d = m$, assuming isospin symmetry.

$\mathcal{L}_4$ is a four-point interaction between quarks and antiquarks (Fig.6.1, (a)), with the coupling strength G. The λ^a are 3×3 matrices in flavour space, with a running from 0 to 8. The λ^1 to λ^8 are the Gell-Mann matrices and λ^0 is proportional to the identity matrix, $\sqrt{2/3}I$. $\mathcal{L}_6$ is a six-point interaction, called the Kobayashi-Maskawa-'t Hooft interaction (Fig.6.1, (b)) with an interaction strength K. Since q and $\bar{q}$ both have three components in flavour $SU(3)$, $\mathcal{L}_6$ consists of 6th order terms in the fermion fields. It can be written in the following form [35, 129]:

$$\mathcal{L}_6 = \frac{K}{6} d_{abc} \Big[\frac{1}{3} (\bar{q}\lambda^i q)(\bar{q}\lambda^j q) + (\bar{q}\gamma_5\lambda^i q)(\bar{q}\gamma_5\lambda^j q) \Big] (\bar{q}\lambda^k q), \tag{6.4}$$

where d_{abc} are the symmetric invariants of $SU(3)$ for $a = 1, \cdots, 8$, in addition $d_{000} = \sqrt{2/3}$, $d_{0bc} = -\sqrt{1/6}$ $(b, c \neq 0)$.

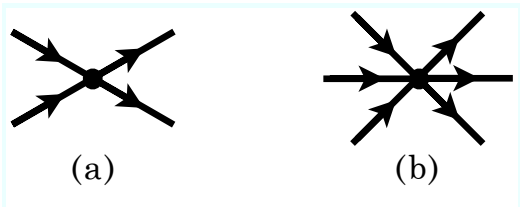

Figure 6.1: (a) 4-point interaction, (b) 6-point interaction.

We use the same effective potential $\mathcal{U}[\bar{\Phi}, \Phi, T]$ as in the two-flavour case studied in Chapter 5, because $\mathcal{U}[\bar{\Phi}, \Phi, T]$ is chosen to mimic the features of the pure gauge theory, so that it is independent of the number of flavours.

$$\mathcal{U}[\bar{\Phi}, \Phi, T]/T^4 = -\frac{1}{2} b_2(T) \bar{\Phi}\Phi - \frac{1}{6} b_3(\bar{\Phi}^3 + \Phi^3) + \frac{1}{4} b_4 (\bar{\Phi}\Phi)^2 \tag{6.5}$$

with

$$b_2(T) = a_0 + a_1 \Big(\frac{T_0}{T}\Big) + a_2 \Big(\frac{T_0}{T}\Big)^2 + a_3 \Big(\frac{T_0}{T}\Big)^3, \tag{6.6}$$

where

$$\Phi = \frac{1}{3} \langle \mathrm{tr}_c L \rangle, \qquad \bar{\Phi} = \frac{1}{3} \langle \mathrm{tr}_c L^\dagger \rangle. \tag{6.7}$$

We note that the relation between L in Eq.(6.7) and the Polyakov loop defined by

$$L(\mathbf{r}) = \mathcal{P}\exp\Big[ig\int_0^\beta d\tau A_4(\mathbf{r},\tau)\Big] \tag{6.8}$$

is not strict. Indeed, in the description of Eq.(6.7) the quarks are embedded in a uniform background gauge field, not fluctuating either in space or in imaginary time.

The parameters in the effective potential $\mathcal{U}[\bar{\Phi},\Phi,T]$ is summarised in Table 6.1.

Table 6.1: Parameters

a_0	a_1	a_2	a_3	b_3	b_4	T_0
6.75	-1.95	2.625	-7.44	0.75	7.5	270 MeV

The partition function is given by

$$Z(T,A_4) = \int [dq][d\bar{q}]\exp\Big[\int_0^\beta d\tau \int d^3x\mathcal{L}(q,\bar{q},A_4)\Big]. \tag{6.9}$$

From the interaction terms, this model can incorporate correlations which generate pseudo-scalar mesons and scalar mesons. For pseudo-scalar mesons, there are nine mesons, three kinds of π, four kinds of K, η and η'. They form a nonet in SU(3) flavour classification. In the chiral limit, the mass of all mesons is exactly zero, and they appear as massless Nambu-Goldstone modes. The axial U(1) symmetry is broken by the 6-point interaction, making the η^0 massive. In addition, the SU(3) flavour symmetry is broken due to the non-vanishing bare quark masses, m_u, m_d, m_s, generating the physical mass of each meson.

There also appear nine scalar mesons in this scheme, not all of which are confirmed by experiments. Especially, the existence of the κ is still very controversial. Besides the κ, all the other scalar mesons are listed in the data compiled by the particle data group [121].

The original model Lagrangian contains 4th and 6th power in the fermion fields. These non-quadratic terms make it difficult to perform the fermion integrals in the partition function. In the two-flavour case, the PNJL model has only four-point interactions that we could eliminate by generating "counter terms" contained in the square of the auxiliary bosonic field shifted by the quadratic quark fields. Then, integration of the quark fields can be performed analytically and the partition function is written in terms of path integral over the newly introduced bosonic fields. This standard Hubbard-Stratonovich transformation [108, 109] cannot be applied directly in the presence of the six-point fermionic interaction. In order to eliminate the

six-point interaction, we need to introduce extra "counter terms" generated by the third power of the auxiliary bosonic fields shifted by a bilinear form of the quark fields with appropriate normalisation, reducing the six-point interaction to same effective four-point interactions. This procedure shifts the coupling G of the 4th order term in the quark fields, which can then be eliminated by the standard procedure.

To be more explicit, we introduce auxiliary bosonic fields ϕ^a and π^a coupled to the quark scalar densities $\bar{q}\lambda^a q$ and to the pseudo-scalar density $i\bar{q}\gamma_5\lambda^a q$ respectively by multiplying $Z(T, A_4)$ by a constant dummy integral:

$$\int [d\phi][d\pi]\exp\Big(\int_0^\beta d\tau \int d^3x \mathcal{L}_b(\phi,\pi)\Big) \tag{6.10}$$

with

$$\begin{aligned}
\mathcal{L}_b \;=\; & \frac{K}{24G^3} d_{abc}(\phi^a - 2G\bar{q}\lambda^a q)\big[\frac{1}{3}(\phi^b - 2G\bar{q}\lambda^b q)(\phi^c - 2G\bar{q}\lambda^c q) \\
& +(\pi^b - 2Gi\bar{q}\lambda^b\gamma_5 q)(\pi^c - 2Gi\bar{q}\lambda^c\gamma_5 q)\big] \\
& +\frac{K}{24G^2} d_{abc}\phi^a\big[(\phi^b - 2G\bar{q}\lambda^b q)(\phi^c - 2G\bar{q}\lambda^c q) \\
& +(\pi^b - 2Gi\bar{q}\lambda^b\gamma_5 q)(\pi^c - 2Gi\bar{q}\lambda^c\gamma_5 q)\big] \\
& -\frac{1}{4G}\big[(\phi^a - 2G\bar{q}\lambda^a q)^2 + (\pi^a - 2Gi\bar{q}\lambda^a\gamma_5 q)^2\big].
\end{aligned} \tag{6.11}$$

Only even terms in the pseudo-scalar fields can appear in order to respect the Lorentz symmetry of the Lagrangian. The desired "counter terms" for the six-point quark interactions can be found in the expansion of the first term, which however also generates additional four-point quark interactions, that are removed by the "counter term" generated by the second term. The third term is introduced in order to eliminate the four-point quark interactions in the original Lagrangian.

Adding $\mathcal{L}_b$, the original Lagrangian is converted to a form which contains the quark fields only up to order two, in addition to second and third power terms in the auxiliary bosonic fields:

$$\begin{aligned}
\mathcal{L} + \mathcal{L}_b \;=\; & \sum_{i,j=1}^{3} \bar{q}_i(i\not{D} - \hat{m} - \Sigma(\phi_a,\pi_a))_{ij} q_j + \frac{K}{18G^3} d_{abc}\phi^a\phi^b\phi^c \\
& -\frac{K}{6G^3} d_{abc}\phi^a\pi^b\pi^c - \frac{1}{4G}(\phi_a^2 + \pi_a^2) - \mathcal{U}[\bar{\Phi},\Phi,T],
\end{aligned} \tag{6.12}$$

where

$$\Sigma(\phi_a,\pi_a) = \frac{K}{4G^2} d_{abc}\lambda^a\phi^b\phi^c - \lambda^a\big[\phi^a + i\gamma_5\pi^a\big] \tag{6.13}$$

is the self-energy matrix of quark quasiparticles due to the coupling to the auxiliary fields.

Now the integration over the Grassmann quark fields can be performed and we obtain the partition function written in terms of the auxiliary bosonic fields ϕ_a and π_a:

$$Z(T, A_4) = \int [d\phi][d\pi] e^{-I(\phi,\pi,A_4)}, \tag{6.14}$$

where

$$\begin{aligned} I(\phi, \pi, A_4) &= -\int_0^\beta d\tau \int d^3x \big[\mathrm{tr}_q \, \ln(\beta S_E^{-1}) + \frac{K}{18G^3} d_{abc}\phi^a\phi^b\phi^c \\ &\quad - \frac{K}{6G^3} d_{abc}\phi^a\pi^b\pi^c - \frac{1}{4G}(\phi_a^2 + \pi_a^2) - \mathcal{U}[\bar{\Phi}, \Phi, T] \big] \end{aligned} \tag{6.15}$$

with the inverse Euclidean quark propagator given by

$$S_E^{-1} = i\not{D}_E + \hat{m} + \Sigma(\phi, \pi, A_4) \tag{6.16}$$

with $\not{D}_E = \sum_{i=1,\cdots,3} \gamma_i \partial_i + \gamma_4(\partial_\tau + igA_4)$. The trace tr_q includes sums over the colour and the Dirac spinor indices of the quark fields.

In order to calculate the pressure of mesonic correlations, we expand the effective action up to the second order in the fluctuations around the stationary point, $\varphi_a = \phi_a - \bar{\phi}_a$,

$$I(\phi, \pi, A_4) = I_0 + \frac{1}{2} \left. \frac{\delta^2 I}{\delta\phi_a \delta\phi_b} \right|_{\phi=\bar{\phi}} \varphi_a\varphi_b \; + \frac{1}{2} \left. \frac{\delta^2 I}{\delta\pi_a \delta\pi_b} \right|_{\phi=\phi_0} \pi_a\pi_b \; \cdots \tag{6.17}$$

with

$$I_0 = I(\bar{\phi}, \pi = 0, A_4), \tag{6.18}$$

where the stationary value of $\bar{\phi}_a$ is determined by the condition:

$$\left. \frac{\delta I}{\delta\phi_a} \right|_{\phi=\bar{\phi}} = 0. \tag{6.19}$$

We have assumed that the stationary values of the pseudo-scalar fields π_a all vanish. Keeping only terms up to quadratic order in the expansion,

$$\begin{aligned} &Z(T, A_4) \simeq e^{-I_0} \\ &\times \int [d\phi][d\pi] \exp\left[-\frac{1}{2} \left. \frac{\delta^2 I}{\delta\phi_a \delta\phi_b} \right|_{\phi=\bar{\phi}} \varphi_a\varphi_b - \frac{1}{2} \left. \frac{\delta^2 I}{\delta\pi_a \delta\pi_b} \right|_{\phi=\bar{\phi}} \pi_a\pi_b \right]. \end{aligned} \tag{6.20}$$

If we stop the expansion at the second order in the fluctuations, ignoring the meson interactions, we can perform the Gaussian integral over the meson fields. Then, we get the following thermodynamic potential;

$$\Omega(T, A_4) = -T \ln Z \tag{6.21}$$

$$= T\Big(I_0 + \frac{1}{2} \mathrm{Tr}_M \ln \frac{\delta^2 I}{\delta\phi_a \delta\phi_b} + \frac{1}{2} \mathrm{Tr}_M \ln \frac{\delta^2 I}{\delta\pi_a \delta\pi_b} \Big). \tag{6.22}$$

The first term of Eq.(6.22) represents the thermodynamic potential in the mean-field approximation and the second and third terms represent the contribution of mesonic correlations to the thermodynamic potential.

6.2 Mean-field approximation

6.2.1 Pressure in the mean-field approximation

The thermodynamic potential in the mean-field approximation, $\Omega_{MF}(T, A_4)$ and the corresponding pressure $p_{MF}(T, A_4)$ are related to the leading term of the effective action Eq.(6.17), I_0 :

$$\Omega_{MF}(T, A_4) = TI_0 = -p_{MF}(T, A_4)V. \tag{6.23}$$

The explicit form of the leading term I_0 is given by

$$\begin{aligned} I_0 &= \beta V\Big[\frac{1}{4G}(\bar{\phi}_u^2 + \bar{\phi}_d^2 + \bar{\phi}_s^2) - \frac{K}{2G^3}\bar{\phi}_u\bar{\phi}_d\bar{\phi}_s \\ &- 2V\sum_i\sum_n\int\frac{d^3p}{(2\pi)^3}\mathrm{tr}_c\ln\big[\beta^2\big((\epsilon_n - gA_4)^2 + \mathbf{p}^2 + M_i^2\big)\big]\Big] \\ &+ \beta V\mathcal{U}[\bar{\Phi}, \Phi, T], \end{aligned} \tag{6.24}$$

where the ϵ_n are the fermionic Matsubara frequencies, $\epsilon_n = (2n+1)\pi T$. The trace is to be performed over the 3×3 colour matrix A_4. We have introduced for convenience the following notations:

$$\bar{\phi}_u \equiv 2G\langle\bar{u}u\rangle = \frac{2}{\sqrt{6}}\bar{\phi}_0 + \bar{\phi}_3 + \frac{2}{2\sqrt{3}}\bar{\phi}_8 \tag{6.25}$$

$$\bar{\phi}_d \equiv 2G\langle\bar{d}d\rangle = \frac{2}{\sqrt{6}}\bar{\phi}_0 - \bar{\phi}_3 + \frac{2}{2\sqrt{3}}\bar{\phi}_8 \tag{6.26}$$

$$\bar{\phi}_s \equiv 2G\langle\bar{s}s\rangle = \frac{2}{\sqrt{6}}\bar{\phi}_0 - \frac{2}{\sqrt{3}}\bar{\phi}_8 \tag{6.27}$$

as implied by the relation $\bar{\phi}_a = G\langle\bar{q}\lambda_a q\rangle$ in the mean-field approximation. The constituent quark masses M_i are given in terms of the quantities $\langle\bar{q}_i q_i\rangle$ defined by Eqs.(6.25)-(6.27);

$$M_u = m_u - 4G\langle\bar{u}u\rangle + 2K\langle\bar{d}d\rangle\langle\bar{s}s\rangle \tag{6.28}$$

$$M_d = m_d - 4G\langle\bar{d}d\rangle + 2K\langle\bar{s}s\rangle\langle\bar{u}u\rangle \tag{6.29}$$

$$M_s = m_s - 4G\langle\bar{s}s\rangle + 2K\langle\bar{u}u\rangle\langle\bar{d}d\rangle. \tag{6.30}$$

$\langle\bar{q}_i q_i\rangle$ is related to the Euclidean i-quark propagator $S_E^i = (i\not{D}_E + M_i)^{-1}$ by

$$\langle\bar{q}_i q_i\rangle = -i\mathrm{Tr}S_E^i = T\sum_n\int\frac{d^3p}{(2\pi)^3}\frac{M_i}{(\epsilon_n - gA_4)^2 + \mathbf{p}^2 + M_i^2}, \tag{6.31}$$

where the fermionic Matsubara frequency sum can be evaluated by the method of contour integration. This leads to

$$\langle \bar{q}_i q_i \rangle = \int \frac{d^3p}{(2\pi)^3} \frac{M_i}{E_i(p)} \left[-1 + 2f(E_i(p) - igA_4) \right] \tag{6.32}$$

with $E_i(p) = \sqrt{\mathbf{p}^2 + M_i^2}$ and

$$f(E) = \frac{1}{e^{\beta E} + 1}. \tag{6.33}$$

Eqs.(6.28)-(6.30) can also be written as

$$M_i = m_i + 4iG\mathrm{tr}S_E^i - 2K\epsilon_{ijk}(\mathrm{tr}S_E^j)(\mathrm{tr}S_E^k), \tag{6.34}$$

which are equivalent to the stationarity conditions for the auxiliary scalar fields Eq.(6.19). These equations are a three-flavour extension of the Nambu-Jona-Lasinio gap equation that determines the quark masses M_i (gaps in the single particle energy spectra) self-consistently.

In the following calculation, we assume unbroken isospin symmetry so that the u and d quarks are degenerate. We then obtain the pressure in the mean-field approximation for the three-flavour model,

$$\begin{aligned} p_{MF}(T, A_4) &= -\frac{1}{4G}(2\bar{\phi}_u^2 + \bar{\phi}_s^2) + \frac{K}{2G^3}\bar{\phi}_u^2\bar{\phi}_s \\ &+ 2T\sum_i \sum_n \int \frac{d^3p}{(2\pi)^3} \mathrm{tr}_c \ln\left[\beta^2\left((\epsilon_n - gA_4)^2 + \mathbf{p}^2 + M_i^2\right)\right] \\ &- \mathcal{U}[\bar{\Phi}, \Phi, T]. \end{aligned} \tag{6.35}$$

Evaluating the discrete sum over the Matsubara frequencies by the standard method of contour integration, we find

$$\begin{aligned} p_{MF}(T, A_4) = p_{MF}^0 + 2\sum_i \int \frac{d^3p}{(2\pi)^3} \frac{\mathbf{p}^2}{3E_i} \mathrm{tr}_c\left[f(E_i + igA_4) + f(E_i - igA_4)\right] \\ -\mathcal{U}[\bar{\Phi}, \Phi, T], \end{aligned} \tag{6.36}$$

where

$$p_{MF}^0 = 3 \times 2 \sum_i \int_f^\Lambda \frac{d^3p}{(2\pi)^3} E_i(p) - \frac{1}{4G}(2\bar{\phi}_u^2 + \bar{\phi}_s^2) + \frac{K}{2G^3}\bar{\phi}_u^2\bar{\phi}_s \tag{6.37}$$

is the pressure due to the quark condensate and the zero point motion of the quark quasiparticles with energy $E_i = \sqrt{\mathbf{p}^2 + M_i^2}$ ($i = u, d, s$) .

$$f(E_i \pm igA_4) = \frac{1}{e^{\beta(E_i \pm igA_4)} + 1} \tag{6.38}$$

is the quark (antiquark) quasiparticle distribution function in an external gauge field.

In the above expressions, the constant temporal gauge field A_4 appears as a phase factor together with the quark quasiparticle energy in the quark (antiquark) distribution function. We then replace $\langle \frac{1}{3}\mathrm{tr}_c f(E_i + igA_4)\rangle$ by

$$f_\Phi(E_i) = \frac{\bar{\Phi}e^{2\beta E_i} + 2\Phi e^{\beta E_i} + 1}{e^{3\beta E_i} + 3\bar{\Phi}e^{2\beta E_i} + 3\Phi e^{\beta E_i} + 1}, \tag{6.39}$$

where $\Phi = \frac{1}{3}\langle \mathrm{tr}_c L\rangle$ and $\bar{\Phi} = \frac{1}{3}\langle \mathrm{tr}_c L^\dagger\rangle$. Φ and $\bar{\Phi}$ behave as an order parameter of the deconfinement phase transition.

We apply the same procedure to the quark condensates that appear in the gap equation, so that $\langle \bar{q}_i q_i\rangle$ is replaced by

$$\langle \bar{q}_i q_i\rangle \quad = \quad -\int_f^\Lambda \frac{d^3p}{(2\pi)^3}\frac{M_i}{E_i(p)} + 2\int \frac{d^3p}{(2\pi)^3}\frac{M_i}{E_i(p)} f_\Phi(E_i(p)), \tag{6.40}$$

where we have indicated a momentum cutoff at $p = \Lambda_f$ in the otherwise ultraviolet divergent vacuum polarisation term.

After replacing the quark distribution function by the statistical average over the gauge field A_4, the pressure in the mean-field approximation is given by

$$p_{MF}(T) = p^0_{MF} + 2\times 3\sum_i \int \frac{d^3p}{(2\pi)^3}\frac{\mathbf{p}^2}{3E_i} f_\Phi(E_i) - \mathcal{U}[\bar{\Phi}, \Phi, T]. \tag{6.41}$$

6.2.2 Behaviour of the order parameters

We show in Fig.6.2 the temperature dependence of the order parameters, the amplitudes of the chiral condensates $\langle \bar{u}u\rangle$, $\langle \bar{s}s\rangle$ and the expectation value of the Polyakov loop $\langle l\rangle = \Phi$. Since both the chiral and the deconfinement transitions are crossovers in this calculation, T_c is a pseudo critical temperature determined by the maximum of the chiral susceptibility, the second derivative of the pressure with respect to $\langle \bar{u}u\rangle$. In this calculation, T_c is found to be 220MeV.

Table 6.2: Parameters

$m_u = m_d$	m_s	Λ_f	$G\Lambda_f^2$	$K\Lambda_f^5$
5.5 MeV	140.7 MeV	602.3 MeV	1.835	12.36

We choose the values of the parameters in accordance with [38]; $m_u = m_d = 5.5$MeV, $m_s = 140.7$MeV, $\Lambda_f = 602.3$MeV, $G\Lambda_f^2 = 1.835$ and $K\Lambda_f^5 = 12.36$. These parameters are determined in order to reproduce the pion

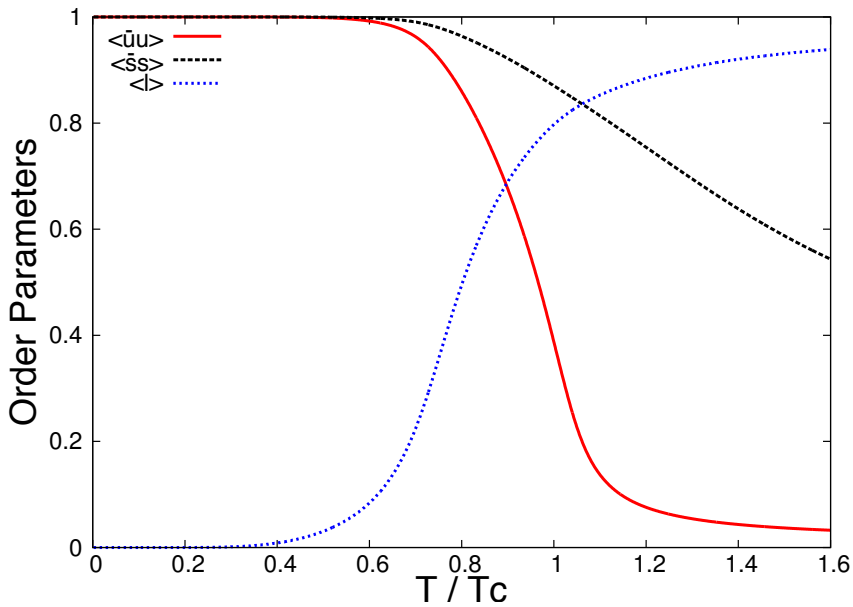

Figure 6.2: Temperature dependence of the order parameters in the mean-field approximation. The bare quark mass is taken to be 5.5 MeV for the u and d quarks, and 140.7 MeV for the s quark. The chiral condensates are normalised by their vacuum expectation values: $\langle \bar{u}u \rangle^{1/3} = -241.9$ MeV, $\langle \bar{s}s \rangle^{1/3} = -257.7$ MeV.

mass $m_\pi = 135.0$MeV, the kaon mass $m_K = 497.7$MeV, the η' mass $m_{\eta'} = 957.8$MeV and the pion decay constant $f_\pi = 92.4$MeV in the vacuum. Note that the Polyakov loop enters only through the quark distribution function so that it does not appear in the vacuum. This implies that our procedure to set the values of the parameters from physical observables in the vacuum is the same as the one taken for the NJL model without the Polyakov loop. The solid red line and the dotted black line are the two chiral condensates, $\langle \bar{u}u \rangle$, $\langle \bar{s}s \rangle$ respectively, scaled by their respective vacuum expectation values. The dotted blue line is the expectation value of the Polyakov loop which characterises the deconfinement transition. The amplitude of the u-quark condensate approaches zero rapidly at temperatures above T_c, while that of the s-quark condensate remains non-zero even at higher temperature due to the larger bare s-quark mass, which is comparable to T_c.

We plot the pressure in the mean-field approximation in Fig.6.3. The solid red line (the dotted blue line) is calculated in the mean-field approximation with (without) the effective potential of the Polyakov loop $\mathcal{U}[\bar{\Phi}, \Phi, T]$, which gives the gluon pressure. The dotted blue line is the pressure only due to the quark quasiparticles. The dotted pink line is the pressure calculated in the NJL model. Comparing the pink and the blue lines, one sees that the quark pressure becomes almost zero at low temperatures because the quark excitations are strongly suppressed by the Polyakov loop in the confined phase, while they persist even at low temperatures in the NJL model without the Polyakov loop.

6.3 Mesonic fluctuations

In the previous section, we have discussed the equation of state obtained in the mean-field approximation with the three-flavour PNJL model. We have observed that the Polyakov loop suppresses the quark pressure in the low temperature confined phase. Now we explore how the mesonic correlations contribute to the equation of state in this section.

The pressure from the mesonic correlations can be calculated from the second and the third terms of Eq.(6.22) for the thermodynamic potential. By the thermodynamic relation $pV = -T\Omega$, the pressure of the mesonic correlations in the background gauge field A_4 is given by

$$p_M(T, A_4) = -\frac{T}{2V}\big(\mathrm{Tr}_M \ln \frac{\delta^2 I}{\delta\phi_a \delta\phi_b} + \mathrm{Tr}_M \ln \frac{\delta^2 I}{\delta\pi_a \delta\pi_b}\big), \tag{6.42}$$

where I is the effective action given in Eq.(6.17). The first term comes from scalar mesons and the second term is from pseudo-scalar mesons. The indices a and b in Eq.(6.42) run from 0 to 8 in the SU(3) flavour space. The trace Tr_M is taken over the space-time coordinates of the auxiliary meson fields which obey a periodic boundary condition in the imaginary time direction.

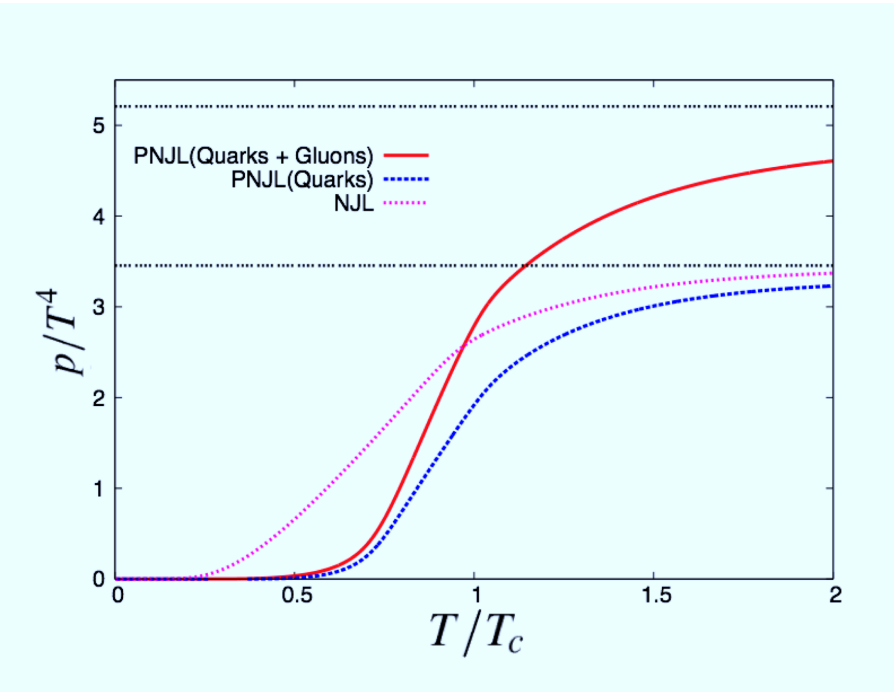

Figure 6.3: Pressure in the mean-field approximation. The dotted blue line is the pressure of quarks calculated with the PNJL model, the solid red line includes the gluon pressure coming from the effective potential of the Polyakov loop. The dotted pink line is the quark pressure calculated with the NJL model without confinement, which allows quark excitations even at low temperatures. In the PNJL model both the quark and the gluon pressures decrease rapidly below the crossover region due to the Polyakov loop which suppresses the quark distribution in the confined phase. The pressures of the massless quark gas and the gas of massless quarks and gluons are indicated by the lower and upper horizontal dashed lines, respectively.

From Eqs.(6.17) and (6.42), we find

$$
\begin{aligned}
p_M &= -\sum_n \int \frac{d^3q}{(2\pi)^3} \Big\{ 3\ln\mathcal{M}_\pi(\omega_n,q) + 4\ln\mathcal{M}_K(\omega_n,q) + \ln\mathcal{M}_\eta(\omega_n,q) \\
&\qquad + \ln\mathcal{M}_{\eta'}(\omega_n,q) + \ln\mathcal{M}_\sigma(\omega_n,q) + 4\ln\mathcal{M}_\kappa(\omega_n,q) \\
&\qquad + 3\ln\mathcal{M}_{a_0}(\omega_n,q) + \ln\mathcal{M}_{f_0}(\omega_n,q) \Big\},
\end{aligned}
\tag{6.43}
$$

where $\mathcal{M}_\alpha$ measures the Gaussian fluctuation of the Fourier component of the mesonic auxiliary fields in the mesonic channel $\alpha(=\pi, K, \eta, \eta', \sigma, \kappa, a_0, f_0)$ with the Matsubara frequencies $\omega_n = 2n\pi T$ and the spatial inverse wavelength q. It contains the information about the existence of collective mesonic excitations in each channel. It can be written in the form

$$
\mathcal{M}_\alpha(\omega_n,q) = \frac{1}{2G'_\alpha} - \Pi_\alpha(\omega_n,q), \tag{6.44}
$$

where $\Pi_\alpha(\omega_n,q)$ is the quark polarisation for each mesonic channel α. We have

$$
\begin{aligned}
\Pi_\alpha(\omega_n,q) &= \beta \sum_m \int \frac{d^3p}{(2\pi)^3} \\
&\quad \times \langle \mathrm{tr}_q \big(\Lambda_\alpha S_E(\omega_n+\epsilon_m, \mathbf{p}+\mathbf{q}, A_4) \Lambda_\alpha S_E(\epsilon_m, \mathbf{p}, A_4) \big) \rangle
\end{aligned}
\tag{6.45}
$$

for the scalar fields (channels $\alpha = \sigma, \kappa, a_0, f_0$) and

$$
\begin{aligned}
\Pi_\alpha(\omega_n,q) &= \beta \sum_m \int \frac{d^3p}{(2\pi)^3} \\
&\quad \times \langle \mathrm{tr}_q \big(\Lambda_\alpha \gamma_5 S_E(\omega_n+\epsilon_m, \mathbf{p}+\mathbf{q}, A_4) \Lambda_\alpha \gamma_5 S_E(\epsilon_m, \mathbf{p}, A_4) \big) \rangle
\end{aligned}
\tag{6.46}
$$

for the pseudo-scalar fields ($\alpha = \pi, K, \eta, \eta'$) while Λ_α is the projector onto the flavour channel α. Each term in the right hand side of Eq.(6.43) is multiplied by the appropriate degeneracy factor: 3 for pions, 4 for kaons, *etc.*

G'_α in Eq.(6.44) is the effective four-point coupling, combination of the original four-point coupling G and the additional four-point coupling generated from the six-point coupling K with appropriate weight for each channel, as indicated pictorially in Fig. 6.4. The explicit form of G' will be given for each meson channel in the following subsections. We note here that this effective four-point coupling depends on the condensate $\langle \bar{q}_i q_j \rangle$ so that it depends on the temperature.

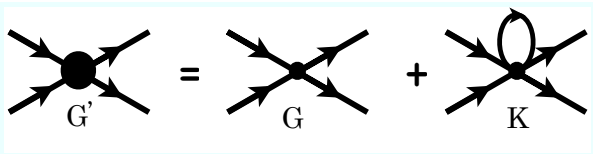

Figure 6.4: The effective four-point coupling G' is a sum of the original coupling G and the coupling induced by the six-point coupling in the presence of the condensate.

The discrete Matsubara frequency sum in Eq.(6.43) for the mesonic correlation pressure can be transformed by the method of contour integration into an integral along the positive real ω axis:

$$\begin{aligned} p_M = &-\int \frac{d^3q}{(2\pi)^3}\int_0^\infty \frac{d\omega}{2\pi i}\left[1+\frac{2}{e^{\beta\omega}-1}\right] \\ &\times\Big\{3\ln\left[\frac{\tilde{\mathcal{M}}_\pi(\omega-i\delta,q)}{\tilde{\mathcal{M}}_\pi(\omega+i\delta,q)}\right]+4\ln\left[\frac{\tilde{\mathcal{M}}_K(\omega-i\delta,q)}{\tilde{\mathcal{M}}_K(\omega+i\delta,q)}\right] \\ &+\ln\left[\frac{\tilde{\mathcal{M}}_\eta(\omega-i\delta,q)}{\tilde{\mathcal{M}}_\eta(\omega+i\delta,q)}\right]+\ln\left[\frac{\tilde{\mathcal{M}}_{\eta'}(\omega-i\delta,q)}{\tilde{\mathcal{M}}_{\eta'}(\omega+i\delta,q)}\right] \\ &+\ln\left[\frac{\tilde{\mathcal{M}}_\sigma(\omega-i\delta,q)}{\tilde{\mathcal{M}}_\sigma(\omega+i\delta,q)}\right]+4\ln\left[\frac{\tilde{\mathcal{M}}_\kappa(\omega-i\delta,q)}{\tilde{\mathcal{M}}_\kappa(\omega+i\delta,q)}\right] \\ &+3\ln\left[\frac{\tilde{\mathcal{M}}_{a_0}(\omega-i\delta,q)}{\tilde{\mathcal{M}}_{a_0}(\omega+i\delta,q)}\right]+\ln\left[\frac{\tilde{\mathcal{M}}_{f_0}(\omega-i\delta,q)}{\tilde{\mathcal{M}}_{f_0}(\omega+i\delta,q)}\right]\Big\}, \end{aligned} \tag{6.47}$$

where

$$\tilde{\mathcal{M}}_\alpha(\omega,q)\equiv\mathcal{M}_\alpha(-i\omega,q)=\frac{1}{2K'_\alpha}-\tilde{\Pi}_\alpha(\omega,q) \tag{6.48}$$

with

$$\begin{aligned} \tilde{\Pi}_\alpha(\omega,q) \;=\; &\int\frac{d^3p}{(2\pi)^3}\int_0^\infty\frac{d\epsilon}{2\pi i}\frac{-1}{e^{\beta\omega}+1} \\ &\times\langle\mathrm{tr}_q\big(\Lambda_\alpha\gamma_5 S(\epsilon+\omega,\mathbf{p}+\mathbf{q},A_4)\Lambda_\alpha\gamma_5 S(\epsilon,\mathbf{p},A_4)\big)\rangle, \end{aligned} \tag{6.49}$$

where $S(\omega,\mathbf{p})$ is the standard Feynman propagator for quarks. We note that each logarithm in the integral Eq.(6.47) is just the argument of $\tilde{\mathcal{M}}_\alpha(\omega+i\delta,q)$ multiplied by 2.

For the computation of the correlation energy or the pressure, it is convenient to decompose the function $\mathcal{M}(\omega\pm i\delta,q)$ into a real part $\mathcal{M}_1(\omega,q)$

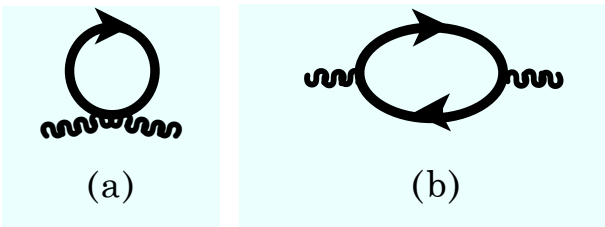

Figure 6.5: The meson self-energy Π_α contains two terms, a non-dispersive contact term (a) and a dispersive term (b).

and an imaginary part $\mathcal{M}_2(\omega, q)$:

$$\mathcal{M}(\omega \pm i\delta, q) \quad = \quad \mathcal{M}_1(\omega, q) \pm i\mathcal{M}_2(\omega, q). \tag{6.50}$$

The imaginary part $\mathcal{M}_2(\omega, q)$ becomes non-zero in the kinematical region of (ω, q) that allows pair excitations of quarks and antiquarks, or scatterings of thermally excited quarks into unoccupied states, as indicated by the non-zero imaginary part of the function $\mathcal{F}^{\rm pair}(\omega \pm i\delta, q)$ and $\mathcal{F}^{\rm scat}(\omega \pm i\delta, q)$, respectively, given explicitly in Appendix E. A long-lived meson collective mode exists when the real part $\mathcal{M}_1(\omega, q)$ vanishes in the region where the imaginary part also vanishes.

6.3.1 Pseudo-scalar mesons: π, K, η, η'

In this section, we consider the contribution to the pressure from the pseudo-scalar mesons that form a nonet in the $SU(3)$ flavour space. From Eq.(6.43), we see that their pressure is written as a sum of contributions from each meson. With the $SU(3)$ flavour symmetry breaking, but keeping the isospin $SU(2)$ symmetry intact, the pseudo-scalar mesons can be classified in four kinds according to their masses.

The difference between these four mesons appears in the meson self-energy due to the quark polarisation Π_α and the effective four-point coupling G'_α. The self-energies Π_α of the pseudo-scalar mesons are given in general by

$$\Pi_{PS} = \Pi^1_{PS}(A_4) + \Pi^2_{PS}(\omega_n, q, A_4), \tag{6.51}$$

where

$$\begin{aligned} \Pi^1_{PS}(A_4) \quad &= \quad -2T \sum_n {\rm tr}_c \int \frac{d^3p}{(2\pi)^3} \qquad (6.52) \\ &\qquad \times \frac{1}{2}\Big(\frac{1}{(\epsilon_n + gA_4)^2 + E_i(p)^2} + \frac{1}{(\epsilon_n + gA_4)^2 + E_j(p)^2} \Big) \\ &= \quad -\big(\frac{\langle \bar{q}_i q_i \rangle}{M_i} + \frac{\langle \bar{q}_j q_j \rangle}{M_j} \big) \qquad (6.53) \end{aligned}$$

is the non-dispersive contact component of the meson self-energy shown diagrammatically in Fig.6.5 (a), while

$$\Pi^2_{PS}(\omega_n, q, A_4) = \left(\omega_n^2 + q^2 + (M_i - M_j)^2\right) F_{ij}(\omega_n, q, A_4) \tag{6.54}$$

with

$$\begin{aligned} F_{ij}(\omega_n, q, A_4) &= 2T \sum_{n'} \mathrm{tr}_c \int \frac{d^3p}{(2\pi)^3} \frac{1}{[(\epsilon_{n'} + gA_4)^2 + E_i(p)^2]} \\ &\quad \times \frac{1}{[(\epsilon_{n'} + gA_4 + \omega_n)^2 + E_j(p+q)^2]} \end{aligned} \tag{6.55}$$

is the dispersive component shown in Fig.6.5 (b). In these expressions, $i, j (= u, d, s)$ indicate the flavours of the quarks and antiquarks constituting the pseudo-scalar meson.

The dispersive part of the meson self-energy needs to be analytically continued to a real frequency ω in order to find the dispersion relation of the collective meson modes. The detail of this computation is given in the Appendix E. Here we present the result of this computation for pseudo-scalar mesons:

$$\tilde{\Pi}^2_{PS}(\omega, q, A_4) = \left(-\omega^2 + q^2 + (M_i - M_j)^2\right) \mathcal{F}_{ij}(\omega, q, A_4), \tag{6.56}$$

where

$$\mathcal{F}_{ij}(\omega, q, A_4) = \mathcal{F}^{\mathbf{scat}}_{ij}(\omega, q, A_4) + \mathcal{F}^{\mathbf{pair}}_{ij}(\omega, q, A_4) \tag{6.57}$$

with the scattering term

$$\begin{aligned} \mathcal{F}^{\mathbf{scat}}_{ij}(\omega, q, A_4) &= \int \frac{d^3p}{(2\pi)^3} \frac{1}{2E_i(p)2E_j(p+q)} \left(\frac{1}{\omega + E_i(p) - E_j(p+q)} \right. \\ &\quad \left. - \frac{1}{\omega - E_i(p) + E_j(p+q)} \right) \\ &\quad \times \mathrm{tr}_c \left[f(E_i(p) - igA_4) - f(E_j(p+q) - igA_4) \right] \end{aligned} \tag{6.58}$$

and the pair creation and annihilation term

$$\begin{aligned} \mathcal{F}^{\mathbf{pair}}_{ij}(\omega, q, A_4) &= \int \frac{d^3p}{(2\pi)^3} \frac{1}{2E_i(p)2E_j(p+q)} \left(\frac{1}{\omega + E_i(p) + E_j(p+q)} \right. \\ &\quad \left. - \frac{1}{\omega - E_i(p) - E_j(p+q)} \right) \\ &\quad \times \mathrm{tr}_c \left[1 - f(E_i(p) - igA_4) - f(E_j(p+q) - igA_4) \right]. \end{aligned} \tag{6.59}$$

These functions have singularities when $\omega = \pm(E_i(p) - E_j(p+q))$ for the scattering term and when $\omega = \pm(E_i(p) + E_j(p+q))$ for the pair term corresponding to real excitations of the medium. Note that the effect of the background gauge field A_4 cancels for these excitations since they are totally colour singlet. However, the gauge field still appears in the distribution functions of the quark quasiparticles as a phase factor in exactly the same way as in the mean-field calculation. We replace this phase factor by the Polyakov loop, and then we take the statistical average, e.g.

$$\mathrm{tr}_c\,[f(E_i(p) - igA_4) - f(E_j(p+q) - igA_4)] \to [f_\Phi(E_i(p)) - f_\Phi(E_j(p+q))] \tag{6.60}$$

for the statistical averages of each component,

$$\mathcal{F}_{ij}^{\mathbf{scat}}(\omega, q) \;=\; \langle \mathcal{F}_{ij}^{\mathbf{scat}}(\omega, q, A_4)\rangle, \quad \mathcal{F}_{ij}^{\mathbf{pair}}(\omega, q) = \langle \mathcal{F}_{ij}^{\mathbf{pair}}(\omega, q, A_4)\rangle. \tag{6.61}$$

Having discussed these generic results for pseudo-scalar mesons, we now present the explicit forms for each pseudo-scalar meson starting with pions. With the SU(2) isospin symmetry, u-quark and d-quark are degenerate so that the contributions to the pressure from the three pions π^+, π^- and π^0 are identical.

$$\tilde{\mathcal{M}}_\pi(\omega, q) = \frac{1}{2G'_\pi} - \tilde{\Pi}^1_\pi - \tilde{\Pi}^2_\pi(\omega, q), \tag{6.62}$$

where

$$G'_\pi \equiv G'_1 = G'_2 = G'_3 = G - \frac{K}{2}\langle \bar{s}s\rangle \tag{6.63}$$

is the effective four-point coupling for the pions. The non-dispersive and dispersive parts of the pion self-energy are given by

$$\tilde{\Pi}^1_\pi = \langle \Pi^1_\pi(A_4)\rangle = -2\frac{\langle \bar{u}u\rangle}{M_u} \tag{6.64}$$

$$\tilde{\Pi}^2_\pi(\omega, q) = \langle \tilde{\Pi}^2_\pi(\omega, q, A_4)\rangle = (-\omega^2 + q^2)\mathcal{F}_\pi(\omega, q). \tag{6.65}$$

An explicit form of $\mathcal{F}_\pi(\omega, q)$ is given in Appendix E.

Comparing Eq.(6.62) with the gap equation for M_u, we observe that the first two terms in the right hand side of Eq.(6.62) can be transformed into a simpler form:

$$\tilde{\mathcal{M}}_\pi(\omega, q) = (-\omega^2 + q^2)\mathcal{F}_\pi(\omega, q) + \frac{m_u}{2G'_\pi M_u}. \tag{6.66}$$

We note that in the limit of the coupling $K = 0$, $\tilde{\mathcal{M}}_\pi$ coincides with our previous results for the two-flavour model.

Similarly, for the kaons, we find,

$$\tilde{\mathcal{M}}_K(\omega,q) = \frac{1}{2G'_K} - \langle\tilde{\Pi}^1_K\rangle - \langle\tilde{\Pi}^2_K(\omega,q)\rangle, \tag{6.67}$$

where

$$G'_K \equiv= G'_4 = G'_5 = G'_6 = G'_7 = G - \frac{K}{2}\langle\bar{u}u\rangle, \tag{6.68}$$

and

$$\langle\tilde{\Pi}^1_K\rangle = -\Big(\frac{\langle\bar{u}u\rangle}{M_u} + \frac{\langle\bar{s}s\rangle}{M_s}\Big) \tag{6.69}$$

$$\langle\tilde{\Pi}^2_K(\omega,q)\rangle = (-\omega^2 + q^2 + (M_s - M_u)^2)\mathcal{F}_K(\omega,q) \tag{6.70}$$

with $\mathcal{F}_K(\omega,q)$ given in the Appendix E. By making use of the gap equation for M_s, Eq.(6.67) can be transformed into

$$\begin{aligned}\tilde{\mathcal{M}}_K(\omega,q) &= (-\omega^2 + q^2 + (M_u - M_s)^2)\mathcal{F}_K(\omega,q) \\ &\quad + \frac{1}{2G'_K} - \frac{M_u - m_u}{4G'_K M_s} - \frac{M_s - m_s}{4G'_K M_u} \\ &\quad - \frac{G}{G'_K}\Big(\frac{\langle\bar{u}u\rangle - \langle\bar{s}s\rangle}{M_s} + \frac{\langle\bar{s}s\rangle - \langle\bar{u}u\rangle}{M_u}\Big).\end{aligned} \tag{6.71}$$

Although it looks rather complicated, this result coincides with that for pions when the flavour $SU(3)$ symmetry becomes exact.

Next we consider the η and η' mesons. If there were no Kobayashi-Maskawa-'t Hooft interaction, in other words if the $U(1)_A$ symmetry is not broken, the masses of these two mesons would be same. Both the η and η' mesons are mixtures of a flavour singlet η^0 and a flavour octet η^8. Without mixing, we find for η^8,

$$\begin{aligned}\tilde{\mathcal{M}}_{\eta^8}(\omega,q) &= \frac{1}{2G'_{\eta^8}} - \langle\tilde{\Pi}_8(\omega,q)\rangle \\ &= (-\omega^2 + q^2)\mathcal{F}_{\eta^8}(\omega,q) \\ &\quad + \frac{1}{2G'_{\eta^8}} - \frac{2}{3}\Big[\frac{1}{3G'_8}\Big(\frac{M_s - m_s}{M_u} + 2\frac{M_u - m_u}{M_s}\Big)\Big(\frac{\langle\bar{s}s\rangle}{4\langle\bar{u}u\rangle} - 1\Big) \\ &\quad + \frac{G}{3G'_8}\Big\{\frac{1}{M_u}\Big(\frac{\langle\bar{s}s\rangle\langle\bar{s}s\rangle}{\langle\bar{u}u\rangle} - 4\langle\bar{s}s\rangle + 3\langle\bar{u}u\rangle\Big) + \frac{8}{M_s}\big(\langle\bar{s}s\rangle - \langle\bar{u}u\rangle\big)\Big\}\Big],\end{aligned} \tag{6.72}$$

where

$$G'_{\eta^8} = G + \frac{K}{6}\big(\langle\bar{s}s\rangle - 4\langle\bar{u}u\rangle\big). \tag{6.73}$$

And for η^0, we have

$$\begin{aligned}
\tilde{\mathcal{M}}_{\eta^0} &= \frac{1}{2G'_{\eta^0}} - \langle\tilde{\Pi}_{00}(\omega,q)\rangle \\
&= (-\omega^2+q^2)\mathcal{F}_{\eta^0}(\omega,q) \\
&\quad -\frac{2}{3}\Big[\frac{1}{3G'_{\eta^0}}\Big(2\frac{M_s-m_s}{M_u}+\frac{M_u-m_u}{M_s}\Big)\Big(\frac{\langle\bar{s}s\rangle}{2\langle\bar{u}u\rangle}+1\Big) \\
&\quad +\frac{G}{3G'_{\eta^0}}\Big\{\frac{1}{M_u}\Big(4\frac{\langle\bar{s}s\rangle\langle\bar{s}s\rangle}{\langle\bar{u}u\rangle}+8\langle\bar{s}s\rangle+6\langle\bar{u}u\rangle\Big)\Big]+\frac{1}{M_s}\big(5\langle\bar{s}s\rangle+4\langle\bar{u}u\rangle\big)\Big\},
\end{aligned} \tag{6.74}$$

where

$$G'_{\eta^0} = G + \frac{K}{3}\big(\langle\bar{s}s\rangle + 2\langle\bar{u}u\rangle\big). \tag{6.75}$$

In order to check these results for the η^8 and η^0, we inspect these formula in some limiting cases. First, we consider the case of an exact $SU(3)_L \times SU(3)_R$ symmetry, taking $m_u = m_d = m_s = 0$, but with a finite Kobatashi-Maskawa-'t Hooft coupling K. In this case, the η^8 becomes a massless Nambu-Goldstone mode, while the η^0 becomes a massive mode. Furthermore, if we set $K = 0$ while keeping the $SU(3)$ chiral symmetry, the η^0 also becomes a massless NG mode. Regarding the mixing of η^0 and η^8, we need an effective coupling G'_{08};

$$G'_{08} = G + \frac{\sqrt{2}K}{6}(\langle\bar{u}u\rangle - \langle\bar{s}s\rangle) \tag{6.76}$$

and $\langle\tilde{\Pi}_{08}(\omega,q)\rangle$.

We show in Fig.6.6 the effective coupling G' scaled by the four-point coupling G as a function of T/T_c in order to check the effect of the Kobayashi-Maskawa-'t Hooft interaction. Each G' indirectly depends on the temperature through the chiral condensates. Although this interaction is introduced to generate the mass splitting of η^8 and η^0, it also influences the couplings of the π and K mesons. One can see that the effective coupling of the π does not vary much compared to others as the temperature increases because of the moderate change of $\langle\bar{s}s\rangle$. Another feature is that only G'_{η^0} becomes smaller than the original four-point coupling G. All the others become larger than G because of the negative effect of the second terms in Eqs. (6.63),(6.68) and (6.73).

6.3.2 Scalar mesons: σ, κ, a_0, f_0

We find for the scalar mesons,

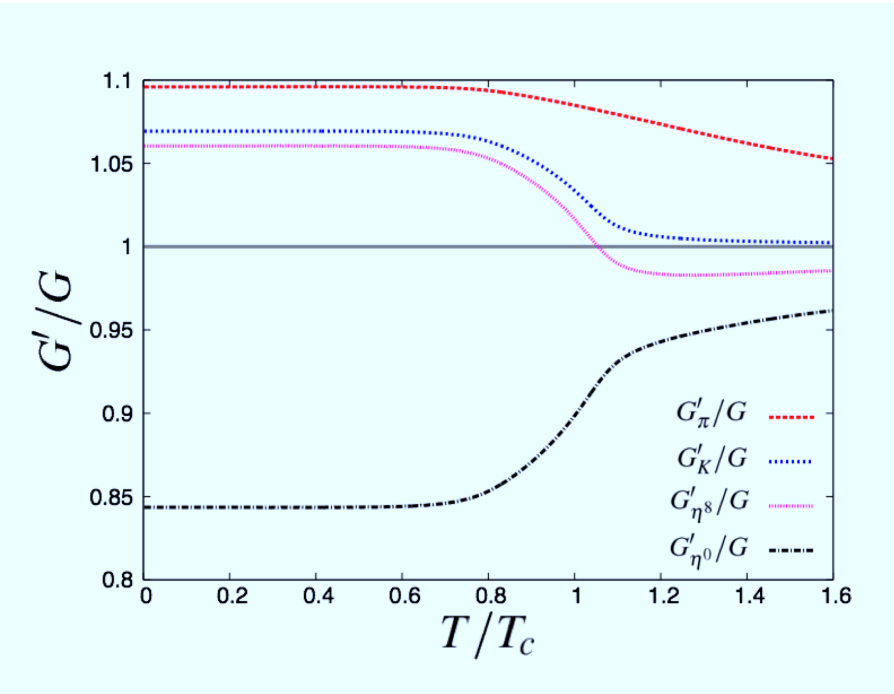

Figure 6.6: Temperature dependence of the effective four-point coupling G' for pions (the dotted red line), kaons (the dotted blue line), η^8 (the dotted pink line), and η^0 (the dashed light black line). The temperature is scaled by the pseudo critical temperature T_c computed in the mean-field approximation.

$$\tilde{\mathcal{M}}_S(\omega,q) = \frac{1}{2G'_S} - \langle\tilde{\Pi}^1_S\rangle - \langle\tilde{\Pi}^2_S(\omega,q)\rangle, \tag{6.77}$$

where

$$G'_S = \begin{cases} G + \frac{K}{2}\langle\bar{s}s\rangle & \text{for} \quad a_0 \\ G + \frac{K}{2}\langle\bar{u}u\rangle & \text{for} \quad \kappa \\ G - \frac{K}{6}\left(\langle\bar{s}s\rangle - 4\langle\bar{u}u\rangle\right) & \text{for} \quad \sigma \\ G - \frac{K}{3}\left(\langle\bar{s}s\rangle + 2\langle\bar{u}u\rangle\right) & \text{for} \quad f_0 \end{cases} \tag{6.78}$$

and where

$$\langle\Pi^1_S\rangle = -\left(\frac{\langle\bar{u}u\rangle}{M_i} + \frac{\langle\bar{s}s\rangle}{M_j}\right) = \langle\Pi^1_{PS}\rangle \tag{6.79}$$

$$\langle\tilde{\Pi}^2_S(\omega,q)\rangle = (-\omega^2 + q^2 + (M_i + M_j)^2)\mathcal{F}_S(\omega,q) \tag{6.80}$$

with $\mathcal{F}_S(\omega,q) = \mathcal{F}_{PS}(\omega,q)$.

The only important difference between Π^2_{PS} for pseudo-scalars and Π^2_S for the scalars resides in the first term of the dispersive parts where the combination $M_i + M_j$ appears for the scalar case instead of $M_i - M_j$. Therefore, if $M_i = M_j$, this factor generates a massless Nambu-Goldstone mode for the pseudo-scalar case, while the scalar mesons become massive with their masses given by $M_S = 2M_i$.

6.3.3 Numerical results

We display the pressure scaled by the fourth power of the temperature as a function of T/T_c in Fig.6.7. On the top panel in Fig.6.7, we plot the pressure of quarks, gluons and mesons (the red line), the pressure of quarks and gluons only (the blue line) which corresponds to the mean-field pressure, and the pressure of free pions and kaons (the lower black line). At low temperatures, our result including mesons agrees with the free meson pressure. As the temperature increases, the free meson pressure approaches the Stefan-Boltzmann constant, $(3+4)\times\pi^2/90 \sim 0.77$, since there is no mechanism to increase the number of degrees of freedom. In contrast, our calculation can describe the change of the number of degrees of freedom from the hadrons to the quarks and gluons. Therefore, the pressure dominated by mesons at low temperature increases as the temperature increases, then it changes to the pressure of the quarks and gluons at high temperatures.

In the bottom panel of Fig.6.7, we compare the pressure in the PNJL model (the red and blue lines) with the pressure calculated from the fit function which is obtained from a lattice QCD calculation (the black line) [130]. Since there are no thermal excitations in the mean-field approximation, where the quark excitations are suppressed by the Polyakov loop and the mesonic excitations are not included, the pressure in the mean-field approximation is zero at low temperatures. Our approach can describe the contribution from mesonic excitations at low temperatures, so that a difference between the red and blue lines appears due to the mesonic excitations. In addition, the behaviour of the pressure gets close to that of the lattice simulation by taking mesonic excitations into account, compared with the mean-field result. The difference between our result and the lattice result at low temperatures comes from the missing contribution from resonances in our result. In our approach, only free pions and kaons are taken into account, so that the contribution from the resonances to the pressure is neglected. There is also a difference between our result and the lattice result at high temperatures. The pressure of the gluon sector in the PNJL model agrees with the pressure in a pure gauge lattice calculation at high temperatures by construction, so that the difference may come from the quark sector. In the lattice calculation, the remainder of the pressure after subtracting the pure glue pressure [130] from the total lattice pressure [130] does not approach quickly the Stefan-Boltzmann limit at high temperatures. While in the PNJL model, the pressure of the quark sector approaches the Stefan-Boltzmann limit, as the expectation value of the Polyakov loop Φ approaches unity at high temperatures. This is because the pressure of the quark excitations in the PNJL model is controlled by Φ through the modified quark distribution function as a result of confinement. As the effect of the Polyakov loop in the quark distribution function becomes weak, the quarks become free, and therefore the pressure of the quark sector gets close

to the free quark pressure. This is the source of the difference between the lattice result and our result at high temperatures, and this may perhaps indicate that the description of the confinement in the PNJL model, which only appears via changes of the quark distribution function, is insufficient.

We have only included the π and K in this calculation. Our approach for taking mesonic excitations can describe only free mesons, and the contribution from free mesons is dominated by their mass. Therefore, we expect that in this model heavier mesons would not contribute much to the pressure at low temperatures. To estimate the contribution of mesons, we plot the pressure of free mesons as a function of temperature in Fig. 6.8. T_c is determined from the chiral transition of the PNJL model. At low temperatures, the pressure of π and K is much larger then that of η and σ. Although the mass difference between the eta meson and the kaon is not very large, the contribution from the kaons to the pressure is much larger than that of the eta mesons because of the kaon degeneracy.

In order to study until which temperature the mesons persist as collective modes, we plot the real part and the imaginary part of $\mathcal{M}(\omega, q)$ as a function of ω/q at several temperatures near T_c. The conditions of isolated meson poles are given by the vanishing of both the real part $\mathcal{M}_1$ and the imaginary part $\mathcal{M}_2$. In particular, the condition $\mathcal{M}_1(\omega, q) = 0$ determines the dispersion relation of collective modes. $\mathcal{M}_2$ corresponds to the excitations of quarks and antiquarks in the continuum. Therefore, collective meson modes exist when both the real part and the imaginary part of $\tilde{\mathcal{M}}(\omega + i\delta, q)$ vanish simultaneously. The latter condition guarantees an infinite lifetime. We derive expressions for the real part and the imaginary part of $\mathcal{M}(\omega, q)$ in Appendix E.

We plot the two components as a function of ω/q in Fig.6.9 for pions and in Fig. 6.10 for kaons, at three different temperatures around T_c. These panels are showing whether collective modes exist or not for the pions and for the kaons. In the shadowed areas, where the imaginary part $\mathcal{M}_2$ has a finite value, the continuum of quarks and antiquarks exists. The time-like region where the imaginary part is finite extends to lower ω/q as the temperature increases because of a decrease of the constituent quark masses along with chiral symmetry restoration.

In Fig.6.9, there is a point where both the real and imaginary parts become zero until $T = 1.15T_c$, but when T reaches $1.2T_c$ such a point disappears. This means that the collective pion modes exist until $T = 1.15T_c$. The same plots for kaons are displayed in Fig.6.10. The collective kaon mode disappears at $T = 1.15T_c$. This melting temperature of kaon pole is lower than that of the pion.

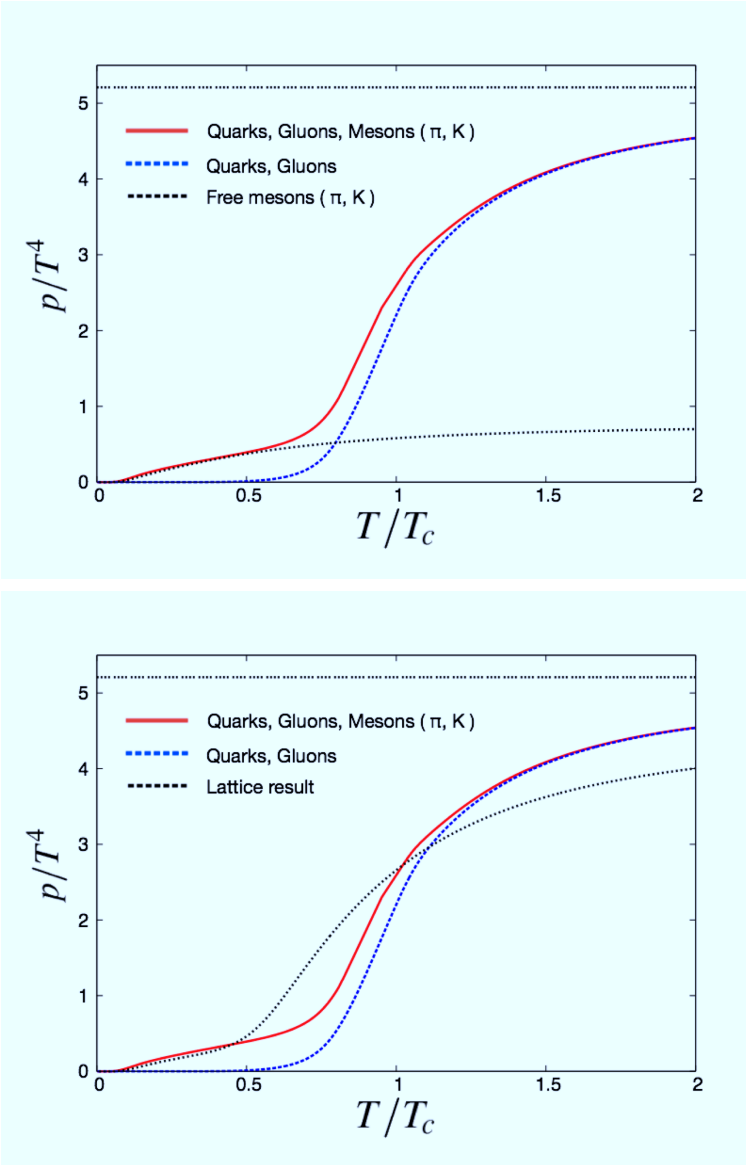

Figure 6.7: Pressure scaled by T^4 as a function of the temperature T scaled by the pseudo critical temperature T_c. The dashed blue line is the result of the mean-field approximation, consisting of the quark pressure and the gluon pressure, while the solid red line contains also the pressure from mesonic correlations in the pion and kaon channels. The top panel is the comparison between our results and the free meson (pion and kaon) pressure. The bottom panel is the comparison between our results and the lattice result [130]. The pressures of massless quarks and gluons is indicated by the horizontal dashed line.

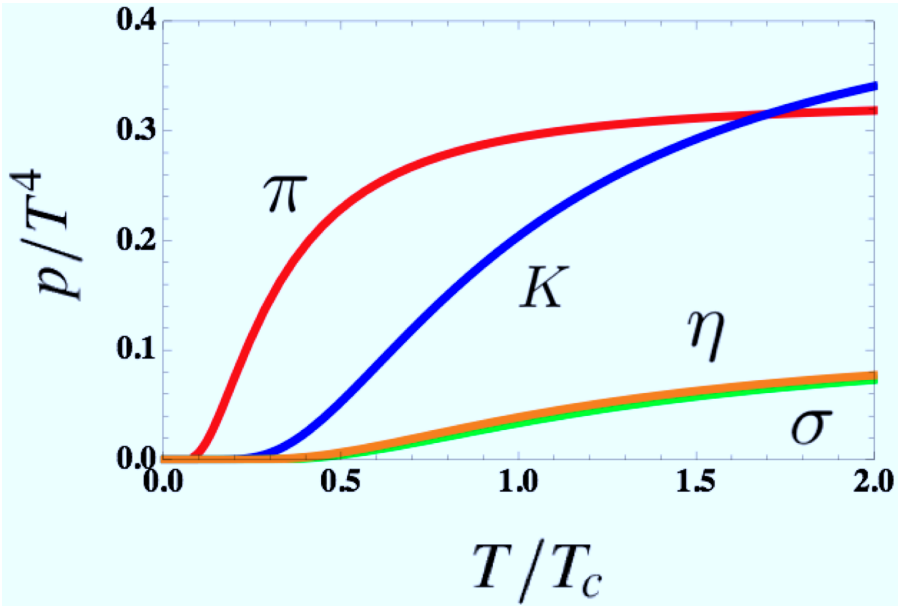

Figure 6.8: Pressure of free mesons scaled by T^4 as a function of the temperature T scaled by the pseudo critical temperature T_c. The red line is three degenerated pion, the blue line is four degenerated kaon, the orange line is the eta meson, and the green line is the sigma meson.

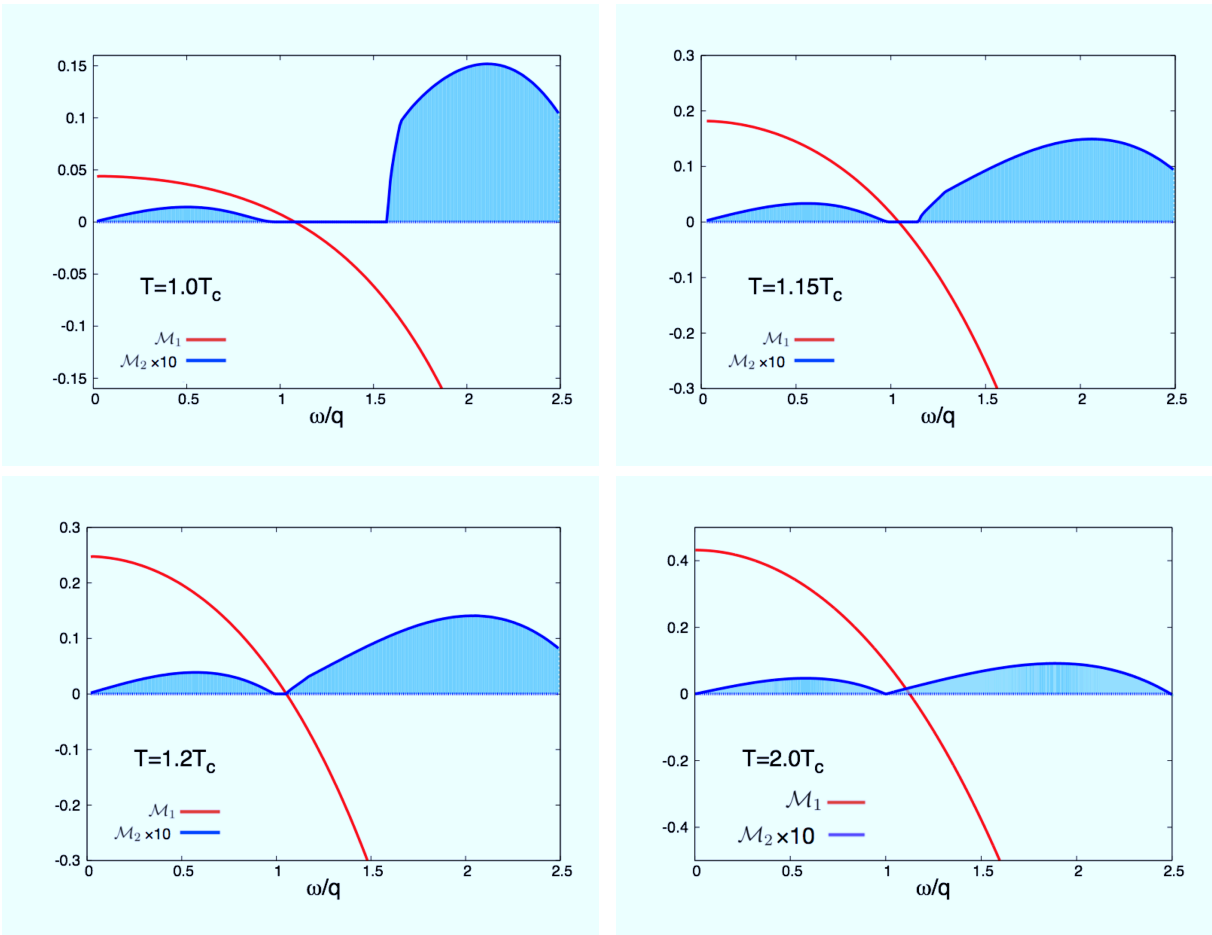

Figure 6.9: $\mathcal{M}_1$ and $\mathcal{M}_2$ of the pion as a function of ω/q calculated at three different values of the temperature $T/T_c = 1.0, 1.15, 1.2, 2.0$ respectively. When $\mathcal{M}_1$ vanishes in the region where $\mathcal{M}_2$ also vanishes, the long-lived pion collective mode exists, as clearly seen below $T = 1.15T_c$. The pion collective mode is absorbed into the continuum of pair excitations at $T = 1.2T_c$.

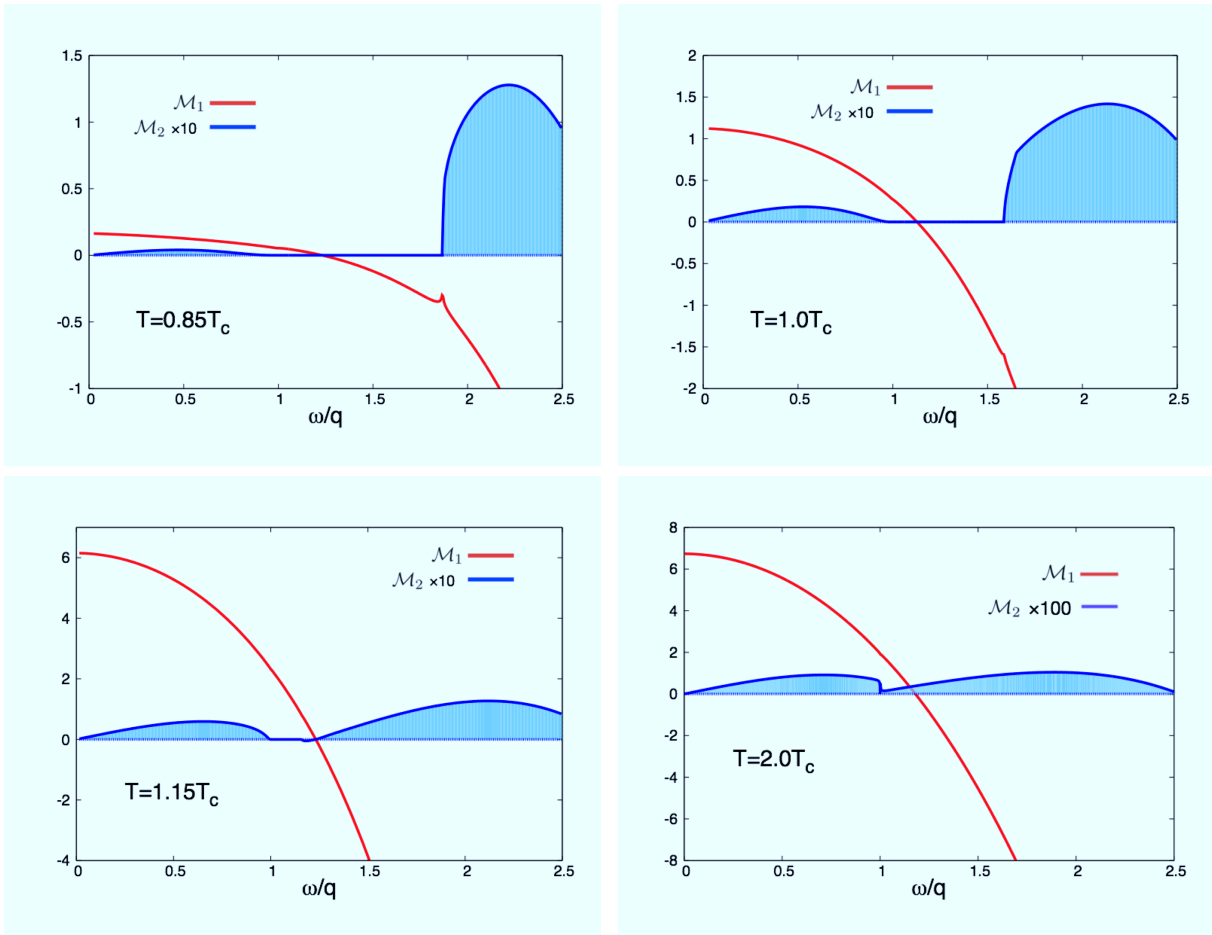

Figure 6.10: The same plots as the Fig. 6.9 for kaons. The collective kaon mode is absorbed into the pair continuum at $T = 1.15T_c$, slightly below the pion melting temperature.

In Fig.6.11, we plot the pressure of the pion and the kaon separately. It is remarkable that the pion and the kaon still survive after the colour confinement is lost. Namely, the quark-gluon excitations and meson excitations coexist in the transition region. The chiral symmetry is still not fully recovered at these temperatures. Therefore, a small window between a continuum in the time-like region and that in the space-like region still persists in the $\omega - q$ plane, where the spectrum of the isolated collective meson excitations resides. As the temperature increases further these windows shrink because of the decrease of the constituent quark masses and the collective meson spectra are absorbed into the continuum of individual quark-antiquark pair excitations.

We also display the entropy in Fig.6.12. At low temperatures, the pions and the kaons carry the entropy. As the temperature increases, the carrier of the entropy changes to the quarks and the gluons in the transition region.

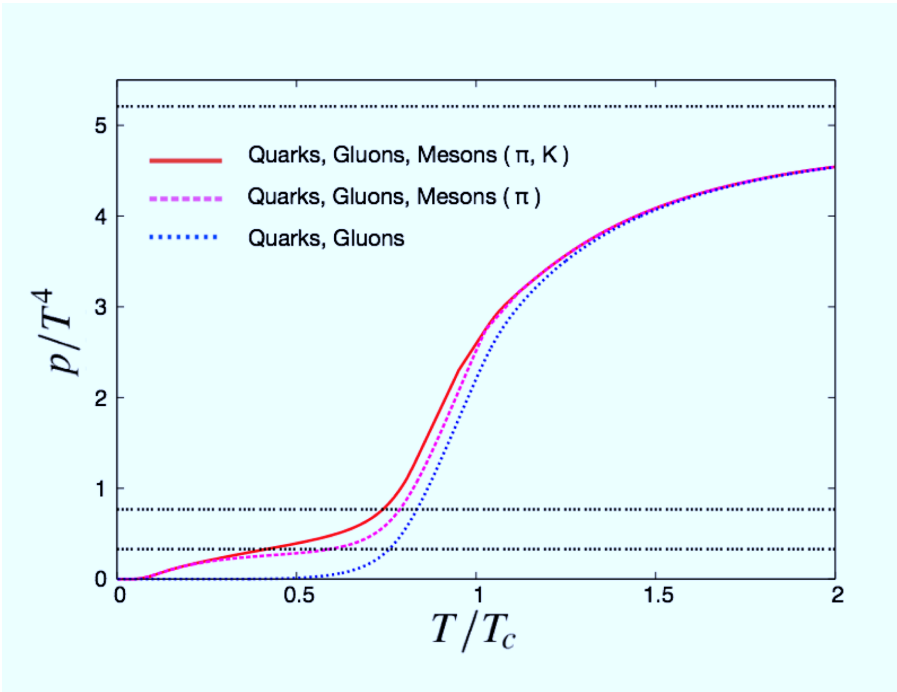

Figure 6.11: Pressure scaled by T^4 as a function of the temperature T scaled by the pseudo critical temperature T_c. The solid red line is the sum of the contributions from the mean-field and mesonic correlations (pion, kaon). The dotted pink line is for the mean-field plus pionic correlation only and the dotted blue line is the pressure without mesonic correlations. The melting temperatures of the pions and the kaons are indicated by arrows. The pressures of the gas of pions, the gas of pions and kaons, and the gas of massless quarks and gluons are indicated by the horizontal dashed lines, going from bottom to top respectively.

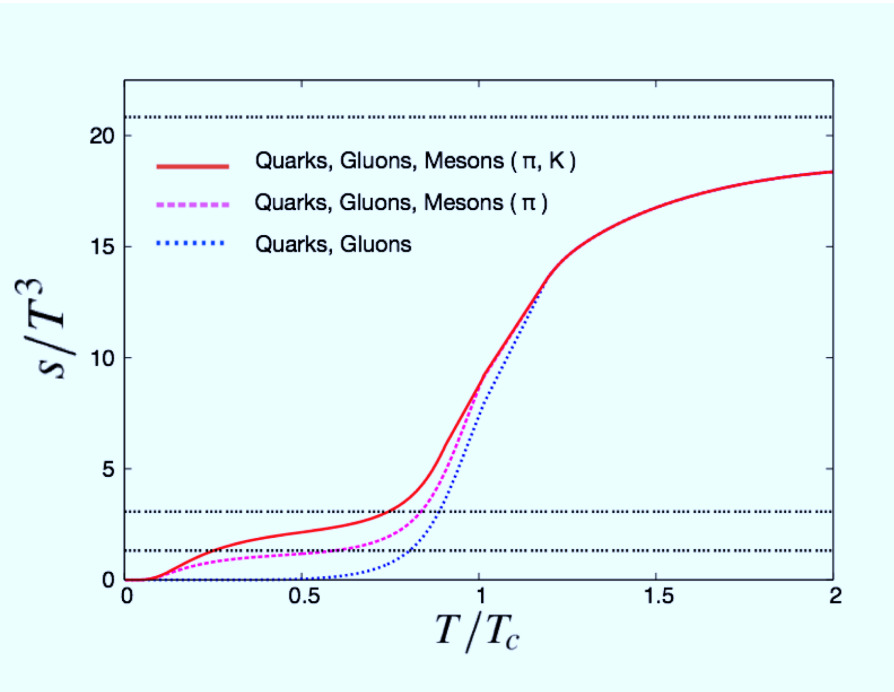

Figure 6.12: Entropy scaled by T^3 as a function of the temperature T scaled by the pseudo critical temperature T_c. The solid red line is the sum of the contributions from the mean-field and mesonic correlations (pion, kaon). The dotted pink line is for the mean-field plus pionic correlation only and the dotted blue line is the pressure without mesonic correlations. The melting temperatures of the pions and the kaons are indicated by arrows. The entropies of the gas of pions, the gas of pions and kaons, and the gas of massless quarks and gluons are indicated by the horizontal dashed lines, going from bottom to top, respectively.

Chapter 7

Perspective of the PNJL model with mesons and baryons

In the chapters 5 and 6, we have taken the mesonic correlations into account in the two- and the three-flavour PNJL model at zero chemical potential, and we have shown that the mesonic excitations dominate the pressure and the entropy at low temperatures, while the quarks and the gluons dominate at high temperatures instead of the mesons. Compared with calculations based on the mean-field approximation, our method can describe a more realistic hadronic phase including the mesonic excitations. However, the baryonic degrees of freedom are still missing, even though there are the quark triads at low temperatures as a remnant of the phase cancellation in the modified quark distribution function [1]. The quark triads look like baryons carrying three times the energy and three times the chemical potential of a single quark, but these degrees of freedom are quite different from baryons: they are essentially the same as those of the original quarks. When we shift our focus to the finite chemical potential, baryons cannot be ignored since they provide the baryon density at finite chemical potential.

It may look unnatural to include baryons into the NJL models whose main focus is the chiral symmetry breaking and its restoration. Unlike the mesons, the baryons are not obtained from the chiral symmetry breaking, so that we need another approach to describe the baryons in the NJL models. We assume that a baryon is composed of a quark and a diquark instead of three quarks. The diquark correlations have been originally introduced in a spectroscopic study of baryons [131–134] . Each quark pair in a baryon is required to have a colour anti-triplet configuration. However, this does not mean that a quark pair has to have correlations. It is possible that two quarks in a baryon which are arranged in a colour anti-triplet state exist without any correlation. The diquark correlations have been more

recently invoked in studies of possible exotic states of hadrons [114] and have been related to the QCD analogue of the BCS states in a superconducting phase. The single gluon exchange interaction between a colour anti-triplet quark pair indeed gives an attraction between the two quarks, which form a bound state on the Fermi surfaces of degenerate quarks at high baryon densities. The diquark correlation has been conjectured as one of the most prominent features of the QCD phenomenology independent from the colour confinement and the chiral symmetry [135].

We introduce an effective quark-quark interaction in the colour anti-triplet diquark channel as a seed in order to induce the baryonic correlations. In principle, a two-body attractive interaction alone can form three-body bound states by repeated actions of the two-body interaction on three different pairs of the three body system. A relativistic version of the Fadeev equation has beens used with a contact interaction of NJL-type in order to construct the baryons in the NJL scheme [136]. Here we follow a different approach.

We begin with the two-flavour PNJL model with a quark-quark four-point interaction which is used to make diquarks, not only a quark-antiquark interaction. Then, we introduce auxiliary fields for mesons, diquarks, anti-diquarks, baryons, and anti-baryons. The meson fields, the diquark and the antidiquark fields are used for replacing the four-point interactions by Yukawa interactions. For the baryons, we need to introduce a coupling constant between quarks and diquarks by hand, since it does not appear in the original Lagrangian. We perform the Hubbard-Stratonovich transformation to eliminate the four-point interactions and get an effective action as a function of the auxiliary fields.

In the next section, we introduce the two-flavour PNJL model for interacting quarks with a quark-antiquark interaction and a quark-quark interaction. We calculate the partition function from the path integral. We introduce dummy integrals over the auxiliary fields for mesons, diquarks, anti-diquarks, baryons and anti-baryons. In this procedure, we need to introduce another coupling between quarks and diquarks, which does not appear in the original Lagrangian. We determine this parameter in the vacuum in order to reproduce the nucleon mass. The four-point interactions in the Lagrangian are replaced by Yukawa interactions with the meson, the diquark and the anti-diquark fields. By this procedure, we turn the fourth power of the fermion fields into quadratic terms in the effective action, and then the Grassmann integral can be performed by using the Nambu-Gorkov basis. Moreover, we show that the gap equations for the constituent quark mass, the diquark condensates, and the Polyakov loop are obtained from the stationarity conditions of the effective action. In Section 7.2, we perform the Gaussian integration over the diquark and the anti-diquark fields in order to obtain an effective action for the mesons and the baryons. For this integral to be doable analytically, we need to approximate the effective action.

We expand up to the second order in the diquark fluctuations around the stationary point determined by the gap equations. In Section 7.3, we set the diquark and the antidiquark condensates to zero for simplification, instead of solving the gap equations. By this procedure, the five gap equations (one for the constituent quark mass, two for the Polyakov loop and the anti Polyakov loop, two for the diquark and the anti-diquark condensates) are reduced to three equations because we do not need to solve the ones for the diquark and the anti-diquark condensates any longer. This approximation can be justified only when the chemical potential is small. In this setting, we obtain the pressure of the diquark and the baryonic fluctuations, and we show that the diquark fluctuations do not give a large contribution at low temperatures and low densities [4].

7.1 Extended PNJL model for mesons, diquarks and baryons

7.1.1 Model setup

In this section, we introduce the two-flavour PNJL model. In this model, only the quarks and the antiquarks are treated as dynamical valuables, and the mesons and the baryons are constructed from the quarks. The gluons are described by an effective potential which has already been introduced in Chapters 5 and 6. Here we assume that a baryon is composed by a quark and a diquark, instead of the three quarks, so that we start from a Lagrangian which has two types of four-point interactions. The first one is a quark-antiquark interaction for the mesons, and the other is a quark-quark interaction for the diquarks. The partition function is written as a path integral over the quark and the antiquark fields with the Lagrangian including the four-point interaction terms for $\bar{q}q$ and qq:

$$Z = \int [d\bar{q}][dq] \exp\Big[\int_0^\beta d\tau \int d^3x \, \big(\mathcal{L}(\bar{q}, q) - i\mu\bar{q}\gamma_0 q\big)\Big] \tag{7.1}$$

and

$$\mathcal{L}(\bar{q}, q) = \bar{q}(i\not{D} - m_0)q + \mathcal{L}_{\bar{q}q} + \mathcal{L}_{qq} - \mathcal{U}[\bar{\Phi}, \Phi, T], \tag{7.2}$$

where the covariant derivative is $D^\mu = \partial^\mu + gA^0\delta^{\mu 0}$. The quark-antiquark interaction is given by

$$\mathcal{L}_{\bar{q}q} = G\big[(\bar{q}q)^2 + (\bar{q}i\gamma_5\tau q)^2\big] \tag{7.3}$$

as already introduced in the previous chapters, with the coupling constant G, and the quark-quark interaction is given by

$$\mathcal{L}_{qq} = H \sum_{i=1,2,3} \big[(\bar{q}i\gamma_5\tau_2\zeta_i C\bar{q}^T)(q^T C i\gamma_5\tau_2\zeta_i q)\big] \tag{7.4}$$

with the coupling constant H. Note that we consider only the scalar diquarks (See Section 4.4 in Chapter 4). Here $\tau_{1,2,3}$ are isospin matrices; ζ_i are 3×3 colour matrices defined in terms of the Gell-Mann matrices λ_a by $\zeta_1 = \lambda_7$, $\zeta_2 = \lambda_5$ and $\zeta_3 = \lambda_2$, so that $\bar{q}\zeta_i\bar{q}^T = i\epsilon_{ijk}\bar{q}_j\bar{q}_k$ ($q^T\zeta_i q = i\epsilon_{ijk}q_jq_k$) give the i-th component of the colour anti-triplet diquark creation (annihilation) operator with respect to colour indices. The charge conjugation operator is defined as $C = i\gamma_0\gamma_2$. The coupling constant H in $\mathcal{L}_{qq}$ is related to the coupling constant G in $\mathcal{L}_{\bar{q}q}$ by a Fierz identity. The effective action $\mathcal{U}[\bar{\Phi},\Phi,T]$ is given as a function of the expectation value of the Polyakov loop by

$$\mathcal{U}[\bar{\Phi},\Phi,T]/T^4 = -\frac{1}{2}b_2(T)\bar{\Phi}\Phi - \frac{1}{6}b_3(\Phi^3+\bar{\Phi}^3) + \frac{1}{4}b_4(\bar{\Phi}\Phi)^2 \tag{7.5}$$

with

$$b_2(T) = a_0 + a_1\Big(\frac{T_0}{T}\Big) + a_2\Big(\frac{T_0}{T}\Big)^2 + a_3\Big(\frac{T_0}{T}\Big)^3, \tag{7.6}$$

as we have seen in Chapters 5 and 6, which gives the gluon pressure at high temperatures. Φ and $\bar{\Phi}$ are the expectation values of the Polyakov loop,

$$\Phi = \frac{1}{3}\langle \mathrm{tr}_c L\rangle \tag{7.7}$$

$$\bar{\Phi} = \frac{1}{3}\langle \mathrm{tr}_c L^\dagger\rangle. \tag{7.8}$$

The Polyakov loop is defined by

$$L(\mathbf{x}) = \mathcal{P}\exp\Big[ig\int_0^\beta d\tau A_4(\mathbf{r},\tau)\Big]. \tag{7.9}$$

In order to obtain the effective action for the mesons, the diquarks, and the baryons, we perform an extended Hubbard-Stratonovich transformation by inserting dummy integrals over the meson, the diquark, the anti-diquark, the baryon, and the anti-baryon fields [137, 138] :

$$\begin{aligned}&\int [d\phi][d\bar{\Delta}][d\Delta][d\bar{B}][dB]\\ &\times\exp\Big(\int_0^\beta d\tau\int d^3x\mathcal{L}_{\mathrm{aux}}(\phi,\bar{\Delta},\Delta,\bar{B},B)\Big)\end{aligned} \tag{7.10}$$

with

$$\begin{aligned}\mathcal{L}_{\mathrm{aux}} = &-\frac{1}{4G}\big((\sigma-2G\bar{q}q)^2+(\boldsymbol{\pi}-2iG\bar{q}\gamma_5\boldsymbol{\tau}q)^2\big)\\ &-\frac{1}{4H}\sum_i(\bar{\Delta}_i-2H\bar{q}\gamma_5\tau_2\xi_iC\bar{q}^T)(\Delta_i-2Hq^TC\gamma_5\tau_2\xi_iq)\\ &-\frac{1}{4\lambda}(\bar{B}-2\lambda\bar{\Delta}\bar{q})(B-2\lambda q\Delta),\end{aligned} \tag{7.11}$$

where $\phi = (\sigma, \boldsymbol{\pi})$ for the mesons and Δ_i ($\bar{\Delta}_i$) for the diquark (the anti-diquarks) are ordinary commuting fields for bosons, while B ($\bar{B}$) for the baryons (the anti-baryons) are anti-commuting Grassmann fields for fermions, as well as the composite fields $q\Delta = \sum_i q_i \Delta_i$. Note that ϕ, Δ, $\bar{\Delta}$ and λ, all have a dimension of energy, and B, $\bar{B}$ have a dimension of energy to the power 3/2, as well as q, $\bar{q}$.

The first term of Eq.(7.11) works to replace the fourth power of the fermion field in $\mathcal{L}_{\bar{q}q}$ by a second power. It can be illustrated as (a) in Fig.7.1. The second term works in the same way for $\mathcal{L}_{qq}$ and is represented as (b) in Fig.7.1. We note here that these two terms are sufficient to eliminate the four-point interactions that make the Grassmann integral in the partition function impossible. However, we have introduced another term in Eq.(7.11) in order to describe the baryons; the coupling constant λ in the last term of Eq.(7.11) can be viewed as a coupling between a baryon and a pair made of a diquark and a quark. We assume that this parameter is constant, and it will be fixed in order to reproduce the nucleon mass in the vacuum. Of course there is no reason that this parameter is independent from the temperature and the chemical potential as well as all other parameters. Indeed it may be possible to deal with it as a variational parameter. If we treat it as a variational parameter and we determine its value by minimising the free energy at each given temperature and chemical potential, it would vary with the temperature and baryon chemical potential. In this case, there is no guarantee that baryons exist as bound states even in the vacuum. However, here we assume that baryons constructed from quarks and diquarks exist in the hadronic phase, and then we study how they evolve upon changes of the temperature and of the chemical potential. Therefore, we treat λ as a parameter fixed in the vacuum by the condition that baryons exist, instead of a variational parameter.

Having inserted the dummy integrals over the five auxiliary fields, the partition function is now written in terms of the path-integrals not only over the quark and anti-quark fields but also over the auxiliary meson, diquark, anti-diquark, baryon and anti-baryon fields,

$$Z = \int d\bar{q} dq d\phi d\bar{\Delta} d\Delta d\bar{B} dB \; e^{-I(\bar{q},q,\phi,\bar{\Delta},\Delta,\bar{B},B)}, \tag{7.12}$$

and the effective action is written in terms of $\bar{q}$, q and the auxiliary fields,

$$\begin{aligned}
&I(\bar{q}, q, \phi, \bar{\Delta}, \Delta, \bar{B}, B) \\
&= \int d\tau \int d^3x \big[-\bar{q}(i\not{D} - m_0 + \mu\gamma_0 + \sigma + i\gamma_5 \boldsymbol{\tau} \cdot \boldsymbol{\pi} - \lambda\bar{\Delta}\Delta)q \\
&-\frac{1}{2}\bar{B}q\Delta - \frac{1}{2}\bar{\Delta}\bar{q}B - \frac{1}{2}\bar{\Delta}_i(qC\gamma_5\tau_2\zeta_i q) - \frac{1}{2}(\bar{q}\gamma_5\tau_2\zeta_i C\bar{q}^T)\Delta_i \\
&+\frac{1}{4G}\big(\sigma^2 + \boldsymbol{\pi}^2\big) + \frac{1}{4H}\bar{\Delta}\Delta + \frac{1}{4\lambda}\bar{B}B + \mathcal{U}[\bar{\Phi}, \Phi, T]\big].
\end{aligned} \tag{7.13}$$

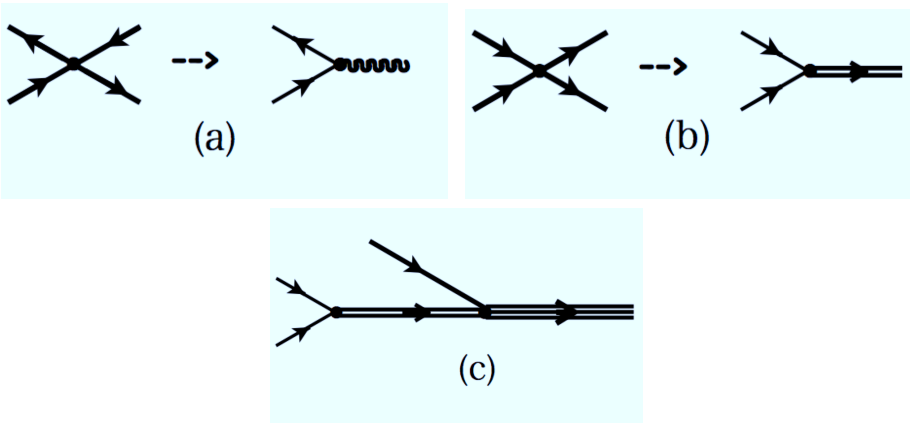

Figure 7.1: (a) $\mathcal{L}_{\bar{q}q}$ is replaced by the dummy integral over the meson field. (b) $\mathcal{L}_{qq}$ is replaced by the dummy integral over the diquark field. (c) Baryons are made from the quarks and diquarks.

If there were no quark-quark interaction $\mathcal{L}_{qq}$ in the Lagrangian, the effective action would become a linear function of $\bar{q}q$ after inserting the dummy integral over the meson field. In that case, one can easily perform the integral over the quark fields, and obtain the effective action of the mesons. However, the effective action Eq.(7.13) is more complicated because of $\mathcal{L}_{qq}$. This effective action now contains terms proportional to q, $\bar{q}$, $\bar{q}\bar{q}$ and qq besides the $\bar{q}q$ term. In order to perform the Grassmann integral over q and $\bar{q}$, we first rewrite the effective action as a bilinear form in terms of a fermion doublet $\boldsymbol{q}$,

$$\boldsymbol{q} = \begin{pmatrix} q \\ C\bar{q}^T \end{pmatrix}, \bar{\boldsymbol{q}} = \left(\bar{q}, q^T C\right) \tag{7.14}$$

and of the inverse of the Nambu-Gorkov propagator,

$$\boldsymbol{G}^{-1} = \begin{pmatrix} i\not{D} + \Sigma & \frac{1}{2}\gamma_5\tau_2\zeta\Delta \\ \frac{1}{2}\bar{\Delta}\zeta\gamma_5\tau_2 & -i\not{D} + \Sigma \end{pmatrix}, \tag{7.15}$$

where

$$\Sigma = -m_0 - i\mu\gamma_0 + \sigma + i\gamma_5\boldsymbol{\tau}\cdot\boldsymbol{\pi} - \lambda\bar{\Delta}\Delta. \tag{7.16}$$

We have used abbreviated notations: $\zeta\Delta = \sum_i \zeta_i\Delta_i$, $\bar{\Delta}\zeta = \sum_i \bar{\Delta}_i\zeta_i$, $\bar{\Delta}\Delta = \sum_i \bar{\Delta}_i\Delta_i$ for the sum over the colour indices. Then the effective action can be rewritten as,

$$\begin{aligned} &I(\bar{q}, q, \phi, \bar{\Delta}, \Delta, \bar{B}, B) \\ &\quad = \int d\tau \int d^3x \Big[-\frac{1}{2}\big(\bar{\boldsymbol{q}}\boldsymbol{G}^{-1}\boldsymbol{q} + \bar{\boldsymbol{q}}\boldsymbol{\xi} + \bar{\boldsymbol{\xi}}\boldsymbol{q}\big) \\ &\qquad + \frac{1}{4G}\sigma^2 + \frac{1}{4H}\bar{\Delta}\Delta + \frac{1}{4\lambda}\bar{B}B + \mathcal{U}[\bar{\Phi}, \Phi, T]\Big], \end{aligned} \tag{7.17}$$

where

$$\boldsymbol{\xi} = \begin{pmatrix} \bar{\Delta} B \\ -\bar{B}\Delta \end{pmatrix}, \quad \bar{\boldsymbol{\xi}} = \left(\bar{B}\Delta, -\bar{\Delta}B\right). \tag{7.18}$$

The terms linear in $\boldsymbol{q}$ and $\bar{\boldsymbol{q}}$ can be absorbed into the bilinear term by shifting the Grassmann fields: $\boldsymbol{q} \to \boldsymbol{q} + \boldsymbol{G}\boldsymbol{\xi}$, $\bar{\boldsymbol{q}} \to \bar{\boldsymbol{q}} + \bar{\boldsymbol{\xi}}\boldsymbol{G}^{-1}$. Performing the Grassmann integral over the quark fields, we get the effective action for the mesons, the baryons and the diquarks:

$$\begin{aligned} &I(\phi, \bar{\Delta}, \Delta, \bar{B}, B) \\ &\quad = \int d\tau \int d^3x \left[\frac{1}{4G}\sigma^2 + \frac{1}{4H}\bar{\Delta}\Delta + \frac{1}{4\lambda}\bar{B}B \right. \\ &\qquad \left. -\frac{1}{2}\bar{\boldsymbol{\xi}}\boldsymbol{G}\boldsymbol{\xi} - \mathcal{U}[\bar{\Phi}, \Phi, T]\right] - \frac{1}{2}\ln(\mathrm{Det}\boldsymbol{G}^{-1}). \end{aligned} \tag{7.19}$$

The first three terms in the integrand form a part of the mass terms of the auxiliary meson, diquark and baryon fields respectively. The fourth term, bilinear in the composite fields $\boldsymbol{\xi}$ and $\bar{\boldsymbol{\xi}}$, which has appeared due to the shift of the quark Grassmann integral, is a baryon-diquark interaction mediated by a quark exchange. The last term, written rather symbolically with a determinant in the functional space, contains some highly non-linear terms in these fields due to the coupling to a quark loop. Although there are no kinetic terms for the auxiliary fields, the energy and the momentum dependence of these fields are hiding in their space-time dependence, that will be retrieved later from the sum over the Matsubara frequencies.

7.1.2 Gap equations

The partition function is now expressed as a path integral over the auxiliary fields with the non-linear effective action Eq.(7.19). We note that no approximation has been done so far. In order to evaluate this path integral, we need to do an approximation, a method of steepest descent, in order to do the Gaussian integral around the stationary point of the effective action.

The stationarity conditions are given by the functional derivatives of this effective action with respect to each auxiliary field:

$$\frac{\delta I}{\delta \phi} = \frac{\delta I}{\delta \Delta} = \frac{\delta I}{\delta \bar{\Delta}} = \frac{\delta I}{\delta B} = \frac{\delta I}{\delta \bar{B}} = 0, \tag{7.20}$$

where the last two conditions for the stationarity with respect to the baryon fields would simply give $B = \bar{B} = 0$.

Since there is no non-linear term in Eq.(7.19), the stationarity conditions for the baryon and the anti-baryon are trivially satisfied. We obtain the explicit form of the gap equation for the constituent quark mass from

Eq.(7.20):

$$
\begin{aligned}
&M_0 - m_0 \\
&= \gamma_q G \mathrm{tr}_c \int \frac{d^3p}{(2\pi)^3} \frac{M_0}{2E_p} \\
&\times \Big(\frac{E_p + \mu}{E^+_{\Delta,A_4}} \big(1 - 2f(E^+_{\Delta,A_4})\big) + \frac{E_p - \mu}{E^-_{\Delta,A_4}} \big(1 - 2f(E^-_{\Delta,A_4})\big) \Big)
\end{aligned}
\tag{7.21}
$$

and for the diquark condensate Δ_0, we have

$$
\Delta_0 = \gamma_q H \Delta_0 \mathrm{tr}_c \int \frac{d^3p}{(2\pi)^3} \tag{7.22}
$$

$$
\times \Big(\frac{1}{E^+_{\Delta,A_4}} \big(\frac{1}{2} - f(E^+_{\Delta,A_4})\big) + \frac{1}{E^-_{\Delta,A_4}} \big(\frac{1}{2} - f(E^-_{\Delta,A_4})\big) \Big), \tag{7.23}
$$

where

$$
E^{\pm}_{\Delta,A_4} = \sqrt{(E_p \pm \mu \mp iA_4)^2 + \Delta_0^2}, \tag{7.24}
$$

and $\gamma_q = 2 \times 2 \times 3 \times N_f$ counts spin, particle-antiparticle, colour, and flavour degeneracy. Note that the gap equation for the constituent quark mass Eq.(7.21) agrees with Eq.(5.29) which has been obtained in Chapter 5 when the diquark condensate is equal to zero and the chemical potential is equal to zero.

In the case where the diquark condensate Δ_0 is equal to zero, the quark distribution function $f(E^{\pm}_{\Delta,A_4})$ can be written in terms of the expectation value of the Polyakov loop. We take the diagonal representation for the Polyakov loop, $L = (e^{i\phi_1}, e^{i\phi_2}, e^{-i(\phi_1+\phi_2)})$, following Fukushima's method, so that the expectation values of the Polyakov loops Φ and $\bar{\Phi}$ become

$$
\Phi = \frac{1}{3} \langle (e^{i\phi_1} + e^{i\phi_2} + e^{-i(\phi_1+\phi_2)}) \rangle \tag{7.25}
$$

$$
\bar{\Phi} = \frac{1}{3} \langle (e^{-i\phi_1} + e^{-i\phi_2} + e^{i(\phi_1+\phi_2)}) \rangle \quad . \tag{7.26}
$$

By using Φ and $\bar{\Phi}$, we get

$$
\begin{aligned}
&\frac{1}{3} \mathrm{tr}_c f(E^{\pm}_{A_4}) = f_{\Phi}(E^{\pm}) \\
&= \frac{\Phi e^{2\beta E^{\pm}} + 2\bar{\Phi} e^{\beta E^{\pm}} + 1}{e^{3\beta E^{\pm}} + 3\Phi e^{2\beta E^{\pm}} + 3\bar{\Phi} e^{\beta E^{\pm}} + 1}.
\end{aligned}
\tag{7.27}
$$

From the effective action Eq.(7.19), we can also obtain the gap equations for the expectation values of the Polyakov loops Φ and $\bar{\Phi}$,

$$
\frac{\delta I}{\delta \Phi} = \frac{\delta I}{\delta \bar{\Phi}} = 0. \tag{7.28}
$$

By solving these equations simultaneously, we get the stationary point.

7.2 Effective action for mesons and baryons

In this section, we derive the effective action for mesons and baryons by performing the diquark and anti-diquark integrals in the partition function,

$$Z = \int d\phi d\bar{\Delta} d\Delta d\bar{B} dB \; e^{-I(\phi,\bar{\Delta},\Delta,\bar{B},B)} \tag{7.29}$$

with the effective action Eq.(7.19). Since the effective action is not bilinear in the diquark and the anti-diquark fields, it is impossible to calculate the partition function analytically, so that we need an approximation of the effective action. We expand Eq.(7.19) up to the second order in the diquark fluctuations around the stationary point determined by the gap equations Eq.(7.20).

$$\begin{aligned} & I(\phi, \bar{\Delta}, \Delta, \bar{B}, B) \\ & \simeq I_0(\phi, \bar{\Delta} = \Delta = \Delta_0, \bar{B}, B) + \frac{1}{2} \sum_{i,j} \frac{\delta^2 I}{\delta \bar{\Delta}_i \delta \Delta_j} \bigg|_{\bar{\Delta}=\Delta=\Delta_0} \bar{\Delta}_i \Delta_j, \end{aligned} \tag{7.30}$$

where the sum in the second term in the right hand side is taken over the colour indices i, j. From the second derivative of the last term in Eq.(7.19) with respect to the diquark fields, we get the diquark self energy Π^k_Δ,

$$\Pi^k_\Delta(q, \omega_n) = \Pi_{1,\Delta} + \Pi^k_{2,\Delta}(q, \omega_n), \tag{7.31}$$

where

$$\Pi_{1,\Delta} = \sum_{m,i} \mathrm{tr} \int \frac{d^3p}{(2\pi)^3} \Big(\frac{1}{\varepsilon_m^2 + E^{-2}_{\Delta,i}} + \frac{1}{\varepsilon_m^2 + E^{+2}_{\Delta,i}} \Big) \tag{7.32}$$

and

$$\Pi^k_{2,\Delta} = (\omega_n^2 + q^2 + 4M_0^2 + \Delta_0^2) F(\omega_n, q) \tag{7.33}$$

with

$$\begin{aligned} F(\omega_n, q) = & \sum_{m,i,j} \epsilon_{ilk} \mathrm{tr} \int \frac{d^3p}{(2\pi)^3} \\ & \times \Big\{ \frac{1}{(\varepsilon_m^2 + E^{-2}_{\Delta,i}(p))((\varepsilon_m + \omega_n)^2 + E^{-2}_{\Delta,j}(p+q))} \\ & + \frac{1}{(\varepsilon_m^2 + E^{+2}_{\Delta,i}(p))((\varepsilon_m + \omega_n)^2 + E^{+2}_{\Delta,j}(p+q))} \Big\}. \end{aligned} \tag{7.34}$$

The $\omega_n = 2n\pi T$ are the bosonic Matsubara frequencies and $\varepsilon_m = (2m+1)\pi T$ are the fermionic Matsubara frequencies. The sum in Eq.(7.32) is taken over the quark Matsubara frequencies and the quark colour index, and the sum

in Eq.(7.34) is taken over the quark Matsubara frequencies and the quark colour indices i, j. The energy $E^{\pm}_{\Delta,i}$ are given as

$$E^{\pm}_{\Delta,i} = \sqrt{(E_p \pm \mu \mp i\phi_i)^2 + \Delta_0^2} \ . \tag{7.35}$$

Note that $\phi_k = -(\phi_i + \phi_j)$. The sum over the fermionic Matsubara frequencies can be replaced by a contour integration like in the previous calculations performed in Chapters 4 to 6. We will show the explicit form of the diquark self energy as a function of the diquark momentum and the diquark energy in the next section, under the assumption that the diquark condensate Δ_0 is equal to zero.

The forth term in the square bracket in Eq.(7.19) contains two types of diagrams shown in Fig.7.2. The intermediate bold line in the diagram (a) is the quark propagator dressed by an even number of diquark field insertions as shown in the top diagram of Fig.7.3, while in (b) it is the quark propagator dressed by an odd number of diquark field insertions, as shown in the bottom diagram of Fig.7.3.

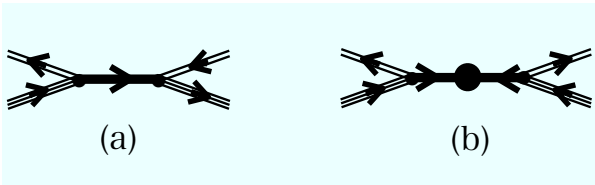

Figure 7.2: (a) Intermediate quark propagator with an even number of diquark fields (shown in the top of Fig.7.3). (b) Quark propagator with an odd number of diquark fields (shown in the bottom in Fig.7.3.)

In order to perform the Gaussian integral over the diquark fields in the partition function, we only need the second order terms in the diquark fields. For this reason, we neglect all the terms beyond the second order, so that only the lowest term in the diagram (a) of Fig.7.2 remains. There is no contribution from the diagram (b) because even the lowest order term contains the third power of the diquark fields. Therefore, we take only the first term in the diagram (a) of Fig.7.2 into account, which is illustrated in Fig.7.4.

Since we stop the expansion at the second order in the diquark fluctuations, we can perform the integral over the diquark fields, and then we obtain the effective action as a function of the meson fields and the baryon fields:

$$I(\phi, \bar{B}, B) = I_0 + \frac{1}{2}\mathrm{Tr}\ \ln \left. \frac{\delta^2 I}{\delta\bar{\Delta}\delta\Delta} \right|_{\Delta_0} , \tag{7.36}$$

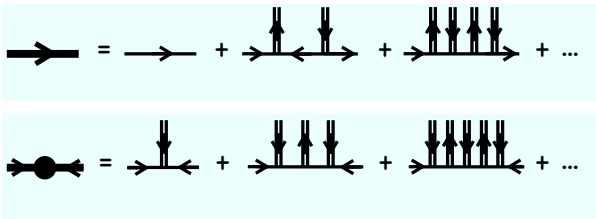

Figure 7.3: The top diagram is the intermediate quark propagator of the diagram (a) in Fig.7.2, which has an even number of diquark fields. The bottom diagram corresponds to the intermediate propagator of the diagram (b) in Fig.7.2, which has an odd number of diquark fields.

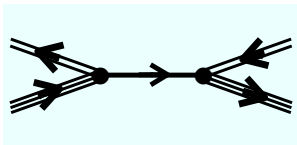

Figure 7.4: The intermediate line is a free quark propagator without diquark fields.

where

$$\left.\frac{\delta^2 I}{\delta\bar{\Delta}\delta\Delta}\right|_{\Delta_0} = \frac{1}{2H} - \Pi_{\Delta_0} - \bar{B}SB \tag{7.37}$$

and where

$$S(\varepsilon, p) = [(\varepsilon - \mu - i\phi_i T)\gamma_0 - \mathbf{p}\cdot\boldsymbol{\gamma} - M_0]^{-1} \tag{7.38}$$

is the quark quasiparticle propagator. This effective action contains all informations about mesons and baryons in this approach.

7.3 The $\Delta_0 = 0$ case

Having derived the effective action for the meson, the diquark and the baryon fields, we now consider the thermal excitations of mesons and baryons in the low temperature confined phase, where the baryons are described as colour singlet bound states of a quark and a diquark, in the same way as the mesons are described as colour singlet bound states of a quark and an antiquark. For this purpose, we assume that there are no diquark condensates ($\Delta_0 = 0$), and integrate out the diquark auxiliary fields around the stationary point. This procedure is very similar to the method used in Chapter 5 to compute

the mesonic correlations (in the absence of diquark correlations) for the pressure and for the entropy. We first recall the procedure for the mesonic correlations in order to apply it for the present purpose.

7.3.1 Scalar meson correlation

In the absence of diquark interaction $\mathcal{L}_{qq}$ Eq.(7.4), the mesonic effective action can be extracted from Eq.(7.19) by expanding in powers of the mesonic auxiliary fields and by setting $\Delta = \bar{\Delta} = \bar{B} = B = 0$:

$$\begin{aligned} & I(\phi, \bar{\Delta} = 0, \Delta = 0, \bar{B} = 0, B = 0) \\ & \simeq I_0(\phi) + \frac{1}{2} \sum_{i,j} \frac{\delta^2 I}{\delta\phi_i \delta\phi_j}\bigg|_{\bar{\Delta}=\Delta=0} \phi_i \phi_j, \end{aligned} \tag{7.39}$$

where the indices i and j run over the sigma meson ($i = 0$) and over the pions ($i = 1, 2, 3$) and the trace is over the other internal degrees of freedom of the meson fields. For example, we find for the sigma meson polarisation:

$$\frac{\delta^2 I}{\delta\sigma\delta\sigma}\bigg|_{\bar{\Delta}=\Delta=0} = \frac{1}{2G} - \Pi_\sigma, \tag{7.40}$$

where

$$\begin{aligned} \Pi_\sigma(q, \omega_n) = & -\frac{1}{\beta} \int \frac{d^3p}{(2\pi)^3} \\ & \times \sum_{m,i} \mathrm{Tr}\left[S_i(i\varepsilon_m + i\omega_n, p + q) S_i(i\varepsilon_m, p)\right]. \end{aligned} \tag{7.41}$$

S_i is the quark quasiparticle propagator at finite chemical potential,

$$S_i(\varepsilon, p) = [(\varepsilon - \mu - i\phi_i T)\gamma_0 - \mathbf{p} \cdot \boldsymbol{\gamma} - M_0]^{-1}. \tag{7.42}$$

The trace is taken over the Dirac indices as well as the flavour indices, and the sum is taken over the quark colour index i. The sum over the fermionic Matsubara frequencies ε_m yields the following Minkowski space expression for the sigma meson polarisation:

$$\begin{aligned} \Pi_\sigma(\omega, q) \quad = \quad & -\int \frac{d^3p}{(2\pi)^3} \int_C \frac{d\varepsilon}{2\pi i} f(\varepsilon) \\ & \times \sum_i \mathrm{Tr}\left[S_i(\varepsilon + \omega, p + q) S_i(\varepsilon, p)\right]. \end{aligned} \tag{7.43}$$

The detailed computation of this scalar meson polarisation is given in Appendix G, where after the statistical average over the background gauge field, we find

$$\Pi_\sigma(\omega, q) \quad = \quad \mathcal{T} + (\omega^2 - q^2 - 4M_0^2)\mathcal{F}(\omega, q), \tag{7.44}$$

where $\mathcal{T}$ is a function of the temperature and of the chemical potential given by

$$\mathcal{T} = \gamma_q \int^{\Lambda} \frac{d^3p}{(2\pi)^3} \frac{1}{E_p} \left[f_\Phi(E_p - \mu) + f_\Phi(E_p + \mu) - 1 \right], \tag{7.45}$$

which is independent of (ω, q). This quantity is just the thermal expectation value of the quark condensate divided by the constituent quark mass, and it is related by the mass gap equation to the NJL coupling G:

$$\mathcal{T} = \frac{\langle \bar{q}q \rangle}{M_0} = -\frac{1}{2G}\left(1 - \frac{m_0}{M_0}\right). \tag{7.46}$$

The second term in Eq.(7.44) contains the scattering term and the pair excitation term,

$$\mathcal{F}(\omega, q) = \mathcal{F}_{\text{scatt}}(\omega, q) + \mathcal{F}_{\text{pair}}(\omega, q). \tag{7.47}$$

The explicit forms of the scattering term $\mathcal{F}_{\text{scatt}}(\omega, q)$ and the pair excitation term $\mathcal{F}_{\text{pair}}(\omega, q)$ at finite chemical potential μ are given in Appendix G.

The contribution from the sigma meson correlations to the pressure is given by

$$\begin{aligned}
p_\sigma &= -\frac{T}{V}\frac{1}{2}\text{Tr}\ \ln\left[\frac{1}{2G} - \Pi_\sigma\right] \\
&= -T\frac{1}{2}\sum_{n,k}\int \frac{d^3q}{(2\pi)^3}\ln\left[\frac{1}{2G} - \Pi_\sigma(\omega_n, q)\right] \\
&= -\frac{1}{2}\int \frac{d^3q}{(2\pi)^3}\int \frac{d\omega}{2\pi i}\left(f_B(\omega) - f_B(-\omega)\right) \\
&\qquad \times \ln\left[\frac{1 - 2G\Pi_\sigma(\omega + i\delta, q)}{1 - 2G\Pi_\sigma(\omega - i\delta, q)}\right] \\
&= -\frac{1}{2}\int \frac{d^3q}{(2\pi)^3}\int \frac{d\omega}{2\pi i}\left(1 + 2f_B(\omega)\right) \\
&\qquad \times \ln\left[\frac{1 - 2G\Pi_\sigma(\omega + i\delta, q)}{1 - 2G\Pi_\sigma(\omega - i\delta, q)}\right],
\end{aligned} \tag{7.48}$$

where we have used $f_B(-\omega) = -1 - f_B(\omega)$ for the Bose distribution function,

$$f_B(\omega) = \frac{1}{e^{\beta\omega} - 1}. \tag{7.49}$$

The scalar meson contribution to the pressure is contained in the pole parts of the argument. In the chiral limit, the collective mesonic pressure can be extracted explicitly thanks to the cancellation between the tadpole term $\mathcal{T}$ of the polarisation.

7.3.2 Diquark correlations

We adopt the same procedure for the diquark field, by expanding Eq.(7.19) up to the second order in the diquark fluctuations

$$\begin{aligned} I(\phi, \bar{\Delta}, \Delta, \bar{B}, B) \quad &\simeq \quad I_0(\phi, \bar{\Delta} = \Delta = 0, \bar{B}, B) \\ &\quad + \frac{1}{2} \sum_{i,j} \frac{\delta^2 I}{\delta \bar{\Delta}_i \delta \Delta_j} \bigg|_{\bar{\Delta}=\Delta=0} \bar{\Delta}_i \Delta_j. \end{aligned} \tag{7.50}$$

Extracting the kinetic term of the diquark fields leads to:

$$\frac{\delta^2 I}{\delta \bar{\Delta}_i \delta \Delta_j} \bigg|_{\bar{\Delta}=\Delta=0} = \left(\frac{1}{2H} + \Pi^i_\Delta - \bar{B} S B \right) \delta_{ij}, \tag{7.51}$$

where $\Pi^i_\Delta(\omega, q)$ is the polarisation of the diquark of a colour index i into a pair of quarks in the mean field distribution (See (b) in Fig.7.5) , while the third term is the interaction of a diquark and a baryon through a quark exchange.

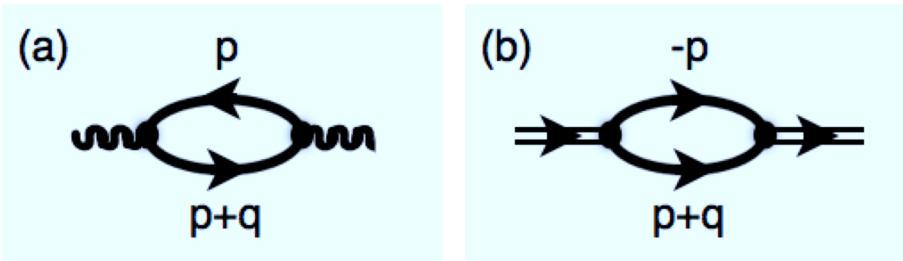

Figure 7.5: Quark polarisation for mesons (a) and for diquarks (b). The solid lines represent quark quasiparticles with effective quark mass M. Note the difference in the sign of momentum.

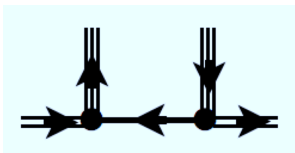

Figure 7.6: Diquark propagation in the presence of "external baryon fields". The intermediate line is a quark propagator in the mean field approximation.

The diquark polarisation is similar to the meson polarisation as shown in the panel (b) in Fig.7.5, and it is given by

$$\Pi^k_\Delta(q,n) = -\frac{1}{\beta}\int \frac{d^3p}{(2\pi)^3} \times \sum_{m,i,j} \epsilon_{ijk} \mathrm{Tr}\left[\gamma_5 S_i(i\varepsilon_m + i\omega_n, p+q)\gamma_5 S_j(-i\varepsilon_m, -p)\right]. \tag{7.52}$$

Performing the sum over the fermionic Matsubara frequencies ε_m by the contour integration methos, we obtain the Minkowski space polarisation in a similar way as the scalar meson polarisation:

$$\begin{aligned}\Pi^k_\Delta(\omega,q) &= -\int \frac{d^3p}{(2\pi)^3}\int_C \frac{d\varepsilon}{2\pi i} f(\varepsilon) \sum_{i,j} \epsilon_{ijk} \\ &\quad \times \mathrm{Tr}\left[\gamma_5 S_i(\varepsilon+\omega, p+q)\gamma_5 S_j(-\varepsilon, -p)\right].\end{aligned} \tag{7.53}$$

We present the details of the computation of the diquark polarisation in the Appendix G and we find that the result is very similar to the scalar meson polarisation:

$$\Pi^k_\Delta(\omega,q) = \mathcal{T} + (\omega'^2 - q^2 - 4M_0^2)\mathcal{F}_\Delta(\omega', q). \tag{7.54}$$

We note that the diquark energy ω is replaced by

$$\omega' = \omega - 2\mu + i\phi_k T. \tag{7.55}$$

This shift reflects that the diquark carries the quark number 2, or the baryon number 2/3, and carries the same colour as an antiquark. In deriving the above results, we have taken the gauge field average for the quark distribution functions ignoring the gauge field dependence in the shifted diquark energy ω'.

After performing the Gaussian integration over the diquark fields, we find the effective action for the meson-baryon system:

$$\begin{aligned} I(\phi,\bar{B},B) &= I_0(\phi,\bar{B},B) \\ &\quad + \frac{1}{2}\mathrm{Tr}\ \ln\left[\frac{1}{2H} - \Pi_\Delta - \bar{B}SB\right],\end{aligned} \tag{7.56}$$

where the baryon fields are contained in the first term I_0 which has been obtained in the mean-field approximation for the quarks, as well as in the second term due to the thermal fluctuations of the diquark field, or the diquark correlations. In this expression, the trace is taken over the bosonic

Matsubara frequencies ω_n of the diquark fields as well as over the diquark momentum $\boldsymbol{q}$.

In order to evaluate the baryon contribution to the partition function, we need to perform the Grassmann integration over the baryon fields. For this purpose, we expand the logarithm in Eq.(7.56) in powers of the term bilinear in the baryon fields:

$$\begin{aligned}&\mathrm{Tr}\ \ln\left[\frac{1}{2H}-\Pi_\Delta-\bar{B}SB\right]\\&\simeq \mathrm{Tr}\ \ln\left[\frac{1}{2H}-\Pi_\Delta\right]-\mathrm{Tr}\Big[\frac{2H\bar{B}SB}{1-2H\Pi_\Delta}\Big].\end{aligned} \tag{7.57}$$

The first term is the contribution of the thermal excitations of the diquarks to the effective action, which gives a contribution of the diquark correlations to the thermodynamic potential:

$$p_\Delta = -\frac{T}{V}\frac{1}{2}\mathrm{Tr}\ \ln\left[\frac{1}{2H}-\Pi_\Delta\right] \tag{7.58}$$

$$= -T\frac{1}{2}\sum_{n,k}\int\frac{d^3q}{(2\pi)^3}\ln\left[\frac{1}{2H}-\Pi^k_\Delta(\omega_n,q)\right] \tag{7.59}$$

$$\begin{aligned}= -\frac{1}{2}\sum_k\int\frac{d^3q}{(2\pi)^3}\int\frac{d\omega}{2\pi i}\,&[f_B(\omega-2\mu-i\phi_kT)\\&-f_B(-\omega-2\mu-i\phi_kT)]\\&\times\ln\left[\frac{1-2H\Pi^k_\Delta(\omega+i\delta,q)}{1-2H\Pi^k_\Delta(\omega-i\delta,q)}\right].\end{aligned} \tag{7.60}$$

f_B is the bosonic distribution function that depends on the diquark energy ω, and contains twice the quark chemical potential μ and a gauge potential ϕ_k. Only when the diquark condensate is equal to zero, the distribution function can be written in terms of the expectation value of the Polyakov loop. To simplify, we write $\beta A_4 = \mathrm{diag}(\phi_1,\phi_2,\phi_3) = \mathrm{diag}(\phi,-\phi,0)$. By taking the trace over the colour index, the diquark distribution function $f_\Delta(E)$ can be written as

$$\begin{aligned}&f_\Delta(\omega)\equiv\langle\frac{1}{3}\mathrm{tr}_c f_B(\omega-2\mu-i\phi_kT)\\&=\frac{1}{3}\frac{e^{2(\omega-2\mu)}(e^{2i\phi}+e^{-2i\phi}+1)-2e^{\omega-2\mu}(e^{2i\phi}+e^{-2i\phi}+1)+3}{e^{3(\omega-2\mu)}-e^{2(\omega-2\mu)}(e^{2i\phi}+e^{-2i\phi}+1)+e^{\omega-2\mu}(e^{2i\phi}+e^{-2i\phi}+1)-1}.\end{aligned} \tag{7.61}$$

It can be also written in terms of the expectation value of the Polyakov loop Φ, then we obtain $f_\Delta(\omega-2\mu)$ as a function of Φ:

$$f_\Delta=\frac{\Phi(3\Phi-2)e^{2(\omega-2\mu)}-2\Phi(3\Phi-2)e^{\omega-2\mu}+1}{e^{3(\omega-2\mu)}-3\Phi(3\Phi-2)e^{2(\omega-2\mu)}+3\Phi(3\Phi-2)e^{\omega-2\mu}-1}. \tag{7.62}$$

Note that in the deconfined phase where $\Phi = 1$, we have a diquark distribution function with diquark energy $E_p + E_{p+q}$,

$$f_\Delta = \frac{1}{e^{\beta(\omega-2\mu)} - 1}. \tag{7.63}$$

On the other hand, in the confined phase where $\Phi = 0$, we have a suppressed distribution function with prefactor 3 times the diquark energy as argument:

$$f_\Delta = \frac{1}{e^{3\beta(\omega-2\mu)} - 1}. \tag{7.64}$$

Now we get the diquark pressure in terms of the diquark distribution function modified by the Polyakov loop,

$$\begin{aligned} p_\Delta &= -\frac{3}{2}\int \frac{d^3q}{(2\pi)^3}\int \frac{d\omega}{2\pi i}\left[f_\Delta(\omega-2\mu) + f_\Delta(\omega+2\mu) + 1\right] \\ &\quad \times \ln\left[\frac{1 - 2H\Pi^k_\Delta(\omega+i\delta, q)}{1 - 2H\Pi^k_\Delta(\omega-i\delta, q)}\right]. \end{aligned} \tag{7.65}$$

Since Eq.(7.64) suppresses the diquark excitations at low temperatures, their contribution to the pressure is small.

We note that the contribution Eq.(7.65) to the pressure from diquark correlation indicates that the diquark collective modes are given by the solutions of

$$1 - 2H\Pi^k_\Delta(\omega + i\delta, q) = 0. \tag{7.66}$$

Like for the meson collective modes, this equation has isolated zeros when the imaginary part of the diquark self-energy is zero,

$$\mathrm{Im}\Pi^k_\Delta(\omega + i\delta, q) = 0, \tag{7.67}$$

which is the kinematical condition that guarantees that the diquark does not decay spontaneously into a pair of quarks. Even if a solution exists for the diquark collective modes, their thermal excitations are suppressed by the colour correlations as the mean-field quark excitations.

7.3.3 Baryon excitations

The second term of Eq.(7.57) can be viewed as a correction to the baryon self-energy, so that we write

$$\Sigma_B = -\frac{2HS}{1 + 2H\Pi_\Delta}. \tag{7.68}$$

Note that Σ_B is a 4×4 Dirac matrix with the quark propagator S. Its diagrammatical representation is shown in Fig.7.7. Then the baryon sector of the effective action becomes,

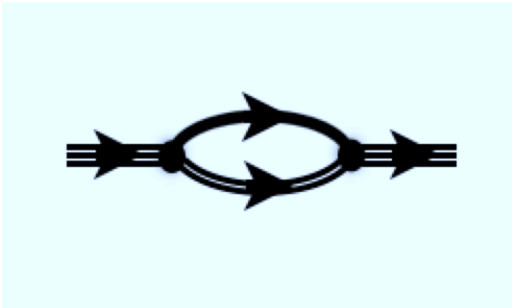

Figure 7.7: Quark-diquark polarisation for baryons.

$$I_B = \mathrm{Tr}\bar{B}\left[\frac{1}{2\lambda} + \Sigma_B\right] B. \tag{7.69}$$

The contribution of the baryonic correlations to the pressure is obtained by performing the Grassmann integration over the baryon fields, which leads to:

$$\begin{aligned} p_B &= \frac{T}{V}\mathrm{Tr}\ \ln\ \det{}_\gamma\left[\frac{1}{2\lambda} + \Sigma_B\right] \\ &= \frac{1}{2}T\sum_n \int \frac{d^3P}{(2\pi)^3}\ln\ \det{}_\gamma\left[1 + 2\lambda\Sigma_B(E_n, P)\right] \\ &= \frac{1}{2}\int \frac{d^3P}{(2\pi)^3}\int \frac{dE}{2\pi i}\left[f(E-3\mu) + f(E+3\mu) - 1\right] \\ &\quad \times \ln\ \det{}_\gamma\left[\frac{1 + 2\lambda\Sigma_B(E+i\delta, P)}{1 + 2\lambda\Sigma_B(E-i\delta, P)}\right], \end{aligned} \tag{7.70}$$

where $\det_\gamma$ denoted the determinant over the Dirac indices and Tr is the trace over all the other indices including the baryon momentum P and the fermionic Matsubara frequencies E_n of the baryon fields.

The baryon excitations are contained in the poles of the argument, like in the calculation of the mesonic pressure. Therefore, the equation that determines the baryon mass M_B is given by

$$\det{}_\gamma\left[1 + 2\lambda\Sigma_B(M_B + i\delta, P = 0)\right] = 0. \tag{7.71}$$

Note that no statistical average over the background gauge fields appear here, since the baryons are colour neutral states (like the mesons). This implies that there is no suppression for the baryon distribution function due to the phase cancellation, unlike the quark or the diquark distributions in the confined phase.

It may be interesting to compare our calculation with the Faddeev approach to make baryons from quarks used by Ishii, Bentz and Yazaki [136]. They also begin with the NJL model (but without the Polyakov loop), and construct baryons from quarks and diquarks by solving the relativistic Faddeev equation. Since their calculation contains the exchange of quarks (see Fig.7.8), while ours does not, our baryons correspond to their lowest order term.

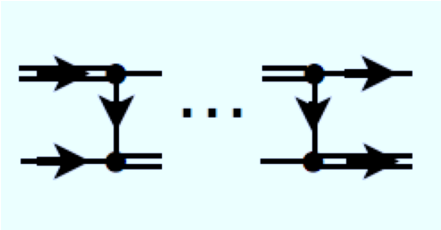

Figure 7.8: An exchange diagram for the polarisation of baryons.

7.4 Conclusions

We have calculated in this chapter the diquark pressure and the baryon pressure. The diquark pressure is written in terms of the modified bosonic distribution function with the diquark energy and the diquark momentum. When the diquark condensate is equal to zero, the distribution function can be rewritten in terms of the expectation value of the Polyakov loop. Since the Polyakov loop suppresses the diquark excitations at low temperatures, the contribution from the diquark fluctuations to the pressure is small. In contrast, the Polyakov loop does not appear in the fermionic distribution function for the baryons. Therefore, the baryonic fluctuations can give a contribution at low temperatures. However, the baryons have a large mass, for instance compared to pions, so that their contribution to the pressure at low temperature is smaller than that of the pions and of the sigma mesons.

Chapter 8

Conclusions

We have proposed a method to describe the mesonic and the baryonic excitations at low temperatures in the PNJL model, in order to better describe the quark-hadron phase transition. First, in Chapter 5, we have focused on the zero chemical potential case, and considered only the mesonic correlations in the two flavour PNJL model, by expanding the effective action including the meson fields (as auxiliary fields) up to second order in the fluctuations around the stationary point determined from the gap equation. Since the Polyakov loop which is coupled to a quark loop suppresses the coloured states at low temperatures, the quark excitations do not appear in the hadronic phase when described in this method, but instead the mesonic correlations appear as the dominant thermal excitations. However, even though the Polyakov loop acts for suppressing quark excitations, the quark triads still continue to exist at low temperatures. They cause a mismatch of degrees of freedom, if one tries to understand them as baryons. This is indeed a problem at least in principle, but we have found numerically that the contribution from the quark triads to the pressure and the entropy is very small, so that mesons, especially pions, dominate the pressure and the entropy at low temperatures. As the temperature increases, the contribution from the mesons becomes smaller, since they melt into quarks and antiquarks in the transition region, then we have a pressure dominated by quarks and gluons at high temperatures.

We have also discussed at which temperature the mesons as collective modes melt into quarks by calculating the real part and the imaginary part of the meson polarisation. The condition that the real part is equal to zero gives the dispersion relation, and the imaginary part gives the thermal excitations of the non-collective modes of quarks and antiquarks. If both the real and the imaginary parts vanish simultaneously at a common value of momentum and energy, it means that there is an isolated meson pole at this momentum and energy. In the two-flavour case, we have found that the sigma meson melts at a lower temperature than the pion. This can be interpreted by the

fact that the sigma meson pole appears at a higher energy than that of the pion with the same momentum because of its heavier mass. Therefore, when the continuum of quarks in the time-like region moves down to lower energy as the temperature increases, the sigma meson pole is absorbed first. The pion pole is absorbed only after the continuum approaches sufficiently the light cone, since the pion pole is located just above the light cone because of its small mass. After being absorbed into the continuum, both the pions and the sigma mesons melt into quarks and antiquarks. We do not allow correlations between mesons in this method. Therefore, there is no process by which a sigma meson would decay into two pions. If one is interested in such a process, the expansion of the effective action up to at least fourth order in the fluctuations is necessary. This may be a direction for future works.

In Chapter 6, we have extended the two-flavour PNJL model to the three-flavour case. The Lagrangian of the three-flavour PNJL model requires a six quark interaction in order to break the axial $U(1)$ symmetry. First, the six quark interaction has been reduced to an effective four quark interaction by making the approximate assumption that quark and antiquark pair is replaced by a condensate. This approximation makes it possible to deal with this effective four-point interaction and the original four-point interaction simultaneously by introducing an effective coupling constant. Once we have rewritten the six-quark interaction as a four-quark interaction, the same calculations as in the two-flavour case have been performed in order to obtain the equation of state including the mesonic fluctuations. In contrast to the two-flavour case, the three-flavour PNJL model contains 9 species of pseudo scalar mesons and 9 species of scalar mesons. We have calculated numerically the pressure including the pions and the kaons. In this calculation of the pressure, we have neglected all the other mesons, such as the η, η', κ, a_0, σ and f_0. These mesons can be expected not to dominate the pressure because of their heavier masses than the π and K.

We have then extended the two-flavour PNJL model to the finite chemical potential case in Chapter 7. In order to consider the baryons, not only the mesons, we have introduced a Lagrangian containing a quark-antiquark interaction and a quark-quark interaction. The quark-antiquark interaction is used for composing the $\bar{q}q$ condensates as shown in Chapter 5, and the quark-quark interaction is used for making the qq condensates. The values of these condensates are determined by solving the gap equations for the constituent quark mass and the diquark condensate. But we have set the diquark condensate equal to zero in order to simplify, then we have solved the gap equation for the constituent quark mass. We have assumed that baryons are composed by a quark and a diquark. Therefore, the baryon polarisation calculated under this assumption is represented by a combination of the quark propagator and the diquark propagator. In this approach, we can calculate the contribution from both the diquark excitations and the

baryonic excitations to the pressure. The pressure of the diquark excitations can be written in terms of a modified bosonic distribution function with the diquark energy and twice the quark chemical potential. The diquark distribution function also depends on the gauge potential. Since the gauge potential appears in the phase factor of the diquark distribution function, it can be replaced by the expectation value of the Polyakov loop in the same way as for the quark distribution function, but this can only be done when the diquark condensate is equal to zero. The Polyakov loop acts at low temperatures to suppress the diquark excitations, so that they do not dominate the pressure at low temperatures. The pressure of baryonic excitations is written in terms of a fermionic distribution function with the baryon energy and three times the quark chemical potential. Since the baryons are colour singlet states, the Polyakov loop does not appear in the baryon distribution function, unlike in the quark and the diquark distribution functions. This means that the baryonic excitations can give a contribution to the pressure at low temperatures as well as the mesonic excitations.

In this work, we have considered only the case with a vanishing diquark condensate. This amounts to looking only at the small chemical potential region. However, it would be interesting to consider also a finite diquark condensate in order to investigate at which chemical potential the colour superconductor phase appears, and how the hadronic phase changes to the colour superconductor phase. This knowledge may play an important role when searching the phase structure in QCD. Moreover, taking correlations between baryons into account is also important. In this work, the baryon-baryon correlations have been neglected, since we have stopped the expansion of the effective action at the second order in the baryonic fluctuations. It may be possible to consider them by continuing the expansion up to higher order in the fluctuations. In addition, it may also be interesting to calculate the baryon number susceptibility at finite temperature and finite chemical potential. Since our method can describe the change of the degrees of freedom from hadrons to quarks, this would be useful to search some important features of the QCD phase diagram, such as a critical point.

Appendix A

Gamma matrices

We summarise some important properties of the Gamma matrices that we have used for the calculations in this work. More details about the Gamma matrices can be found in the following reference [139].

The Gamma matrices γ^μ ($\mu = 0, 1, 2, 3$) are defined as satisfying this relation;

$$\{\gamma^\mu, \gamma^\nu\} = 2g^{\mu\nu}, \tag{A.1}$$

and γ_5 is defined by

$$\gamma_5 \equiv i\gamma^0\gamma^1\gamma^2\gamma^3 = -i\gamma_0\gamma_1\gamma_2\gamma_3. \tag{A.2}$$

The set of γ^μ that satisfies Eq.(A.1) is not unique. Indeed, the following two representations are often used. The first one is the chiral representation:

$$\gamma^0 = \begin{pmatrix} 0 & 1 \\ 1 & 0 \end{pmatrix}, \quad \boldsymbol{\gamma} = \begin{pmatrix} 0 & -\boldsymbol{\sigma} \\ \boldsymbol{\sigma} & 0 \end{pmatrix}, \quad \gamma_5 = \begin{pmatrix} 1 & 0 \\ 0 & -1 \end{pmatrix}, \tag{A.3}$$

and the second one is the Dirac representation:

$$\gamma^0 = \begin{pmatrix} 1 & 0 \\ 0 & -1 \end{pmatrix}, \quad \boldsymbol{\gamma} = \begin{pmatrix} 0 & \boldsymbol{\sigma} \\ -\boldsymbol{\sigma} & 0 \end{pmatrix}, \quad \gamma_5 = \begin{pmatrix} 0 & 1 \\ 1 & 0 \end{pmatrix}, \tag{A.4}$$

where $\boldsymbol{\sigma} = (\sigma^1, \sigma^2, \sigma^3)$ are the Pauli matrices,

$$\sigma^1 = \begin{pmatrix} 0 & 1 \\ 1 & 0 \end{pmatrix}, \quad \sigma^2 = \begin{pmatrix} 0 & -i \\ i & 0 \end{pmatrix}, \quad \sigma^3 = \begin{pmatrix} 1 & 0 \\ 0 & -1 \end{pmatrix}. \tag{A.5}$$

Note that the Gamma matrices also satisfy the relation,

$$\gamma^\mu\gamma_\mu = 4. \tag{A.6}$$

We summarise some useful properties results for traces of products of Gamma matrices:

$$\text{tr } \gamma^\mu = 0 \tag{A.7}$$

$$\text{tr (any odd number of } \gamma\text{'s)} = 0 \tag{A.8}$$

$$\text{tr } (\gamma^\mu \gamma^\nu) = 4g^{\mu\nu} \tag{A.9}$$

$$\text{tr } \gamma^5 = 0 \tag{A.10}$$

$$\text{tr } (\gamma^\mu \gamma^\nu \gamma^5) = 0. \tag{A.11}$$

Appendix B

Pressure from non-collective mesonic excitations in the chiral limit

Here we present the detail of the computation of the pressure exerted by the non-collective mesonic excitation modes given by Eq.(5.62).

We first perform the sum over the bosonic Matsubara frequencies ω_n in (5.62) by the contour integration in the complex z-plane:

$$\Delta p_M(T, A_4) = -2T \int \frac{d^3q}{(2\pi)^3} \frac{1}{2\pi i} \int_{\mathcal{C}} dz \frac{1}{e^{\beta z} - 1} \ln F(-iz, q, A_4), \tag{B.1}$$

where the contour $\mathcal{C}$ encloses the imaginary axis counter-clockwise. The function $1 \,/\, (e^{\beta z} - \ 1\ )$ has poles at $z = 2\pi n T i = i\omega_n$ and this function is analytic everywhere else. We change the integration path along the contour $\mathcal{C}$ to the path that encloses the real z-axis clockwise. Denoting the integration variable z by ω on the real z-axis and then converting the integration along the paths in the negative ω region into an integration around the positive real axis, we find

$$\Delta p_M(T, A_4) = -2 \int \frac{d^3q}{(2\pi)^3} \frac{1}{2\pi i} \int_0^\infty d\omega \left[1 + \frac{2}{e^{\beta\omega} - 1}\right] \ln \left[\frac{\mathcal{F}(\omega + i\epsilon, q, A_4)}{\mathcal{F}(\omega - i\epsilon, q, A_4)}\right], \tag{B.2}$$

where we have defined $\mathcal{F}$ as

$$\begin{aligned} &\mathcal{F}(\omega, q, A_4) = F(-i\omega, q, A_4) \\ &= 2T \sum_{n'} \mathrm{tr}_c \int \frac{\mathrm{d}^3p}{(2\pi)^3} \frac{1}{\left[(\epsilon_{n'} + gA_4)^2 + E_p^2\right] \cdot \left[(\epsilon_{n'} + gA_4 - i\omega)^2 + E_{p+q}^2\right]}, \end{aligned} \tag{B.3}$$

where the $\epsilon_{n'} = (2n'+1)\pi T$ are the fermionic Matsubara frequencies for the quark-quasiparticles. If it is necessary, we can rewrite the above expression

by partial integration into

$$\Delta p_M(T, A_4) = -2T \int \frac{d^3q}{(2\pi)^3} \frac{1}{2\pi i} \int_0^\infty d\omega \\ \times \big[\omega + \frac{2}{\beta}\ln(1 - \mathrm{e}^{\beta\omega})\big] \frac{d}{d\omega} \ln\Big[\frac{\mathcal{F}(\omega + i\epsilon, q, A_4)}{\mathcal{F}(\omega - i\epsilon, q, A_4)}\Big]. \tag{B.4}$$

We now perform the sum over the fermionic Matsubara frequencies $\epsilon_{n'}$ by contour integration:

$$\mathcal{F}(\omega, q, A_4) = \mathrm{tr}_c \int \frac{\mathrm{d}^3p}{(2\pi)^3} \int_{\mathcal{C}} \frac{dz}{2\pi i} \frac{-1}{e^{\beta z} + 1} \\ \times \frac{1}{\big[(-(z + igA_4)^2 + E_p^2\big] \cdot \big[-(z + igA_4 + \omega)^2 + E_{p+q}^2\big]}, \tag{B.5}$$

where the function $-1/(e^{\beta z} + 1)$ is chosen because it has poles at the fermionic Matsubara frequencies on the imaginary axis. The minus sign is necessary for ensuring the right sign of the residues at these poles. The integration path is chosen in the same way as for the bosonic contour integration. We change the integration path again to the path enclosing the real z-axis, and we perform the integral around the poles of the integrand at the real values of z. The result can be written as a sum of two terms:

$$\mathcal{F}(\omega, q, A_4) = \mathcal{F}_{\mathrm{scat}}(\omega, q, A_4) + \mathcal{F}_{\mathrm{pair}}(\omega, q, A_4). \tag{B.6}$$

The first term is scattering term

$$\mathcal{F}_{\mathrm{scat}}(\omega, q, A_4) = \int \frac{d^3p}{(2\pi)^3} \frac{1}{2E_p 2E_{p+q}} \left(\frac{1}{\omega + E_p - E_{p+q}} - \frac{1}{\omega - E_p + E_{p+q}}\right) \\ \times \mathrm{tr}_c \left(f(E_p - igA_4) - f(E_{p+q} - igA_4)\right), \tag{B.7}$$

while the second term corresponds to pair creation and pair annihilation

$$\mathcal{F}_{\mathrm{pair}}(\omega, q, A_4) = \int \frac{d^3p}{(2\pi)^3} \frac{1}{2E_p 2E_{p+q}} \left(\frac{1}{\omega + E_p + E_{p+q}} - \frac{1}{\omega - E_p - E_{p+q}}\right) \\ \times \mathrm{tr}_c \left(1 - f(E_p - igA_4) - f(E_{p+q} - igA_4)\right). \tag{B.8}$$

The external gauge field again appear in a phases factor in the quark distribution function as well as in the mean-field approximation. We therefore replace these phase factors by the expectation values of the Polyakov loops, and then we substitute them by statistical average as in Eq.(5.30):

$$\mathcal{F}(\omega, q) \equiv \langle \mathcal{F}(\omega, q, A_4) \rangle = \mathcal{F}_{\mathrm{scat}}(\omega, q) + \mathcal{F}_{\mathrm{pair}}(\omega, q), \tag{B.9}$$

where

$$\mathcal{F}_{\rm scat}(\omega,q) = 3\int \frac{d^3p}{(2\pi)^3}\frac{1}{2E_p 2E_{p+q}}\left(\frac{1}{\omega+E_p-E_{p+q}}-\frac{1}{\omega-E_p+E_{p+q}}\right) \times\left(f_\Phi(E_p)-f_\Phi(E_{p+q})\right) \tag{B.10}$$

and

$$\mathcal{F}_{\rm pair}(\omega,q) = 3\int \frac{d^3p}{(2\pi)^3}\frac{1}{2E_p 2E_{p+q}}\left(\frac{1}{\omega+E_p+E_{p+q}}-\frac{1}{\omega-E_p-E_{p+q}}\right) \times\left(1-f_\Phi(E_p)-f_\Phi(E_{p+q})\right). \tag{B.11}$$

We may interpret these correlation energies as the non-collective fluctuations of the system carrying mesonic quantum numbers with quenched quark distributions.

In order to compute the correlation energy and the pressure, it is convenient to decompose the function $\mathcal{F}(\omega\pm i\epsilon,q)$ into its real part $\mathcal{F}_1(\omega,q)$ and its imaginary part $\mathcal{F}_2(\omega,q)$:

$$\mathcal{F}(\omega\pm i\epsilon,q) = \mathcal{F}_1(\omega,q)\pm i\mathcal{F}_2(\omega,q) = \sqrt{\mathcal{F}_1(\omega,q)^2+\mathcal{F}_2(\omega,q)^2}\,e^{\pm i\phi(\omega,q)}, \tag{B.12}$$

where the argument ϕ is given by

$$\phi(\omega,q) = \tan^{-1}\frac{\mathcal{F}_2(\omega,q)}{\mathcal{F}_1(\omega,q)} \quad . \tag{B.13}$$

The real part and the imaginary part of the function $\mathcal{F}$ are further decomposed into two parts: the scattering term and the pair excitation term. The two components of the real part are given by the principal part integrals:

$$\mathcal{F}_{\rm scatt.,1}(\omega,q) = \mathcal{P}\int \frac{d^3p}{(2\pi)^3}\frac{1}{2E_p 2E_{p+q}}\left(\frac{1}{\omega+E_p-E_{p+q}}-\frac{1}{\omega-E_p+E_{p+q}}\right) \times\left(f_\Phi(E_p)-f_\Phi(E_{p+q})\right) \tag{B.14}$$

and

$$\mathcal{F}_{\rm pair,1}(\omega,q) = \mathcal{P}\int \frac{d^3p}{(2\pi)^3}\frac{1}{2E_p 2E_{p+q}}\left(\frac{1}{\omega+E_p+E_{p+q}}-\frac{1}{\omega-E_p-E_{p+q}}\right) \times\left(1-f_\Phi(E_p)-f_\Phi(E_{p+q})\right), \tag{B.15}$$

while the two components of the imaginary part contain the energy conserving δ-functions:

$$\mathcal{F}_{\text{scatt.},2}(\omega, q) = -\pi \int \frac{d^3p}{(2\pi)^3} \frac{1}{2E_p 2E_{p+q}} \left(f_\Phi(E_p) - f_\Phi(E_{p+q})\right) \times \left(\delta(\omega + E_p - E_{p+q}) - \delta(\omega - E_p + E_{p+q})\right) \tag{B.16}$$

$$\mathcal{F}_{\text{pair},2}(\omega, q) = -\pi \int \frac{d^3p}{(2\pi)^3} \frac{1}{2E_p 2E_{p+q}} \left(1 - f_\Phi(E_p) - f_\Phi(E_{p+q})\right) \times \left(\delta(\omega + E_p + E_{p+q}) - \delta(\omega - E_p - E_{p+q})\right). \tag{B.17}$$

Similar functions have been computed for the vector channel in the NJL model without the Polyakov loop [140] and for the finite temperature bosonic system [141, 142]. It is obvious that the scattering term has a non-zero imaginary part in the space-like energy-momentum region ($\mathrm{q}^2 > \omega^2$), while the pair creation-annihilation term is non-zero only in the time-like region ($\mathrm{q}^2 < \omega^2$). It is important to note that the non-collective mesonic correlations arise only from the non-vanishing imaginary part of $\mathcal{F}(q, \omega)$.

Appendix C

Computation of $\mathcal{F}_{\rm scat}(\omega, q)$ and $\mathcal{F}_{\rm pair}(\omega, q)$

Here we present the computation of the phase space integral in the functions $\mathcal{F}_{\rm scat}(\omega, q)$ and $\mathcal{F}_{\rm pair}(\omega, q)$. As we have seen in Appendix B, the function $\mathcal{F}$ can be separated into a scattering term and a pair excitation term, and both terms have a real part and an imaginary part. It is convenient to rewrite the scattering term and the pair excitation term as functions of new variables that will be introduced soon instead of E_p and E_{p+q}.

We first adopt the polar coordinate system, $d^3p = dpp^2 d\cos\theta d\phi$, and then change the variables $(p, \cos\theta)$ to new variables (E, ε) defined by

$$E = \frac{1}{2}(E_p + E_{p+q}) \tag{C.1}$$

and

$$\varepsilon = E_{p+q} - E_p. \tag{C.2}$$

Note that $2E$ represents the energy absorbed by pair excitations, while ε is the energy transferred by scatterings. The Jacobian of this transformation is

$$\frac{\partial(E, \varepsilon)}{\partial(p, \cos\theta)} = \frac{p^2 q}{E_p E_{p+q}}, \tag{C.3}$$

so that the new integration measure absorbs the Lorentz factor $E_p E_{p+q}$:

$$\frac{d^3p}{E_p E_{p+q}} = \frac{dpp^2 d\cos\theta d\phi}{E_p E_{p+q}} = \frac{1}{q} dE d\varepsilon d\phi. \tag{C.4}$$

Note that by construction

$$2E\varepsilon = E_{p+q}^2 - E_p^2 = 2pq\cos\theta + q^2, \tag{C.5}$$

so that the domain of integration in the (E, ε) plane is constrained by the condition

$$\cos^2\theta = \frac{E\varepsilon - \frac{q^2}{2}}{pq} \leq 1. \tag{C.6}$$

The relation,

$$p = \sqrt{E_p^2 - m^2} = \sqrt{(E - \frac{1}{2}\varepsilon)^2 - m^2} \tag{C.7}$$

implies

$$E^2\varepsilon^2 \leq q^2\left(E^2 + \frac{1}{4}\varepsilon^2 - m^2 - \frac{q^2}{4}\right). \tag{C.8}$$

The allowed region of integration in the (E, ε) plane is indicated by the grey zone in Fig. C.1.

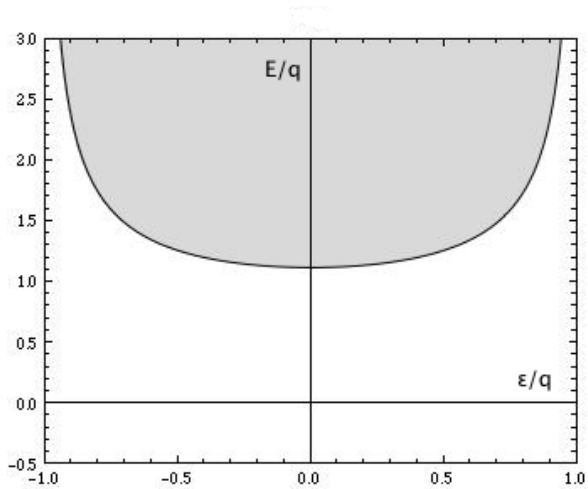

Figure C.1: The allowed region of integration in the (ε, E) plane is shown by the gray area.

We can now rewrite Eq.(B.10) and Eq.(B.11) in simpler, physically more transparent, forms. The scattering term Eq.(B.10) can be written as

$$\mathcal{F}_{\rm scat}(\omega, q) \;=\; \frac{1}{2\pi}\int_{-q}^{q} d\varepsilon \left(\frac{1}{\omega - \varepsilon} - \frac{1}{\omega + \varepsilon}\right) N_{\mathbf{scat}}(\varepsilon), \tag{C.9}$$

where

$$N_{\mathbf{scat}}(\varepsilon, q) \;=\; \frac{1}{2\pi q}\int_{E_0} dE \left(f_\Phi(E - \frac{1}{2}\varepsilon) - f_\Phi(E + \frac{1}{2}\varepsilon)\right). \tag{C.10}$$

This may be interpreted as the number of scattering states with the energy-momentum transfer (ε, q). The lower boundary of the E-integration, E_0, is

given from the constraint Eq.(C.8) as a function of (ε, q):

$$E_0(\varepsilon, q) = \frac{q}{2}\sqrt{1 + \frac{4m^2}{q^2 - \varepsilon^2}}. \tag{C.11}$$

If the condition $\varepsilon \ll q$ is satisfied, the integration can be performed approximately as

$$N_{\mathbf{scat}}(\varepsilon, q) \simeq -\frac{1}{2\pi}\frac{\varepsilon}{q}\int_{E_0} dE \frac{df_\Phi(E)}{dE} = \frac{1}{2\pi}\frac{\varepsilon}{q} f_\Phi(E_0). \tag{C.12}$$

Note that the number of scattering final states decreases exponentially for large q.

Similarly, we can express the pair excitation term Eq.(B.11) as

$$\mathcal{F}_{\rm pair}(\omega, q) = \frac{1}{2\pi}\int_{E_0} dE \left(\frac{1}{\omega - 2E} - \frac{1}{\omega + 2E}\right) N_{\mathbf{pair}}(E, q), \tag{C.13}$$

where

$$N_{\mathbf{pair}}(E, q) = \frac{1}{2\pi q}\int_{\varepsilon_-}^{\varepsilon_+} d\varepsilon \left(1 - f_\Phi(E - \frac{1}{2}\varepsilon) - f_\Phi(E + \frac{1}{2}\varepsilon)\right). \tag{C.14}$$

This may be interpreted as the number of pair excitation states with the energy-momentum $(2E, q)$. The boundary of the ε-integration is obtained from Eq.(C.8) as a function of E and q:

$$\varepsilon_\pm(E, q) = \pm q\sqrt{1 - \frac{m^2}{E^2 - q^2/4}}. \tag{C.15}$$

Since the value of ε is constrained by $-q < \varepsilon < q$, we can estimate the integration approximately, and we find

$$N_{\mathbf{pair}}(E, q) \simeq \frac{1}{2\pi q}(\varepsilon_+ - \varepsilon_-)\left(1 - 2f_\Phi(E)\right) \tag{C.16}$$

$$= \frac{1}{\pi}\sqrt{1 - \frac{m^2}{E^2 - q^2/4}}\left(1 - 2f_\Phi(E)\right). \tag{C.17}$$

The functions $N_{\mathbf{scat}}(\varepsilon)$ and $N_{\mathbf{pair}}(E)$ determine the imaginary part of $\mathcal{F}_{\rm scat}(\omega+i\epsilon,q)$ and $\mathcal{F}_{\rm pair}(\omega+i\epsilon,q)$, respectively. Using the expression Eq.(C.9), we find

$$\begin{aligned}\mathcal{F}_{\rm scat,2}(\omega,q) &= \frac{1}{2\pi}\int_{-q}^{q} d\varepsilon\,(-\pi\delta(\omega-\varepsilon)+\pi\delta(\omega+\varepsilon))\,N_{\mathbf{scat}}(\varepsilon)\\ &= -N_{\mathbf{scat}}(\omega), \end{aligned} \tag{C.18}$$

where we have used the fact that $N_{\mathbf{scat}}(\varepsilon)$ defined by Eq.(C.10) is an odd function of ε when extended to negative values of ε. Similarly, from Eq.(C.13) we obtain

$$\begin{aligned}\mathcal{F}_{\rm pair,2}(\omega,q) &= \frac{1}{2\pi}\int_{E_0} dE\,(-\pi\delta(\omega-2E)+\pi\delta(\omega+2E))\,N_{\mathbf{pair}}(E)\\ &= -N_{\mathbf{pair}}(\omega/2). \end{aligned} \tag{C.19}$$

Appendix D

Separation of the collective mesonic modes with finite bare quark mass

In the case of a non-vanishing bare quark mass, collective meson modes are also contained in Eq.(5.81), or in the pressure as a function of the gauge field A_4, i.e. before replacing A_4 by the expectation value of the Polyakov loop,

$$\begin{aligned}\Delta p_M(T,A_4) &= -\int \frac{d^3q}{(2\pi)^3}\frac{1}{2\pi i}\int_0^\infty d\omega\left[1+\frac{2}{e^{\beta\omega}-1}\right] \\ &\quad\times\left\{3\ln\left[\frac{\mathcal{M}_\pi(\omega+i\epsilon,q)}{\mathcal{M}_\pi(\omega-i\epsilon,q)}\right]+\ln\left[\frac{\mathcal{M}_\sigma(\omega+i\epsilon,q)}{\mathcal{M}_\sigma(\omega-i\epsilon,q)}\right]\right\}\end{aligned} \tag{D.1}$$

together with the non-collective excitation modes. In this case, we can still separate the contribution from the collective and the non-collective meson modes.

We first note that for small, but finite ϵ, the real parts of the function $\mathcal{M}(\omega,q)$ for the pion and the sigma meson read,

$$\mathcal{M}^1_\pi(\omega,q) = (-\omega^2+\mathrm{q}^2)\mathcal{F}_1(\omega,q)+\frac{m_0}{2GM_0} \tag{D.2}$$

$$\mathcal{M}^1_\sigma(\omega,q) = (-\omega^2+\mathrm{q}^2+4M_0^2)\mathcal{F}_1(\omega,q)+\frac{m_0}{2GM_0}, \tag{D.3}$$

while their imaginary parts are

$$\mathcal{M}^2_\pi(\omega,q) = -2\omega\epsilon\mathcal{F}_1(\omega,q)+(-\omega^2+\mathrm{q}^2)\mathcal{F}_2(\omega,q) \tag{D.4}$$

$$\mathcal{M}^2_\sigma(\omega,q) = -2\omega\epsilon\mathcal{F}_1(\omega,q)+(-\omega^2+\mathrm{q}^2+4M_0^2)\mathcal{F}_2(\omega,q). \tag{D.5}$$

The imaginary parts $\mathcal{M}^2_{\pi/\sigma}$ depend on both $\mathcal{F}_1$ and $\mathcal{F}_2$. In the kinematical region where no individual excitation exists, we have $\mathcal{F}_2(\omega, q) = 0$ and

$$\mathcal{M}^2_{\pi/\sigma}(\omega, q) \quad = \quad -2\omega\epsilon\mathcal{F}_1(\omega, q). \tag{D.6}$$

Since $\mathcal{M}^1_{\pi/\sigma} = 0$ at the meson poles, the argument of $\mathcal{M}_\sigma(\omega + i\epsilon, q)$ becomes $\pm\pi/2$, depending only on the sign of $\mathcal{F}_1(\omega, q)$. In the limit $\epsilon \to 0$, the poles move to the real ω axis.

The locations of the meson poles in the (ω, q) plane are determined by the conditions:

$$\mathcal{M}^1_\sigma(\omega, q) \quad = \quad (-\omega^2 + \mathrm{q}^2 + 4M_0^2)\mathcal{F}_1(\omega, q) + \frac{m_0}{2GM_0} = 0 \tag{D.7}$$

$$\mathcal{M}^1_\pi(\omega, q) \quad = \quad (-\omega^2 + \mathrm{q}^2)\mathcal{F}_1(\omega, q) + \frac{m_0}{2GM_0} = 0 \tag{D.8}$$

for the σ meson pole and the pion pole respectively. The bare quark mass parameter m_0 is determined so that it generates the physical mass of the pions in the vacuum, hence it should satisfy near $q = 0$ the on-the-mass-shell condition $\omega = \sqrt{q^2 + m_\pi^2}$. Therefore, we obtain

$$-m_\pi^2\mathcal{F}_{\mathrm{vac}}(m_\pi, q) + \frac{m_0}{2GM_0} = 0, \tag{D.9}$$

where $\mathcal{F}_{\mathrm{vac}}(\omega, q)$ is the vacuum piece of the function $\mathcal{F}(\omega, q)$:

$$\mathcal{F}_{\mathrm{vac}}(\omega, q) = -\pi \int^\Lambda \frac{d^3p}{(2\pi)^3} \frac{1}{2E_p 2E_{p+q}}. \tag{D.10}$$

Subtracting Eq.(D.9) from Eq.(D.7) and Eq.(D.8), we obtain

$$\mathcal{M}_\sigma(\omega, q) \quad = \quad (-\omega^2 + \mathrm{q}^2 + 4M_0^2)\mathcal{F}(\omega, q) + m_\pi^2\mathcal{F}_{\mathrm{vac}}(m_\pi, 0) \tag{D.11}$$

and

$$\mathcal{M}_\pi(\omega, q) \quad = \quad (-\omega^2 + \mathrm{q}^2)\mathcal{F}(\omega, q) + m_\pi^2\mathcal{F}_{\mathrm{vac}}(m_\pi, 0). \tag{D.12}$$

The contribution of these "pole terms" to the ω-integral is essentially the same as in the chiral limit, except that the masses of the mesons are shifted.

The contribution from the cuts comes from the non-vanishing imaginary part of $\mathcal{F}(\omega \pm i\epsilon, q)$, which generates the non-zero imaginary parts in $\mathcal{M}_\sigma(\omega \pm i\epsilon, q)$ by

$$\mathcal{M}^2_\sigma(\omega, q) \quad = \quad (-\omega^2 + \mathrm{q}^2 + 4M_0^2)\mathcal{F}_2(\omega, q) \tag{D.13}$$

and

$$\mathcal{M}^2_\pi(\omega, q) \quad = \quad (-\omega^2 + \mathrm{q}^2)\mathcal{F}_2(\omega, q), \tag{D.14}$$

while the real parts of $\mathcal{M}_{\pi/\sigma}(\omega \pm i\epsilon, q)$ remain non-zero on the cuts, so that we have the phases

$$\phi_\pi(\omega, q) \quad = \quad \tan^{-1} \frac{\mathcal{M}^2_\pi(\omega, q)}{\mathcal{M}^1_\pi(\omega, q)} = \tan^{-1} \left(\frac{\mathcal{F}_2}{\mathcal{F}_1 + \dfrac{m_0}{2GM_0} \dfrac{1}{\mathrm{q}^2 - \omega^2}} \right) \tag{D.15}$$

and

$$\phi_\sigma(\omega, q) \quad = \quad \tan^{-1} \frac{\mathcal{M}^2_\sigma(\omega, q)}{\mathcal{M}^1_\sigma(\omega, q)} = \tan^{-1} \left(\frac{\mathcal{F}_2}{\mathcal{F}_1 + \dfrac{m_0}{2GM_0} \dfrac{1}{\mathrm{q}^2 + 4M_0^2 - \omega^2}} \right). \tag{D.16}$$

They are slightly shifted compared to their values in the chiral limit. These phases may be interpreted as the phase-shift of the scatterings of a quark off a quark or an anti-quark [143–145] . A constraint on the phase shift, due to Levingson's theorem, has been exploited recently for studying the dissolution of the mesonic bound states in a model similar to ours [146] .

Appendix E

Explicit form of $\mathcal{F}(\omega, q)$ in the three-flavour PNJL model

Here we show the explicit form of $\mathcal{F}(\omega, q)$ for the pseudo-scalar mesons. They can be written in terms of $\mathcal{F}_{uu}(\omega, q)$, $\mathcal{F}_{ss}(\omega, q)$ and $\mathcal{F}_{us}(\omega, q)$. Since we assume SU(2) isospin symmetry, $\mathcal{F}_{ud} = \mathcal{F}_{dd} = \mathcal{F}_{uu}$. These functions contain a scattering term and a pair excitation term, and both terms can be written in terms of the modified quark distribution function f_Φ.

$$\begin{aligned}
\mathcal{F}_{uu}(\omega, q) &= \mathcal{F}_{uu}^{\mathbf{scat}}(\omega, q) + \mathcal{F}_{uu}^{\mathbf{pair}}(\omega, q) && \text{(E.1)}\\
&= \int \frac{d^3p}{(2\pi)^3} \frac{1}{2E_u(p)2E_u(p+q)} \\
&\times \Big(\frac{1}{\omega + E_u(p) - E_u(p+q)} - \frac{1}{\omega - E_u(p) + E_u(p+q)}\Big) \\
&\times \big(f_\Phi(E_u(p)) - f_\Phi(E_u(p+q))\big) && \text{(E.2)}\\
&+ \int \frac{d^3p}{(2\pi)^3} \frac{1}{2E_u(p)2E_u(p+q)} \\
&\times \Big(\frac{1}{\omega + E_u(p) + E_u(p+q)} - \frac{1}{\omega - E_u(p) - E_u(p+q)}\Big) \\
&\times \big(1 - f_\Phi(E_u(p)) - f_\Phi(E_u(p+q))\big) && \text{(E.3)}
\end{aligned}$$

$$
\begin{aligned}
\mathcal{F}_{ss}(\omega,q) &= \mathcal{F}_{ss}^{\mathbf{scat}}(\omega,q)+\mathcal{F}_{ss}^{\mathbf{pair}}(\omega,q) && \text{(E.4)}\\
&= \int \frac{d^3p}{(2\pi)^3}\frac{1}{2E_s(p)2E_s(p+q)}\\
&\times \Big(\frac{1}{\omega+E_s(p)-E_s(p+q)}-\frac{1}{\omega-E_s(p)+E_s(p+q)}\Big)\\
&\times \big(f_\Phi(E_s(p))-f_\Phi(E_s(p+q))\big) && \text{(E.5)}\\
&+ \int \frac{d^3p}{(2\pi)^3}\frac{1}{2E_s(p)2E_s(p+q)}\\
&\times \Big(\frac{1}{\omega+E_s(p)+E_s(p+q)}-\frac{1}{\omega-E_s(p)-E_s(p+q)}\Big)\\
&\times \big(1-f_\Phi(E_s(p))-f_\Phi(E_s(p+q))\big) && \text{(E.6)}
\end{aligned}
$$

$$
\begin{aligned}
\mathcal{F}_{us}(\omega,q) &= \mathcal{F}_{us}^{\mathbf{scat}}(\omega,q)+\mathcal{F}_{us}^{\mathbf{pair}}(\omega,q) && \text{(E.7)}\\
&= \int \frac{d^3p}{(2\pi)^3}\frac{1}{2E_u(p)2E_s(p+q)}\\
&\times \Big(\frac{1}{\omega+E_u(p)-E_s(p+q)}-\frac{1}{\omega-E_u(p)+E_s(p+q)}\Big)\\
&\times \big(f_\Phi(E_u(p))-f_\Phi(E_s(p+q))\big) && \text{(E.8)}\\
&+ \int \frac{d^3p}{(2\pi)^3}\frac{1}{2E_u(p)2E_s(p+q)}\\
&\times \Big(\frac{1}{\omega+E_u(p)+E_s(p+q)}-\frac{1}{\omega-E_u(p)-E_s(p+q)}\Big)\\
&\times \big(1-f_\Phi(E_u(p))-f_\Phi(E_s(p+q))\big). && \text{(E.9)}
\end{aligned}
$$

Since the pions are written as collective modes of u-quark, $\mathcal{F}_\pi$ is written in terms only of $\mathcal{F}_{uu}$;

$$\mathcal{F}_\pi(\omega,q)=\mathcal{F}_{uu}(\omega,q). \tag{E.10}$$

For kaons,

$$\mathcal{F}_K(\omega,q)=\mathcal{F}_{us}(\omega,q) \tag{E.11}$$

because they are collective modes of u-quarks and s-quarks. The η^8 and η^0 mesons contain both $\bar{u}u$ and $\bar{s}s$, so that we have

$$\mathcal{F}_{\eta^8}(\omega,q)=\mathcal{F}_{uu}(\omega,q)+2\mathcal{F}_{ss}(\omega,q) \tag{E.12}$$

for the η^8 meson, and

$$\mathcal{F}_{\eta^0}(\omega,q)=2\mathcal{F}_{uu}(\omega,q)+\mathcal{F}_{ss}(\omega,q) \tag{E.13}$$

for the η^0 meson.

Appendix F

Polarisations of mesons, diquarks and baryons

F.1 Scalar meson polarisation

The integrand of the scalar meson polarisation given in Eq.(7.41) contains the factor:

$$\begin{aligned}
&\mathrm{Tr}\left[S_i(\varepsilon+\omega,p+q)S_i(\varepsilon,p)\right] \\
&= \frac{N_\sigma}{\left[(\varepsilon+\omega-\mu+i\phi_i T)^2-E_{p+q}^2\right]\left[(\varepsilon-\mu+i\phi_i T)^2-E_p^2\right]},
\end{aligned} \tag{F.1}$$

where the numerator is given by

$$\begin{aligned}
N_\sigma &= -\mathrm{Tr}\left\{\left[(\varepsilon+\omega-\mu+i\phi_i T)\gamma_0+(\mathbf{p}+\mathrm{q})\cdot\boldsymbol{\gamma}+M_0\right]\right. \\
&\qquad\qquad \left.\times\left[(\varepsilon-\mu+i\phi_i T)\gamma_0+\mathbf{p}\cdot\boldsymbol{\gamma}+M_0\right]\right\} \\
&= -2\left\{\left[(\varepsilon+\omega-\mu+i\phi_i)^2-E_{p+q}^2\right]\right. \\
&\qquad + \left[(\varepsilon-\mu+i\phi_i T)^2-E_p^2\right] \\
&\qquad \left. + (-\omega^2+q^2+4M_0^2)\right\}.
\end{aligned} \tag{F.2}$$

Hence,

$$
\begin{aligned}
\Pi_\sigma(q,n) &= -\gamma_q \int \frac{d^3p}{(2\pi)^3} \int_C \frac{d\varepsilon}{2\pi i} f(\varepsilon) \\
&\qquad \times \sum_i \mathrm{Tr}\left[S_i(\varepsilon + i\omega_n, p+q) S_i(\varepsilon, p)\right] \qquad \text{(F.3)} \\
&= -2\gamma_q \int \frac{d^3p}{(2\pi)^3} \int_C \frac{d\varepsilon}{2\pi i} f(\varepsilon) \\
&\qquad \times \sum_i \left[\frac{1}{(\varepsilon - \mu + i\phi_i T)^2 - E_p^2} \right. \\
&\qquad + \frac{1}{(\varepsilon + i\omega_n - \mu + i\phi_i T)^2 - E_{p+q}^2} \\
&\qquad + \frac{(\omega_n^2 + q^2 + 4M_0^2)}{\left[(\varepsilon + i\omega_n - \mu + i\phi_i T)^2 - E_{p+q}^2\right]} \\
&\qquad \left. \times \frac{1}{\left[(\varepsilon - \mu + i\phi_i T)^2 - E_p^2\right]} \right] . \qquad \text{(F.4)}
\end{aligned}
$$

The contour integral of the first term picks up the residues of the poles at $\epsilon = \pm E_p + \mu - i\phi_i T$, so that

$$
\begin{aligned}
&-2\gamma_q \int \frac{d^3p}{(2\pi)^3} \int_C \frac{d\varepsilon}{2\pi i} f(\varepsilon) \sum_i \frac{1}{(\varepsilon - \mu + i\phi_i T)^2 - E_p^2} \\
&= -\gamma_q \int \frac{d^3p}{(2\pi)^3} \frac{1}{E_p} \sum_i \left[f(E_p + \mu - i\phi_i T) \right. \\
&\qquad \left. + f(-E_p + \mu - i\phi_i T) \right] \\
&= -\gamma_q \int \frac{d^3p}{(2\pi)^3} \frac{1}{E_p} \sum_i \left[f(E_p + \mu - i\phi_i T) \right. \\
&\qquad \left. + f(E_p - \mu + i\phi_i T) - 1 \right] , \qquad \text{(F.5)}
\end{aligned}
$$

where we have used

$$
f(-\epsilon) = f(\epsilon) - 1 \qquad \text{(F.6)}
$$

for the fermionic distribution function for particles with a negative energy. The integral of the second term in Eq.(F.4) picks up the residues of the poles

at $\epsilon = \pm E_{p+q} - i\omega_n + \mu - i\phi_i T$, so that

$$
\begin{aligned}
-2\gamma_q \int \frac{d^3p}{(2\pi)^3} \int_C \frac{d\varepsilon}{2\pi i} f(\varepsilon) \\
\times \sum_i \frac{1}{(\varepsilon + i\omega_n - \mu + i\phi_i T)^2 - E_{p+q}^2} \\
= -\gamma_q \int \frac{d^3p}{(2\pi)^3} \frac{1}{E_{p+q}} \sum_i [f(E_{p+q} - i\omega_n + \mu - i\phi_i T) \\
+ f(-E_{p+q} - i\omega_n + \mu - i\phi_i T)] \\
= -\gamma_q \int \frac{d^3p}{(2\pi)^3} \frac{1}{E_{p+q}} \sum_i [f(E_{p+q} + \mu - i\phi_i T) \\
+ f(E_{p+q} - \mu + i\phi_i T) - 1] \,, \qquad \text{(F.7)}
\end{aligned}
$$

where we have used $e^{i\beta\omega_n} = 1$ for the bosonic Matsubara frequencies $\omega_n = 2\pi n T$ in deriving the last equality. By making the shift of the momentum integration variable $\boldsymbol{p} \to \boldsymbol{p} + \boldsymbol{q}$, this integral becomes identical to the first one. Performing the statistical average over the gauge fields, they give a tadpole term $\mathcal{T}$, given by Eq.(7.45), which is independent from both ω and q. This term is exactly the same as the integral that appears in the gap equation for the constituent quark mass. Therefore, this can be rewritten simply in terns of the effective quark mass M_0 and the four-point coupling G,

$$
\mathcal{T} = -\frac{1}{2G}\left(1 - \frac{m_0}{M_0}\right). \qquad \text{(F.8)}
$$

The integration of the last dispersive term can be performed by performing a similar change of variable and it gives the two dispersive terms, the scattering term and the pair excitation term, with a quark distribution function whose energy argument is shifted by the chemical potential and by the background gauge field as $\epsilon \to \epsilon - \mu + i\phi_i T$ for quarks or $\epsilon \to \epsilon + \mu - i\phi_i T$

for antiquarks.

$$
\begin{aligned}
& -\gamma_q \int \frac{d^3p}{(2\pi)^3} \int_C \frac{d\varepsilon}{2\pi i} f(\varepsilon) \\
& \quad \times \sum_i \frac{1}{\left[(\varepsilon + i\omega_n - \mu + i\phi_i T)^2 - E_{p+q}^2\right]} \\
& \quad \times \frac{1}{\left[(\varepsilon - \mu + i\phi_i T)^2 - E_p^2\right]} \Bigg] \\
= \; & -\gamma_q \int \frac{d^3p}{(2\pi)^3} \sum_i \\
& \quad \times \Bigg[\frac{f(E_{p+q} + \mu - i\phi_i T) - f(-E_{p+q} + \mu - i\phi_i T)}{2E_{p+q}\left[(E_{p+q} - i\omega_n)^2 - E_p^2\right]} \\
& \quad + \frac{f(E_p - \mu + i\phi_i T) - f(-E_p - \mu + i\phi_i T)}{2E_p\left[(E_p - i\omega_n)^2 - E_{p+q}^2\right]} \Bigg] \\
= \; & -\gamma_q \int \frac{d^3p}{(2\pi)^3} \sum_i \\
& \quad \times \Bigg[\frac{f(E_{p+q} + \mu - i\phi_i T) + f(E_{p+q} - \mu + i\phi_i T) - 1}{2E_{p+q}\left[(E_{p+q} - i\omega_n)^2 - E_p^2\right]} \\
& \quad + \frac{f(E_p - \mu + i\phi_i T) + f(E_p + \mu - i\phi_i T) - 1}{2E_p\left[(E_p - i\omega_n)^2 - E_{p+q}^2\right]} \Bigg],
\end{aligned}
\tag{F.9}
$$

where we have again used $e^{i\beta\omega_n} = 1$ and the relation Eq.(F.6).

After taking the statistical average over the background gauge fields, we find the expression Eq.(7.44) for the Minkowski representation of the scalar meson polarisation

$$
\Pi_\sigma(\omega, q) \;=\; \mathcal{T} + (\omega^2 - q^2 - 4M^2)\mathcal{F}(\omega, q), \tag{F.10}
$$

where

$$
\mathcal{F}(\omega, q) = \mathcal{F}_{\text{scatt}}(\omega, q) + \mathcal{F}_{\text{pair}}(\omega, q). \tag{F.11}
$$

The two functions $\mathcal{F}_{\text{scatt}}$ and $\mathcal{F}_{\text{pair}}$ are given respectively by

$$
\begin{aligned}
\mathcal{F}_{\text{scatt}}(\omega, q) \;=\; & \gamma_q \int \frac{d^3p}{(2\pi)^3} \Bigg[\frac{f_\Phi(E_p - \mu) - f_\Phi(E_{p+q} - \mu)}{2E_p\; 2E_{p+q}} \\
& + \frac{f_\Phi(E_p + \mu) - f_\Phi(E_{p+q} + \mu)}{2E_p\; 2E_{p+q}} \Bigg] \\
& \times \left(\frac{1}{\omega + E_p - E_{p+q}} - \frac{1}{\omega - E_p + E_{p+q}} \right)
\end{aligned}
\tag{F.12}
$$

and

$$\begin{aligned}\mathcal{F}_{\rm pair}(\omega,q) &= \gamma_q \int \frac{d^3p}{(2\pi)^3}\left[\frac{1-f_\Phi(E_p-\mu)-f_\Phi(E_{p+q}-\mu)}{2E_p\ 2E_{p+q}}\right.\\ &\qquad \left.+\frac{1-f_\Phi(E_p+\mu)-f_\Phi(E_{p+q}+\mu)}{2E_p\ 2E_{p+q}}\right]\\ &\times \left(\frac{1}{\omega+E_p+E_{p+q}}-\frac{1}{\omega-E_p-E_{p+q}}\right).\end{aligned} \tag{F.13}$$

The function $\mathcal{F}_{\rm scatt}(\omega+i\delta,q)$ has a non-zero imaginary part in the space-like region, namely $\omega^2<\boldsymbol{q}^2$, corresponding to the scatterings of a quark and an antiquark that carry the energy-momentum $(\epsilon,\boldsymbol{p})$ and $(\epsilon+\omega,\boldsymbol{p}+\boldsymbol{q})$. While the non-vanishing imaginary part of the function $\mathcal{F}_{\rm pair}(\omega+i\delta,q)$ appears in the time-like region, namely $\omega^2>\boldsymbol{q}^2$, corresponding to the pair excitations of a quark and an antiquark carrying the energy-momentum $(\epsilon,\boldsymbol{p})$ and $(\epsilon+\omega,\boldsymbol{p}+\boldsymbol{q})$. We note that the gauge potential does not appears in the energy denominator due to the cancellation of the two gauge potentials associated to a quark-antiquark pair, reflecting the fact that the meson is colour singlet. This is not the case for diquarks since they are not colour singlet.

F.2 Scalar diquark polarisation

The scalar diquark polarisation contains the factor:

$$\begin{aligned}&{\rm Tr}\left[i\gamma_5 S_i(\varepsilon+\omega,p+q)i\gamma_5 S_j(-\varepsilon,-p)\right]\\ &=\frac{N_{ij}}{\left[(\varepsilon+\omega-\mu+i\phi_iT)^2-E_{p+q}^2\right]\left[(\varepsilon+\mu-i\phi_jT)^2-E_p^2\right]},\end{aligned} \tag{F.14}$$

where

$$\begin{aligned}N_{ij} &= -{\rm Tr}\left\{i\gamma_5\left[(\varepsilon+\omega-\mu+i\phi_iT)\gamma_0+(\mathbf{p}+\mathrm{q})\cdot\boldsymbol{\gamma}+M\right]\right.\\ &\qquad \left.\times i\gamma_5\left[(\varepsilon+\mu-i\phi_jT)\gamma_0+\mathbf{p}\cdot\boldsymbol{\gamma}-M\right]\right\}\\ &= -2\left\{\left[(\varepsilon+\omega-\mu+i\phi_iT)^2-E_{p+q}^2\right]\right.\\ &\qquad +\left[(\varepsilon+\mu-i\phi_jT)^2-E_p^2\right]\\ &\qquad \left.+(-\omega'^2+q^2+4M^2)\right\}\end{aligned} \tag{F.15}$$

with

$$\begin{aligned}\omega' &= \omega-2\mu+i\phi_iT+i\phi_jT\\ &= \omega-2\mu-i\phi_kT.\end{aligned} \tag{F.16}$$

In this formula we have used the traceless condition for the background gauge field which implies $\sum_i \phi_i = 0$.

Inserting Eqs.(F.14)-(F.15) into Eq.(7.52) and performing the integral over ε , we pick up the residues of the poles at $\varepsilon = \pm E_{p+q} - \omega + \mu - i\phi_i T$ and at $\varepsilon = \pm E_p - \mu + i\phi_j T$. The first non-dispersive term is exactly the same as in the scalar meson polarisation. In the derivation of the second dispersive term, we encounter the computation of the following integral

$$\begin{aligned}
& -\gamma_q \int \frac{d^3p}{(2\pi)^3} \int_C \frac{d\varepsilon}{2\pi i} f(\varepsilon) \\
& \quad \times \sum_{i,j} \epsilon_{ijk} \frac{1}{\left[(\varepsilon + i\omega_n - \mu + i\phi_i T)^2 - E_{p+q}^2\right]} \\
& \quad \times \frac{1}{\left[(\varepsilon + \mu - i\phi_i T)^2 - E_p^2\right]} \Bigg] \\
= & -\gamma_q \int \frac{d^3p}{(2\pi)^3} \sum_{i,j} \epsilon_{ijk} \\
& \quad \times \Bigg[\frac{f(E_{p+q} + \mu - i\phi_i T) - f(-E_{p+q} + \mu - i\phi_i T)}{2E_{p+q}\left[(E_{p+q} - i\omega_n + 2\mu + i\phi_k T)^2 - E_p^2\right]} \\
& \quad + \frac{f(E_p + \mu - i\phi_i T) - f(-E_p + \mu - i\phi_i T)}{2E_p\left[(E_p - i\omega_n + 2\mu + i\phi_k T)^2 - E_{p+q}^2\right]} \Bigg] \\
= & -\gamma_q \int \frac{d^3p}{(2\pi)^3} \sum_{i,j} \\
& \quad \times \Bigg[\frac{f(E_{p+q} + \mu - i\phi_i T) + f(E_{p+q} - \mu + i\phi_i T) - 1}{2E_{p+q}\left[(E_{p+q} - i\omega_n + 2\mu + i\phi_k T)^2 - E_p^2\right]} \\
& \quad + \frac{f(E_p - \mu + i\phi_i T) + f(E_p + \mu - i\phi_i T) - 1}{2E_p\left[(E_p - i\omega_n + 2\mu + i\phi_k)^2 - E_{p+q}^2\right]} \Bigg],
\end{aligned} \tag{F.17}$$

where we have used $e^{\beta\omega_n} = 1$ again for the bosonic Matsubara frequencies ω_n and the traceless condition $\phi_i + \phi_j = -\phi_k$ for the background gauge fields. This integral is similar to the one encountered in the computation of the scalar meson polarisation. The gauge potential dependence now appears not only in the quark distribution function (as in the scalar meson polarisation) but also in the energy denominator, reflecting the fact that the diquarks carry a colour charge. If we replace the quark distribution function by its statistical average over the external gauge potential while ignoring the gauge field in the energy denominator, we find

$$\Pi_\Delta^k(\omega, q) = \mathcal{T} - (-\omega'^2 + q^2 + 4M^2)\mathcal{F}_\Delta(\omega, q), \tag{F.18}$$

where

$$\mathcal{F}_\Delta(\omega, q) = \mathcal{F}(\omega', q) \tag{F.19}$$

with ω' given by Eq.(F.16). We note that the scattering term in $\mathcal{F}(\omega', q)$ is now given by

$$\begin{aligned}
\mathcal{F}_{\rm scatt}(\omega', q) &= \gamma_q \int \frac{d^3p}{(2\pi)^3} \left[\frac{f_\Phi(E_p+\mu) - f_\Phi(E_{p+q}-\mu)}{2E_p\ 2E_{p+q}} \right. \\
&\qquad \left. + \frac{f_\Phi(E_p-\mu) - f_\Phi(E_{p+q}+\mu)}{2E_p\ 2E_{p+q}} \right] \\
&\quad \times \left(\frac{1}{\omega' + E_p - E_{p+q}} - \frac{1}{\omega' - E_p + E_{p+q}} \right),
\end{aligned} \tag{F.20}$$

which may be physically interpreted as a scattering of a quark quasiparticle off an antiquark by an emission of a diquark whose energy is shifted by $-2\mu - i\phi_k T$ and *vice versa*. Similarly,

$$\begin{aligned}
\mathcal{F}_{\rm pair}(\omega', q) &= \gamma_q \int \frac{d^3p}{(2\pi)^3} \frac{1}{2E_p\ 2E_{p+q}} \\
&\quad \times [2 - f_\Phi(E_p-\mu) - f_\Phi(E_{p+q}-\mu) \\
&\qquad - f_\Phi(E_p+\mu) - f_\Phi(E_{p+q}+\mu)] \\
&\times \left(\frac{1}{\omega' + E_p + E_{p+q}} - \frac{1}{\omega' - E_p - E_{p+q}} \right)
\end{aligned} \tag{F.21}$$

can be interpreted as the diquark polarisation from a pair of quark quasiparticles.

In the vacuum, the scalar particle-antiparticle polarisation for the mesons becomes identical to the particle-particle polarisation for the diquarks. This is known as the Pauli-Gürsey symmetry.

The replacement of ω_n by ω'_n brings two important differences. The first one is that the quark chemical potential shifts the kinematics of the non-vanishing imaginary parts in the absence of the external colour gauge potential. For positive values of μ, the scattering term which is associated with a transition of a thermally excited quark to an excited antiquark is excluded from the space-like region for small value of the momentum q. The other difference is that the threshold for quark pair excitations moves down from the value of $2M_0$ to $2(M_0 - \mu)$ at small momentum q.

In the presence of the non-vanishing gauge potential A_4, that adds imaginary parts to ω', these dispersive terms acquire extra imaginary parts $i(\phi_i + \phi_j)T$ in the energy denominators as well as in the imaginary parts in the quark distribution functions, and their physical effects become more complicated.

The gauge potential dependence that appears in the quark distribution functions is the same as the one encountered in the case of the meson polarisation. Taking a statistical average over the gauge fields, this gauge field acts to suppress the thermal excitations of the quarks, replacing the quark distribution function by f_Φ. We will keep the gauge field dependence in the energy denominator for later use to suppress the thermal excitations of diquarks in the confining phase, by ignoring the correlations between the gauge fields in the quark distribution functions and the gauge fields in the energy denominator while taking the statistical average [147].

F.3 Baryon self-energy

The Fourier components of the baryon self-energy Σ_B is given by

$$\Sigma_B(P,\epsilon_n) = \sum_{l,m} \int \frac{d^3p}{(2\pi)^3} \frac{2HS(p,\epsilon_m)}{1-2H\Pi_\Delta(P-p,\omega_l)} \delta_{l+m,n}, \tag{F.22}$$

where

$$\begin{aligned} S(p,\epsilon_m) &= \frac{1}{(i\epsilon_m - 2\mu - i\phi_i T)\gamma_0 - \boldsymbol{p}\cdot\boldsymbol{\gamma} - M_0} \\ &= \frac{-(i\epsilon_m - 2\mu - i\phi_i T)\gamma_0 + \boldsymbol{p}\cdot\boldsymbol{\gamma} - M_0}{(i\epsilon_m - 2\mu - i\phi_i T)^2 - \boldsymbol{p}^2 - M_0^2} \end{aligned} \tag{F.23}$$

with $\epsilon_m = (2m+1)\pi T$ the fermionic Matsubara frequencies, $\omega_l = 2\pi l T$ the bosonic Matsubara frequencies. In this equation, the Fourier components of the diquark polarisation read

$$\begin{aligned} \Pi_\Delta(P-p,\omega_l) &= \mathcal{T} + \big[(i\omega_l - 2\mu + i\phi_k T)^2 \\ &\quad -(\boldsymbol{P}-\boldsymbol{p})^2 - M_0^2\big]\, \mathcal{F}_\Delta(i\omega_l, P-q), \end{aligned} \tag{F.24}$$

where

$$\mathcal{F}_\Delta(i\omega_l, P-q) = \mathcal{F}(i\omega_l - 2\mu - i\phi_k T, P-q). \tag{F.25}$$

The Kronecker delta $\delta_{l+m,n}$ in Eq.(F.22), that reflects energy conservation, originates from the integral over the imaginary time,

$$T\int_0^\beta d\tau e^{i\tau(\omega_l+\epsilon_m-\epsilon_n)} = \delta_{l+m,n},$$

where we have used $\omega_l = 2l\pi T$, $\epsilon_m = (2m+1)\pi T$ and $\epsilon_n = (2n+1)\pi T$. Performing the sum over the fermion Matsubara frequencies ϵ_n by contour integration, we obtain

$$\begin{aligned}\Sigma_B(P,n) &= \int_C \frac{d\epsilon}{2\pi i} f_F(\epsilon) \int \frac{d^3p}{(2\pi)^3} \\ &\quad \times \frac{2HS(\epsilon,p)}{1-2H\Pi_\Delta(i\epsilon_n-\epsilon,P-p)}.\end{aligned} \tag{F.26}$$

The contour integral over ϵ picks up the residues from the energy denominator in the quark Dirac propagator $S(\epsilon,p)$ at $\epsilon = \pm E_p + \mu + i\phi_i T$ and from the energy denominator $1-2H\Pi_\Delta(\epsilon_n-\epsilon,P-p)$ for the propagator of the scalar diquark. The latter contributions are better seen by rewriting the integral with a change of integration variable from ϵ to $\omega = i\epsilon_n - \epsilon$, which gives

$$\begin{aligned}\Sigma_B(P,n) &= -\int_C \frac{d\omega}{2\pi i} f_F(i\epsilon_n-\omega) \int \frac{d^3p}{(2\pi)^3} \\ &\quad \times \frac{2HS(\epsilon_n-\omega,p)}{1-2H\Pi_\Delta(\omega,P-p)} \\ &= -\int_C \frac{d\omega}{2\pi i}(1+f_B(\omega)) \int \frac{d^3p}{(2\pi)^3} \\ &\quad \times \frac{2HS(\epsilon_n-\omega,p)}{1-2H\Pi_\Delta(\omega,P-p)}.\end{aligned} \tag{F.27}$$

Note that in this expression, the fermion distribution changes to a boson distribution by

$$f_F(\epsilon) = 1 + f_B(\omega) \tag{F.28}$$

due to the identity $e^{i\beta\epsilon_n} = -1$ for a fermionic Matsubara frequency $\epsilon_n = (2n+1)\pi T$ with overall minus sign for integration. Therefore, the poles from the quark propagator contribute to the baryon self-energy because of the fermion distribution function, while the poles and cuts of the diquark propagator contribute to it because of the boson distribution function as they should.

Acknowledgements

This thesis contains many results of the collaboration works with Professor Tetsuo Matsui and Professor Gordon Baym. I thank them for discussing and collaborating. By working with them, I have learned a lot. I also thank the members of the Komaba nuclear theory group, especially Professor Hirotsugu Fujii, for giving useful comments and questions on this work.

I appreciate Professor Jean-Paul Blaizot and Dr. Veronique Bernard for accepting me as a visitor to their groups for two months respectively, at IPhT and at IPN-Orsay, and discussing. Also, I would like to thank Professor Brigitte Hiller for useful discussions and her interests on this work.

I would also thank Professor Tetsuo Hatsuda, Professor Kenji Fukushima, Professor Koich Yazaki, Professor Krzysztof Redlich, and Professor Michael Buballa for discussions.

Finally, I am grateful to Dr. François Gelis for giving a lot of comments on this work and on this thesis. All his supports have been exceedingly helpful.

Bibliography

[1] Kanako Yamazaki and T. Matsui. Quark-Hadron Phase Transition in the PNJL model for interacting quarks. *Nucl.Phys.*, A913:19–50, 2013.

[2] Kanako Yamazaki and T. Matsui. Quark-hadron phase transition in a three flavor PNJL model for interacting quarks. *Nucl.Phys.*, A922:237–261, 2014.

[3] Kanako Yamazaki, T. Matsui, and Gordon Baym. Entropy in the quark-hadron transition. *Nucl.Phys.*, A933:245–255, 2015.

[4] Kanako Yamazaki and T. Matsui. Baryons in an extended PNJL model for quark-hadron phase transition. *in preparation.*

[5] G. Baym. DECONFINED PHASES OF STRONGLY INTERACTING MATTER. (TALK). 1982.

[6] G. Baym. CLOSING REMARKS. *Nucl.Phys.*, A418:433C–444C, 1984.

[7] Krishna Rajagopal and Frank Wilczek. The Condensed matter physics of QCD. 2000.

[8] Kenji Fukushima and Tetsuo Hatsuda. The phase diagram of dense QCD. *Rept.Prog.Phys.*, 74:014001, 2011.

[9] T. Matsui and H. Satz. J/ψ Suppression by Quark-Gluon Plasma Formation. *Phys.Lett.*, B178:416, 1986.

[10] M.C. Abreu et al. Anomalous J / psi suppression in Pb - Pb interactions at 158 GeV/c per nucleon. *Phys.Lett.*, B410:337–343, 1997.

[11] M.C. Abreu et al. Evidence for deconfinement of quarks and gluons from the J / psi suppression pattern measured in Pb + Pb collisions at the CERN SPS. *Phys.Lett.*, B477:28–36, 2000.

[12] CERN PressRelease. *PR01.00 1002.00*, http://press.web.cern.ch/press/pressreleases /Releases2000/PR01.00EQuarkGluonMatter.html.

[13] K. Adcox et al. Formation of dense partonic matter in relativistic nucleus-nucleus collisions at RHIC: Experimental evaluation by the PHENIX collaboration. *Nucl.Phys.*, A757:184–283, 2005.

[14] John Adams et al. Experimental and theoretical challenges in the search for the quark gluon plasma: The STAR Collaboration's critical assessment of the evidence from RHIC collisions. *Nucl.Phys.*, A757:102–183, 2005.

[15] B.B. Back, M.D. Baker, M. Ballintijn, D.S. Barton, B. Becker, et al. The PHOBOS perspective on discoveries at RHIC. *Nucl.Phys.*, A757:28–101, 2005.

[16] I. Arsene et al. Quark gluon plasma and color glass condensate at RHIC? The Perspective from the BRAHMS experiment. *Nucl.Phys.*, A757:1–27, 2005.

[17] H. David Politzer. Reliable Perturbative Results for Strong Interactions? *Phys.Rev.Lett.*, 30:1346–1349, 1973.

[18] David J. Gross and Frank Wilczek. Ultraviolet Behavior of Nonabelian Gauge Theories. *Phys.Rev.Lett.*, 30:1343–1346, 1973.

[19] Bertrand C. Barrois. Superconducting Quark Matter. *Nucl.Phys.*, B129:390, 1977.

[20] R. Rapp, Thomas Schfer, Edward V. Shuryak, and M. Velkovsky. Diquark Bose condensates in high density matter and instantons. *Phys.Rev.Lett.*, 81:53–56, 1998.

[21] D. Bailin and A. Love. Superfluidity and Superconductivity in Relativistic Fermion Systems. *Phys.Rept.*, 107:325, 1984.

[22] Mark G. Alford, Krishna Rajagopal, and Frank Wilczek. QCD at finite baryon density: Nucleon droplets and color superconductivity. *Phys.Lett.*, B422:247–256, 1998.

[23] N. Cabibbo and G. Parisi. Exponential Hadronic Spectrum and Quark Liberation. *Phys.Lett.*, B59:67–69, 1975.

[24] R. Hagedorn. Statistical thermodynamics of strong interactions at high-energies. *Nuovo Cim.Suppl.*, 3:147–186, 1965.

[25] R. Hagedorn and J. Ranft. Statistical thermodynamics of strong interactions at high-energies. 2. Momentum spectra of particles produced in p p collisions. *Nuovo Cim.Suppl.*, 6:169–354, 1968.

[26] John C. Collins and M.J. Perry. Superdense Matter: Neutrons Or Asymptotically Free Quarks? *Phys.Rev.Lett.*, 34:1353, 1975.

[27] T.D. Lee and G.C. Wick. Vacuum Stability and Vacuum Excitation in a Spin 0 Field Theory. *Phys.Rev.*, D9:2291–2316, 1974.

[28] T. Hatsuda and T. Kunihiro. Critical Phenomena Associated with Chiral Symmetry Breaking and Restoration in QCD. *Prog.Theor.Phys.*, 74:765, 1985.

[29] T. Hatsuda and T. Kunihiro. Fluctuation Effects in Hot Quark Matter: Precursors of Chiral Transition at Finite Temperature. *Phys.Rev.Lett.*, 55:158–161, 1985.

[30] T. Hatsuda and T. Kunihiro. Character Changes of Pion and Sigma Meson at Finite Temperature. *Phys.Lett.*, B185:304, 1987.

[31] Teiji Kunihiro and Tetsuo Hatsuda. Effects of Flavor Mixing Induced by Axial Anomaly on the Quark Condensates and Meson Spectra. *Phys.Lett.*, B206:385, 1988.

[32] Veronique Bernard, R.L. Jaffe, and Ulf G. Meissner. Strangeness Mixing and Quenching in the Nambu-Jona-Lasinio Model. *Nucl.Phys.*, B308:753, 1988.

[33] M. Asakawa and K. Yazaki. Chiral Restoration at Finite Density and Temperature. *Nucl.Phys.*, A504:668–684, 1989.

[34] S. Klimt, Matthias F.M. Lutz, and W. Weise. Chiral phase transition in the SU(3) Nambu and Jona-Lasinio model. *Phys.Lett.*, B249:386–390, 1990.

[35] U. Vogl and W. Weise. The Nambu and Jona Lasinio model: Its implications for hadrons and nuclei. *Prog.Part.Nucl.Phys.*, 27:195–272, 1991.

[36] S.P. Klevansky. The Nambu-Jona-Lasinio model of quantum chromodynamics. *Rev.Mod.Phys.*, 64:649–708, 1992.

[37] Tetsuo Hatsuda and Teiji Kunihiro. QCD phenomenology based on a chiral effective Lagrangian. *Phys.Rept.*, 247:221–367, 1994.

[38] P. Rehberg, S.P. Klevansky, and J. Hufner. Hadronization in the SU(3) Nambu-Jona-Lasinio model. *Phys.Rev.*, C53:410–429, 1996.

[39] Michael Buballa. NJL model analysis of quark matter at large density. *Phys.Rept.*, 407:205–376, 2005.

[40] Yoichiro Nambu and G. Jona-Lasinio. Dynamical Model of Elementary Particles Based on an Analogy with Superconductivity. 1. *Phys.Rev.*, 122:345–358, 1961.

[41] Yoichiro Nambu and G. Jona-Lasinio. DYNAMICAL MODEL OF ELEMENTARY PARTICLES BASED ON AN ANALOGY WITH SUPERCONDUCTIVITY. II. *Phys.Rev.*, 124:246–254, 1961.

[42] Wojciech Florkowski and Wojciech Broniowski. Melting of the quark condensate in the NJL model with meson loops. *Phys.Lett.*, B386:62–68, 1996.

[43] Emil N. Nikolov, Wojciech Broniowski, Christo V. Christov, Georges Ripka, and Klaus Goeke. Meson loops in the Nambu-Jona-Lasinio model. *Nucl.Phys.*, A608:411–436, 1996.

[44] M. Oertel, M. Buballa, and J. Wambach. Meson properties in the 1/N(c) corrected NJL model. *Nucl.Phys.*, A676:247–272, 2000.

[45] M. Oertel, M. Buballa, and J. Wambach. Meson loop effects in the NJL model at zero and nonzero temperature. *Phys.Atom.Nucl.*, 64:698–726, 2001.

[46] M. Kitazawa, T. Koide, T. Kunihiro, and Y. Nemoto. Precursor of color superconductivity in hot quark matter. *Phys.Rev.*, D65:091504, 2002.

[47] Mei Huang, Peng-fei Zhuang, and Wei-qin Chao. Massive quark propagator and competition between chiral and diquark condensate. *Phys.Rev.*, D65:076012, 2002.

[48] Masakiyo Kitazawa, Tomoi Koide, Teiji Kunihiro, and Yukio Nemoto. Chiral and color superconducting phase transitions with vector interaction in a simple model. *Prog.Theor.Phys.*, 108:929–951, 2002.

[49] Mei Huang, Peng-fei Zhuang, and Wei-qin Chao. Charge neutrality effects on 2 flavor color superconductivity. *Phys.Rev.*, D67:065015, 2003.

[50] D. Blaschke, M.K. Volkov, and V.L. Yudichev. Coexistence of color superconductivity and chiral symmetry breaking within the NJL model. *Eur.Phys.J.*, A17:103–110, 2003.

[51] Igor Shovkovy and Mei Huang. Gapless two flavor color superconductor. *Phys.Lett.*, B564:205, 2003.

[52] Hiroaki Abuki, Gordon Baym, Tetsuo Hatsuda, and Naoki Yamamoto. The NJL model of dense three-flavor matter with axial anomaly: the low temperature critical point and BEC-BCS diquark crossover. *Phys.Rev.*, D81:125010, 2010.

[53] Takashi Sano and Kanako Yamazaki. Random matrix model for chiral and color-flavor locking condensates. *Phys.Rev.*, D85:094032, 2012.

[54] Kenji Fukushima. Chiral effective model with the Polyakov loop. *Phys.Lett.*, B591:277–284, 2004.

[55] Alexander M. Polyakov. Thermal Properties of Gauge Fields and Quark Liberation. *Phys.Lett.*, B72:477–480, 1978.

[56] Leonard Susskind. Lattice Models of Quark Confinement at High Temperature. *Phys.Rev.*, D20:2610–2618, 1979.

[57] E. Megias, E. Ruiz Arriola, and L.L. Salcedo. Polyakov loop in chiral quark models at finite temperature. *Phys.Rev.*, D74:065005, 2006.

[58] Claudia Ratti, Michael A. Thaler, and Wolfram Weise. Phases of QCD: Lattice thermodynamics and a field theoretical model. *Phys.Rev.*, D73:014019, 2006.

[59] Zhao Zhang and Yu-Xin Liu. Coupling of pion condensate, chiral condensate and Polyakov loop in an extended NJL model. *Phys.Rev.*, C75:064910, 2007.

[60] Simon Roessner, Claudia Ratti, and W. Weise. Polyakov loop, diquarks and the two-flavour phase diagram. *Phys.Rev.*, D75:034007, 2007.

[61] C. Sasaki, B. Friman, and K. Redlich. Susceptibilities and the Phase Structure of a Chiral Model with Polyakov Loops. *Phys.Rev.*, D75:074013, 2007.

[62] H. Hansen, W.M. Alberico, A. Beraudo, A. Molinari, M. Nardi, et al. Mesonic correlation functions at finite temperature and density in the Nambu-Jona-Lasinio model with a Polyakov loop. *Phys.Rev.*, D75:065004, 2007.

[63] Claudia Ratti, Simon Roessner, and Wolfram Weise. Quark number susceptibilities: Lattice QCD versus PNJL model. *Phys.Lett.*, B649:57–60, 2007.

[64] D. Blaschke, M. Buballa, A.E. Radzhabov, and M.K. Volkov. Effects of mesonic correlations in the QCD phase transition. *Yad.Fiz.*, 71:2012–2018, 2008.

[65] H. Abuki, R. Anglani, R. Gatto, G. Nardulli, and M. Ruggieri. Chiral crossover, deconfinement and quarkyonic matter within a Nambu-Jona Lasinio model with the Polyakov loop. *Phys.Rev.*, D78:034034, 2008.

[66] M. Kobayashi and T. Maskawa. Chiral symmetry and eta-x mixing. *Prog.Theor.Phys.*, 44:1422–1424, 1970.

[67] Gerard 't Hooft. Symmetry Breaking Through Bell-Jackiw Anomalies. *Phys.Rev.Lett.*, 37:8–11, 1976.

[68] Larry D. McLerran and Benjamin Svetitsky. A Monte Carlo Study of SU(2) Yang-Mills Theory at Finite Temperature. *Phys.Lett.*, B98:195, 1981.

[69] Larry D. McLerran and Benjamin Svetitsky. Quark Liberation at High Temperature: A Monte Carlo Study of SU(2) Gauge Theory. *Phys.Rev.*, D24:450, 1981.

[70] Kazuyuki Kanaya. Finite Temperature QCD on the Lattice – Status 2010. *PoS*, LATTICE2010:012, 2010.

[71] Szabocls Borsanyi, Zoltan Fodor, Christian Hoelbling, Sandor D. Katz, Stefan Krieg, et al. Full result for the QCD equation of state with 2+1 flavors. *Phys.Lett.*, B730:99–104, 2014.

[72] Szabolcs Borsanyi, Zoltan Fodor, Christian Hoelbling, Sandor D. Katz, Stefan Krieg, et al. Continuum EoS for QCD with N f=2 + 1 flavors. *PoS*, LATTICE2013:155, 2014.

[73] M.E. Berbenni-Bitsch, A.D. Jackson, S. Meyer, A. Schafer, J.J.M. Verbaarschot, et al. Random matrix universality in the small Eigenvalue spectrum of the lattice dirac operator. *Nucl.Phys.Proc.Suppl.*, 63:820–822, 1998.

[74] J.J.M. Verbaarschot and T. Wettig. Random matrix theory and chiral symmetry in QCD. *Ann.Rev.Nucl.Part.Sci.*, 50:343–410, 2000.

[75] M.A. Stephanov, J.J.M. Verbaarschot, and T. Wettig. Random matrices. 2005.

[76] Edward V. Shuryak. Which chiral symmetry is restored in hot QCD? *Comments Nucl.Part.Phys.*, 21:235–248, 1994.

[77] Robert D. Pisarski and Frank Wilczek. Remarks on the Chiral Phase Transition in Chromodynamics. *Phys.Rev.*, D29:338–341, 1984.

[78] Tetsuo Hatsuda, Motoi Tachibana, Naoki Yamamoto, and Gordon Baym. New critical point induced by the axial anomaly in dense QCD. *Phys.Rev.Lett.*, 97:122001, 2006.

[79] H. Georgi. LIE ALGEBRAS IN PARTICLE PHYSICS. FROM ISOSPIN TO UNIFIED THEORIES. *Front.Phys.*, 54:1–255, 1982.

[80] Benjamin Svetitsky and Laurence G. Yaffe. Critical Behavior at Finite Temperature Confinement Transitions. *Nucl.Phys.*, B210:423, 1982.

[81] K.A. Olive et al. Review of Particle Physics. *Chin.Phys.*, C38:090001, 2014.

[82] Barry R. Holstein. How large is f(pi)? *Phys.Lett.*, B244:83–87, 1990.

[83] M. Cheng, N.H. Christ, S. Datta, J. van der Heide, C. Jung, et al. The QCD equation of state with almost physical quark masses. *Phys.Rev.*, D77:014511, 2008.

[84] V. Bernard, U.G. Meissner, and I. Zahed. Decoupling of the Pion at Finite Temperature and Density. *Phys.Rev.*, D36:819, 1987.

[85] Robert D. Pisarski and Orlando Alvarez. Strings at Finite Temperature and Deconfinement. *Phys.Rev.*, D26:3735, 1982.

[86] T. Hell, Simon Roessner, M. Cristoforetti, and W. Weise. Dynamics and thermodynamics of a non-local PNJL model with running coupling. *Phys.Rev.*, D79:014022, 2009.

[87] Kouji Kashiwa, Thomas Hell, and Wolfram Weise. Nonlocal Polyakov-Nambu-Jona-Lasinio model and imaginary chemical potential. *Phys.Rev.*, D84:056010, 2011.

[88] G.A. Contrera, A.G. Grunfeld, and D.B. Blaschke. Phase diagrams in nonlocal Polyakov-Nambu-Jona-Lasinio models constrained by lattice QCD results. *Phys.Part.Nucl.Lett.*, 11:342–351, 2014.

[89] Yuji Sakai, Takahiro Sasaki, Hiroaki Kouno, and Masanobu Yahiro. Entanglement between deconfinement transition and chiral symmetry restoration. *Phys.Rev.*, D82:076003, 2010.

[90] Yuji Sakai, Takahiro Sasaki, Hiroaki Kouno, and Masanobu Yahiro. Equation of state in the PNJL model with the entanglement interaction. *J.Phys.*, G39:035004, 2012.

[91] Mrcio Ferreira, Pedro Costa, Dbora P. Menezes, Constana Providncia, and Norberto Scoccola. Deconfinement and chiral restoration within the SU(3) Polyakov–Nambu–Jona-Lasinio and entangled Polyakov–Nambu–Jona-Lasinio models in an external magnetic field. *Phys.Rev.*, D89:016002, 2014.

[92] Alexander A. Osipov, Brigitte Hiller, and Joao da Providencia. Multiquark interactions with a globally stable vacuum. *Phys.Lett.*, B634:48–54, 2006.

[93] Brigitte Hiller, Alexander A. Osipov, Veronique Bernard, and Alex H. Blin. Functional integral approaches to the bosonization of effective multi-quark interactions with U(A)(1) breaking. *SIGMA*, 2:026, 2006.

[94] W. Heisenberg and W. Pauli. On Quantum Field Theory. (In German). *Z.Phys.*, 56:1–61, 1929.

[95] W. Heisenberg and W. Pauli. On Quantum Field Theory. 2. (In German). *Z.Phys.*, 59:168–190, 1930.

[96] R.P. Feynman. Space-time approach to nonrelativistic quantum mechanics. *Rev.Mod.Phys.*, 20:367–387, 1948.

[97] G. Parisi and Yong-shi Wu. Perturbation Theory Without Gauge Fixing. *Sci.Sin.*, 24:483, 1981.

[98] Mariusz Sadzikowski and Wojciech Broniowski. Nonuniform chiral phase in effective chiral quark models. *Phys.Lett.*, B488:63–67, 2000.

[99] Oliver Schnetz, Michael Thies, and Konrad Urlichs. Phase diagram of the Gross-Neveu model: Exact results and condensed matter precursors. *Annals Phys.*, 314:425–447, 2004.

[100] Oliver Schnetz, Michael Thies, and Konrad Urlichs. Full phase diagram of the massive Gross-Neveu model. *Annals Phys.*, 321:2604–2637, 2006.

[101] E. Nakano and T. Tatsumi. Chiral symmetry and density wave in quark matter. *Phys.Rev.*, D71:114006, 2005.

[102] Dominik Nickel. Inhomogeneous phases in the Nambu-Jona-Lasino and quark-meson model. *Phys.Rev.*, D80:074025, 2009.

[103] Stefano Carignano, Dominik Nickel, and Michael Buballa. Influence of vector interaction and Polyakov loop dynamics on inhomogeneous chiral symmetry breaking phases. *Phys.Rev.*, D82:054009, 2010.

[104] T.M. Schwarz, S.P. Klevansky, and G. Papp. The Phase diagram and bulk thermodynamical quantities in the NJL model at finite temperature and density. *Phys.Rev.*, C60:055205, 1999.

[105] D. Ebert, K.G. Klimenko, and H. Toki. Chromomagnetic catalysis of color superconductivity in a (2+1)-dimensional NJL model. *Phys.Rev.*, D64:014038, 2001.

[106] F. Gastineau, R. Nebauer, and J. Aichelin. Thermodynamics of the three flavor NJL model: Chiral symmetry breaking and color superconductivity. *Phys.Rev.*, C65:045204, 2002.

[107] Benoit Vanderheyden and A.D. Jackson. Random matrix study of the phase structure of QCD with two colors. *Phys.Rev.*, D64:074016, 2001.

[108] R.L. Stratonovich. . *Dokl. Akad. Nauk SSSR*, 115:1097, 1957.

[109] J. Hubbard. Calculation of partition functions. *Phys.Rev.Lett.*, 3:77–80, 1959.

[110] David J. Gross and Andre Neveu. Dynamical Symmetry Breaking in Asymptotically Free Field Theories. *Phys.Rev.*, D10:3235, 1974.

[111] Julian S. Schwinger. On gauge invariance and vacuum polarization. *Phys.Rev.*, 82:664–679, 1951.

[112] Martine Jaminon, Ramon Mendez Galain, Georges Ripka, and Pierre Stassart. Chiral theory of mesons in dense baryonic matter. 1. *Nucl.Phys.*, A537:418–456, 1992.

[113] W. Pauli and F. Villars. On the Invariant regularization in relativistic quantum theory. *Rev.Mod.Phys.*, 21:434–444, 1949.

[114] Robert L. Jaffe and Frank Wilczek. Diquarks and exotic spectroscopy. *Phys.Rev.Lett.*, 91:232003, 2003.

[115] R.L. Jaffe. Exotica. *Nucl.Phys.Proc.Suppl.*, 142:343–355, 2005.

[116] C. Itzykson and J.B. Zuber. QUANTUM FIELD THEORY. 1980.

[117] E. Quack and S.P. Klevansky. Effective 1/N(c) expansion in the NJL model. *Phys.Rev.*, C49:3283–3288, 1994.

[118] Simon Roessner, T. Hell, C. Ratti, and W. Weise. The chiral and deconfinement crossover transitions: PNJL model beyond mean field. *Nucl.Phys.*, A814:118–143, 2008.

[119] A. Fetter and J.D. Walecka. Quantum Theory of Many-Particle System. 1971.

[120] J.I. Kapusta and Charles Gale. Finite-temperature field theory: Principles and applications. 2006.

[121] J. Beringer et al. Review of Particle Physics (RPP). *Phys.Rev.*, D86:010001, 2012.

[122] Muneyuki Ishida. Possible classification of the chiral scalar sigma nonet. *Prog.Theor.Phys.*, 101:661–669, 1999.

[123] Shin Ishida, Muneyuki Ishida, Taku Ishida, Kunio Takamatsu, and Tsuneaki Tsuru. Analysis of K pi scattering phase shift and existence of kappa (900) particle. *Prog.Theor.Phys.*, 98:621–629, 1997.

[124] Amir H. Fariborz, Renata Jora, and Joseph Schechter. Global aspects of the scalar meson puzzle. *Phys.Rev.*, D79:074014, 2009.

[125] H. Abuki, M. Ciminale, R. Gatto, G. Nardulli, and M. Ruggieri. Enforced neutrality and color-flavor unlocking in the three-flavor Polyakov-loop NJL model. *Phys.Rev.*, D77:074018, 2008.

[126] Kenji Fukushima. Phase diagrams in the three-flavor Nambu-Jona-Lasinio model with the Polyakov loop. *Phys.Rev.*, D77:114028, 2008.

[127] Philip D. Powell and Gordon Baym. Axial anomaly and the three-flavor Nambu–Jona-Lasinio model with confinement: Constructing the QCD phase diagram. *Phys.Rev.*, D85:074003, 2012.

[128] Hiroaki Kouno, Takahiro Makiyama, Takahiro Sasaki, Yuji Sakai, and Masanobu Yahiro. Confinement and $\mathbb{Z}_3$ symmetry in three-flavor QCD. *J.Phys.*, G40:095003, 2013.

[129] S. Klimt, Matthias F.M. Lutz, U. Vogl, and W. Weise. GENERALIZED SU(3) NAMBU-JONA-LASINIO MODEL. Part. 1. MESONIC MODES. *Nucl.Phys.*, A516:429–468, 1990.

[130] Szabolcs Borsanyi, Gergely Endrodi, Zoltan Fodor, Antal Jakovac, Sandor D. Katz, et al. The QCD equation of state with dynamical quarks. *JHEP*, 1011:077, 2010.

[131] Murray Gell-Mann. A Schematic Model of Baryons and Mesons. *Phys.Lett.*, 8:214–215, 1964.

[132] Masakuni Ida and Reido Kobayashi. Baryon resonances in a quark model. *Prog.Theor.Phys.*, 36:846, 1966.

[133] D.B. Lichtenberg and L.J. Tassie. Baryon Mass Splitting in a Boson-Fermion Model. *Phys.Rev.*, 155:1601–1606, 1967.

[134] Mauro Anselmino, Enrico Predazzi, Svante Ekelin, Sverker Fredriksson, and D.B. Lichtenberg. Diquarks. *Rev.Mod.Phys.*, 65:1199–1234, 1993.

[135] R.L. Jaffe. Exotica. *Phys.Rept.*, 409:1–45, 2005.

[136] N. Ishii, W. Bentz, and K. Yazaki. Faddeev approach to the nucleon in the Nambu-Jona-Lasinio (NJL) model. *Phys.Lett.*, B301:165–169, 1993.

[137] L.J. Abu-Raddad, A. Hosaka, D. Ebert, and H. Toki. Path integral hadronization for the nucleon and its interactions. *Phys.Rev.*, C66:025206, 2002.

[138] Jin-cheng Wang, Qun Wang, and Dirk H. Rischke. Baryon formation and dissociation in dense hadronic and quark matter. *Phys.Lett.*, B704:347–353, 2011.

[139] Michael E. Peskin and Daniel V. Schroeder. An Introduction to quantum field theory. 1995.

[140] H. Fujii and M. Ohtani. Sigma and hydrodynamic modes along the critical line. *Phys.Rev.*, D70:014016, 2004.

[141] T. Matsui and M. Matsuo. Quantized meson fields in and out of equilibrium. I. Kinetics of meson condensate and quasi-particle excitations. *Nucl.Phys.*, A809:211–245, 2008.

[142] M. Matsuo and T. Matsui. Quantized meson fields in and out of equilibrium. II: Chiral condensate and collective meson excitations. 2008.

[143] P. Zhuang, J. Hufner, and S.P. Klevansky. Thermodynamics of a quark - meson plasma in the Nambu-Jona-Lasinio model. *Nucl.Phys.*, A576:525–552, 1994.

[144] J. Hufner, S.P. Klevansky, P. Zhuang, and H. Voss. Thermodynamics of a quark plasma beyond the mean field: A generalized Beth-Uhlenbeck approach. *Annals Phys.*, 234:225–244, 1994.

[145] Z. Yu, G. Baym, and C.J. Pethick. Calculating energy shifts in terms of phase shifts. *J. Phys. B : Mol. Opt. Phys.*, 44:195207, 2011.

[146] A. Wergieluk, D. Blaschke, Yu.L. Kalinovsky, and A. Friesen. Pion dissociation and Levinson‘s theorem in hot PNJL quark matter. *Phys.Part.Nucl.Lett.*, 10:660–668, 2013.

[147] Larry McLerran, Krzystof Redlich, and Chihiro Sasaki. Quarkyonic Matter and Chiral Symmetry Breaking. *Nucl.Phys.*, A824:86–100, 2009.